Framework for Multi-Purpose Utility Tunnel Location Selection Considering Social Costs

Kelechukwu Tersoo Genger

A Thesis

In the department

of

Concordia Institute for Information Systems Engineering (CIISE)

Presented in Partial Fulfillment of the Requirements
for the Degree of
Doctor of Philosophy (Information & Systems Engineering) at

Concordia University

Montreal, Québec, Canada

March 2023

CONCORDIA UNIVERSITY

School of Graduate Studies

This is to certify that the thesis prepared

By: Kelechukwu Tersoo Genger

Entitled: **Framework for Multi-Purpose Utility Tunnel Location Selection Considering Social Costs**

and submitted in partial fulfillment of the requirements for the degree of

Doctor of Philosophy (Information & Systems Engineering)

complies with the regulations of the University and meets the accepted standards with respect to originality and quality.

Signed by the final examining committee:

_____ Chair
Dr.

_____ External Examiner
Dr. Dexter Hunt

_____ Examiner
Dr. Anjali Awasthi

_____ Examiner
Dr. Farnoosh Naderkhani

_____ Examiner
Dr. Fuzhan Nasiri

_____ Thesis Supervisor
Dr. Amin Hammad

Approved by _____
Dr. Zachary Patterson, Graduate Program Director

March 2023 _____
Dr. Mourad Debbabi, Dean,
Gina Cody School of Engineering and Computer Science

ABSTRACT
Framework for Multi-Purpose Utility Tunnel Location Selection Considering Social Costs

Kelechukwu Tersoo Genger, Ph.D.

Concordia University, 2023

The unsustainable way of burying utilities has resulted in difficulties in regular maintenance, which is one of the main reasons for the poor state of these utilities. Accessing these utilities through open-cut excavation leads to detrimental socioeconomic and environmental impacts, which can be quantified as social costs incurred during the asset's lifecycle. To reduce social costs, synchronized interventions of collocated assets (e.g., water and sewer pipes and pavements) can minimize excavations in a specific street segment over time for preventive maintenance. Few studies have prioritized street segments based on the socioeconomic impacts from intervention activities, such as street closures. Additionally, synchronized interventions are not a long-term solution as they do not eliminate the need for future excavations.

A more sustainable solution is the Multi-Purpose Utility Tunnels (MUTs), as they integrate all underground utilities in one accessible tunnel. MUTs eliminate the need for future excavations and their associated costs, as well as the resulting socioeconomic impacts. Meanwhile, both the synchronized interventions and the MUT are not generally practiced. Although several MUTs have been implemented in different parts of the world, their locations have either been politically influenced or selected to preserve heritage sites. In some cases, MUTs are built to take advantage of some opportunities, such as a newly developed area. Nevertheless, choosing the street segments for MUTs is affected by several criteria with different spatial characteristics. Combining these characteristics and managing their trade-offs determine the ranking of alternative MUT locations. Therefore, a systematic approach for MUT location selection that is based on the spatial characteristics of the criteria, as well as the lifecycle costs of each alternative is needed. Furthermore, the social cost of maintaining, repairing, or replacing utility assets during synchronized interventions or MUT implementation can be reduced by predicting the closure of street segments based on the need for intervention determined by asset conditions.

The main goal of this research is to develop a framework for MUT location selection considering social costs. To achieve this goal, the specific objectives are: (1) Establishing the relationships between intervention activities and their socioeconomic impacts; (2) Classifying the conditions of

different spatially collocated underground municipal assets (i.e., pavements, water and sewer pipes) within a segment; (3) Determining street closures based on the synchronized or unsynchronized interventions at the segment level; (4) Developing a multi-criteria decision-making model (MCDM) for MUT location selection; and (5) Optimizing the location selection of MUTs considering agency and social lifecycle costs.

The main contributions developed in the context of this thesis are: (1) Developing a geospatial visual analytics model that supports the understanding of the socioeconomic impacts of unsynchronized intervention practices; (2) Developing an ML method for systematic condition classification of different spatially collocated underground municipal assets (i.e., pavements, water and sewer pipes) within a segment. To the best of our knowledge, there is no existing research about determining street closures based on the combined conditions of spatially collocated municipal infrastructure assets at the segment level; (3) Applying a heuristic approach for determining street closures based on the synchronized or unsynchronized interventions at the segment level induced by combining the interventions of individual assets within each segment; (4) Defining a comprehensive MCDM model that identifies and quantifies the criteria that influence the MUT location selection using subjective and objective methods; (5) Defining a multi-objective optimization model that was able to identify the potential MUT locations and a multi-year plan for MUT implementation that offers lifecycle savings; (6) Developing a systematic method for comparing the results of the MUT optimization with those of the synchronized interventions. This comparison is based on the agency and social LCCs, and the network deterioration generated by the MUTs and synchronized method of utility interventions at the network and segment levels; and (7) Developing three regression models for capturing the social cost of both alternatives at the network and segment levels.

ACKNOWLEDGEMENT

My deepest gratitude to God Almighty, my Lord and personal savior Jesus Christ whom I trust.

I would like to extend my immeasurable gratitude to my brilliant supervisor, Dr. Amin Hammad, who is always ready to offer insightful guidance no matter the time of day. His work ethic and commitment to the area of sustainable infrastructure management are an inspiration to me.

I would also like to thank the members of my committee, Dr. Dexter Hunt, Dr. Anjali Awasthi, Dr. Farnoosh Naderkhani, and Dr. Fuzhan Nasiri for their vital input toward improving this research.

I would like to give special thanks to Mr. Michel Saindon and Ms. Salamatou Modieli from Centre d'expertise et de recherche en infrastructures urbaines (CERIU), Mr. Serge Boileau from Commission des Services Electriques De Montreal (CSEM), and Mr. Martin Gaudette, Mr. Jean-Pierre Bossé, and Mr. Sacha Volcy from the City of Montreal, for providing the invaluable data required for this research.

This research has been funded by MITACS project number IT12902, Concordia University Gina Cody School of Engineering and Computer Science, and TETFund. I sincerely appreciate the support provided.

Furthermore, I also appreciate Dr. Ali Alaghbandrad and Miss Yisha Luo for laying the foundation for this research.

On a personal level, I would like to thank my lovely parents, Mrs. Edith Ngozi Genger and Late Mr. Francis Utume Genger, for the gift of life, my father-in-law Mr. Marcus Idemudia Imhafuegbe, and my siblings Mrs. Chinwe, Arch. Francis, Ms. Eldoo, and Mr. Okechukwu for their continuous prayers and support.

Dedicated to my lovely wife Susan Mary Genger and my three beautiful children, Gabriella, Alvin, and Nathan.

TABLE OF CONTENTS

LIST OF FIGURES

LIST OF TABLES

LIST OF ACRONYMS

AADT	Annual Average Daily Traffic
AHP	Analytic Hierarchy Process
ANN	Artificial Neural Networks
ANP	Analytic Network Process
AOC	Average Operating Cost
BDT	Boosted Decision Tree
BIM	Building Information Modeling
BLR	Binary Logistic Regression
BOCR	Benefits, Opportunities, Cost, and Risks
COF	Consequence of Failure
CR	Consistency Ratio
CSEM	Commission Des Services Electriques De Montreal
DL	Deep Learning
DT	Decision Trees
DSS	Decision Support System
EA	Evolutionary Algorithm
EDT	Ensemble Decision Tree
EGB	Extreme Gradient Boosting
ELECTRE	ELimination Et Choice Translating Reality
ELM	Extreme Learning Machine
EPR	Evolutionary Polynomial Regression
GA	Genetic Algorithm
GBT	Gradient-Boosted Trees
GHG	Greenhouse Gases
GIS	Geographical Information System
IRI	International Roughness Index
LCC	Lifecycle Cost
LGR	Logistic Regression
LightGBM	Light Gradient Boosted Machine
LOS	Level of Service
LR	Linear Regression
M&R	Maintenance and Repair
MACBETH	Measuring Attractiveness by a Categorical-Based Evaluation Technique
MAUT	Multi-Attribute Utility Theory
MCDM	Multi-Criteria Decision Making
ML	Machine Learning
MUT	Multi-Purpose Utility Tunnel
NIS	Negative Ideal Solution

OAT	One-at-a-time
OCR	Overall Change Rate
PCI	Pavement Condition Index
PCM	Pairwise Comparison Matrix
PDC	Pedestrian Delay Costs
PIS	Positive ideal solution
POF	Probability of Failure
PROMETHEE II	Preference Ranking Organization METHod for Enrichment Evaluation II
PSI	Present Serviceability Index
PSO	Particle Swarm Optimization
RD	Rut Depth
RF	Random Forest
RFR	Random Forest Regression
RQI	Road Quality Index
RSL	Remaining Service Life
SAW	Simple Additive Weighting
SDSS	Spatial Decision Support System
SVM	Support Vector Classification
SVC	Support Vector Machine
SVR	Support Vector Regression
SWOT	Strength, Weakness, Opportunity, and Threat
TNP	Transportation Network Performance
TOPSIS	Technique for Order of Preference by Similarity to Ideal Situation
UUS	Urban Underground Space
VA	Visual Analytics
VDC	Vehicle Delay Costs
VE	Voting-based Ensemble
VEC	Vehicle Emission Cost
VMO	Vehicle Maintenance and Operating
VOT	Value of Time
WLC	Weighted Linear Combination

CHAPTER 1. INTRODUCTION

1.1 Background

Traditionally, most urban utilities, such as water, sewer, and gas pipes, and telecommunication and electricity cables, are laid underground. In addition, cable networks have extensive networks aboveground on poles and towers. In most cases, the layout of these utilities makes interventions not only challenging but expensive for both utility providers and utility consumers (i.e., social cost) (Roberts *et al.*, 2006; Valdenebro and Gimena, 2018). Utility providers face challenges in increasing the lifespan of these assets against damages ranging from natural disasters and manmade risks to deterioration over time. To increase the lifespan and ensure service continuity of utility assets, preventive maintenance and repair are needed. In the case of underground utilities, such as sewer pipes, potable water pipes, etc., these maintenance and repair activities, as well as network expansions, often require open-cut excavations. These interventions lead to the closure of streets and local businesses, noise pollution, air pollution, the diversion of traffic from the intervention area, and the reduction in the life of the pavement and walkways (Hao *et al.*, 2012; Parker, 2008).

All around the world, utility interventions account for a large number of pavement excavations. In the United Kingdom, an average of 1.5 million road excavations causing partial and complete street closures occur yearly, resulting in an estimated loss in earnings (e.g., loss of street parking revenue, social costs, dry holes related to utility excavations, etc.) of £5.5B per year (Caffoor, 2019). Several cities in North America have also quantified the number of pavement excavations. For example, the District of Columbia (Washington DC) estimated over 6,000 excavations in 2000. Meanwhile, based on the requests for excavation permits made by utility owners in Montreal, 7,000 requests for excavations were made by telecom, gas, Commission des services électriques de Montréal (CSEM), and electricity transmission and distribution companies from 2017 to 2019. These figures paint a picture of the number of interventions needed to install, maintain, or expand existing utility networks and the number of resulting business closures, increased travel delays, tax revenue losses, service interruptions, and air pollution (Oum, 2017). This recognition of the need for excavation for utility interventions, especially in urban centers, reiterates the need for coordinated and sustainable utility interventions and placement.

Incorporating sustainability into the early stages of utility intervention planning ensures the implementation of optimal solutions through innovative strategic planning (Maleti *et al.*, 2014;

Morioka and Monteiro De Carvalho, 2016). A sustainability-based utility interventions plan aims at achieving the right balance between reducing the socioeconomic and environmental impacts of the utility interventions and the cost of the interventions (de Magalhães *et al.*, 2019). In the short term, some level of sustainability can be achieved by conducting synchronized integrated interventions.

One main reason street segments undergo repeated excavations is unsynchronized interventions (Palsat *et al.*, 2020; Wilde *et al.*, 2002). An example is when a recently reconstructed or rehabilitated pavement of a street segment later experiences a pipe failure. These repeated excavations mean the user costs (e.g., traffic congestion because of street closures) associated with this street segment are increased due to both events. The negative socioeconomic impacts of unsynchronized utility interventions can be minimized by implementing a holistic form of utility intervention.

In most cases, the maintenance and management of utility networks are performed in isolation from one another even though these systems operate as a system of systems (Clarke *et al.*, 2017). Due to this interdependency, there is a need to holistically coordinate their intervention activities (Rashedi and Hegazy, 2016). This coordination means factoring in variables (e.g., the type and number of utility assets under a road segment, the remaining service life (RSL) of an asset, the nature of the required intervention, deterioration level, budget, social cost implications, etc.) into the decision-making process.

Synchronized utility interventions are coordinated interventions that simultaneously target pavement interventions with private and municipal underground utility interventions (Abu-Samra et al., 2018). Although these interventions are practiced in several countries, e.g., Canada, Norway, Sweden, and the USA (Braun, 2012; Chacon and Normand, 2016; FCM and NRC, 2003; Hafskjold, 2010; Hafskjold and Bertelsen, 2008), some asset owners conduct their interventions in insolation from one another as their respective budgets are not coordinated. The effect of synchronizing intervention activities includes reducing project costs by eliminating repeated repair costs (FCM and NRC, 2003) and the associated social costs (Abu-Samra et al., 2018). Due to these benefits, synchronized interventions are encouraged (FCM and NRC, 2003). Practices such as corridor/street segment (i.e., part of a street between two intersections) upgrades are seen as opportunities for synchronized interventions, where the road is repaved when underground utility interventions are completed (FCM and NRC, 2003). Although this practice promotes coordination and reduces the frequency of utility interventions, there is a possibility of premature replacement

of utility assets before the end of their useful life. In addition, from the perspective of sustainable urban development, the practice of synchronized interventions does not guarantee the elimination of future excavations on the same street segment in which collocated assets exist. Also, it relies on adequate collaboration between utility owners, which seldom exists among most utility owners.

To evaluate the conditions of these assets, most researchers have focused on asset-level condition assessment, prediction, or classification (Harvey and McBean, 2014; Kumar et al., 2018; Tavakoli et al., 2020). However, treating municipal assets as interrelated systems and synchronizing their interventions is paramount to reducing user costs. Therefore, multi-asset conditions should be determined at the segment level.

However, in the long term, under certain conditions (e.g., high utility density, traffic density, etc.), a major shift can be made toward the sustainable placement of underground utilities using multi-purpose utility tunnels (MUTs). MUTs offer a sustainable, long-term alternative by hosting utilities in an underground tunnel capable of housing several utilities in one or more compartments. In so doing, utility assets in the MUT are less vulnerable to damage, thus, increasing their lifespan (Laistner and Laistner, 2012). Also, expansion, inspection, and maintenance of the underground utilities can be executed all year round with the possibility of eliminating social costs. Other advantages of implementing MUTs include a significant reduction in utility intervention costs, reduced utility strikes and improved planning of underground space (Luo, Alaghbandrad, *et al.*, 2020).

Despite these advantages, there is a general lack of enthusiasm towards building MUTs in most countries, as several barriers exist in the widespread acceptance and adoption of MUTs. Some of the challenges include the high cost of construction (Canto-Perello *et al.*, 2013; Hunt *et al.*, 2012), the dominance of the bury-it and forget-it approach (Laistner, 2012), safety and security risks related to the incompatibility of utilities (Calvo-Peña *et al.*, 2006; Canto-Perello and Curiel-Esparza, 2013; Hunt *et al.*, 2014a), reluctant cooperation between utility owners (Hunt and Rogers, 2005), lack of a standardized method of construction (Hunt *et al.*, 2014a), lack of political will (Curiel-Esparza *et al.*, 2004), and the business model of utility owners (Luo, 2019a).

The short-term cost of construction is a significant setback in implementing MUTs. Most decision-makers focus mainly on direct costs and pay little attention to long-term social and economic impacts in their decision-making process (Hojjati *et al.*, 2018). When faced with cheaper alternatives, such as the traditional method of burying utilities and trenchless technologies, the decision, in most cases, does not favor the adoption of MUTs. However, when considering the

lifecycle costs of these alternatives, the MUT is a better solution because it offers a sustainable and resilient solution to hosting utilities (Valdenebro and Gimena, 2018; Wang *et al.*, 2018; Yang and Peng, 2016).

MUT location selection is vital because the decision-makers who are willing to consider the construction of MUTs are faced with a limited budget versus the high initial cost of construction of the MUT. In some countries (e.g., China), the decision of where to build MUTs is mainly political (Wang, 2018). In other set-ups (e.g., private establishments, universities, etc.), the decision is less complicated. Having a systematic process of identifying the most suitable locations (i.e., street segments) based on predetermined criteria will ensure that constructing the MUTs in the selected locations provides the maximum benefits of MUTs to utility owners and consumers as well as to the utility assets.

1.2 Problem Statement

This section expounds on the problems of interest:

P1: Limited research related to the visualization and interpretation of the relationships between multi-asset interventions and their socioeconomic implications: To aid the decision-making process, insights can be drawn from the visualization and interpretation of the multivariate datasets that capture the relationship that exists between the interventions of spatially collocated assets. The use of methods such as Visual analytics (VA) has been effectively applied to understand the phenomena associated with individual infrastructure assets. However, this method of individual asset analysis is inefficient when considering synchronized or multi-asset interventions.

P2: Need for a systematic process for predicting street closures based on the conditions of spatially collocated assets at the segment-level: From the social cost point of view, based on the scale and number of utility assets maintained, repaired, or replaced during synchronized interventions or MUT implementation, there is a need to either partially or completely close street segments. Therefore, predicting the closure of street segments based on the need for intervention (determined by the asset conditions) can provide a window to plan street closures to reduce socioeconomic impact while offering a more accurate estimate of the intervention duration (Oum, 2017). Accurately classifying the conditions of the spatially collocated assets improves the planning and budgeting phase of synchronized interventions, as well as MUT location selection, which will lead to better planning/decision-making for utility owners, city planners, business owners around the intervention area, transit departments, and the public.

P3: Limited research focusing on MUT location selection: Several MUTs have been implemented in different parts of the world. Their locations have either been politically influenced or selected to preserve heritage sites or to meet the conditions of a newly developed city (Valdenebro and Gimena, 2018; Wang, 2018). Nevertheless, selecting the location in an existing city under street segments is affected by several criteria that have different spatial characteristics. Combining these characteristics and managing the trade-offs that exist between them determine the ranking of the alternative street segments. Previous research has achieved MUT location selection using the Analytic Hierarchical Process (AHP) to determine the weights of eight criteria and the subsequent ranking of alternative street segments using Weighted Linear Combination (WLC) (Luo, et al., 2020). However, AHP does not factor in interrelated criteria (Saaty, 2004). Using the Analytic Network Process (ANP) eliminates this drawback (Saaty, 2004). In terms of problem structure, AHP structures an MCDM problem in the form of a hierarchy, while ANP uses a network structure factoring in dependencies between different criteria. Furthermore, the weights obtained from applying both AHP and ANP are subjective weights that are based on expert judgments, which are in most cases biased to favor each expert's area of expertise. In addition, using subjective methods that factor in dependencies, and objective methods that objectively assign weights to the criteria will affect the outcome of the decision-making process. Although, the use of subjective and objective weights will offer different perspectives from the decision-maker's point of view and from the data itself.

On the other hand, past research has compared the LCC of direct burial versus the MUT for built-up areas with existing underground utility infrastructure. The literature shows that it is generally accepted that the MUT can be a more sustainable alternative to the traditional method of burying underground utilities (Canto-Perello et al., 2016; Valdenebro et al., 2019; Hunt et al., 2014), especially on street segments with high utility and traffic densities. Studies have used agent-based simulations, breakeven point analysis, etc., to show how the MUT in the long term, has the potential to be more economically sustainable than the synchronized method of utility intervention for buried utilities. However, these researchers used single isolated projects in their analyses. Therefore, more research is needed to apply optimization techniques to find the optimal MUT locations at the network and segment levels.

1.3 Research Objectives

The main goal of this research is to develop a framework for MUT location selection considering social costs. The specific objectives of this research regarding the problem statements given in Section 1.2 are as follows:

1. Developing a visual analytics model to establish the relationships between intervention activities and their socioeconomic impacts visually and statistically. This model identifies critical areas where the current infrastructure practices will potentially result in a relatively high socioeconomic impact.
2. Developing a machine learning (ML) method for systematic condition classification of different spatially collocated underground municipal assets (i.e., pavements, water and sewer pipes) within a segment.
3. Applying a heuristic approach for determining street closures based on the synchronized or unsynchronized interventions at the segment level induced from combining the interventions of individual assets within each segment.
4. Developing a multi-criteria decision-making model for the spatial analysis for location selection of MUTs.
5. Developing a multi-objective optimization model for selecting potential locations of MUTs considering agency and social lifecycle costs.

1.4 Thesis Organization

This thesis is structured as follows:

Chapter 2 Literature Review: This chapter presents a critical review of several areas including: (1) the history, benefits, and implementation challenges of MUTs; (2) MUT location selection and the influencing criteria; (3) MCDM techniques; (4) underground asset condition classification and prediction; (5) synchronized utility intervention; (6) optimizing synchronized interventions (7) social costs; and (8) visual analytics. The chapter also summarizes the identified research gaps based on the limitations in the literature.

Chapter 3 Research Framework: This chapter expounds on the different modules that make up the proposed methodology.

Chapter 4 Geospatial Visual Analytics for Utility Intervention Decision-Making: This chapter presents an analysis of the relationship between the socioeconomic impacts of the current

infrastructure intervention practices and the conditions of two municipal assets (i.e., water pipes and pavements).

Chapter 5 Street Closure Prediction Based on the Combined Conditions of Spatially Collocated Assets: This chapter is centered on the prediction of street closures using the discrete classification of the conditions of the three municipal assets. The conditions are used to determine asset-level intervention strategies, which are combined to obtain segment-level interventions. The nature of the segment-level interventions determines the required street closures. The applicability of the proposed model is demonstrated through a case study.

Chapter 6 Multi-Criteria Decision-Making for MUT Location Selection: In this chapter, the selection of the locations for the placement of MUTs is accomplished using MCDM methods. The criteria that affect the placement of MUTs are identified and weighed using both subjective and objective MCDM techniques. Furthermore, ranking of the potential street segments is achieved by combining the weights and criteria scores of the segments. A case study demonstrating the implementation and applicability of the proposed method is also presented.

Chapter 7 Multi-Objective Optimization for Selecting Potential Locations of MUT Considering Social Costs: This chapter expounds on the selection of street segments for MUT implementation based on the segments that offer agency and social lifecycle cost savings. This component of the research is achieved using two optimization models that optimize the agency and social lifecycle costs for the synchronized intervention and MUT. The outputs of both models are compared at the network and segment levels to identify the streets with lifecycle cost savings. The implementation and applicability of this proposed model are demonstrated through a case study.

Chapter 8 Summary, Conclusions, Contributions, and Future Work: This chapter summarizes this research, and the contributions are highlighted. In addition, the limitations of this research are also stated, and recommendations for future research are suggested.

CHAPTER 2. LITERATURE REVIEW[1]

2.1 Introduction

The MUT location selection problem is complex and multifaceted. This chapter focuses on exploring the literature related to MUT location selection and the synchronized method of utility intervention, which is considered the best practice. The chapter begins by discussing the history of MUTs, their implementation in North America and Europe, as well as their advantages and implementation challenges. Moreover, the chapter delves into MUT planning, highlighting the criteria considered for location selection from the MCDM perspective. This section emphasizes the techniques used in weighting criteria applied in this research.

Following this, the chapter examines scholarly works related to optimizing both the MUT location selection and the synchronized method of utility interventions. In addition, the chapter showcases literature on the application of machine learning algorithms in the decision-making process of several asset management practices. Furthermore, the chapter provides an analysis of the social cost indicators used in this research to estimate the negative socioeconomic impacts of underground utility asset intervention. The literature also discusses the application of geospatial visual analytics as a way of portraying the relationship between the intervention activities and their socioeconomic impacts.

Overall, this chapter provides a comprehensive overview of the literature related to MUT location selection and synchronized utility intervention. It highlights the challenges and opportunities associated with these practices, and the potential benefits of incorporating cutting-edge technologies such as machine learning, optimization algorithms, and geospatial visual analytics.

2.2 Multi-Purpose Utility Tunnels

MUT, as defined by APWA, (1997), is "*any system of underground structures containing one or more utility services which permit the placement, renewal, maintenance, repair or revision of the service without the necessity of making excavations; this implies that the structure is traversable by people and, in some cases, traversable by some sort of vehicle as well".*

[1] This chapter is partially based on the following journal paper: Luo, Y., Alaghbandrad, A., Genger, T.K. and Hammad, A. (2020), "History and recent development of multi-purpose utility tunnels", Tunnelling and Underground Space Technology, Pergamon, 1 September, doi: 10.1016/j.tust.2020.103511.

According to Canto-Perello and Curiel-Esparza (2013), MUT is "an underground utilidor containing one or more utility systems, permitting the installation, maintenance, and removal of the system without making street cuts or excavations."

2.2.1 MUT advantages and implementation challenges

2.2.1.1 MUT advantages

According to Luo et al. (2020) the advantages of MUTs are classified into two groups: advantages to utility owners and to users.

The benefits to the utility owners are as follows: (1) Significant reduction of agency costs; (2) Improved inspection and maintenance of utilities; (3) Minimized damage and corrosion of utilities; (4) Cost savings for future upgrades; (5) significant reduction in accidental injuries and death associated with underground utility interventions; (6) Significant reduction of municipal revenue loss resulting from street closures; and (7) Improved underground space planning.

The societal and environmental benefits to the users are as follows: (1) Significant reduction in intervention-related traffic congestions; (2) Improved health and environment; (3) Improved quality of service; (4) Elimination of street closure for utility interventions; and (5) Major reduction in the temporary closures of recreational facilities and businesses around the intervention area.

2.2.1.2 MUT implementation challenges

There is a general lack of enthusiasm in developed countries, as several barriers exist in the acceptance and adoption of MUTs. Some of the challenges include; the high cost of construction (Canto-Perello *et al.*, 2013; Hunt *et al.*, 2012), the bury-it and forget-it approach (Laistner, 2012), incompatibility of utilities (Calvo-Peña *et al.*, 2006), reluctant cooperation between utility owners (Hunt and Rogers, 2005), security and safety (Canto-Perello et al., 2013; Hunt et al., 2014), lack of a standardized method of construction (Hunt et al., 2014), and the business model of utility owners (Luo, 2019).

2.2.2 History of MUTs

MUTs have been in existence since the 19th century. The first countries to implement the use of MUTs were France (1850s) (Cano-Hurtado and Canto-Perello, 1999; Canto-Perello and Curiel-Esparza, 2001; Wang *et al.*, 2018), England (1860s)(Canto-Perello *et al.*, 2009; Laistner and

Laistner, 2012; Rogers and Hunt, 2006), and Germany (1893) this shown in Figure 2-1(a). There was a lag from 1893 to about 1920 in the construction of MUTs. Figure 2-1(b) shows that between 1921 and 1960, several MUTs were constructed in parts of North America (Alaska), Asia (Japan), and Europe (France, Germany, Czech, etc.). Figure 2-1(c) shows that from 1961 to 1980, there was a rise in the construction of MUTs with a total of about 30 MUTs constructed. During this period, about 50% of the world's MUTs were built in France in cities like Angers, Paris, Rouen, Lyon, etc. Following the Utility Tunnel, Law passed in 1963, Japan was able to build approximately 2000 km of utility tunnels in 80 Japanese cities (Wang *et al.*, 2018).

Countries like Belgium, the Czech Republic, Germany, Switzerland, etc., were also involved in the construction of MUTs. Subsequently, between 1981 and 2000, the Czech Republic increased the construction of MUTs with a total of 10 out of a total of about 36 MUTs constructed worldwide during this period. These MUTs were built in cities like Prague, Brno, etc. Japan increased the construction of MUTs during this period to about 30% of the world's MUTs. However, countries like France and Germany continued to build MUTs. This period also saw the construction of MUTs in countries like Norway, Spain, China, and the USA as shown in Figure 2-1(d).

The 21st century has seen a relative increase in the construction of MUTs in Asia. 80% of the world's MUTs are currently being constructed in China as shown in Figure 2-1(e). Countries like Israel, Malaysia, India, Qatar, Singapore, and Canada have also implemented MUTs, while countries like the Czech Republic, England, USA, have continued to construct MUTs with the latter two having MUTs constructed mainly on university campuses, hospitals, private establishments, and military installations.

2.2.3 MUT projects in North America

The feasibility study carried out by the (American Public Works Association (APWA), 1971) on the implementation of utility tunnels concluded that the choice for the construction of MUTs will be determined on case-by-case bases. Considering the utilities to be hosted, the cost of construction, installation, operation, and maintenance as well as quantifiable and unquantifiable benefits. The report also pointed out that economic feasibility is expected to be found only in high-density urban areas. Also, the report concluded that MUTs will be better suited for the distribution of utility services as opposed to the transmission of services. As a way of quantifying the economic justification of MUTs, three different types of demonstration projects were recommended; (a) An

urban renewal project with municipally-owned utilities to reduce the problems of regulation; (b) New town/community projects, where the planning and construction of the utility network are fused into the overall plan of the new community; and (c) An urban street that will undergo complete reconstruction and relocation of its existing utilities into the tunnel. However, these projects have never been realized because of the lack of interest from the stakeholders.

On the other hand, a large number of university campuses, hospitals, military installations, and airports in North America appreciate the advantages of adopting MUTs in the long term (Laistner and Laistner, 2012). One reason for this adoption is that these bodies own and operate their utility infrastructure (Hunt *et al.*, 2012). Furthermore, barriers such as utility coordination, security, funding, and operation of the utilities hosted in the MUTs are easily overcome in this case. However, in the public sector, very little work has been done in recent years related to MUTs in North America. Most states in the US are interested in MUTs according to a survey (Kuhn *et al.*, 2002). However, security and operational issues are the main concerns for undertaking MUT projects.

Figure 2-2 is a map of some of the universities with MUTs on their campuses. Information regarding the utilities hosted, date of construction, etc. is difficult to acquire because most universities are not willing to share this data. Most of the data used in the generation of Figure 2-2 was retrieved from the websites of the universities.

The University of Rochester constructed tunnels that connect campus buildings for easier all-year-round maintenance in the 1920s and 1930s. These tunnels were designed to be linked to the basements of their respective buildings (Chris, 2015). Central Connecticut University received the Connecticut Engineering Excellence Award in 2005 for the construction of a 2000-foot underground utility tunnel costing about $13.5 M. The MUT was built in 2002 to connect 36 buildings to an energy center, hosting water, sanitary sewage, stormwater, natural gas, telecommunication, and electricity (BVH Integrated Services, 2018a). The University of Massachusetts is currently in the process of constructing a campus wide MUT estimated at $148 M for new facilities and infrastructure construction. The MUT is to host hot and chilled water pipes, domestic water and fire protection pipes, electricity, and telecommunication cables, and sanitary and gas pipes (BVH Integrated Services, 2018b). In Canada, the University of Alberta has a series of underground tunnels on-campus that convey utilities such as telecommunication cables, steam and chilled water, domestic water, natural gas, compressed air, and electricity cables. These

MUTs cover over 14 km in length with a wide section enough to accommodate the movement of small motorcycles (Justin and Ryan, 2012).

(a) 19th Century (3 MUTs).

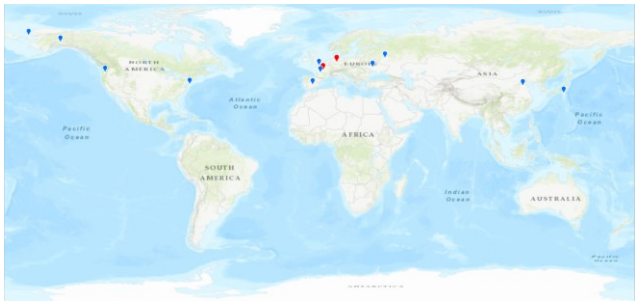

(b) 1921 to 1960 (11 MUTs).

(c) 1961 to 1980 (30 MUTs).

(d) 1981 to 2000 (36 MUTS).

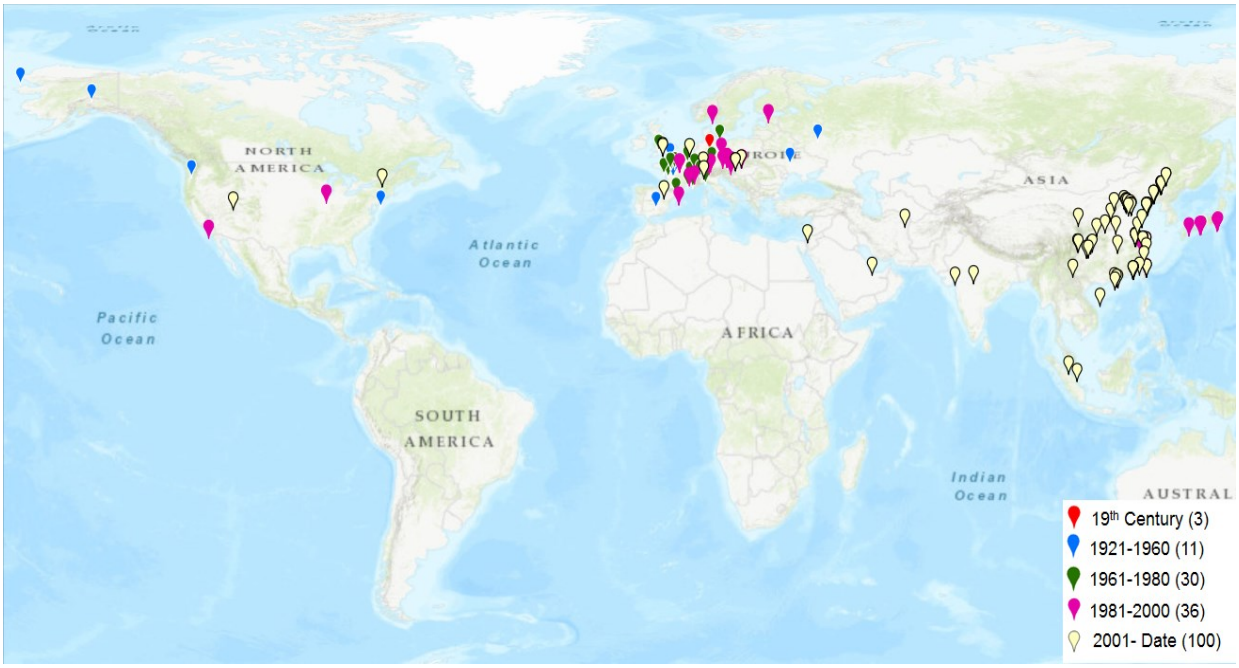

(e) 2001 to 2019 (100 MUTs).

Figure 2-1. Location of MUTs built at different periods.

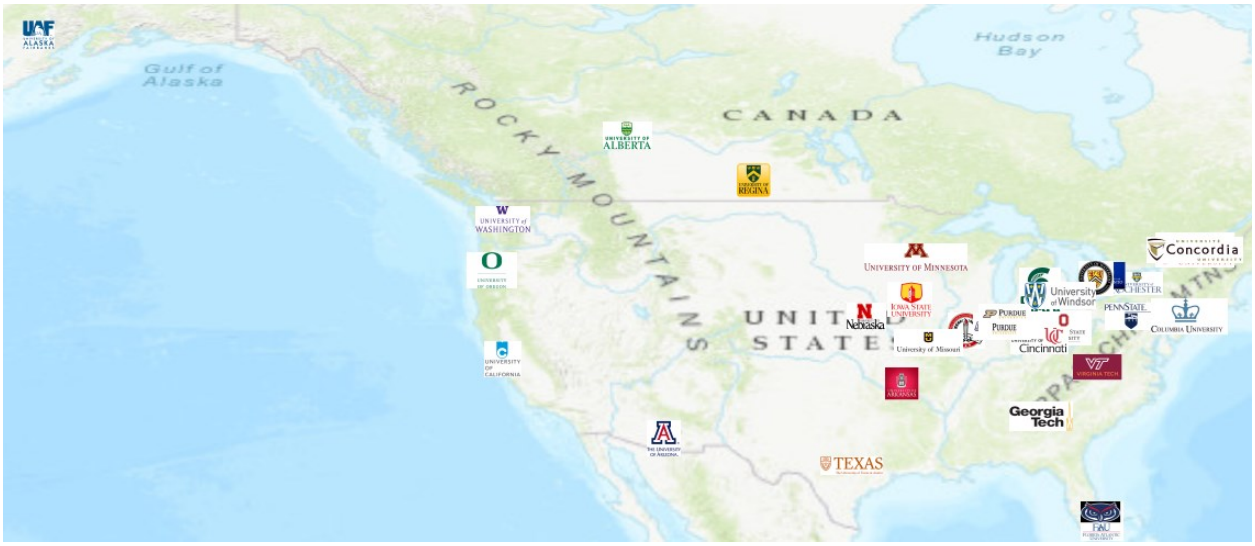

Figure 2-2. Universities with MUTs in North America.

Although the development of MUT projects in North America has been limited to some institutions such as universities, the awareness of their importance as a viable solution for achieving sustainability and resilience for cities has been emphasized by a report published by the US National Research Council (National Research Council., 2013). It was mentioned in this report that "The viability, value, and benefits of utilidors may be effectively communicated with (1) development of workable scenarios for secure multi-utility facilities; (2) development of workable scenarios for effective transitioning from current configurations; (3) lifecycle cost-benefit analyses comparing separate and combined utility corridors, and (4) demonstration projects".

In the context of a research project carried on by the authors in the city of Montreal, Canada, the authors conducted a survey (Luo, 2019a) to understand the specific barriers to implementing MUTs from the point of view of private utility companies. The survey showed that cable utility owners are presently comfortable with the low cost of maintaining their above-ground cable networks and hosting their underground cable networks in ducts. They claim that the benefit of hosting their cables in MUTs is limited because they usually do not need excavation for repair activities. For example, Bell Canada owns its underground cable ducts while Videotron and Hydro Quebec rent ducts belonging to the Electric Services Commission of Montreal at a low cost. Due to the large difference between the cost of hosting these utilities in cable ducts and the initial construction cost of MUTs, these cable utility providers do not see the direct benefit of implementing MUTs. Therefore, incentives, regulations, and cost-sharing agreements between these private entities and the municipalities should be negotiated in a way to achieve a certain compromise among them.

2.2.4 MUT projects in Europe

Several MUTs have been constructed in Europe, with countries like the Czech Republic, France, and Germany having the highest number of MUTs. Different countries in Europe built MUTs as a solution to one or more challenges, for example, France and the UK both built MUTs to stop the spread of cholera. Subsequently, the UK later built MUTs to eliminate traffic congestion caused by excavations for utility repairs. The Czech Republic on the other hand built MUTs to reduce the excavation impact in historical areas.

Figure 2-3 shows some MUTs constructed in Europe, depicting the utilities hosted as well as the shapes of the MUTs. The color of each segment represents the different utilities present in the MUTs. The map shows the different shapes of the MUTs ranging from rectangular and circular to the arch-topped shape (Cano-Hurtado & Canto-Perello, 1999; Canto-Perello & Curiel-Esparza, 2001; Laistner & Laistner, 2012; Makana, Jefferson, Hunt, & Rogers, 2014; Rogers & Hunt, 2006; Yang & Peng, 2016). The location and size of each segment used in representing the MUTs on the map do not represent the precise locations or actual dimensions of the utilities in the MUTs.

Figure 2-4 represents the relative lengths of the MUTs constructed in Europe. Spain and Russia have implemented the longest MUTs of about 100 km built in 1940 and 1943, respectively.

2.2.4.1 Examples of MUT projects in Europe

MUT projects in two European cities (Prague and Barcelona) are selected as examples. The reason for selecting Prague is that it has one of the most extensive MUT networks in Europe. On the other hand, the MUT network in Barcelona is interesting because it was built in a short period as part of the preparation for the summer Olympic Games in 1992.

(a) MUT projects in Prague, Czech Republic

The first MUTs, also known as collectors, were built in the 1970s in Prague's satellite housing estates, with the oldest MUT commissioned in the residential district North Town- Ďáblice in 1971. Several other MUTs were built in the 1970s and 1980s in several cities. The overall length of MUTs in Prague is about 90 km. These MUT networks were built and financed by the City of Prague. MUTs are classified based on their mode of construction and according to their location and capacity. Figure 2-5 shows the MUT classification in Prague. Driven MUTs in Prague's city center could not be excavated from the surface because of the built-up areas, which posed a challenge in

terms of construction technology. As a solution, the tunnels were driven at depths of 5 to 45 m using micro tunneling techniques. This was in contrast to MUTs built on the outskirts of Prague and in newly built areas using the open-cut method. The 1st category MUTs (feeding traversal MUTs) are intended to serve either a state-wide or city-wide area, although they are yet to be constructed in Prague. The 2nd and 3rd category MUTs also have been constructed as supply MUTs and distribution MUTs respectively (Chmelar & Sila, 2006; Kolektory Praha, n.d; Pokorný, 2017). The MUTs were built to house utilities such as water mains of all pressure ranges, hot water, and steam pipes, natural gas pipes, electricity supply, telecommunication cables, sewage, and rain-water networks. Figure 2-6 shows a typical cross-section of Category 2 MUTs. High-quality dispatch control and monitoring centers are achieved in Prague's MUT networks using state-of-the-art computers with several visualization systems unparalleled in the world (ITUSA, n.d.; Sochurek, 2006).

Figure 2-3. Cross-section, shape, and utilities hosted in MUTs in Europe.

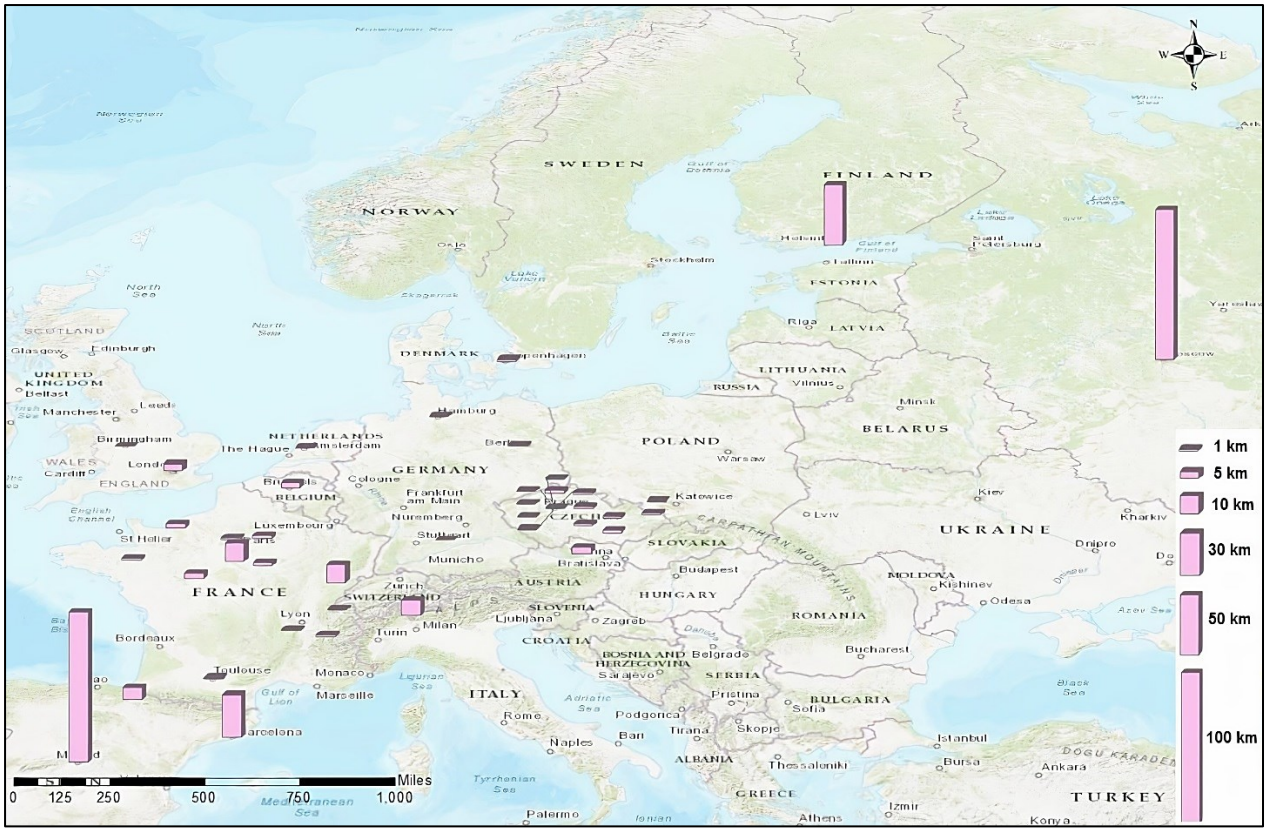

Figure 2-4. Lengths of MUTs in Europe.

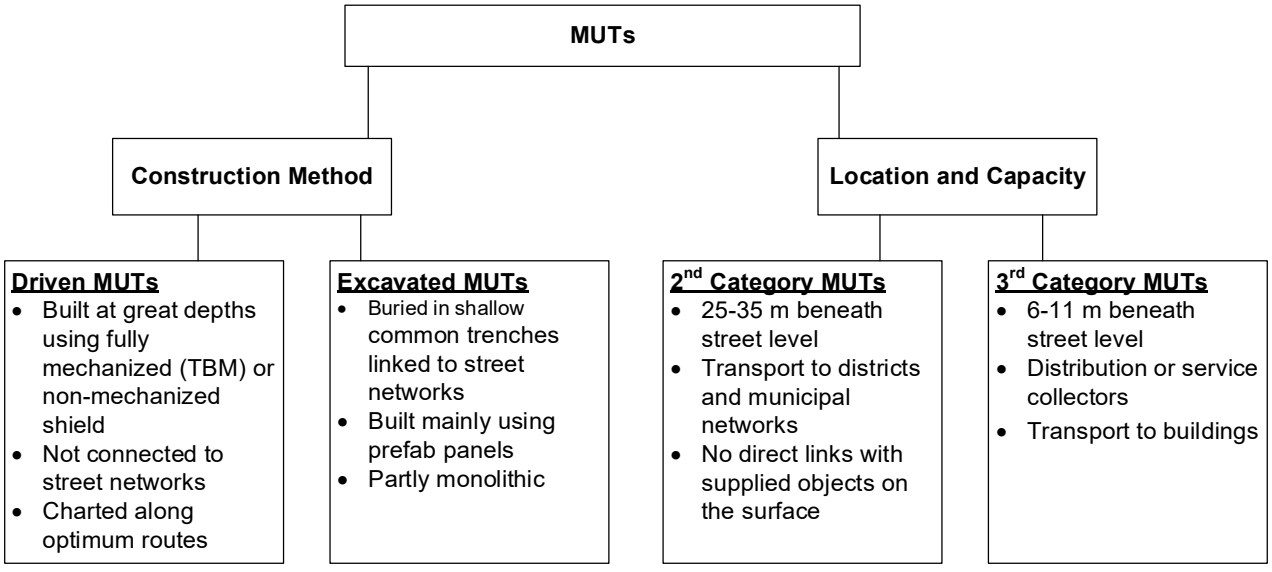

Figure 2-5. MUT classification in Prague (adapted from (Kolektory Praha, 2014).

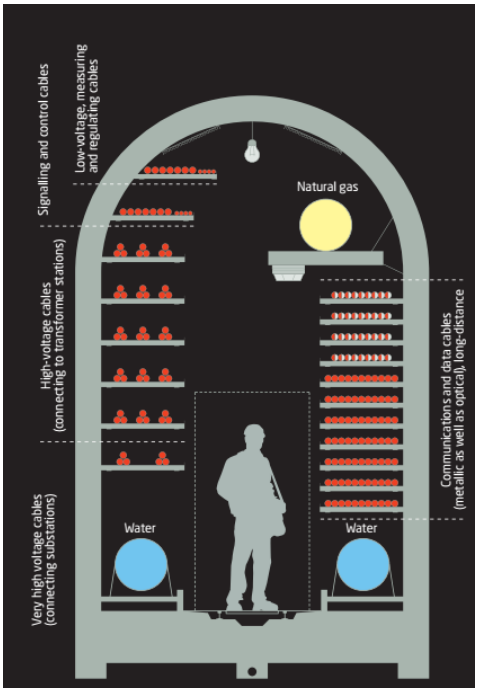

Figure 2-6. Typical cross-section of Category 2 MUTs (Praha Kolektory, 2018).

(b) MUT Projects in Barcelona, Spain

In preparation for the 1992 Olympic Games in Barcelona, The Rondes MUT was constructed under a 36 km ring road that encircles a densely built-up area. The MUT houses all electrical and communication cables originally buried under the road. Other utilities such as public lighting cables owned by the local authorities were later hosted in the MUT. Figure 2-7 is a map of the main MUTs constructed in Barcelona. This network of tunnels includes Barcelona's Rondes and Glòries Square Tunnels (36 km), Besòs Tunnels: Santa Coloma de Gramenet (1.7 km), Sant Adrià de Besòs (2.4 km), and Tarragona St. Tunnel (0.6 km) (Gimeno, 2019). The Rondes transport tunnel has both rectangular (2 x 2.5 m) and circular (2.4 m in diameter) sections running under different main roads. Each MUT is built with reinforced concrete prefabricated pieces, 20 cm thick. Four brackets per module are used for the installation of corbels and the transportation of utilities. The utilities hosted range from electrical and telecom cables to city council services.

The control and monitoring of Barcelona's MUT network are achieved through automated devices connected by an optical fiber network. Smoke and gas sensors trigger acoustic alarms while temperature detectors control the ventilation system. These along with several control systems ensure the optimal operation of the MUT (Gimeno, 2019).

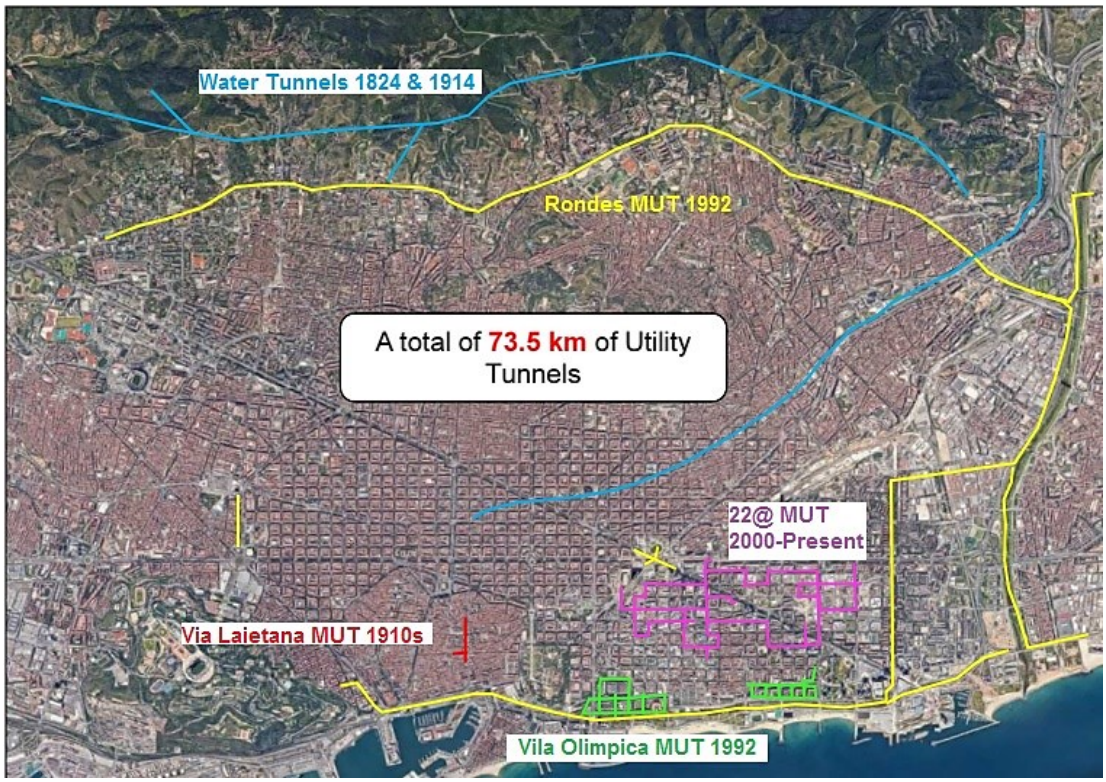

Figure 2-7. Existing MUTs in Barcelona (Gimeno, 2019).

2.3 MUT Planning

2.3.1 MUT location selection

MUT planning is a vital component in underground space planning. Although several MUTs have been constructed over the past century, and more recently in some cities in China (Wang *et al.*, 2018) and the Middle East (Elsawah *et al.*, 2016), details of the planning processes used in determining the optimal location for MUTs are vague. This is partly because local priorities and conditions are the main drivers of MUTs.

A review conducted by Wang *et al.* (2018) on the applications of MUTs in China shows that significant progress is being made in the construction of MUTs. In China, the MUT location and routing are dependent on the status of utilities, the development of new urban settlements, and government policies. The factors influencing these decisions are geology, existing utility pipelines, existing city metro systems, and reserved underground space plans for development. Some MUTs are placed under street segments to fit with the city's design. Examples are the ring-type utility route designs in Zhuhai, Xiaoguwei, and Baiyin. These MUTs were built based on the radial nature

of the road network in these cities. In this research (Wang *et al.* (2018)) no mention was made of the use of any computing or spatial analysis in location selection.

2.3.1.1 MCDM-based MUT location selection

The work of Bobylev (2011) is an example of using the Analytical network process (ANP) in the decision-making process of selecting underground construction technologies for utility placement. The selection process was based on the environmental impact of each of the alternative technologies (open-cut excavation, MUT, and micro tunnelling). The ANP network was made up of four clusters: Benefits, Opportunities, Cost, and Risks (BOCR). These clusters were used in grouping 23 criteria. The result of the sensitivity analysis showed that the MUT had a relatively robust performance compared to the other alternatives when all the BOCR coefficients are equal.

An AHP-Delphi model was proposed (Curiel-Esparza and Canto-Perello, 2013) to aid decision-makers in planning urban underground spaces. This was carried out to select utility placement techniques through a hierarchical model made up of seven criteria and five alternatives: traditional trenching, common conduit, and MUTs (flat MUT, shallow MUT, and deep MUT). Based on seven criteria, the result of the model showed that deep MUT had the highest global priority, and therefore it was chosen as the best alternative.

In terms of MUT construction plans, Liu *et al.* (2018) used five criteria: geological condition, environmental benefits, initial construction cost, number of different pipes, and maintenance cost. They account for the technical, economic, and environmental factors used in evaluating MUT construction plans for multiple energy systems. Each criterion's combined weight is determined using experts' opinions based on the minimum deviation method. The radar chart method was used to determine the evaluation result by using the polygon area of the chart to represent the effectiveness of the construction plan.

Regarding MUT placement location selection, Luo et al. (2020) proposed an AHP-based MCDM model using eight criteria to determine the priority of ten alternative MUT placement locations. The ranking of the ten alternative street segments was achieved using the weighted linear combination (WLC), which combined the criteria evaluation scores derived from the spatial attributes of the ten alternatives, and criteria weights computed using AHP.

2.3.1.2 Criteria for MUT location selection

Table 2-1 contains several publications regarding the criteria and methods used in selecting the locations for the placement of MUTs. In addition, the table also shows the criteria and methods used in the current research. Over the years, the papers related to the spatial decision-making process related to MUT location selection are relatively fewer compared to other areas of MUT planning and implementation.

MUT location selection is complicated due to several factors that should be included in the planning phase, such as population density, existing utilities, metro lines, roads, utility reconstruction, excavation planning, etc. According to (Jiang and Wang, 2016), old city MUTs should consider the scale of existing cables and pipes, including priority and quantity.

According to (DHURD.Liaoning, 2016) and (MHURD, 2015a), route planning factors are as follows: (1) main users (power plants, water plants), (2) main road intersections, intersections of roads and railways or rivers, (3) road attributes (road level, road width, roads which affect city landscape), (4) existing utility pipelines and cables, (5) metro lines, (6) road, metro and utility reconstruction and excavation planning, (7) land-use and intensity (commercial, residence, industrial, vegetation, etc.), (8) underground space utilization (underground complex, underground roads), (9) central area & important plaza, (10) population, (11) geological and hydrological conditions (slopes, precipitation, etc.). These factors are vital since they are related to the city's conditions, especially for old cities.

According to (Zhang, 2016a) and (Gao, 2010), the planning of Xiamen MUT projects in China is based on the following factors: (1) the selection of locations in high-density areas; (2) the planning of relocation of high voltage cables, which need excavation; and (3) the selection of locations with future metros or other underground planning.

In 2013, the State Council of the People's Republic of China decided to start MUT construction nationwide, and it identified 25 pilot cities in 2015 and 2016. The pilot city qualifications consist of: (1) high construction density areas with a population of more than 200,000, (2) heavy transportation, (3) high demand for underground space development and utilization, such as for subways or cables, (4) MUT length more than 10 km, (5) availability of utility types more than three, (6) suitable geological and hydrological conditions, (7) financial conditions and whether public-private partnership (PPP) investment model is reasonable, and (8) new areas at first and then important old areas (MHURD, 2015b, 2015c).

The framework described in (Makana *et al.*, 2016) is based on sustainability science and resilience theory for evaluating the potential implementation of MUTs for both present and future socio-ecological scenarios incorporated as performance indicators. This was achieved by quantifying the spatial and temporal impacts of MUTs, including the impacts on sub-surface environments.

The overall MUT location selection is based on three aspects (Peng *et al.*, 2018): (1) High-density areas such as commercial areas, and high-density underground areas. This aspect can be represented by population density, land use, locations near public facilities and high-rise buildings, etc.; (2) Areas with high traffic volume and high utility density; and (3) Areas with construction or repairs of roads, utilities, metro, underground roads/passages, underground commercial areas, etc. This aspect can be represented by the number of expected excavations of repair works, underground development projects, etc.

MUT location selection can significantly affect the lifecycle cost, method of construction, type of utilities hosted in the MUT, environmental impacts, social costs accrued during construction, etc. From Table 2-1 it can be noticed that the current research has a more comprehensive list of criteria that represent different aspects that affect MUT location selection. In addition, the only other study that has applied spatial MCDM methods for MUT planning is (Makana *et al.*, 2016). However, the focus of this study was the sustainable use of urban underground space rather than the location selection of MUT.

Table 2-1. Related works on MUT implementation.

Reference	Considered criteria													Method(s)	Scope
	AADT	Road class	Population density	Land-use	Number of expected excavations	Utility density	Underground development projects	Proximity to public facilities	Proximity to high-rise buildings	Soil type	Slope of road segment	Proximity to Floodplain	Others		
(Gao, 2010)			✓		✓		✓							Qualitative	MUT design
(Bobylev, 2011)	✓			✓						✓			Functionality, integration, flexibility, vulnerability, etc.	ANP	The selection of underground construction techniques
(Curiel-Esparza and Canto-Perello, 2013)													Urban environment, governance, security, etc.	AHP, Delphi	The selection of underground utility placement techniques
(MHURD, 2015b, 2015d)	✓	✓	✓			✓	✓							Qualitative	Selection of pilot cities
(Jiang and Wang, 2016)						✓								Qualitative	General
(DHURD.Liaoning, 2016)	✓	✓	✓	✓	✓		✓						Metro lines, main road intersections, etc.	Qualitative	Route planning
(Zhang, 2016b)			✓		✓		✓							Qualitative	General
(Makana *et al.*, 2016)			✓	✓		✓				✓	✓		Groundwater depth, real estate value, etc.	ANP, GIS	Sustainable use of urban underground space
(Peng *et al.*, 2018)	✓		✓	✓		✓	✓	✓	✓					Qualitative	
(Luo *et al.*, 2019)	✓	✓	✓	✓	✓	✓	✓	✓						AHP, GIS, WLC	MUT location selection
Chapter 6	✓	✓	✓	✓	✓	✓	✓	✓	✓	✓	✓	✓		AHP, ANP, Entropy, TOPSIS	MUT location selection

2.3.2 MUT economic analyses

Quantitative studies compared the LCC of burying utilities and the MUT. For example, Alaghbandrad and Hammad (2020) used the breakeven point to determine the payback period which, is in turn used to determine how economical the MUT is compared to the synchronized intervention. Wu et al. (2020) used an agent-based simulation to evaluate the socioeconomic benefits of implementing the MUT rather than the buried utilities. Hunt et al. (2014) used the cost-benefit analysis to show how the utility density, the number of avoided interventions, the type of MUT, the location, and the number of excavations is related to the economic benefits of MUTs. In addition, urban locations with the optimal combination of these factors make MUTs more economically sustainable than suburban or undeveloped locations in general. However, even in urban locations, certain street segments might offer more benefits (e.g., cost savings, reduced intervention-related traffic density, etc.) than others.

All these studies show that, even though the MUT has a higher initial cost of construction and implementation, the LCC of the buried utility is greater than the LCC of the MUT when the social cost is considered. Furthermore, the results of the research conducted by (Li *et al.*, 2019) corroborate that MUTs are more sustainable. Heyermann et al. (2022) conducted a lifecycle cost-benefit analysis (LCCBA) to determine the long-term value of MUTs compared to the open-cut method of utility intervention for an isolated street segment. Using a 100-year planning period, the researchers concluded that the benefit-cost ratio is 1.29 with a payback period of 47 years. In addition, Genger *et al.* (2021) used multicriteria decision-making (MCDM) to assign subjective and objective weights to a combination of criteria (e.g., traffic density, utility density, population density, etc.) that influence the location selection of MUTs. However, this study involved a limited number of preselected urban locations. Table 2-2 summarizes most of the related research on the economic analysis of the MUT and the traditional method of buried utilities.

From the table, all the previous studies were achieved using single isolated projects. Furthermore, in terms of quantifying the social LCC benefit, only Wu et al. (2020) considered one social cost indicator (vehicle delay) at the project level. In essence, the selection of potential locations should consider the agency and social LCC at network and segment levels for the MUT compared with the synchronized intervention, which is currently considered the best practice (FCM and NRC, 2003).

Table 2-2. Research related to economic analysis.

Reference	Compared Alternatives		Social Cost Components			Method	Application scope	Objectives
	MUT	Synchronized Intervention/ Buried Utilities	Vehicle Delay	Vehicle Maintenance and Operation	Air Pollution			
Huck et al. (1976)	✓					Economic analysis	Project level	MUT implementation
Hunt et al. (2014)	✓	✓				Cost-benefit analysis	Project level	Breakeven point
Li et al. (2019)	✓					Cost-benefit analysis	Project level	Economic viability
Alaghbandrad and Hammad (2020)	✓	✓				Lifecycle cost analysis	Project level	Breakeven point
Wu et al. (2020)	✓	✓	✓			Agent-based simulation	Project level	LCC
Heyermann et al. (2022)	✓	✓				LCCBA	Project level	MUT benefits
Genger *et al.* (2021)	✓					MCDM	Segment level	Location selection
Chapter 7	✓	✓	✓	✓	✓	Multi-objective optimization	Segment and network level	Location selection

2.4 Synchronized Utility Intervention

The general level of deterioration of underground utility assets, budget constraints, intervention methods, and the socioeconomic impacts of the intervention methods that require excavations have given rise to the need for synchronized intervention for spatially collocated assets. However, synchronized interventions are not practiced in several countries, they are encouraged (FCM and NRC, 2003). In addition, several municipalities in Canada currently conduct integrated interventions, also known as corridor rehabilitation or upgrades.

Table 2-3 is a summary of some municipalities currently practicing synchronized interventions and the different methods used to ensure the synchronization of their interventions. Based on the table, methods of achieving synchronization are driven by factors that are specific to the city or area in question. These factors include community or political policies and council infrastructure approach which varies across different areas. These practices are also limited by the presence of privately owned and managed utility assets that share the right-of-way. Most of these assets are subject to short-term planning periods and are not under the control of the municipalities. In addition, these methods of synchronization are most effective in the context of regular or timed preventive maintenance and are least effective when corrective interventions are required.

Table 2-3. Municipalities currently practicing synchronized interventions.

City/Province/ Country	Method of achieving synchronization	Assets	Reference
Sudbury, Ontario. Canada	Formal internal and external committees	Pavement, water and sewer pipes, private utility companies	(Braun, 2012; Chacon and Normand, 2016; FCM and NRC, 2003; Hafskjold, 2010; Hafskjold and Bertelsen, 2008)
Winnipeg, Manitoba. Canada			
Kelowna, British Columbia. Canada	Development of multi-year plans	Pavement, water, and sewer pipes	
Surrey, British Columbia. Canada	Coordination of development-related works		
Yellowknife, Northwest Territories. Canada			
Hamilton, Ontario. Canada			
Montreal, Quebec. Canada	Restrictive practices e.g., permit requirements, no-cut rules, etc.		(Chacon and Normand, 2016)
Middletown, Ohio. USA	Condition-based corridor renewal		(Braun, 2012)
Bergen, Norway	Penalty systems or permit requirements, long-term planning, portal for planned infrastructure activities, etc.		(Hafskjold, 2010)
Trelleborg, Sweden	Corridor rehabilitation		(Hafskjold and Bertelsen, 2008)
Trondheim, Norway	Corridor rehabilitation	Pavement, water and sewer pipes, electrical cables	(Hafskjold, 2010)

2.4.1 Optimization for synchronized utility intervention

Effectively executing synchronized interventions of spatially collocated assets requires addressing the inevitable tradeoffs in these interventions (Carey and Lueke, 2013). Tradeoffs exist in the form of conflicting stakeholder objectives that include budgets, acceptable performance and risk levels, minimal social cost thresholds, etc. (Soliman, 2018). Tradeoffs could also appear in the form of stakeholder objectives at the network level or project level. Network-level objectives are centered around prioritizing and scheduling the interventions, while project-level objectives focus on selecting the type/strategy of interventions (Uddin *et al.*, 2013). Saad *et al.* (2018) discussed the

tradeoffs for spatially collocated assets as follows: (1) different rates of deterioration, (2) different service lives, (3) limited budget, (4) different intervention methods and strategies, and (5) varying performance levels.

Several methods have been proposed to find a solution that balances the tradeoffs in synchronized buried utility interventions. They include the use of mathematical optimization techniques (e.g., Genetic Algorithms (GA) and Particle Swarm Optimization (PSO)) to find near-optimal/optimal solutions to either single or multi-objective problems (Elshaboury and Marzouk, 2022). Ideally, these methods simultaneously consider the tradeoffs at the network or project levels.

Some of the objectives include minimizing LCC or the risks associated with failures in the network/project level while operating above a performance threshold (Elsawah *et al.*, 2014), maximizing performance, and respecting the budget constraint (Soliman, 2018). Other frameworks have focused on bringing forward or deferring the interventions (Osman, 2016; RCCAO, 2020; Shahata, 2013), minimizing repair time and resources, and maximizing Return on Investment (ROI), safety, and resilience (Dong and Frangopol, 2016; Frangopol and Liu, 2007). Saad et al. (2018) proposed a concurrent bilevel optimization model that combines both the network and project levels into a single mathematical model. The results showed that the model could deal with conflicting stakeholder objectives while reaching a near-optimum solution regarding infrastructure fund allocation. Zangenehmadar et al. (2020) formulated a budget-based optimization model for planning intervention activities on water distribution networks over a 20-year planning period. The model aims to maximize the budget allocation by reducing the variance between maintenance costs and the budget.

Similar to network and project-level tradeoffs, segment-level tradeoffs focus on the combination of prioritizing/scheduling segments, as well as determining the type/strategy of intervention unique to a segment. Researchers (e.g., Carey and Lueke, 2013) applied a GA to optimize the annual segment score, which is the summation of the scores assigned to each segment's condition and criticality indices. The higher the scores, the higher the intervention priority assigned to the segment. Marzouk and Osama (2017) optimized the intervention strategies (repair, rehabilitation, replacement, or do nothing) at the segment level by calculating the risk index derived from the probability of failure and the consequence of failure. The objective functions include minimizing the risk and LCC while maximizing the level of service and performance. In addition to optimizing the LCC, Abu-Samra et al. (2018) optimized the social costs, physical state, and replacement value

for the synchronized interventions of water and road networks. Their research aimed to balance the tradeoff in scheduling segment interventions by either bringing forward or delaying intervention activities by using a combination of dynamic programming and goal optimization. Similarly, Abu-Samra et al. (2020) developed a trilevel framework to optimize segment intervention scheduling by minimizing repair time and LCC while maximizing segment health.

2.5 Multi-Criteria Decision-Making Techniques

The MCDM process consists of several methods that can handle the trade-offs between different alternatives based on multiple criteria. The goal is to identify one or more alternatives that meet the decision-maker's preference subject to criteria that are often conflicting with each other (French and Roy, 1997; Yoon and Hwang, 1981). When considering the spatial nature of the criteria that make up the MUT location selection problem, MCDM alone is insufficient (Grimaldi *et al.*, 2017). Therefore, combining MCDM techniques with GIS offers better visualization of the problem and alternatives as structured spatially referenced data through the creation of thematic maps that improve spatial decision-making (Malczewski, 2007).

The combination of GIS and MCDM is well established, and its application includes areas related to utility infrastructure management, underground space planning, the ranking of construction techniques, urban spatial planning, suitability analysis, and location and site selection. (Peng and Peng, 2018) presented a method for evaluating urban underground space (UUS) resource planning using GIS and AHP along with other mathematical tools. The result was ranking the UUS resources based on the criteria that represent urban planning, construction suitability, and environmental conditions. In the area of water infrastructure planning, (Grimaldi *et al.*, 2017) analyzed the relationship between regulations and planning using a combination of GIS and ANP. Some authors have used a combination of MCDM methods to prioritize criteria or rank the alternatives. (Yildirim *et al.*, 2017) proposed a spatial MCDM method for routing a gas transmission pipeline using the weights obtained from applying AHP and the ranking of alternative routes using simple additive weighting (SAW) TOPSIS. Abdel-Basset *et al.*, (2021) presented a hybrid MCDM method, a combination of AHP and PROMETHEE II for the location selection of offshore wind energy stations. They argued that the need for the combinations of MCDM techniques was due to the incomplete utilization of information and loss of data in the decision-making process.

2.5.1 Analytic hierarchy process

The AHP method uses a weighted aggregation. The weights of the criteria and alternatives are obtained using pairwise comparison based on the decision maker's preferences. The AHP method was introduced by (Saaty, 1982). The steps include: (1) Creating a hierarchical model which consists of the goal, criteria, sub-criteria, and alternatives, (2) A pairwise comparison of main criteria and sub-criteria, (3) Deriving the scale of weights and checking the consistency index (C.I.) using Equation 2-1, (4) Ranking the options (Saaty, 1987, 2002).

$$C.I. = \frac{\lambda_{max} - n}{n - 1} \qquad (2\text{-}1)$$

where λ_{max} is the largest eigenvalue of the pairwise comparison matrix, and *n* is the size of the comparison matrix.

2.5.2 Analytic network process

ANP is a generalized form of AHP used in MCDM. Unlike AHP which structures the decision problem into a hierarchy consisting of goals, criteria, and alternatives, ANP uses a network structure (Saaty, 2004). Nevertheless, both MCDM techniques use a pairwise comparison process that signifies a judgment using a fundamental scale. In the ANP, the strength of dominance is derived by answering two questions: (a) Given a criterion, which of the two elements is more dominant with respect to that criterion; (b) Which of the two elements influences the third element more with respect to a criterion?

A unique feature of ANP is the ability to accommodate the dependencies (inner dependencies and outer dependencies) that may exist within and between clusters in the network. The steps involved in ANP are as follows: (1) creating a network model showing all the clusters, the criteria contained in each cluster, the relationships (dependencies/feedback), and the alternatives; (2) pairwise comparison to identify the strength of dominance between elements of the network; (3) formation of supermatrices (unweighted, weighted, and limit matrix) and estimating the consistency ratio (CR); and (4) Prioritizing the component of the ANP network based on the output of the limit matrix W, calculated using Equation 2-2 (Saaty, 2004).

$$\lim_{k\to\infty} \frac{1}{N} \sum_{k=1}^{N} W^k \qquad (2\text{-}2)$$

where *k= 1, 2, ...* the raising power of *W*.

2.5.3 Technique of order preference similarity to the ideal solution (TOPSIS)

In TOPSIS, it is assumed that there is an ideal (positive-ideal) solution and a non-ideal (negative-ideal) solution for every problem. Therefore, the ranking aims at finding the solution(s) that have the shortest distance to the positive-ideal solution (PIS) and the farthest distance from the negative ideal solution (NIS). Thus, the PIS, also known as the Zenith, maximizes the benefit criteria and minimizes the cost criteria. In contrast, the NIS, also known as the Nadir, maximizes the cost criteria and minimizes the benefit criteria (Behzadian *et al.*, 2012; Papathanasiou and Ploskas, 2018).

The standard TOPSIS consists of seven steps which are: (1) Constructing a decision matrix, (2) normalizing the decision matrix, (3) calculating the weighted decision matrix, (4) selecting the PIS and NIS (5) calculating the distance between each alternative and PIS and NIS, (6) determining the relative closeness to the ideal solution, and (7) ranking the alternatives (Yoon and Hwang, 1981).

2.5.4 Entropy weights

Also known as Shannon's Entropy, the method of entropy weights was initially developed from statistical thermodynamics and transferred to information systems by Shannon (1948). The concept of Shannon's Entropy is used to find the measure of uncertainty associated with the source of an information. This measure of uncertainty is calculated using the probability theory (Shannon, 1948). By using the discrimination that exists between the criteria performance values, the relative importance of each criterion in the MCDM problem is determined. The greater the entropy value of a criterion, the smaller the weight, and therefore the lesser the relative importance of the criterion in the decision-making process (Jat *et al.*, 2008).

The combination of Entropy weights and other ranking methods has been applied in various areas of research. (Dehdasht *et al.*, 2020) proposed an Entropy-weighted TOPSIS combination for the selection of key drivers in sustainable lean construction. (Shad *et al.*, 2017) used Entropy-derived weights to increase the reliability of the weights derived from AHP in developing a green building assessment tool. (Lee and Chang, 2018) compared the ranking of renewable energy sources by

applying four different MCDM ranking methods with Entropy weights. Some authors have used Entropy weights to eliminate the use of subjective weights (Chen, 2020). Others used them to handle imprecise judgments by decision-makers (Wang and Lee, 2009).

The steps required to obtain the Entropy weights for a set of alternative criteria values are presented as follows (Wang *et al.*, 2017). For a set of *m* alternatives A_i $(i = 1,2 \dots, m)$ and *n* corresponding criteria values $C_j (j = 1,2 \dots, n)$, the performance matrix $[a_{ij}]_{m \times n}$ is:

$$A = \begin{bmatrix} a_{11} & a_{12} & \dots & a_{1n} \\ a_{21} & a_{22} & \cdots & a_{2n} \\ \vdots & \vdots & \ddots & \vdots \\ a_{m1} & a_{m2} & \cdots & a_{mn} \end{bmatrix}$$

Step 1: Perform linear normalization on the performance matrix: r_{ij} is the normalized value that implies the probability of occurrence.

$$r_{ij} = \frac{a_{ij}}{\sum_{i=1}^{m} a_{ij}}, i = 1, 2, \dots, m; j = 1, 2, \dots, n \qquad (2\text{-}3)$$

Step 2: Calculate the entropy.

$$e_j = -\frac{1}{ln\, m} \sum_{i=1}^{m} r_{ij}\, ln\, r_{ij}\ , i = 1, 2, \dots, m; j = 1, 2, \dots, n \qquad (2\text{-}4)$$

where e_j is the normalized entropy value*;* $ln\, r_{ij}$*=0 if* $r_{ij} = 0$

Step 3: Calculate the relative importance weights of each criterion.

$$w_j = \frac{1 - e_j}{\sum_{1}^{n} 1 - e_j}, j = 1, 2, \dots, n \qquad (2\text{-}5)$$

where $1 - e_j$ is the degree of information divergence of criterion *j*.

2.6 Underground Asset Condition Prediction and Classification

The above sections focused on the application of MCDM and optimization techniques in the MUT location selection problem. As part of the location selection problem, identifying street segments for implementing either the MUT or synchronized intervention can also be achieved using condition-based asset intervention. Machine learning (ML) algorithms have been applied to the decision-making process for several asset management practices, including predicting or classifying the conditions of utility assets for maintenance, repair, and replacement strategies, failure rate prediction, identification of contributing factors, intervention prioritization, etc. The

following sections focus on the literature related to applying different ML algorithms in predicting/classifying various aspects of underground utility assets and pavement networks.

2.6.1 Pipe condition prediction and classification

ML-based intervention priority has been achieved at a network level by combining ML models with expert opinion (Kerwin *et al.*, 2020), survival analysis (Rahbaralam *et al.*, 2020), etc. While at an asset level, other methods have been used to determine failure impact (Weeraddana *et al.*, 2019), the time of failure of each asset (Jafar *et al.*, 2010), etc. Failure prediction and condition classification are two common areas used to ascertain the need for an intervention. Regarding failure prediction, (Weeraddana *et al.*, 2019) predicted the probability of water mains failure using a supervised ML algorithm known as random forest regression (RFR). (Jafar *et al.*, 2010) used six artificial neural networks (ANN) models to predict the failure of urban water mains. Concerning condition classification, several researchers have classified asset conditions as binary classifications (i.e., good or bad) (Harvey and McBean, 2014; Kumar et al., 2018; Laakso et al., 2018; Mohammadi et al., 2019; Rahbaralam et al., 2020; Robles-Velasco et al., 2020; Tavakoli et al., 2020; Winkler et al., 2018). The misclassification errors resulting from the use of binary classification models may increase the economic loss of the remaining service life of assets prematurely replaced. When binary models are deployed, the misclassification errors will lead to the scheduled replacement of pipes in relatively good condition (i.e., good pipes misclassified as bad). In other words, some pipes scheduled for replacement (true positives) might still be in an "acceptable" condition and their premature replacement will mean a loss of remaining service life. These losses can be significant when considering large networks and budgetary constraints.

However, some researchers (i.e., (Caradot *et al.*, 2018) and (Hernández *et al.*, 2021)) classified the conditions of sewers into three classes signifying good, medium, and bad pipes using random forest and support vector machine (SVM)-based models. They did so at the asset and network levels for management and inspection objectives.

Several combinations of features have been used to achieve either pipe failure prediction or condition classification. The accuracy of the ML model is mainly dependent on the available features. Moreover, processes related to selecting ML algorithms, data preprocessing, hyperparameter tuning, and data quality also contribute to the model's accuracy (Kuhn and Johnson, 2013). As shown in Table 2-4, utility network features (e.g., pipe material, length,

diameter, installation date, pipe location (e.g., right-of-way, jurisdiction, etc.), sewer pipe type (e.g., sanitary, combined), etc.) and external data (e.g., soil, pressure, depth) are commonly used in failure prediction and condition classification ML problems. Other features not listed in Table 2-4 but used by some authors include the number of connections and valves, rainfall, soil resistivity, pipe thickness, water table, slope, etc. Also, Table 2-4 summarizes some related research conducted in applying ML algorithms to the condition prediction of both water and sewer pipes. It includes details of the ML model used, the features considered, and the output of the ML algorithm.

2.6.2 Pavement condition prediction and classification

Planning an optimal synchronized intervention requires prior information on pipe conditions alongside pavement conditions. The use of regression analysis (linear, nonlinear, and multiple linear), Bayesian models, and probabilistic models in predicting asset conditions are often limited by ambiguous, imprecise, and incomplete input data (Flintsch and Chen, 2004). Despite these limitations, ML algorithms have achieved relatively high accuracy when dealing with large sample sizes and a balanced dataset (Harvey and McBean, 2014). For example, (Bashar and Torres-Machi, 2021) performed a meta-analysis to compare the performance of regression-based models to three ML algorithms (ANN, random forest (RF), and support vector machine (SVM)) in the prediction of the international roughness index (IRI) values. The results showed that the ML algorithms outperformed the traditional models, with the RF having the highest performance ($R^2 = 0.995$) while the regression-based models achieved a performance of $R^2 = 0.791$.

In addition to tabular data, ML algorithms have also been applied to images (i.e., computer vision) to detect pavement surface defects (e.g., potholes, cracks, etc.) (Hoang and Nguyen, 2018). Also, pavement condition rating has been determined using other indicators such as the IRI, Pavement Condition Index (PCI), Road Quality Index (RQI), Present Serviceability Index (PSI), etc. For example, Nabipour et al. (2019) used PCI values to predict the remaining service life for flexible pavement. Guo et al. (2021) used an ensemble learning model to predict IRI and rut depth. Some researchers focused on predicting one of the indicators and subsequently assigning the pavement condition based on the value of that indicator (Abdelaziz *et al.*, 2020; Bashar and Torres-Machi, 2021; Kirbaş and Karaşahin, 2016; Zhou *et al.*, 2021; Ziari *et al.*, 2015).

Different ML algorithms and features have been used in IRI prediction. For example, Marcelino et al. (2021) developed a pavement performance prediction model using the Random Forest (RF)

algorithm to predict IRI for five and ten years using the Long-Term Pavement Performance database. Marcelino et al. (2020) predicted IRI values as an indicator to determine pavement performance using a modified version of the TrADABoost algorithm, The researchers used several features, including Annual Average Daily Traffic (AADT), pavement thickness, annual precipitation, average temperature, etc. Table 2-5 summarizes the research on applying ML algorithms toward pavement condition prediction and classification. It also includes the significant features considered in the ML process, the model used, and the output of the ML algorithms based on the problem stated by the researchers. The majority of the researchers used ANN to predict the IRI and set the pavement condition based on the predicted value. Even though relationships exist between several performance indicators (Arhin et al., 2015a), using one indicator alone may not sufficiently capture the condition of a street segment, considering that different standards exist for acceptable indicator thresholds (Arhin et al., 2015b). Regardless of the output of the ML model, most of the researchers used a combination of pavement features such as age, IRI, distress type, and thickness, along with features that represent the climate, such as precipitation and temperature. However, the values representing climate features are assumed to have a negligible variation when considering the research scale; therefore, they have not been used in this research. Few researchers considered the PCI, road class, and distress severity, and none of the listed researchers used the pavement surface area. Furthermore, some researchers used other features not included in the table, such as the number of potholes, soil condition, evaporation, etc.

2.7 Machine Learning Algorithms

This section contains brief details of the machine learning algorithms used in this research. A voting-based ensemble is used mainly because of the statistical, computational, and representational advantages of using multiple base learners (Dietterich, 2000). In this research, base learners consist of RF, gradient-boosted trees (GBT), and deep learning (DL) algorithms.
Both RF and GBT are tree-based methods that apply greedy splitting rules, and DL uses stochastic gradient descent. These three base learners are mainly selected because RF is known to perform well even with statistical noise data, and GBT performs well even with imbalanced data. DL simultaneously uses all the available features in the dataset, unlike RF and GBT, which improve their accuracy by using random subsets of the features as new trees are added. Also, the output of

both the RF and GBT is relatively easy to interpret, unlike the black-box nature of DL algorithms. Details on each ML algorithm are elaborated on in the subsequent sections.

2.7.1 Random forest algorithm

The RF algorithm works by growing a specified number (ensemble) of unpruned decision trees, subsequently combined into a single forest of trees. Using bootstrap aggregation, the model uses sub-sets of randomly sampled instances from the original dataset to generate a tree. These subsets are then replaced based on the number of trees in the ensemble, and the aggregation of the resulting classifier is obtained using the majority vote of each tree classification. However, because a randomly selected subset of predictors generates each tree, this selection method can lead to poor performance in cases where the ratio of relevant predictors to the total number of predictors is low. Although the application of ML is problem and data-dependent, it should be noted that tuning parameters, such as the number of randomly selected predictors, number of trees in the ensemble, minimum leaf node size, etc., may increase the accuracy of an RF model.

The RF aggregated predictor for a classification problem is shown in Equation 2-6 (Pavlov, 2019).

$$\hat{h}_{RF}(x) = \underset{1 \le c \le C}{arg\,max} \sum_{l=1}^{q} 1_{\hat{h}(x,\Theta_l)=c} \qquad (2\text{-}6)$$

where $\hat{h}_{RF}(x)$ is the RF classifier for input vector x; Θ_l is a vector of random variables that are independent and identically distributed used in determining the class c of trees 1 to q; C is the aggregated vote assigned to x; $\hat{h}(x, \Theta_l)$ is the predictor of tree l.

2.7.2 Gradient boosted trees

The GBT algorithm works by sequentially building trees that attempt to compensate for the weaknesses of the previous trees until no further improvements are made, or a stopping criterion is satisfied (Brownlee, 2019). This nonlinear algorithm improves the model's accuracy by optimally reducing the loss function, referred to as the degree of error, by adding weak learners using additive training (Friedman, 2001).

Similar to the RF algorithm, where samples are randomly drawn, having many trees could overfit the model. Increasing the number of trees in a GBT model may also slowly overfit the model. Still, sequentially building more trees ensures that the new trees learn and improve from previous trees.

However, this increase in trees can be computationally expensive on a large dataset (Brownlee, 2019). A classification problem with a labeled dataset $\{x_i, y_j\}$, where x_i is a subset of input features and, y_j is the target or label *{j = 1,2,3…,M},* from training samples *{i = 1,2,3…,N},* GBT initially fits a DT model (weak learner) $F_o = h_t(x_i, a)$ where a is a set of parameter values such as the splitting variables and the terminal node of the weak learner. As new variables are iteratively added, new trees are created such that the loss function L (Equation 2-7) is minimized by applying the risk minimization principle. Equation 2-8 shows the output of the GBT classifier (Friedman, 2001).

Table 2-4. Summary of research applying machine learning to water and sewer pipes.

Reference	Assets		Common Features Considered														ML Model	Output
	Water	Sewer	Age	Depth	Diameter	Failure date	Failure rate	Failure type	Installation date	Length	Pipe Location	Material	Number of failures	Pressure	Soil	Pipe Type		
Jafar *et al.* (2010)	✓		✓		✓	✓				✓	✓	✓	✓	✓	✓		ANN	Failure prediction
Winkler *et al.* (2018)	✓		✓		✓							✓	✓	✓			BDT*	
Weeraddana *et al.* (2019)	✓		✓		✓				✓	✓			✓			✓	RFR	
Mohammadi *et al.* (2019)		✓	✓	✓	✓					✓		✓			✓		LGR*	
Rahbaralam *et al.* (2020)	✓		✓		✓					✓	✓		✓				EGB*	
Robles-Velasco *et al.* (2020)	✓		✓		✓					✓		✓	✓	✓		✓	SVC*	
Kerwin *et al.* (2020)	✓				✓	✓		✓	✓	✓		✓	✓		✓		ANN	
Harvey and McBean (2014)		✓	✓	✓	✓				✓	✓		✓				✓	RF*	Condition classification
Caradot *et al.* (2018)		✓	✓	✓					✓	✓		✓			✓	✓	RF	
Kumar et al. (2018)	✓		✓		✓				✓				✓	✓	✓		GBDT*	
Laakso *et al.* (2018)		✓	✓	✓	✓				✓	✓		✓				✓	RF, BLR*	
Tavakoli *et al.* (2020)		✓	✓	✓	✓				✓	✓		✓					RF*	
Hernández *et al.* (2021)		✓	✓	✓	✓					✓	✓	✓			✓	✓	SVM	
Chapter 5	✓	✓	✓		✓	✓	✓		✓	✓	✓	✓	✓			✓	RF, GBT, DL, VE	

*Notes: ANN: Artificial Neural Networks, BDT: Boosted Decision Tree, BLR: Binary Logistic Regression, DT: Decision Trees, EGB: eXtreme Gradient Boosting, GBDT: Gradient-Boosted Decision Tree, LGR: Logistic regression, RF: Random Forest, RFR: Random Forest Regression, SVC: Support Vector Classification, SVR: Support Vector Regression, VE: Voting-based Ensemble, * Binary classification*

Table 2-5. Summary of research related to pavement condition prediction and classification.

Reference	Common Features Considered												ML Model	Output
	Age	IRI	PCI	AADT	Road class	Distress type	Severity	Surface area	Pavement thickness	Precipitation	Temperature	Freeze index		
Gong *et al.* (2018)	✓	✓		✓		✓				✓	✓	✓	RF	IRI prediction
(Abdelaziz *et al.*, 2020)	✓	✓				✓							ANN	
Ziari *et al.* (2015)	✓			✓					✓	✓	✓	✓	ANN	
Marcelino *et al. (*2020)		✓		✓					✓	✓	✓		TrAdaBoost	
Marcelino *et al.* (2021)		✓		✓					✓	✓	✓	✓	RF	
Zhou *et al.* (2021)	✓	✓		✓		✓				✓	✓		ANN, RNN	
Kirbaş and Karaşahin (2016)	✓												ANN	PCI prediction
Nabipour *et al.* (2019)		✓	✓			✓	✓						SVR	RSL
Guo *et al.* (2021)		✓				✓			✓	✓	✓	✓	LightGBM	IRI, RD prediction
Piryonesi and El-Diraby (2021a)	✓	✓	✓	✓	✓				✓	✓			GBT, RF, LR	IRI, PCI prediction and classification
Hoang and Nguyen (2018)	✓	✓				✓			✓				SVM, ANN, RF	Pavement crack classification
Chapter 5	✓	✓	✓		✓		✓	✓					RF, GBT, DL, VE	Condition classification

Notes: ANN: Artificial Neural Networks, GBT: Gradient Boosted Trees, IRI: International Roughness Index, LightGBM: Light Gradient Boost Machine, LR: Linear Regression, M&R: Maintenance and Repair, PCI: Pavement Condition Index, RD: Rut Depth, RF: Random Forest, RNN: Recurrent Neural Networks, RSL: Remaining Service Life, SVM: Support Vector Machine, SVR: Support Vector Regression, VE: Voting-based Ensemble

$$F_0(x) = arg\ min_\rho \sum_{i=1}^{N} L(y_j, \rho) \quad (2\text{-}7)$$

$$F_T(x) = F_0(x) + \sum_{t=1}^{T} \rho h_t(x; a_t) \quad (2\text{-}8)$$

2.7.3 Deep learning

Deep learning (DL) uses stochastic gradient descent with back-propagation to train a multi-layer feed-forward ANN (RapidMiner, 2020). The neural network is initialized with the input dataset, and the activation function is calculated for each hidden layer while the corresponding weights are initialized. Weights are recalculated and aggregated for each hidden layer (Equation 2-9) using gradient descent. The output signal is transmitted to the connected neuron until the error is below a threshold or the loss function is minimized (Candel and Parmar, 2015). The output signal $f(\alpha)$ which is a nonlinear activation function of the learning rate α, is transmitted to the connected neuron until the error is below a threshold or the loss function is minimized for each training example *j*. Equation 2-10 is the cross-entropy loss function used for a classification problem. Biases are added in all the non-output network layers, and the weights linking the biases and the neurons determine the output of the network (Candel and Parmar, 2015).

$$\alpha = \sum_{i=1}^{n} w_i x_i + b \quad (2\text{-}9)$$

$$L(W, B \mid j) = \sum_{y \in \mathcal{O}} \left\{ ln\left(o_y^{(j)}\right) t_y^{(j)} + ln\left(1 - o_y^{(j)}\right)\left(1 - t_y^{(j)}\right) \right\} \quad (2\text{-}10)$$

where w_i is the neuron's input values, x_i is the neuron weight, b is the bias which is the threshold for a neuron's activation, $W = \{W_i\}_{1:N-1}$, W_i is the weight matrix connecting layers i to $i+1$, N is the number of layers, $B = \{b_i\}_{1:N-1}$, b_i is the column vector of biases for layer $i+1$, j is a training example, y is the output units, $\mathcal{O}$ is the output layer, $o_y^{(j)}$ is the predicted and $t_y^{(j)}$ is the actual output of the *j*.

2.7.4 Voting-based ensemble ML algorithm

The voting-based ensemble algorithms improve stability and classification accuracy and reduce variance and overfitting (Friedman *et al.*, 2000). Ensemble classifiers are generally a set of base learners (classifiers) whose individual decisions are combined to predict new cases. In most cases, the accuracy of an ensemble classifier is higher than the accuracy of its base learners (Dietterich, 2000). This statement is true when the individual decisions of each base learner are not identical (diverse), and the classification errors are uncorrelated (Kuncheva and Rodríguez, 2012).

The voting-based ensemble classifier trains a subset of the training dataset with at least two classifiers. It then aggregates the predicted class with the maximum votes of each classifier to the unknown example. In theory, if there are m independent classifiers, each classifier has the probability p of making the correct prediction. If $p = 0.5 + \epsilon > 0.5$. then the probability of the ensemble classifiers $P(m, p)$ majority voting making the correct prediction is greater than p (Equation 2-11), and p approaches one as m increases(Leon *et al.*, 2017). However, if $p < 0.5$, then $P(m, p)$ decreases and tends to *0 as m* increases. *If* $p = 0.5$, there is no change on $P(m, p)$.

$$P(m,p) = \sum_{i=\lceil m/2 \rceil}^{m} \left(\frac{m!}{(m-i)!\,.\,i!} \right) . p^{i} \,.\, (1-p)^{m-i} \qquad (2\text{-}11)$$

2.7.5 Machine Learning Model Evaluation

Several methods are used in evaluating the performance of an ML algorithm. The confusion matrix is a common method for evaluating the performance of classifiers (Kuhn and Johnson, 2013). The confusion matrix is an $m \times m$ matrix made up of the elements $c_{jk,}$ which are the number of assets in actual condition j that are predicted to be in condition k where $j \in \{1 \ldots m\}$ and $k \in \{1 \ldots m\}$. Elements on the diagonal of the matrix indicate that the predicted condition matches the actual condition. Elements off the diagonal represent the misclassification of the predicted conditions.

The confusion matrix also helps to calculate two other vital metrics: precision and recall. Precision is the ratio of correct positive predictions (true positives, TP) to the overall number of positive predictions (TP + false positives (FP)). The recall is the ratio of correct positive predictions to the overall positive examples (TP + false negatives (FN)) in the dataset. There is a tradeoff in achieving high precision and recall (Andriy, 2019). In asset condition classification, the tradeoff between precision and recall has different consequences ranging from the waste of resources (misclassifying

good assets as bad) to sudden failures (misclassifying bad assets as good). Another helpful metric when errors in predicting multiple classes are essential is the accuracy of a model. The number of correctly classified examples (TP) is divided by the number of classified examples (TP +TN +FP +FN).

Furthermore, the Kappa value measures the accuracy of an ML classifier in predicting different classes against the probability of random occurrence. The Kappa value of a binary classification is estimated using Equation 2-12. Equation 2-13 is used in estimating the Kappa value of a multi-class classification with $k = 1,2,3,\ldots, K$ number of classes (Tallón-Ballesteros and Riquelme, 2014). The higher the Kappa value, the better the performance of the classifier. According to (Landis and Koch, 1977), Table 2-6 provides a benchmark for classifying Kappa values.

Table 2-6. Interpretation of Kappa values.

Kappa value	**Strength of agreement**
<0.00	Poor
0.00-0.20	Slight
0.21-0.40	Fair
0.41-0.60	Moderate
0.61–0.80	Substantial
0.81–1.00	Almost perfect

$$\kappa_{binary} = \frac{P_o - P_r}{1 - P_r} \qquad (2\text{-}12)$$

where P_o is the observed accuracy and P_r is the random accuracy.

$$\kappa = \frac{c \times s - \sum_k^K p_k \times t_k}{s^2 - \sum_k^K p_k \times t_k} \qquad (2\text{-}13)$$

where $c = \sum_k^K C_{kk}$ is the total number of correctly predicted classes, $s = \sum_i^K \sum_j^K C_{ij}$ is the total number of elements; $p_k = \sum_i^K C_{ki}$ is the number of predictions for class k; $t_k = \sum_i^K C_{ik}$ is the number of observations of class k.

2.8 Social Cost Indicators

Social costs have been defined as the monetary equivalent of resources used by parties in construction projects, which are often implicitly accounted for (Matthews *et al.*, 2015). Even

though no one pays the accrued amount, it is necessary to quantify social costs in monetary terms for their socioeconomic effects to be considered in any intervention (Manuilova *et al.*, 2009). Intangible social costs of interventions, such as the loss of human life and the value of time (VOT), are more difficult to quantify. Additionally, it might also be difficult to quantify some of the tangible social costs (e.g., car occupancy rates, traffic accidents, etc.) due to the nature of uncertainty involved. The estimation and prediction of social costs is not a straightforward process (Gilchrist and Allouche, 2005; Zamojska and Próchniak, 2017). According to Matthews et al. (2015), the main deterrent is the inconsistency that exists in the current methods used in calculating various social indicators. However, several authors have proposed methods that can be classified into the direct calculation, generalized ranges, and conservative estimates (Matthews and Allouche, 2010). Oum (2017) modeled several tangible and intangible social cost indicators for municipal infrastructure interventions at a macro level. The aim was to use non-linear regression functions in quantifying the social cost indicators associated with three municipal infrastructure assets. Several studies have used different techniques to quantify some tangible and intangible social cost indicators. McKim (1997) proposed a bidding methodology that includes social costs in the award process. According to this research, this inclusion is desirable by the public because it ensures the least disturbance and it identifies the most economically efficient bid since it estimates the project's true cost (i.e., actual cost and social cost). (Tighe *et al.*, 1999) proposed a method of estimating and comparing the cost of traffic disruptions when both trenchless technologies and open-cut excavations are used. Their method involved comparing three traffic control strategies and estimating the cost of implementing each strategy relative to the duration of the open-cut and trenchless technologies. Gilchrist and Allouche (2005) designed and implemented a tool specifically for forecasting and calculating five social cost categories considering project-specific parameters.

In addition to the elimination of repeated excavations for utility interventions and intervention-related traffic disruptions, MUTs have been associated with several tangible and intangible benefits. This research focuses on the benefits directly related to synchronized utility interventions and the MUT. These social indicators are expressed as the cost of disruptions grouped into road traffic and ecological environment.

2.8.1 Road traffic disruptions

The impact of traffic disruptions considered in this research is divided into three types: vehicle maintenance and operating cost (VMO), vehicle delay costs (VDC), and pedestrian delay costs (PDC). The pedestrian delay cost is not estimated in this research. Traffic disruptions resulting from intervention-related activities lead to an increase in travel time and routes. The estimation of the impact of traffic disruptions can be achieved using field studies, empirical formulae, or traffic modeling tools (Ormsby, 2009). One common method of estimating the social cost of traffic disruptions is by setting the value of time lost in traffic as the hourly wage rate (Oum, 2017; Tighe *et al.*, 1999).

(a) Vehicle maintenance and operating costs

According to Chatti and Zaabar (2012), Vehicle operating costs (VMO) costs are grouped into the additional fuel consumption and costs of increased maintenance and repair. Increased maintenance refers to vehicle depreciation resulting from longer travel routes or time and increased stop-and-go cycles that accelerate the deterioration of vehicle mufflers, tires, axles, and chassis. VMO cost can be assessed by using an average operating cost (AOC) in dollars per vehicle-kilometer driven that considers both fuel and maintenance (CAA, 2013). In case of a partial road closure allowing traffic through the work zone, VMO cost can be also divided into two parts: VMO_q for queuing vehicles and VMO_d for vehicles taking detours (de Marcellis-Warin *et al.*, 2013; Najafi *et al.*, 2021). Specifically, VMO_f cost is assessed for each type of vehicle (automobile, bus, light, and heavy truck) to reflect their differences in fuel consumption (de Marcellis-Warin *et al.*, 2013).

(b) Vehicle delay costs

VDC is assessed as opportunity costs of forgone work activities by setting the value of time (VOT) lost in traffic at the hourly wage rate. The latter is borne by each passenger in circulation. In the case of a partial road closure allowing traffic through the work zone, VDC is divided into two parts: VDC_q for queuing vehicles and VDC_d for vehicles taking detours (de Marcellis-Warin *et al.*, 2013). VDC is assessed for each type of vehicle to give higher VOT to light and heavy trucks. In the literature, case studies were presented with knowledge of detour patterns; thus, removing the need for traffic simulation tools to forecast behaviors of drivers' choice between taking detours and waiting in queues.

Researchers like (Wu *et al.*, 2020) used agent-based simulation to estimate and integrate the increase in travel time into LCC analysis. The effect of the inclusion and exclusion of the cost associated with travel time at the breakeven point between the MUT and the direct burial method was estimated. Although the generated results on the benefits of MUT are consistent with the literature, the LCC model for the MUT does not capture the social costs accrued during the MUT construction phase which can significantly affect the breakeven point.

2.8.2 Ecological environment disruption

The impact on the ecological environment is determined by the volume of pollutants emitted into the environment. Air pollution resulting from fuel consumption is due to two factors: the use of heavy machinery, and increased vehicle emissions (Manuilova *et al.*, 2009). Air pollution costs from machinery are based on the volumetric emission cost (VEC) for different pollutants, where greenhouse gases (GHGs) can be converted to carbon dioxide (CO_2) equivalent (CO_{2eq}) units, thus simplifying the calculations (Sambe and Dogoua, 2016).

2.9 Geospatial Visual Analytics

Visual analytics (VA) is the science of analytical reasoning supported by interactive visual interfaces" (Thomas and Cook, 2005). The term geospatial analytics involves the combination of geographic analysis, data visualization, and applying a specific domain intelligence to aid decision-making (Ting *et al.*, 2018). VA has been applied in several domains, including decision-making in healthcare (Reinert *et al.*, 2020) and bioinformatics (Vehlow *et al.*, 2015), economics (Savikhin *et al.*, 2008), transportation, aviation (Andrienko *et al.*, 2020), predictive analytics (Lee *et al.*, 2020; Lu *et al.*, 2017), social media (Chen *et al.*, 2017), etc. It helps combine interactive visualization and computational analysis of large amounts of complex datasets and monitor their interactions. Geospatial visual analytics involves combining geographic analysis, data visualization, and applying a specific domain intelligence to aid decision-making (Ting *et al.*, 2018). Also, spatiotemporal clusters and concentrations can be identified using statistical tests (Rey *et al.*, 2015) combined with computational and human reasoning.

Several researchers have proposed spatio-temporal visualization; for example, Ferreira et al. (2013) proposed a visualization interface to explore extensive spatio-temporal data and show the attributes' variability and relationships. Packer et al. (2013) proposed a distance-based approach to splitting data and visualizing the shapes of each cluster in an interactive process by combining

spatial clustering and heuristic computations. The deviation between the clusters and the data points is minimized to identify each class (Ester *et al.*, 1995). Lee et al. (2020) developed a predictive VA system to monitor and forecast traffic congestion using real-time and historical data. VA tools have been applied in asset management, sustainable lifecycle design (Ramanujan *et al.*, 2017), and revealing complex tradeoffs in multi-objective optimization (Guo *et al.*, 2009). For example, Motamedi et al. (2014) combined VA and Building Information Modeling (BIM) to detect and visualize failure root causes in facility management. Zhou et al. (2016) used VA tools, such as parallel coordinates and sunburst visualization, to represent the relationships between water pipe attributes and the probability of pipe failure. In the multi-objective optimization of a water distribution system, Fu et al. (2012) demonstrated the use of VA in revealing the tradeoffs among the objectives, thereby improving decision-making via the understanding of the interactions between the objectives. VA has been effectively applied to understand the phenomena associated with individual infrastructure assets. However, this method of individual asset analysis is inefficient when considering synchronized or multi-asset interventions.

To address this gap, this research aims to establish the relationships between multi-asset intervention activities and their socioeconomic impacts visually and statistically. The critical areas where the current infrastructure practices will potentially result in a relatively high socioeconomic impact are identified using density maps. By exploring the spatial distribution of the pipes where the interventions require excavation, the location of aging utility assets, and the traffic density, the interpretation of the correlation between the different attributes can be portrayed to aid decision-makers.

2.10 Summary

This chapter provides an overview of various aspects related to the implementation of MUTs. It begins with a concise history of MUT implementation in different parts of the world, followed by an explanation of the planning process and location selection criteria. Additionally, the chapter explores the literature on synchronized utility intervention and the optimization algorithms involved in this process. The socioeconomic impact of utility interventions is also discussed, specifically in terms of social costs incurred due to current practices that necessitate pavement excavations. Finally, the chapter delves into the application of machine learning techniques for

predictive maintenance in asset condition classification and the application of geospatial visual analytics to improve the decision-making process for utility interventions.

Based on the literature review, the research gaps related to MUT location selection can be summarized as follows: (1) As presented in Table 2-1, there is limited research in the area of MUT location selection. The table clearly shows that the reviewed literature has focused on different areas of MUT implementation. However, Luo et al. (2019) successfully achieved MUT location selection using eight criteria, without accounting for the dependencies that exist within the criteria.; (2) Currently, there is limited research on the quantification of the socioeconomic impact of the MUT and the synchronized method of utility interventions at a macro level. In addition, there is also limited research that provides quantitative support for the long-term benefits of MUTs. Meanwhile, most studies have compared the benefits of implementing the MUT using only isolated projects; (3) Previous research focuses on binary or multi-class classification models to determine the need for intervention at an asset or network level for single infrastructure assets. A systematic approach is required at a segment level to holistically combine the conditions of spatially collocated assets to foster synchronized interventions; and (4) As presented in Table 2-3, existing methods used to achieve synchronized utility interventions are specific to a municipality or city. Therefore, limiting their applicability and replicability.

CHAPTER 3. OVERVIEW OF RESEARCH METHODOLOGY

3.1 Introduction

This chapter presents an overview of the proposed research methodology for determining the MUT location selection from the lifecycle point of view, the socioeconomic perspective, and spatial characteristics while considering the synchronized method of utility interventions. Section 3.2 highlights the key modules that make up the methodology.

3.2 Research Methodology

The proposed research method is shown in Figure 3-1. The method is centered around four core areas, namely: (1) A geospatial visual analytics model to analyze and determine the relationships between interventions practices, asset conditions, and their socioeconomic impacts using statistical tools and geospatial analysis; (2) Street closure prediction model based on the combined conditions of spatially collocated assets (i.e., pavements, water and sewer pipes) within a segment using machine learning; (3) A multi-criteria decision-making model that uses spatial data in the MUT location selection problem; and (4) A multi-objective optimization model, to optimize the agency and social lifecycle costs for identifying the potential locations of MUTs. The following four sections introduce each module of the methodology.

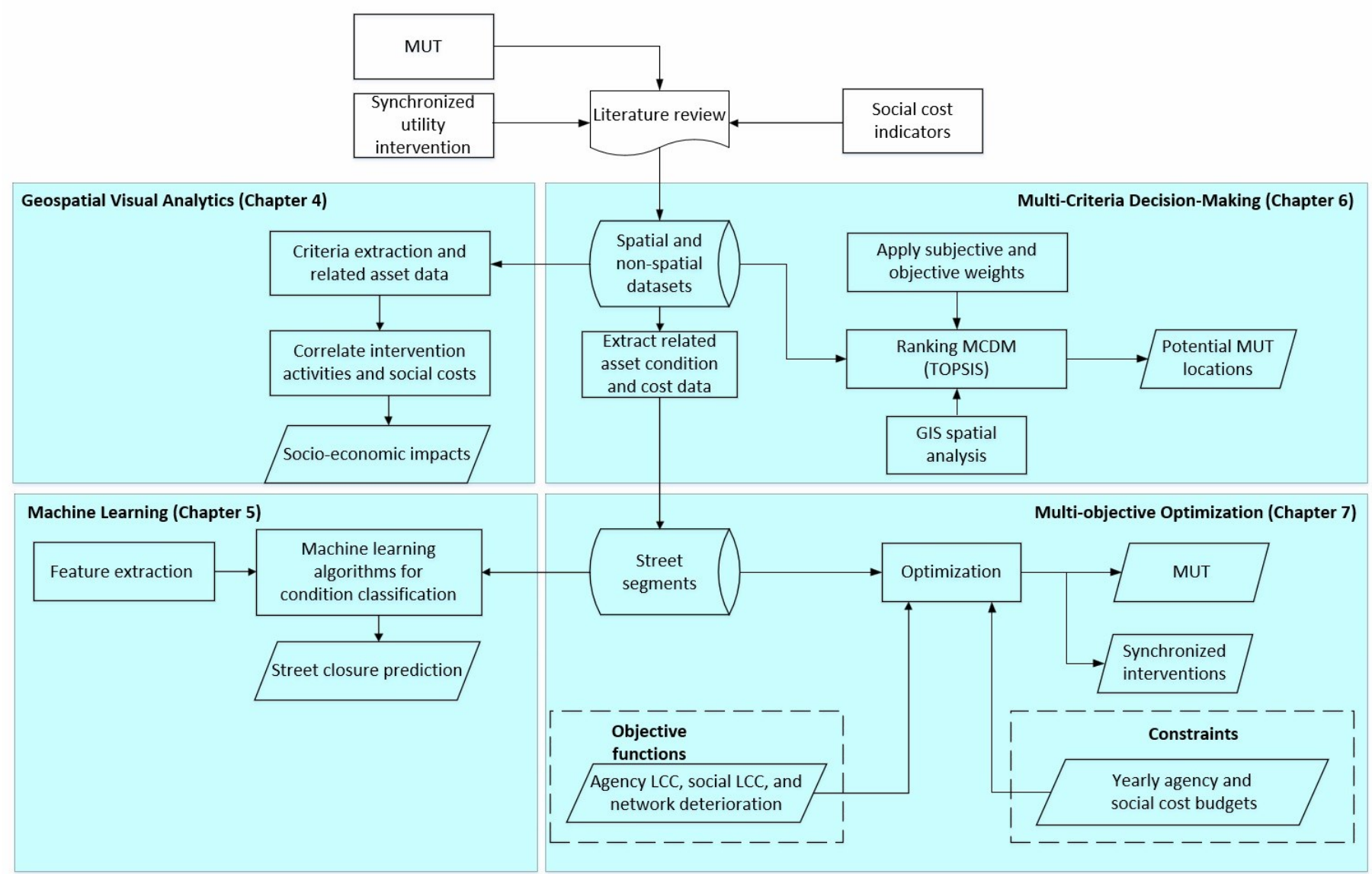

Figure 3-1. Overview of research methodology

3.3 Geospatial Visual Analytics for Utility Intervention Decision-Making

As discussed in Section 1.2, both the synchronized intervention and the MUT have the potential to significantly reduce the agency and social cost of utility interventions, compared to conventional unsynchronized methods. However, despite their benefits, these alternatives are not widely practiced or implemented, which underscores the need to highlight the socioeconomic implications of unsynchronized interventions to decision-makers.

To achieve this, a holistic approach is necessary to identify and understand patterns in the multivariate datasets that represent utility asset interventions. Statistical tests are used to interpret the relationship between spatiotemporal clusters and concentrations (Rey *et al.*, 2015).

Following data collection and criteria extraction, the next phase of this chapter focuses on establishing the relationships between intervention activities and their socioeconomic impacts. By analyzing the correlation between different attributes of the multivariate dataset, critical areas can be identified where current infrastructure practices will likely result in high socioeconomic impacts. This module of the research is presented in detail in Chapter 4.

3.4 Street Closure Prediction Based on the Combined Conditions of Spatially Collocated Assets

As explained in Section 1.1, partial and complete street closures are a common occurrence in both asset-level and segment-level interventions. As the number of unsynchronized interventions increases, so does the frequency of street closures. Once segment-level interventions are determined, the two alternatives of synchronized interventions and MUTs can be considered. In this research, synchronized interventions are considered best practice and MUT is investigated as an opportunity primarily for segment-level interventions that require excavations, such as pipe replacement.

To aid municipal decision-makers in identifying and prioritizing synchronized segment-level interventions, this research predicts street closures. This will improve the planning and estimation of intervention durations and street closures, thereby reducing the social costs resulting from utility interventions. The prediction of street closures is based on the combined conditions of spatially collocated assets, such as street pavements and water and sewer pipes. Different policy-based methods have been implemented for synchronization, but their replicability is limited. A condition-

based method is proposed to classify the condition of each spatially collocated asset and simplify their combination on a segment level.

Feature extraction is used to obtain the most influential asset attributes, which are subsequentially used in the machine learning process. A multi-class classification approach is used to determine the condition of each asset, based on independent ML models that capture their respective conditions. Subsequently, intervention strategies are applied to restore the condition of each asset. These strategies, known as asset-level intervention strategies, are then combined systematically at a segment level to obtain segment-level intervention strategies, including synchronized or unsynchronized interventions and MUTs. Finally, the combination of the output of these strategies determines the nature of the required street closures.

This module not only predicts street closures, but also serves as a way to identify potential street segments for MUT implementation, based on the need for asset-level interventions and segment-level intervention strategies. The details of this module are presented in Chapter 5.

3.5 Multi-Criteria Decision-Making Model for MUT Location Selection

The third module of this research focuses on prioritizing street segments for MUT location selection using a combination of subjective and objective MCDM techniques and GIS spatial analysis. The effect of considering the dependencies in the MCDM process will be determined by comparing the ranking obtained from the TOPSIS that are based on the weights derived from AHP or ANP. The module is divided into four phases, including criteria definition, selection and scoring of the alternatives, aggregation, and decision-making. To prioritize the street segments, 12 criteria, based on the literature review, are considered, including annual average daily traffic, road class, utility density, population density, number of expected excavations, underground development projects, land-use, proximity to public facilities, high-rise buildings, soil type, the slope of the terrain, and proximity to the floodplain.

Different sets of criteria weights are estimated using both AHP and ANP, and the ranking of street segments is achieved using TOPSIS. The subjective weights derived from aggregating expert opinions are represented by criteria weights obtained from both MCDM techniques. To determine the effects of the dependencies considered in the ANP methodology, the weights and the subsequent ranking results are compared. Furthermore, although the AHP and ANP methodologies have the consistency index to check the transitivity of expert responses, not all pairwise

comparisons are transitive. This further complicates the decision maker's ability to compare the criteria from an expert point of view. Also, since 12 criteria are used in the MCDM process, their relative weights would be small. Therefore, a consistency error is likely to considerably distort the relative weights of the criteria (Saaty, 1987). Thus, an objective approach is implemented in this chapter using Shannon's Entropy (Shannon, 1948). The calculated Entropy weights are subsequently integrated into the TOPSIS method. Furthermore, the ranking results from both AHP and ANP are compared to the ranking obtained from using Entropy weights applied with TOPSIS to determine the difference or similarity between the application of objective and subjective weights for a set of alternative MUT locations. Nevertheless, using subjective weights (AHP or ANP) in the context of selecting MUT placement locations is also essential due to the input of experts and because only a handful of authors have covered this area of research as compared to other areas of study.

The proposed method prioritizes street segments from both the decision-makers' perspective and the data itself, providing vital information to the MUT location selection decision-making process. Chapter 6 provides a detailed explanation of this module.

3.6 Multi-Objective Optimization for Selecting Potential Locations of MUT Considering Social Costs

The fourth module of this research aims to identify potential street segments for MUT placement using a mathematical optimization technique. Unlike the method proposed in Chapter 6 where preselected street segments were considered, this module of the research considers all street segments in the network to identify potential locations for MUT implementation. The selection involves modeling agency and social LCC and network deterioration resulting from implementing MUTs and the synchronized method of infrastructure interventions at the network and segment levels. Two independent optimization models are used to optimize both alternatives, and the results are compared at the network and segment levels. Both models are constrained by the yearly agency and social cost budgets. Two solutions that satisfy the decision-maker's preferences are selected from the Pareto fronts of each optimization model and compared. By comparing both optimization results, the street segments in the network where the LCCs of implementing MUTs are less than the LCCs of the synchronized utility intervention are identified as the optimal locations for MUT implementation that guarantee LCC savings.

The search space for finding an optimal or near-optimal solution is complex due to several variables considered, including the number of intervention scenarios, the number of utility assets, the intervention strategies, the number of segments in the network, and the planning period. Similar to the second module, asset conditions determine the asset-level intervention strategies, and their combination determines the applied segment-level intervention strategies. Linear deterioration models for each type of asset are used to determine the yearly change in asset conditions. Three social cost indicators are used to quantify the socioeconomic implication of each intervention alternative using three regression models for each social cost indicator.

This module is presented in detail in Chapter 7 and provides a comprehensive approach to identifying optimal street segments for MUT placement. The proposed framework considers various factors and helps decision-makers make informed decisions that result in efficient and cost-effective interventions.

3.7 Summary

This chapter provides an overview of the proposed research, addressing the research gaps in MUT location selection. The framework is composed of several essential components, including geospatial analysis to establish the correlation between intervention needs and their negative socioeconomic impact, identification of street segments that may require partial or complete closures due to intervention for assets with poor conditions, street segment ranking using MCDM techniques that prioritize them based on subjective and objective weights, and optimization of street segment selection based on the value of agency and social LCCs and network deterioration. In the subsequent chapters, each module of the proposed research is thoroughly explained and validated through case studies. The integration of these components will result in a comprehensive and efficient method for MUT location selection that accounts for various socioeconomic and infrastructure factors.

CHAPTER 4. GEOSPATIAL VISUAL ANALYTICS FOR UTILITY INTERVENTION DECISION-MAKING[2]

4.1 Introduction

Section 1.2 highlights the interdependency between underground utility networks and explains why relying solely on individual asset analysis is inefficient in understanding how the intervention of spatially collocated assets affects their interactions and relationships, as well as the associated negative socioeconomic impacts. This chapter focuses on using VA to comprehend the relationships between the location and condition of underground utility assets, their intervention-related activities, and socioeconomic impacts, to improve the effectiveness of interventions and reduce negative impacts on society. A case study is established to demonstrate these relationships both visually and statistically. This chapter aims to aid decision-making by emphasizing the importance of sustainability considerations (i.e., environmental, social, and governance factors) while exploring alternative intervention practices and utility infrastructure asset placement techniques such as the MUT.

4.2 Geospatial VA Model

The conducted analysis is based on existing and historical datasets grouped into three categories: utility networks (i.e., water pipe network and road pavement), auxiliary datasets, and the surrounding environment, as shown in Figure 4-1. The auxiliary datasets include the intervention plan, emergency repair data, water pipe breakage data, and Info-Excavation data (data representing the *locate* requests of underground infrastructures) for underground assets. All of these play an essential role in establishing the relationships between the attributes of each utility asset, utility interventions that require excavations, and selecting sustainable asset management or placement system.

The feature selection process is carried out to determine which dataset attributes substantially influence asset conditions. Raster maps are generated to enhance the visualization of clusters.

[2] This chapter is based on the following conference paper: Genger, T.K. and Hammad, A. (2022), "Geospatial Visual Analytics for Supporting Decision Making for Underground Utility Integrated Interventions", International Conference on Transportation and Development 2022, American Society of Civil Engineers, Reston, VA, pp. 46–59, doi: 10.1061/9780784484364.005

Spatial relationships are established to identify clusters representing the likelihood of socioeconomic impacts (i.e., high traffic volume resulting from street closures due to pavement excavation for infrastructure interventions). These clusters are made up of locations with high levels of asset damage (e.g., high break rate), aging assets, high traffic density, and high requests. Finally, the spatial and statistical relations between the selected features will be discussed. The details of these steps are explained below.

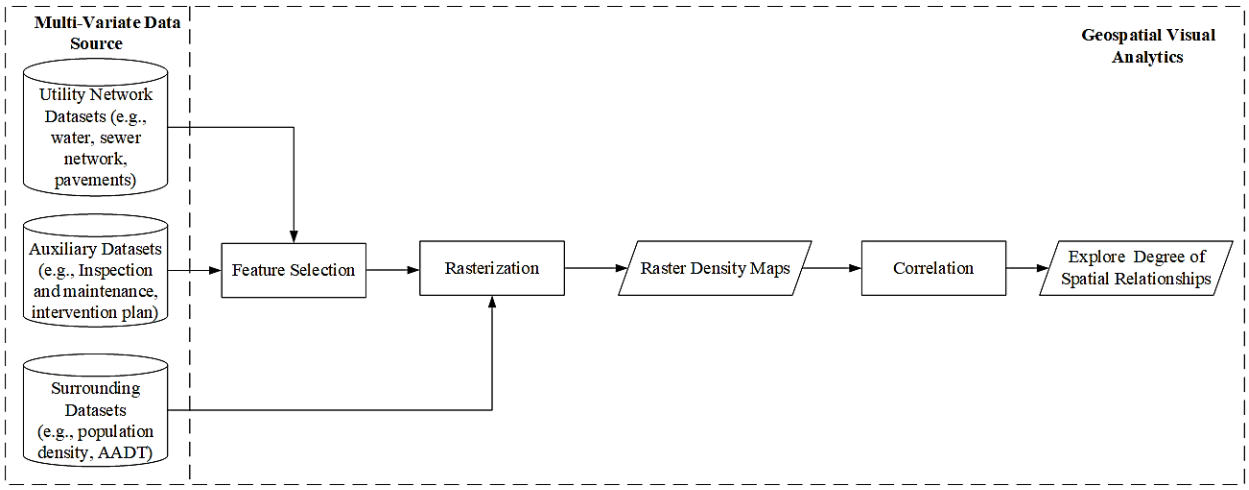

Figure 4-1. Geospatial visual analytics model.

4.2.1 Multi-variate data source

The datasets include both municipal and private networks buried under the roads. By combining both the network and the auxiliary datasets, the relationships between several attributes can be analyzed, such as the condition of the assets, location of failures, age, material, and frequency of repairs. In addition, the combination with surrounding datasets will help establish the relationship between the intervention activities and the social costs. The AADT is used as the surrounding dataset to understand the relationship with social costs.

4.2.2 Geospatial VA

Feature selection is commonly used to improve the performance of a predictive model by reducing the complexity and dimensionality of a dataset (Ting *et al.*, 2018). Here, feature selection is used to search for the most influential set of attributes for determining the condition of pavement and water pipes. Spatial maps are rasterized to create density maps that help identify and visualize

geospatial hotspots based on the identified attributes. The correlation between a subset of the raster density maps is calculated using Equations 4-1 and 4-2 (Poldrack, 2018). Finally, the relationship between each dataset pair is analyzed using a correlation matrix.

$$Cov_{ij} = \frac{\sum_{k=1}^{N}(Z_{ik} - \mu_i)\left(Z_{jk} - \mu_j\right)}{N - 1} \quad (4\text{-}1)$$

$$Corr_{ij} = \frac{Cov_{ij}}{\delta_i \delta_j} \quad (4\text{-}2)$$

where: Cov_{ij} is the covariance of layers *i, j* of a stack, μ is the mean of a layer, N is the number of cells, k is a particular cell, Z is the value of a cell, $Corr_{ij}$ is the correlation coefficient, and δ is the standard deviation.

4.3 Case Study

The study area highlighted in Figure 4-2 comprises nine boroughs in the City of Montreal, including Ville Marie, Mercier–Hochelaga-Maisonneuve, Le Plateau-Mont-Royal, Rosemont–La Petite-Patrie, Outremont, Côte-des-Neiges–Notre-Dame-de-Grâce, Le Sud-Ouest, LaSalle, and Verdun. The data sources include the Traffic Department and the Geomatics Department of Montreal City, the Montreal Open Data Portal (Montreal City, 2021), and Statistics Canada (Statistics Canada, 2020).

4.3.1 Utility networks

Various utility networks exist on the underground surface; however, only the drinking water pipe network is selected for analysis and the road pavement network. The water pipe network (Figure 4-3) consists of about 127,716 pipes, with laid pipes ranging from 1900 to 2019. The pavement network in the study area (Figure 4-4) comprises 15,603 road segments with an average length of 215.4 m. Both assets' conditions are classified as 1, 2, and 3, signifying excellent/good (minor defects with an estimated time of failure ≥ 20 years), fair (moderate defects with an estimated time of failure between 10 to 20 years), and critical (severe defect requiring immediate attention) conditions, respectively (LLA, 2007).

Table 4-1 and Table 4-2 summarize the attribute values for the pavement and water pipes datasets (Montreal City, 2018).

Figure 4-2. Study area.

4.3.2 Auxiliary datasets

The auxiliary dataset comprises the intervention and inspection data for the water pipe and pavement networks. Furthermore, the emergency repair data and water pipe breakage data provide information on the condition of water pipes, the location of pipe breaks, and the frequency of the pipe breaks. This breakage dataset contains 11,794 historical breaks dated to 2020. Both the water pipe breaks, and pipe break rate attributes offer different perspectives. The breakage data provides information on the frequency and location of breaks on each pipe, while the break rate is the amount of breaks/km/year. A pipe with repeated breaks can be translated as the presence of undetected phenomena (e.g., soil type, high traffic loads, etc.). The break rate discloses the rate at which one or more pipes break every kilometer/year. Figure 4-5 is a GIS map of the study area showing the location of previous breaks, and Figure 4-6 shows the different break rates for each road segment. Road segments with high break rates can be candidates for MUTs because this will eliminate the need for repeated excavation. The water pipe and pavement dataset represent the interventions

determined by the City of Montreal's intervention plan for 2016-2021. This plan includes the infrastructure deficit, and the maintenance needs during this period.

Part of the auxiliary dataset is the Info-Excavation data. The Info-Excavation dataset signifies the safety aspects of an excavation-related intervention as it ensures acquiring information on the assets buried underground before excavation. This information reduces the possibility of utility strikes. Figure 4-7 shows the trend from 2015 to part of 2019 for the locate requests made for pavement and water pipe maintenance and repair-related interventions. The trend shows a gradual increase in the locate requests made from 2015 to 2017 and a decline from 2017 to 2019. The information contained in this data is vital to understanding the excavations' frequency and location.

4.3.3 Surrounding datasets

The AADT for 2,396 intersections from 2008 to 2018 is used to analyze the relationship between the surrounding traffic conditions and the intervention activities. Each point in Figure 4-8 represents an intersection, and the hotspots in the figure signify areas with relatively high traffic volume. The correlation between the AADT and the attributes that represent the need for asset replacement or repair (condition of the assets, age) can indicate the degree of the negative socioeconomic impact of the interventions.

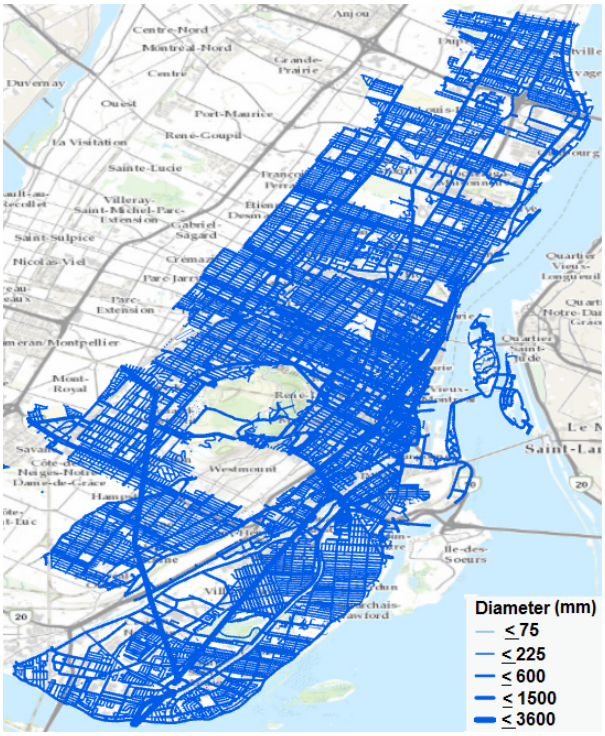

Figure 4-3. Water pipe network.

Figure 4-4. Road pavement network.

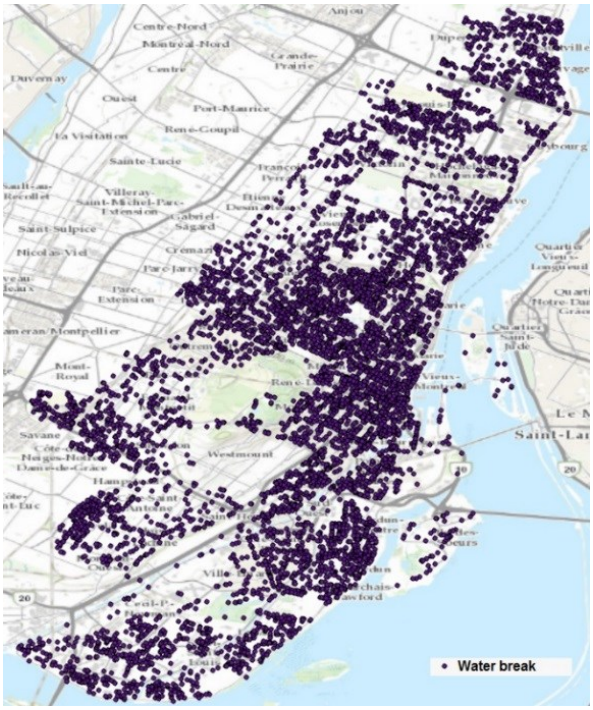

Figure 4-5. Water pipe breaks.

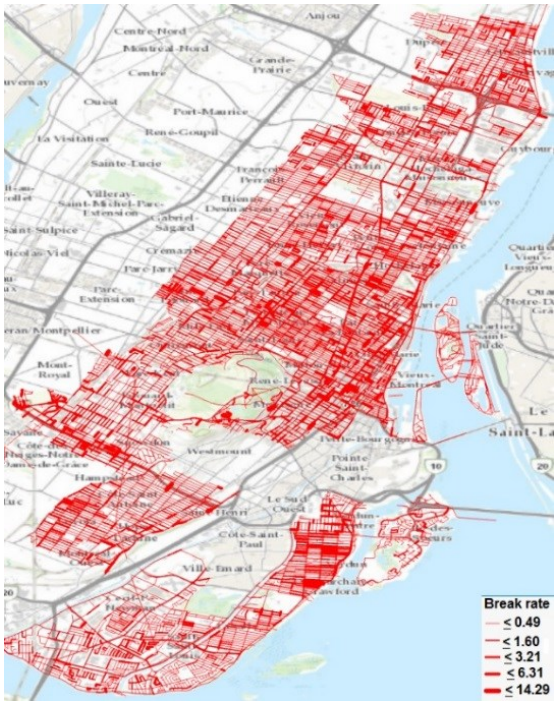

Figure 4-6. Water pipe break rate.

Table 4-1. Summary of pavement features.

Number of road segments	15,603
Performance condition index (PCI) Average PCI	1-100 52
International roughness index (IRI) Average IRI	0 - 13.9 5
Road class	0-9
Average length (m)	215.4
Average surface area (m^2)	2245.1
Category	Arterial, local
Hierarchy	I, II, III
Pavement conditions	1, 2, 3

Table 4-2. Summary of water pipe features.

Number of pipes	127,716
Mean age (yrs.), Std. Dev.	73.84 40.79
Major materials	Gray cast iron, ductile iron, copper, reinforced concrete
Major types	Connection, feed, network
Diameter range (mm)	15-3,900
Average pipe length (m)	215.4
Break rate (brk/km/yr) Average break rate	0 - 15 0.4
Range of failure dates	1973 - 2020
Major failure types	Circular crack, pipe burst, seal leak
N_failures (Number of previous failures in the segment) Average	0 – 26 4
R_life (Inspection age/estimated useful life**)** Average	0 – 1.68 0.55
T_length (Average total length of pipes in a segment) (m)	212
N_p_bad (Number of pipes in a road segment with a bad or very bad status) Average	0 – 8 0.12
Pipe conditions	1, 2, 3

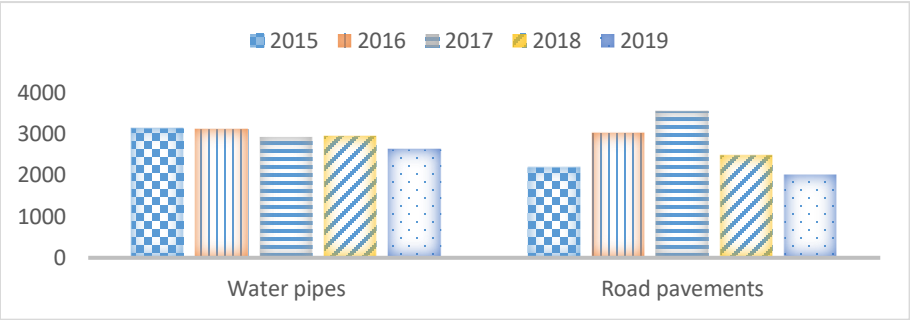

Figure 4-7. Frequency of information requests for excavation.

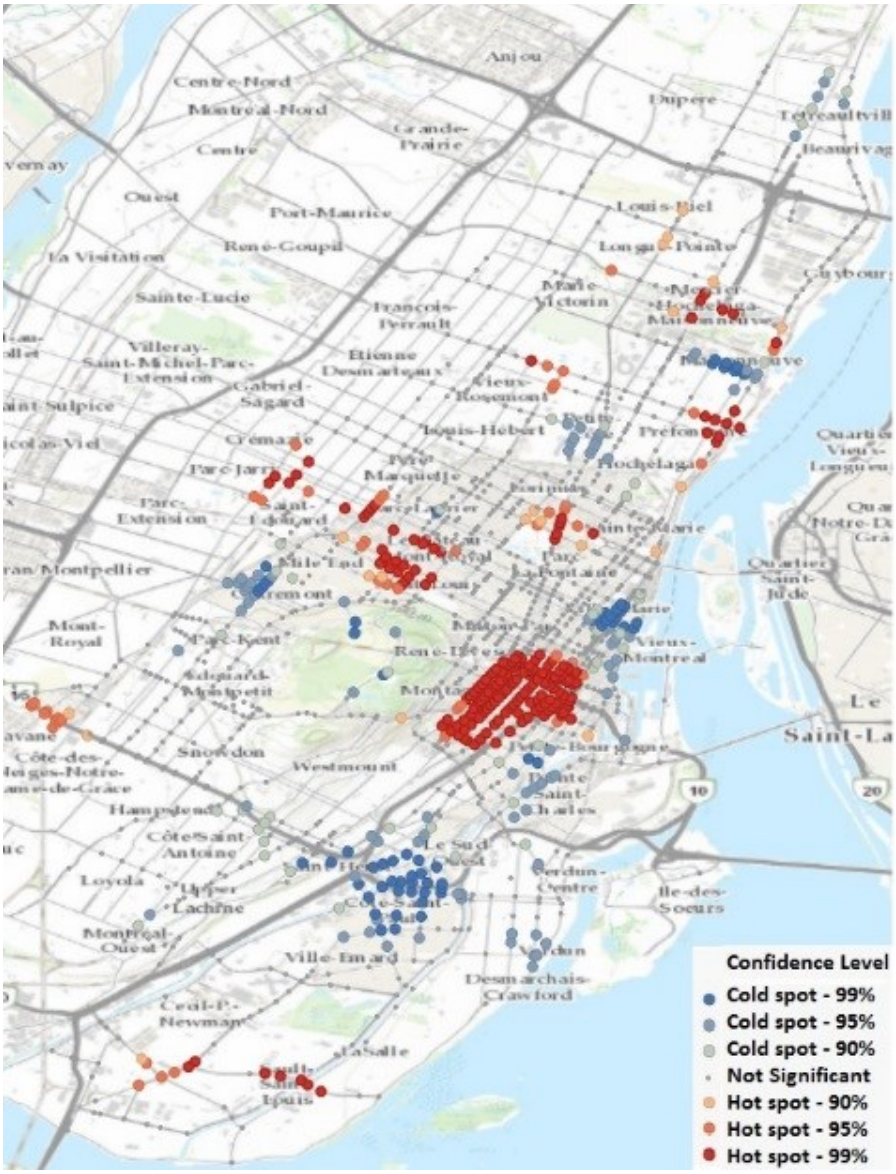

Figure 4-8. AADT Hotspots.

4.3.4 Feature selection

Feature selection was carried out on the water pipes and pavement attributes. Seven of the initial 12 water pipe attributes as shown in Table 4-2 were identified as the key features using the Naive Bayes algorithm and forward selection analysis (Visalakshi and Radha, 2014). These features and their corresponding weights are shown in Figure 4-9. This process revealed that pipe break rate has the most substantial influence in classifying the condition of the water pipes, followed by inspection age/estimated useful life. Similarly, Figure 4-10 shows the key features that determine the pavement conditions. The pavement PCI has the most substantial influence in classifying the pavement conditions, followed by IRI. The parallel coordinates plots in Figure 4-11 and Figure 4-12 are used to visualize the trend between the identified key features for the water pipes and pavement condition. For example, Figure 4-11 shows a linear relationship between break age and pipe age, while Figure 4-12 shows an inverse relationship between PCI and IRI.

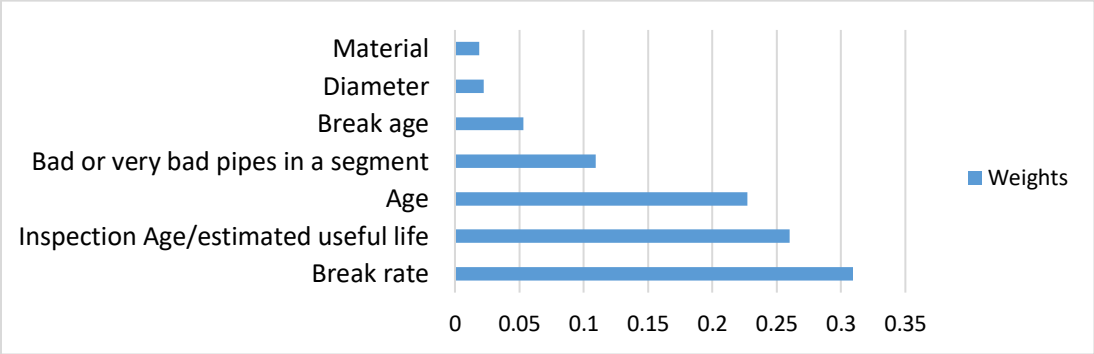

Figure 4-9. Water pipe attributes vs. their weights after feature selection.

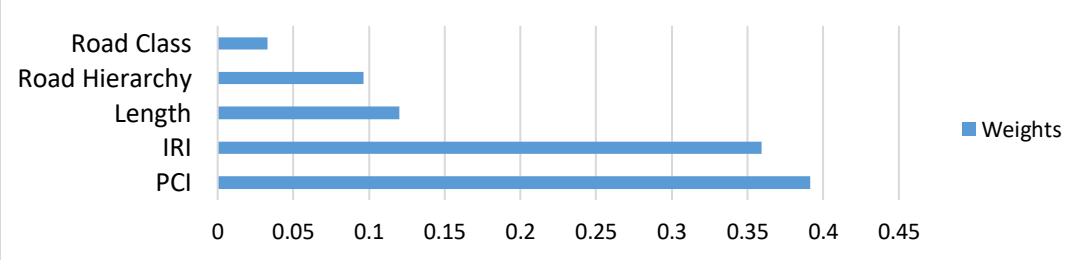

Figure 4-10. Pavement attributes vs. their weights after feature selection.

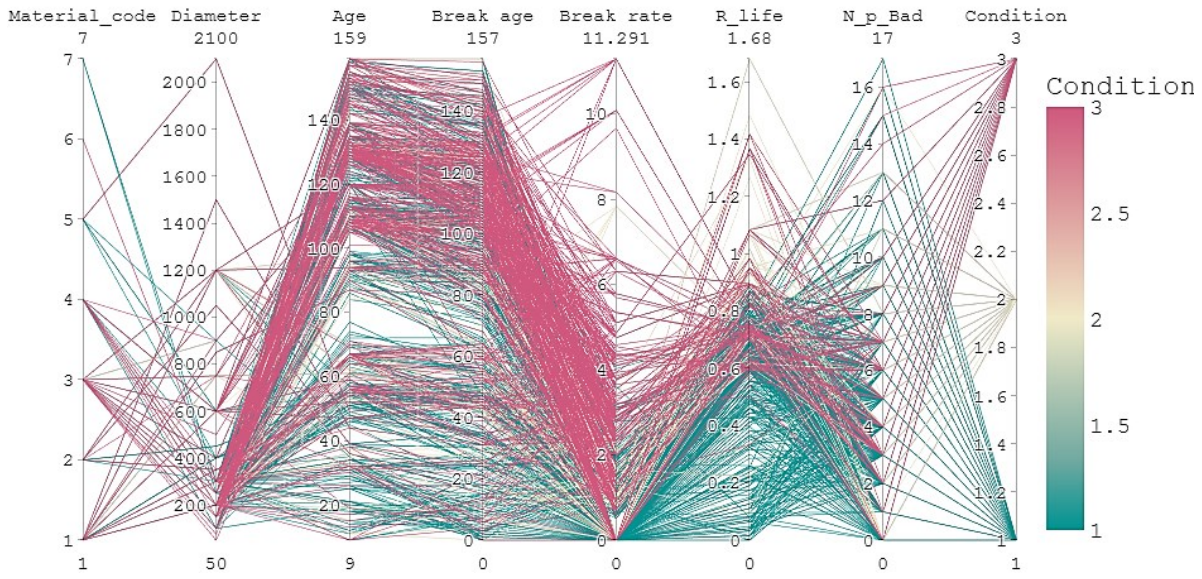

Figure 4-11. Relationship between multi-attributes and water pipe condition.

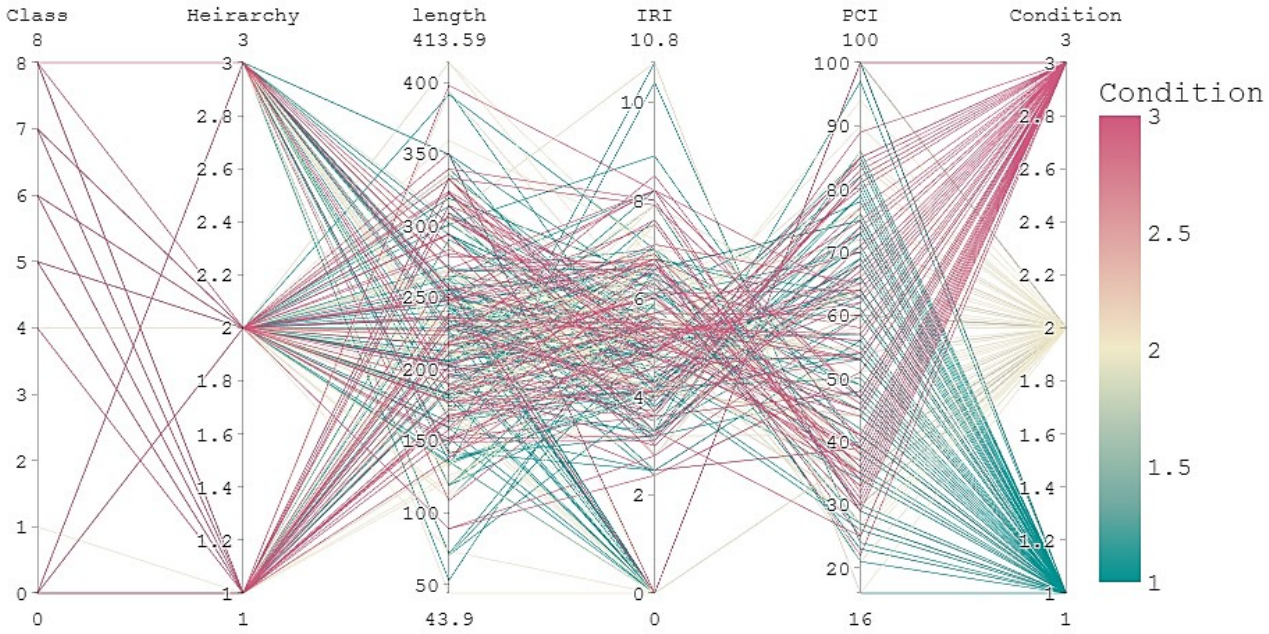

Figure 4-12. Relationship between multi-attributes and pavement condition.

4.3.5 Correlation

The correlation coefficient is used to determine the degree of relationship between the asset conditions, the need for asset replacement or repair, and the socioeconomic impacts of interventions. The PCI and water pipe break rate are used as the variables representing the asset

conditions, while the water pipes older than 100 years and pavements with PCI less than 55 represent the need for intervention (Shah *et al.*, 2013). Furthermore, the excavation activities and the AADT imply the socioeconomic impacts of intervention activities. Due to the different units of the attribute of the datasets, raster maps of equal cell size (50 m) are created for each dataset. Figure 4-13 shows density raster maps used to visualize the locations with the high magnitude-per-unit area.

The maps show common areas with relatively high magnitudes with a darker shade of purple. A correlation matrix is used to show the degree of relationship between any two variables, which is the correlation coefficient of any two raster maps. The ArcGIS tool Band Collection Statistics (Esri, 2016a) is used to calculate the correlation matrix shown in Table 4-3. The matrix shows a positive correlation exists between all the paired datasets. However, there are relatively stronger relationships between locations with water pipes older than 100 years and the excavation rate and, more obviously, between water pipe breaks and break rates.

Table 4-3. Correlation matrix.

	AADT	PCI<55	Water pipes older than 100 years	Water breaks	Excavation	Water pipe break rate
AADT	1	0.533	0.691	0.695	0.717	0.676
PCI<55		1	0.664	0.712	0.737	0.850
Water pipes ≥100 years			1	0.761	0.877	0.708
Water breaks				1	0.810	0.858
Excavation					1	0.761
Water pipe break rate						1

4.4 Intervention Activities and Sustainability Considerations

Montreal has experienced an increase in its population by about 4.6% between 2016 and 2021 (The Canadian Press, 2022). This increase means a rise in every spectrum of its economy. There is a need for sustainable investing in utility infrastructure that identifies, mitigates, and manages environmental, social, and governance (ESG) risks. Meanwhile, making such investment advantageous to both the utility owners and users. The ESG factors are broken as follows.

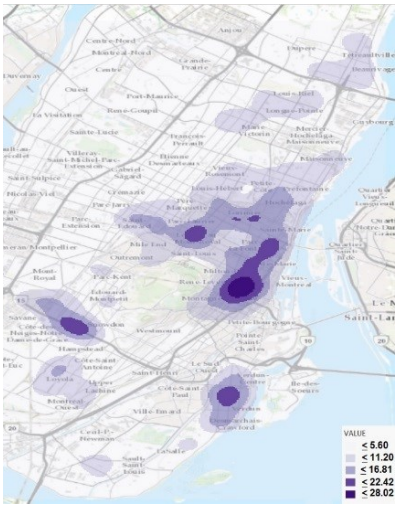

(a) Water pipe break rate

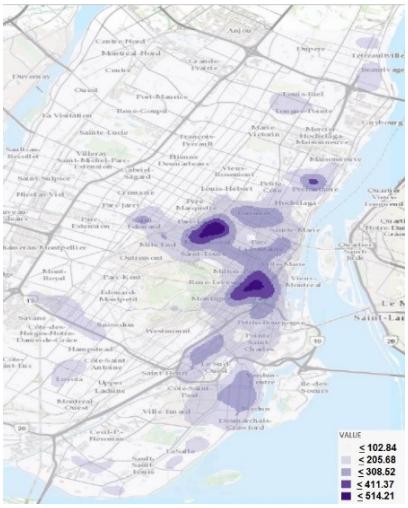

(b) Water pipe breaks

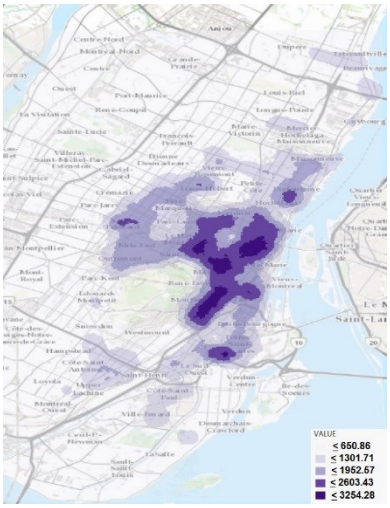

(c) Water pipes older than 100 years

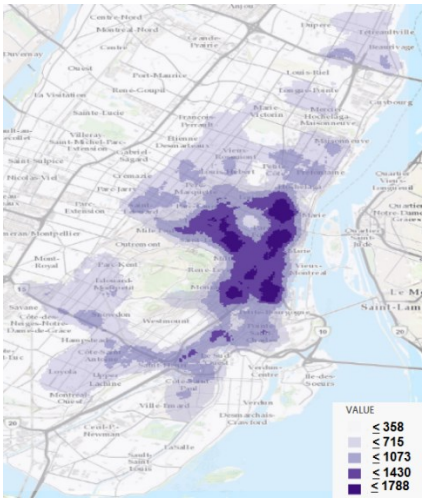

(d) Excavation activities

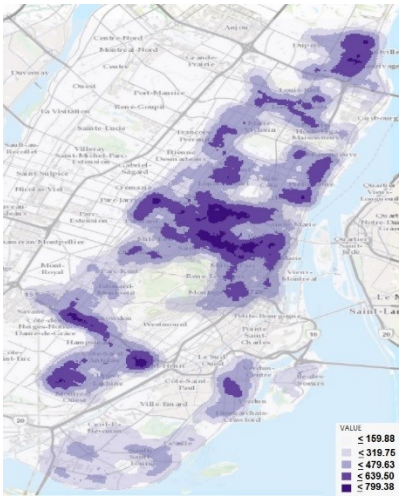

(e) Pavement PCI<55

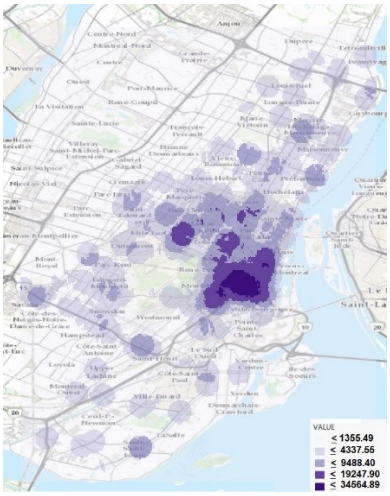

(f) AADT

Figure 4-13 Density raster maps.

Environmental: As underground assets continue aging, the excavation-related interventions will continue to increase, as shown in the positive correlation between excavation and pipes older than 100 years. Despite the increased use of trenchless technologies, intervention-related excavations are synonymous with street or lane closures that increase traffic delays and travel time. Meanwhile,

increasing CO_2 emissions resulting from higher fossil fuel consumption and a significant increase in air pollution pose public health risks.

Social: The positive correlation between the age of pipes and break rate shows that older pipes are likely to break more. More breaks mean more service disruptions (increased loss of service) and emergency interventions to mitigate the breaks (i.e., more unplanned street or lane closures). Meanwhile, unless synchronized, these interventions will further reduce the quality of the pavements, as evident in the relationship between excavations and PCI.

Governance: The placement of underground utility assets makes regular inspection difficult and interventions expensive for both shareholders and stakeholders. Regulations can be implemented to mandate synchronized interventions between utility owners whose assets share the same right-of-way. However, this is a short-term and unsustainable solution mainly because buried assets will need future excavations accompanied by negative environmental and social factors (as shown by the positive correlation between areas with water pipe breaks, break rate, excavation, and PCI). Making the transition to the MUT has been hindered by issues that include the high initial cost of construction, safety concerns, and management issues. Public-private partnerships for cost-sharing (Alaghbandrad and Hammad, 2018), IoT for smart sensing (Luo *et al.*, 2019), and a MUT regulatory body for management and coordination have the potential to address the hindrances mentioned above, respectively. Policies that mandate the construction of MUTs in new developments and areas prone to high break rates and AADT can help ensure future positive ESG returns.

4.5 Summary

This chapter has presented the relationship between the conditions of pavement and water pipe assets with intervention related to excavations, and their socioeconomic activities using geospatial visual analytics. This relationship was established using a list of multivariate datasets, including AADT, intervention plan, emergency repair data, water pipe networks, and excavation data. The link between the need for intervention and the adverse socioeconomic effects was established by relating the asset conditions and excavation-related activities. A feature selection algorithm is used to identify the most influential features in determining the condition of each utility asset. These features were then subsequently used in creating spatial density maps for visualization. These density maps help identify hotspots. For instance, areas with a high number of breaks and high

excavation represent problematic segments where traditional or synchronized interventions have occurred in the past, which translates to unresolved issues responsible for repeated breaks. With this information, decision-makers can recommend further studies to identify the reason for repeated breaks.

The correlation matrix showed the strength of the relationships between features. These relationships can also aid the decision-making process. For example, the positive medium correlation between AADT and break rates does not necessarily mean a cause-effect relationship but that a sustainable method of utility placement (e.g., MUT) is required in areas prone to high traffic (Genger et al., 2021). In addition, the strong positive correlation between pipes older than 100 years, water pipe breaks, and water pipe break rate translates to the influence of pipe age on breaks and the rate at which pipes break. Moreover, the relatively strong correlation between excavation activities and AADT shows that both entities will increase at a relatively high rate (0.716). This relationship shows that areas that experience high excavation activities are also prone to high AADT.

CHAPTER 5. STREET CLOSURE PREDICTION BASED ON THE COMBINED CONDITIONS OF SPATIALLY COLLOCATED ASSETS[3]

5.1 Introduction

As discussed in Section 1.2, one way to reduce the negative socioeconomic impacts of intervention-related activities such as street closures is to undertake synchronized interventions at the street segment level. To conduct efficient synchronized interventions, it is necessary to have the conditions of all spatially collocated assets in the street segment. As explained in Section 2.6 most researchers have focused on condition predictions or classifications of individual assets. This chapter focuses on classifying the conditions of three spatially collocated assets (i.e., road pavement, sewer and water pipes) using a uniform scale to aid their combination in determining synchronized interventions at the segment level.

In this chapter, we present a detailed explanation of the proposed method for determining street closures. Section 5.2 covers the various stages of the proposed approach, including data preparation and preprocessing, ML model development, condition classification, and segment-level combination. The subsequent section expounds on the heuristics that generate the asset and segment-level intervention strategies and street closure decisions. To demonstrate the applicability of the proposed method, a case study is presented, followed by a sensitivity analysis of the various features that contribute to the condition classification of each asset.

5.2 Machine Learning Model

The proposed methodology shown in Figure 5-1 is developed to determine street closures at a segment level by combining the conditions derived from three ML models for each asset and subsequently applying intervention strategies. This methodology starts with preparing raw GIS data for each asset's failure, inspection, and network datasets, then several data preprocessing steps are executed on the datasets. The data is then split into training/cross-validation and testing. The selected features for each asset are fed into their respective ML model, each consisting of a voting-based ensemble ML algorithm.

[3] This chapter is based on the following journal paper:

0.

Hyperparameter tuning is carried out on each ML model to obtain the highest accuracy. Each model is evaluated, and the output (the conditions of the three assets) is combined at a segment level. The mapping between assets and segments is done using assets' unique identifiers and the unique identifiers of the street segment where each asset is located. Finally, the combined conditions of the assets are integrated with intervention strategies that determine the nature of street closures (partial or complete) and the need for synchronized or unsynchronized interventions.

5.2.1 Data preparation

This first phase of the method involves generating the datasets used for the ML process. The selection of attributes is guided by literature, data quality, and data availability. For this purpose, a large amount of data regarding several features of each asset is gathered and used in the classification process. Table 5-1 to Table 5-3 contains the attributes/features for each utility asset. These tables show the features, the source dataset, and the data types generated after the preparation phase.

5.2.2 Data preprocessing

Data combination was achieved using the intersect tool of the ArcGIS geoprocessing toolbox. This tool combines the different data sources using a unique identifier. Data preprocessing was carried out to identify duplicate records, missing data, erroneous data, and outlier values. Subsequently, corrective measures are applied to each dataset to remove the duplicate, outliers, and erroneous records from the training, validation, and testing datasets. Instances with missing attribute values were either removed or replaced using mean (numeric features) or median imputation (nominal features).

Data preprocessing methods such as feature selection and dimensionality reduction will be executed to reduce the complexity and possibly improve the model's accuracy. Feature selection identifies crucial subsets while eliminating noncrucial and redundant features. The process aims to generate the optimal features to achieve the highest accuracy. In theory, a fewer subset of features also reduces the dimensionality and computational complexity of the models and could increase the classification accuracy (Kuhn and Johnson, 2013). Furthermore, data normalization using the Z-transformation method is performed on the numeric features. The data is shuffled to avoid bias by ensuring that each subset used in the training/cross-validation and testing is representative of the overall distribution of the data (Kuhn and Johnson, 2013).

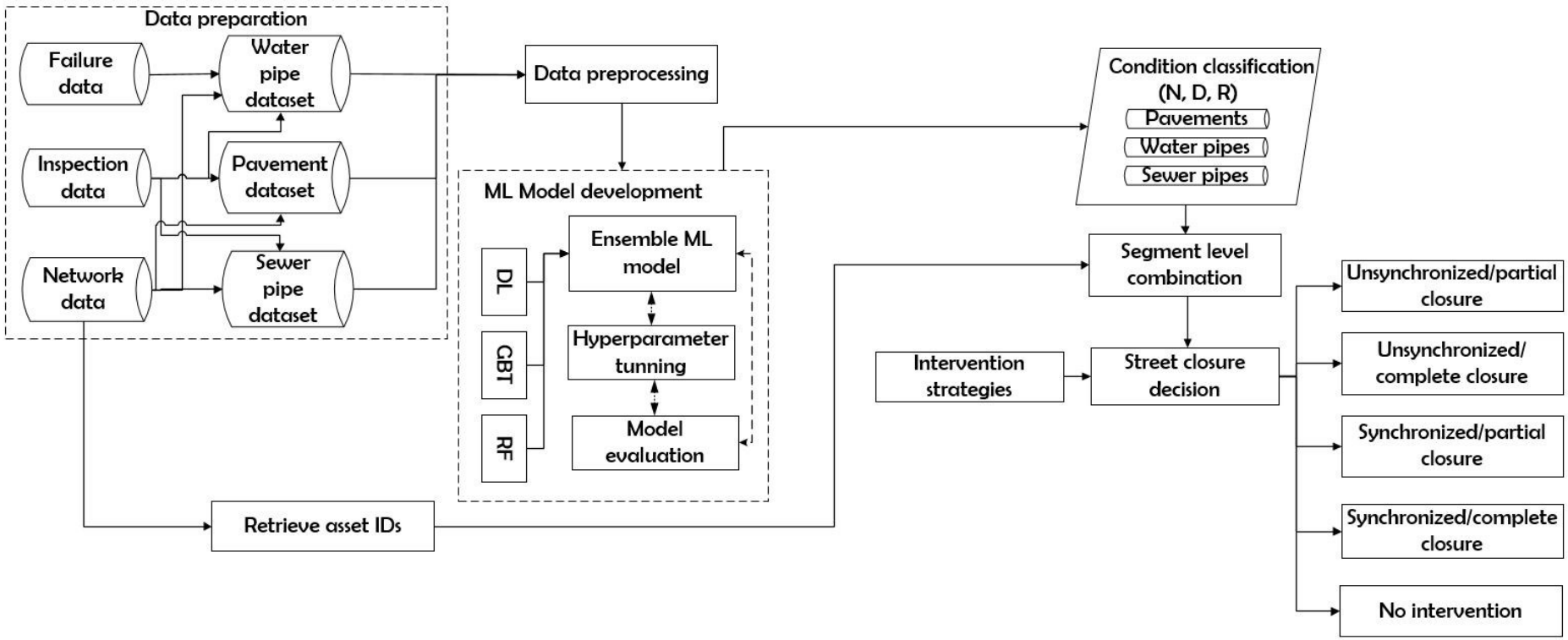

Figure 5-1. Proposed method.

Class imbalance in the training dataset is handled using the Synthetic Minority Over-sampling TEchnique (SMOTE upsampling). SMOTE upsampling uses the K nearest neighbor to find a random neighbor for a subset of randomly selected instances of the minority class and creates new instances (Chawla *et al.*, 2002). The newly created instances for the minority classes balance the missing instances, but they do not provide new information to the model.

Table 5-1. Pavement features.

Source dataset	**Description (Feature name)**	**Type**
Network	Unique street ID (Pavement_ID)	Nominal
	Street class (Category)	
	Type of pavement (rigid or flexible) (Pavement type)	
	Pavement coating material (Pavement coating)	
	Length	Numerical
	Surface area (Surface_area)	
Inspection	PCI (PCI_measure)	
	IRI (IRI_measure)	
	Rutting length (Rutting)	
	Road Intervention class (Label) (Condition)	**Nominal**

Table 5-2. Water pipe features.

Source dataset	**Feature name (description)**	**Type**
Network	Pipe_ID (Water pipe ID)	Nominal
	Material	
	Jurisdiction of the pipe (Jurisdiction)	
	Length	Numerical
	Diameter	
Water pipe breaks	Age	
	Type of failure	
	Break age	
	Sum of lengths of all pipes in the section (T_length)	
	Total number of drinking water pipes in the section (T_n_pipe)	
	Number of drinking water pipes in the street section with a bad status. (N_p_bad)	
Indicators	Break rate (number of water pipe breaks per kilometer per year)	
	Age of drinking water pipe divided by estimated useful life (R_life)	
	Number of previous failures (N_failures)	
	Water Intervention class (Label) (Condition)	**Nominal**

Table 5-3. Sewer pipe features.

Source dataset	Description (Feature name)	Type
Network	Sewer pipe ID (Pipe_ID)	Nominal
	Material	
	Type (Pipe type)	
	Hierarchy (Pipe_hierarchy)	
	Date of pipe installation (Installation year)	Date
	Diameter	Numerical
	Length	
Inspection	Sum of lengths of all pipes in the section (T_length)	
	Total number of sewer pipes in the section (T_n_pipe)	
	Age at inspection divided by estimated useful life (R_life)	
	Remaining life (Rem_life)	
	Number of sewer pipes in the street section with a bad status (N_p_bad)	
	Date of pipe inspection (Inspection year)	Date
	Jurisdiction of the sewer line (Jurisdiction)	Nominal
	Sewer Intervention class (Label) (Condition)	

5.2.3 ML model development

After data preparation and preprocessing, each dataset was split into training/cross-validation and testing datasets. 70% of the dataset was used for training/cross-validation and 30% for testing. The learning model's performance was estimated and improved using the cross-validation process with ten mutually exclusive subsets of equal folds. In addition, each fold was created using either shuffled or stratified sampling. Furthermore, each fold was trained using a voting-based ensemble algorithm consisting of RF, GBT, and DL algorithms. This combination was necessary because the output of each algorithm was diverse and, therefore, the voting generated the highest accuracy. Finally, hyperparameter optimization was done using the grid search technique for each base learner in the ensemble.

5.2.4 Condition classification

Multi-class classification is carried out to determine the conditions of each of the three assets from their independent models. The condition of each asset is labeled using a uniform scale of *N* (No intervention required, assets are unlikely to fail in the near future), *D* (intervention is desirable as assets have an estimated time of failure between 10 to 20 years), and *R* (immediate attention

required i.e., assets have failed or assets likely to fail between 0 to 10 years). However, the focus lies on identifying street segments with conditions with a combination of classes *D* and *R* for all the assets. These conditions determine the required asset-level intervention strategies needed to restore the asset to an *N* condition.

5.2.5 Segment level combination

Figure 5-2 shows a street segment (usually between two intersections) and the spatially collocated assets in the segment. Each segment is assigned a unique identifier, and this ID is assigned to each located asset in the segment in addition to the unique identifier of the asset.

5.3 Intervention Strategies

After classifying the conditions of all three assets, the next step is to determine the asset-level intervention strategies unique to each asset and the segment-level interventions unique to each street segment. These decisions will determine the closures necessary for each segment-level intervention. Most street segments have several water pipes with different diameters and lengths and sewer pipes with varying depths based on the slope. However, in many cases where water and sewer pipes share the right-of-way, a common practice involves burying the water pipes above the sewer pipes to reduce contamination when a sewer pipe failure occurs (Max, 2022; Paige, 2021).

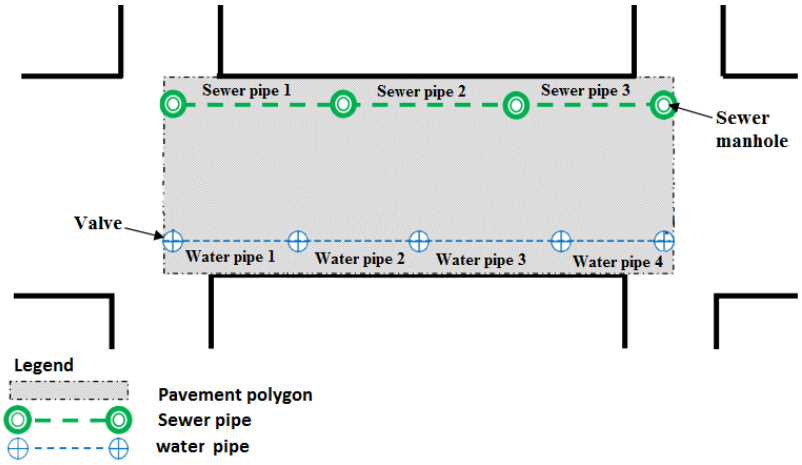

Figure 5-2. Schematic street segment (al Amari et al., 2013).

Therefore, most interventions on the sewer pipes require excavating below the water pipes. This placement method creates an opportunity to implement interventions on water pipes when the main goal is to undertake interventions on sewer pipes (i.e., synchronized interventions). Although this

increases the intervention costs and creates losses due to the premature replacement of water pipes if the water pipes are still in an acceptable condition, it avoids future excavations for the inevitable replacement of the water pipes. In the case of an unsynchronized interventions for a sewer pipe, there is the possibility of damaging the water pipe while assessing the sewer for intervention (utility strikes) (Makana *et al.*, 2018); depending on the sewer pipe condition, trenchless methods such as cured-in-place pipes (CIPP) or sliplining can be used (Najafi, 2010).

The individual intervention strategies depend on the collocated asset and criteria, including the present asset condition, performance indicators (e.g., PCI and IRI for pavements, hydraulic integrity for sewer and water pipes), past intervention practices, etc. Furthermore, synchronized interventions must consider the combined strategies of the collocated assets at a segment level. As shown in Figure 5-3, based on the intervention guidelines of Montreal City, the pavement intervention strategy for R class pavements with $PCI \leq 40$ and $IRI \geq 6$ will undergo a reconstruction (i.e., the complete removal and replacement of existing pavement structure including granular layers) if the pavement is rigid, or a major rehabilitation (i.e., increasing the structural load carrying capacity of the pavement using structural overlays) if the pavement is flexible (Chacon and Normand, 2016). On the other hand, major rehabilitation is required if the pavement condition is bad. In contrast, *D*-class pavements will require minor rehabilitation (i.e., restoring the structural capacity of a pavement structure, e.g., rout and crack sealing). Finally, for *N*-class pavements, no intervention is required. However, these interventions depend on the intervention strategy of other spatially collocated assets (e.g., sewer replacements that require excavations will result in pavement reconstruction rather than rehabilitation). Algorithm 5.1 shows the detailed process depicted in Figure 5-3 and how the pavement intervention strategy is implemented.

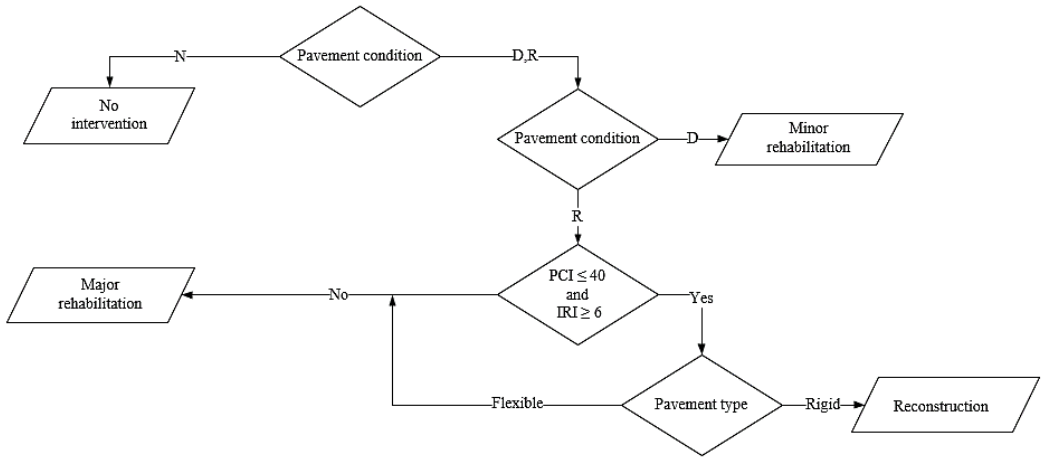

Figure 5-3. Pavement intervention strategy.

Algorithm 5.1: Pavement intervention strategy.

***Input**: Pavement condition (N, D, R), PCI, IRI, and pavement type*
***Output**: Pavement intervention strategy*
for** all segments: **do
{
if** pavement condition == N **then
    Pavement intervention strategy ←No intervention
else if** pavement condition == D **then
    Pavement intervention strategy ← Minor rehabilitation
else:
    if** PCI is less than **40** and IRI ≥ **6** **then
        ***if** Pavement type == Rigid:*
            Pavement intervention strategy ← Reconstruction
        else:
            Pavement intervention strategy ← Major rehabilitation
        end if
    else:
        Pavement intervention strategy ← Major rehabilitation
    end if
end if
}
end for

The sewer intervention strategy shown in Figure 5-4 relies on the condition, hydraulic integrity, and nature of the last intervention executed on the sewer pipe. *N*-class sewer pipes require no intervention, while *D*-class pipes require structural rehabilitation (i.e., extending the service life of an existing sewer pipe using methods such as inserting a sheath inside the sewer pipe). *R*-class sewer pipes are replaced with the recommended diameter if the pipes have lost their hydraulic integrity or if the last intervention conducted on the pipe required structural rehabilitation. Otherwise, structural rehabilitation of *R*-class sewer pipes is conducted. Algorithm 5.2 shows the

detailed process depicted in Figure 5-4 and it expresses how the sequence of the sewer intervention strategy is implemented.

Algorithm 5.2: Sewer intervention strategy.

```
    Input: Sewer pipe condition (N, D, R), hydraulic integrity, last intervention
    Output: Sewer pipe intervention strategy
 1  for all segments do
 2  {
 3    if Sewer pipe condition == N then
 4            Sewer intervention strategy ←No intervention
 5    else if Sewer pipe condition == D then
 6            Sewer intervention strategy ←Structural rehabilitation
 7    else:
 8            if pipe lost hydraulic integrity == true then
 9                  Sewer intervention strategy ←Replacement with a recommended diameter
10            else:
11                  if last intervention == Structural rehabilitation
12                        Sewer intervention strategy ←Replacement
13                  else:
14                        Sewer intervention strategy ←Rehabilitation
                    end if
            end if
     end if
15  }
16  end for
```

Figure 5-5 shows the intervention strategy for water pipes based on the intervention guidelines of Montreal City. This strategy relies on several water pipe attributes: the number of historical repairs, break rate, hydraulic integrity, diameter, material, presence of lead, pipe hierarchy (i.e., ranking assigned by the municipality that is based on the socioeconomic impact of a temporary loss of service), and elapsed life. Similar to the pavement and sewer intervention strategies, *N*-class water will require no intervention, while *D*-class water pipes will also require structural rehabilitation (i.e., extending the service life of a water pipe using methods such as cure-in-place pipe (CIPP)).

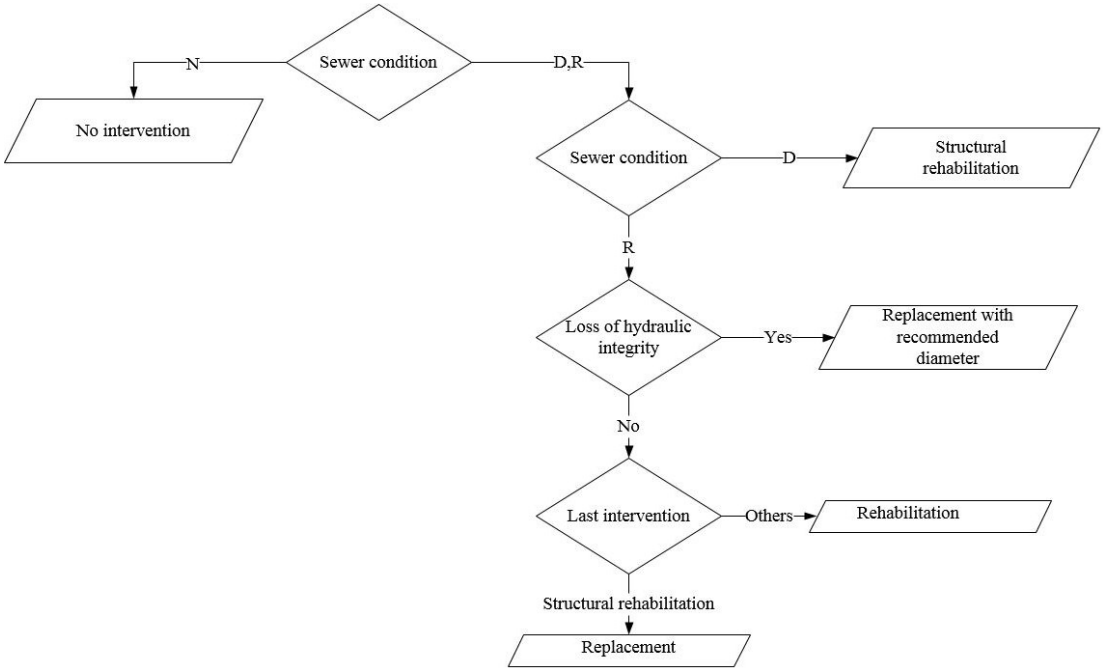

Figure 5-4. Sewer intervention strategy.

In the case of *R*-class pipes, the nature of the intervention is determined by the combination of the different water pipe attribute criteria presented in Figure 5-5. For instance, if the number of historical breaks is less than six and the water pipe has a break rate of less than two, the pipe will undergo structural rehabilitation. On the other hand, if the break rate is greater than two and the number of repairs in the last ten years is greater than two, the pipe is replaced. Furthermore, pipes with a number of historical breaks greater than six that have lost their hydraulic integrity are replaced with the recommended diameter. Otherwise, if their diameter is less than 150 mm, they are replaced with larger-diameter pipes. Pipes with a diameter greater than 1200 mm are replaced, together with pipes with diameters less than 1200 mm made of pre-stressed concrete, installed between 1966 - 1987. Pipes that do not satisfy these criteria and do not contain lead undergo structural rehabilitation. Pipes containing lead and assigned the highest hierarchy (I) are replaced in addition to pipes of lower hierarchy with an elapsed life greater than 90%. Otherwise, the pipes undergo structural rehabilitation. The process depicted in Figure 5-5 is also presented in Algorithm 5.3, and it shows in detail the water pipe intervention strategy.

Algorithm 5.3: Water pipe intervention strategy.

Inputs: *Water pipe condition (N, D, R), number of historical breaks, break rate, loss of hydraulic integrity, Number of repairs, diameter, material, installation date, presence of lead, pipe hierarchy, and elapsed life*

Output*: Water pipe intervention strategy*

```
1   For all segments
2   { if pipe condition == N then
3         Water intervention strategy ←No intervention
4   else if pipe condition == D then
5         Water intervention strategy ←Structural rehabilitation
6   else:
7         if number of historical breaks ≤ 6 then
8               if break rate is ≤ 2 then
9                   Water intervention strategy ←Structural rehabilitation
10              else:
11                  if Number of repairs in the last 10 years ≥ 2 then
12                        Water intervention strategy ←Replacement
13                  else:
14                        if loss of hydraulic integrity == true then
15                              Water intervention strategy ←Replacement with recommended diameter
16                        else:
17                              if diameter < 150 mm then
18                                    Water intervention strategy ←Replacement with larger diameter
19                              else:
20                                    if diameter > 1200 mm then
21                                          Water intervention strategy ←Replacement
22                                    else:
23                                          if Material == stressed concrete & installation date between 1987-1966
                                            then
24                                                Water intervention strategy ←Replacement
25                                          else:
26                                                if presence of lead == true then
27                                                      if pipe hierarchy == 1 then
28                                                            Water intervention strategy ←Replacement
29                                                      else:
30                                                            if Elapsed life > 90% then
31                                                                  Water intervention strategy ←Replacement
32                                                            else:
33                                                                  Water intervention strategy←Structural rehabilitation
34                                                            end if
35                                                      end if
36                                                else:
37                                                      Water intervention strategy ←Structural rehabilitation
38                                                end if
39                                          end if
40                                    end if
41                              end if
42                        end if
43                  end if
44              end if
45        else: go to line 154
47        end if
48    end if }
49  end for
```

Figure 5-6 shows the segment-level intervention strategy used to decide the type of street closures. As presented in the figure, complete closures are necessary when either sewer or water pipes require replacements or when pavements require major rehabilitation or reconstructions. Alternatively, if street segments are completely closed, rather than simply replacing the underground assets, the closures can be considered an opportunity to implement the MUT. On the other hand, partial closures are sufficient when trenchless methods are used for pipe rehabilitation or when the only needed intervention is pavement minor rehabilitation. The process in Figure 5-6 is simplified in Table 5-4, which shows the possible combination of asset conditions, intervention strategies, and street closures decisions at a segment level.

As shown in Table 5-4, there are street segments with a combination such as *N, N,* and *R*. This combination means that although two of the three assets in the segments do not require intervention, a third asset is critical. Suppose the asset in *R* condition is a water or sewer pipe where excavation is required to replace the pipe. In that case, a synchronized intervention is needed due to the reconstruction of the pavement after the pipe replacement is completed. However, if the *R*-class asset is the pavement, it is an unsynchronized intervention requiring a complete street closure for pavement rehabilitation or reconstruction. Unsynchronized interventions could also lead to partial street closures on segments requiring rehabilitation for either *D*-class water or sewer pipes.

On the other hand, a combination such as *R, R*, and *R* could also be considered an opportunity for implementing a MUT. However, MUT placement depends on several other criteria (e.g., utility density, proximity to public facilities, etc.) (Genger et al., 2021); these street segments could be considered potential locations for MUT placement due to the scale of the intervention. In addition, MUTs can also be considered for street segments with water and sewer pipe combinations of *R* and *R* because such sections will require excavation irrespective of the pavement condition. This intervention will lead to the complete closure of the street segment.

Furthermore, synchronized interventions on street segments where either the water or sewer pipe has an *R* and *D* class combination means excavation is required to replace the asset with the *R* condition. In such cases, a replacement is done instead of rehabilitating the *D*-class pipes (Oum, 2017). The replacement of either the sewer or water pipes means excavating the subsurface and subsequently reconstructing the pavement, which is also irrespective of the pavement condition. Therefore, condition combinations representing such scenarios (e.g., *N, D, R*) have been removed from Figure 5-6. Synchronized interventions resulting from combinations such as *R, D*, and *D*,

where the pavement has the *R* condition, will encounter partial and complete street closures. This combination reduces the social costs during the water and sewer pipe rehabilitation phase, where partial closures are needed mainly because trenchless technologies are used (Oum, 2017). After completing the rehabilitation phase, complete closures are required for pavement reconstructions or rehabilitation.

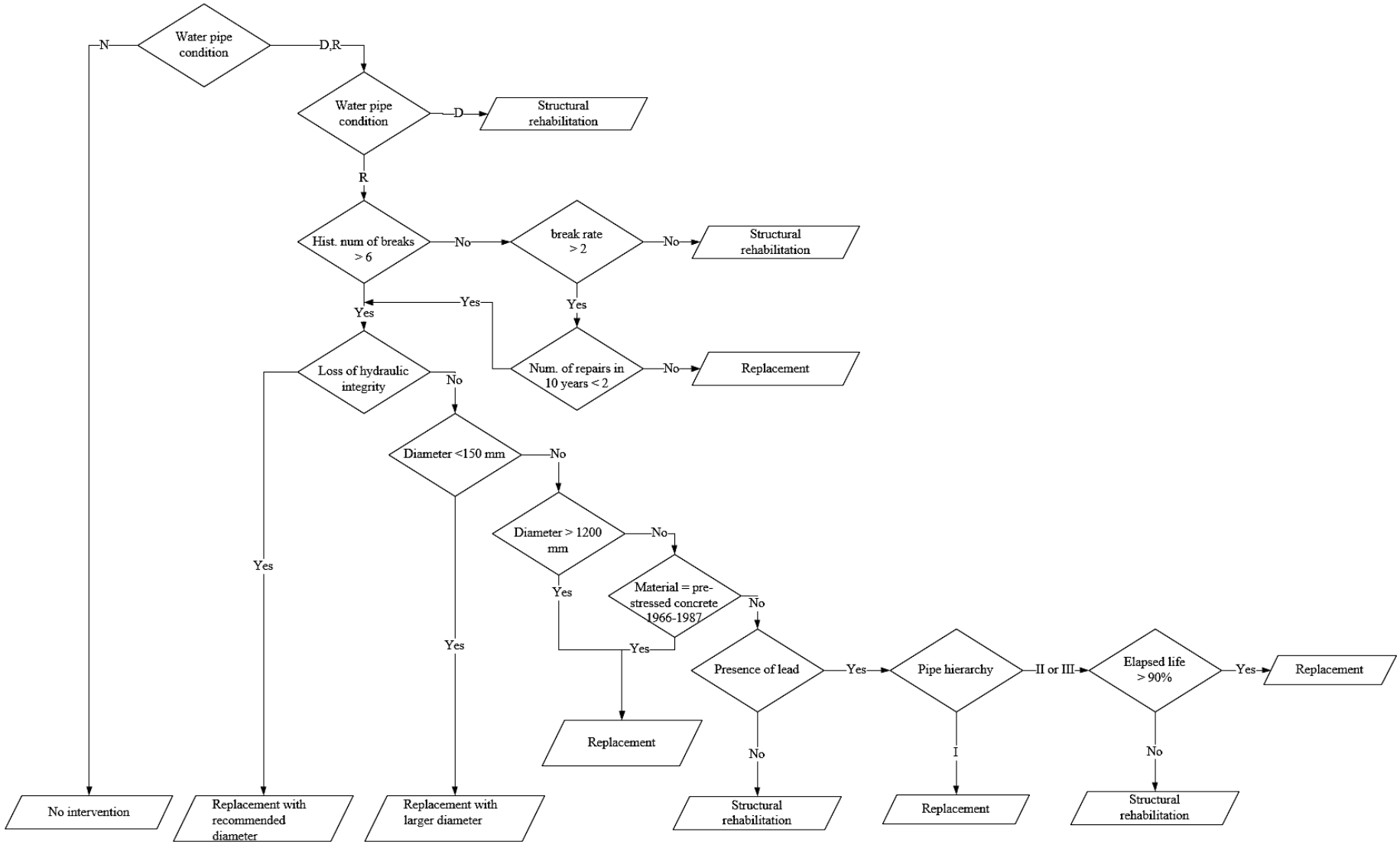

Figure 5-5. Water pipe intervention strategy.

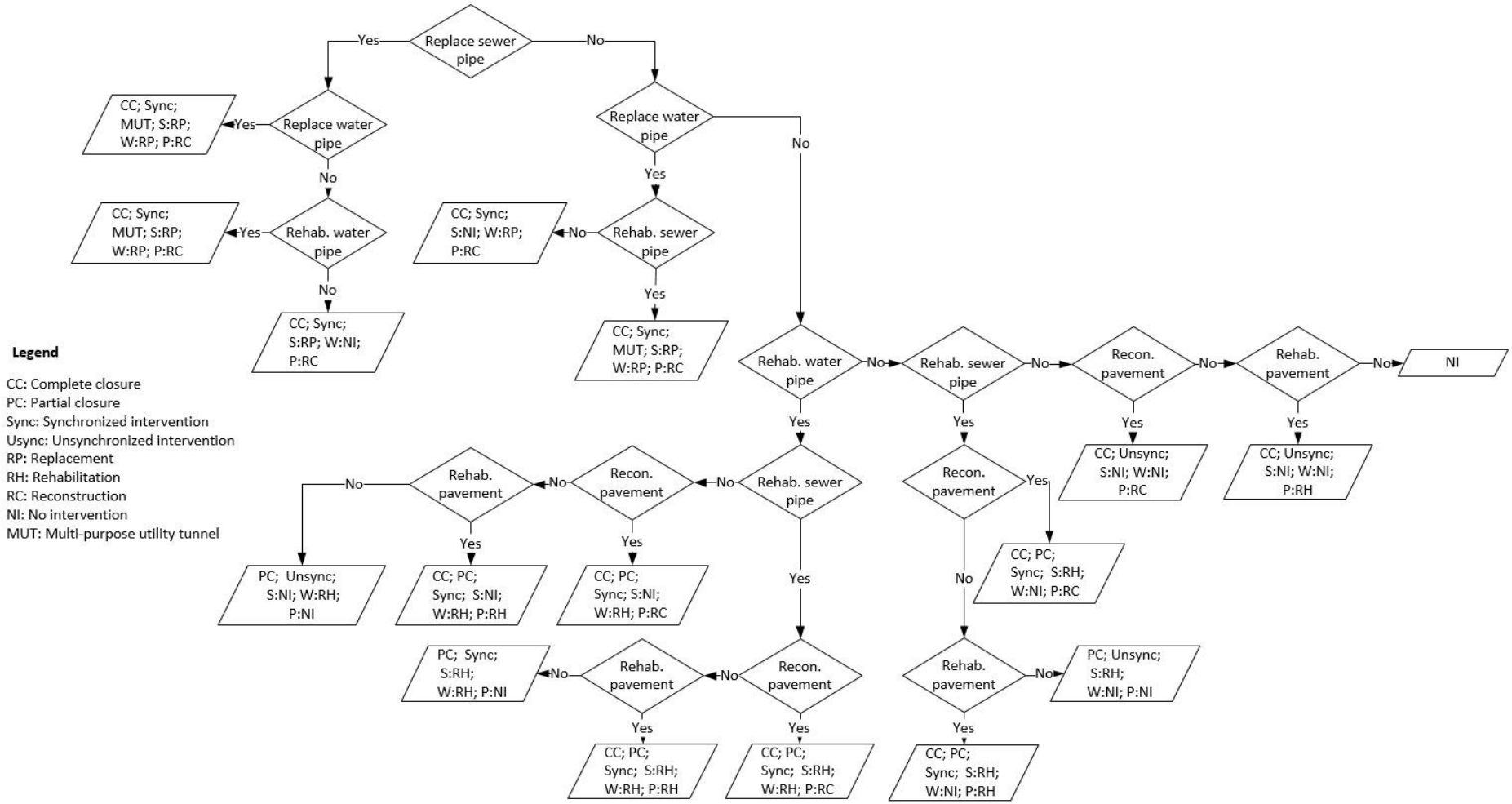

Figure 5-6. Segment-level intervention strategy.

Table 5-4. Possible condition combinations and segment-level interventions.

Condition (Intervention class)			Pavement			Water			Sewer			Synchronized		Unsynchronized		NI
Pavement	**Water**	**Sewer**	**RC**	**RH**	**NI**	**RP**	**RH**	**NI**	**RP**	**RH**	**NI**	**PC**	**CC**	**PC**	**CC**	
D	D	D		✓			✓			✓		✓	✓			
D	D	N		✓			✓				✓	✓	✓			
D	D	R	✓			✓			✓				✓			
D	N	D		✓				✓		✓		✓	✓			
D	N	N		✓				✓			✓				✓	
D	N	R	✓					✓	✓				✓			
D	R	D	✓			✓			✓				✓			
D	R	N	✓			✓					✓		✓			
D	R	R	✓			✓			✓				✓			
N	D	D			✓		✓			✓		✓				
N	D	N			✓		✓				✓			✓		
N	D	R	✓				✓		✓				✓			
N	N	D			✓			✓		✓				✓		
N	N	N			✓			✓			✓					✓
N	N	R	✓					✓	✓				✓			
N	R	D	✓			✓			✓				✓			
N	R	N	✓			✓					✓		✓			
N	R	R	✓			✓			✓				✓			
R	D	D	✓				✓			✓		✓	✓			
R	D	N	✓				✓				✓	✓	✓			
R	D	R	✓			✓			✓				✓			
R	N	D	✓					✓		✓		✓	✓			
R	N	N	✓					✓			✓				✓	
R	N	R	✓					✓	✓				✓			
R	R	D	✓			✓			✓				✓			
R	R	N	✓			✓					✓		✓			
R	R	R	✓			✓			✓				✓			

***Notes**: RC: Reconstruction, RH: Rehabilitation, NI: No intervention, RP: Replacement, PC: Partial closure, CC: Complete closure*

5.4 Street Closure Decisions

The social costs caused by street closures include traffic delays for pedestrians and vehicle users, increased travel time, loss of municipal revenue (e.g., parking meters), etc. Several factors such as the size of the excavation, traffic volume, policies enforced by transportation ministries of municipalities, the estimated duration of the intervention, etc., also contribute to deciding on partial or complete street closures (Valdenebro *et al.*, 2019). However, for worker safety and to ease the movement of heavy machinery and equipment, most interventions on the right-of-way require the complete, partial, or both complete and partial closures of street segments (le Gauffre *et al.*, 2002a; Matthews *et al.*, 2015; Oum, 2017). Another practice involves undertaking intervention activities at night for streets with high traffic volumes and temporarily covering the excavated area with steel plates during the day to reduce the impact on both pedestrian and vehicular traffic (City of Charleston, 2013; Klimas, 2020). Therefore, it is safe to assume that the decision to either partially or entirely close a street segment for intervention is based on the combined (segment-level) intervention strategy of the spatially collocated assets in the street segment.

Figure 5-7 presents the process of determining the street closure decisions. The output of the ML process (the asset condition classes) is combined with the criteria values extracted from the inspection data to determine the asset-level intervention strategies. Asset-level interventions are then combined at a segment level using the segment-level intervention strategies outlined in Figure 5-6. The outcomes are asset-level interventions combined at a segment level and the corresponding street closure decisions.

5.5 Implementation and Case Study

All ML processes were performed on a computer with the following specifications: Ubuntu 20.04.3LTS, AMD Ryzen Threadripper 3960x 24-core processor x 48 threads, and 251 GB memory. RapidMiner Studio Educational 9.10.001 is used to build all ML processes. The GBT and DL algorithms were executed using the H2O 3.30.0.1 (RapidMiner, 2020, 2021) . H2O is developed by H2O.ai as an open-source machine learning and deep learning for applications. H2O uses a supervised training protocol for its deep learning architectures, unlike other architectures that use a combination of unsupervised pretraining and supervised training. It uses in-memory

compressions techniques and implements ML algorithms such as Linear and logistic regression, Naive Bayes, etc. (Candel and Parmar, 2015).

The dataset comprises all boroughs in Montreal. However, a part of the data was reserved from the Ville-Marie Borough to implement the intervention strategies and street closures. Considering that several machine learning data processing and splitting processes involve random sampling, this reserved dataset was necessary to ensure that all three models had a common area that could be later analyzed at a segment level. Based on the city block sizes, the intervention dataset is structured by the geomatic department of the City of Montreal to capture segments with a length of approximately 200 m. The average length of each street segment is 212 m.

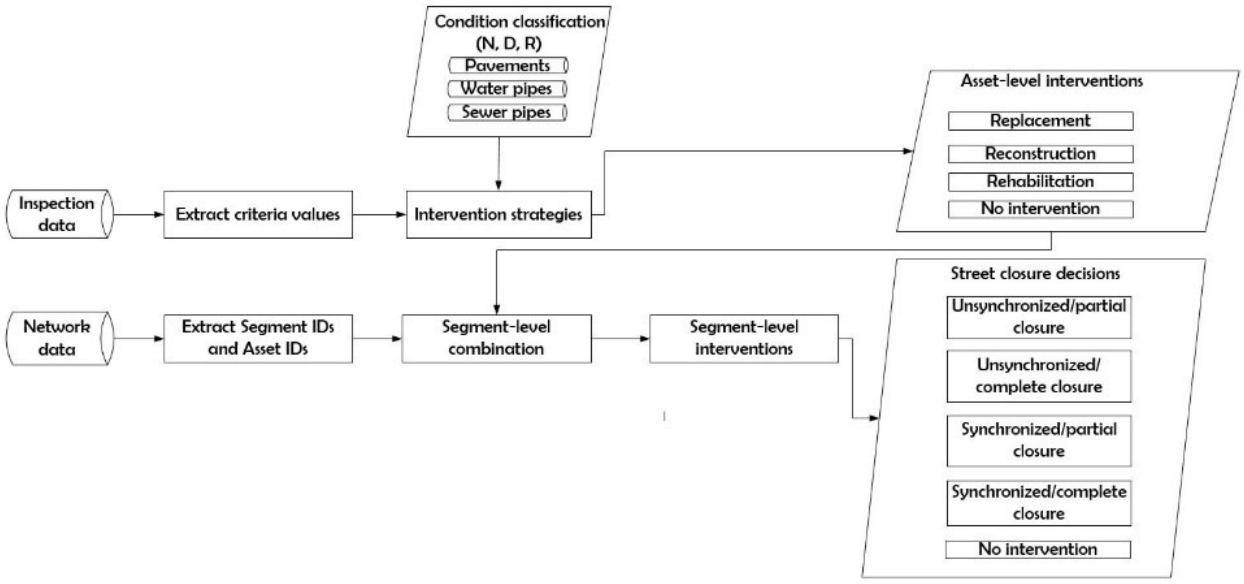

Figure 5-7. Street closure process.

Table 5-5 to Table 5-7 summarize the features of all three assets, and Figure 5-8 is a sample street segment showing all three municipal assets. The list of pavement features used in this research does not include AADT. This feature was removed from the dataset because it had 76% missing values. Its removal is compensated by features such as the road class, pavement surface area, and two indicators (PCI and IRI), whose values are correlated to traffic volume (Amin and Amador-Jiménez, 2017). Both indicators provide valuable information on pavement condition classification, as street segments may have an excellent IRI and a poor PCI or vice versa (Genger and Hammad, 2022).

The pavement model uses eight input features in the classification process. Numeric features such as the *surface area* and *length* were normalized using the Z-transformation method. Other numeric features (i.e., PCI, IRI, and rutting length) were not normalized, as normalizing them did not improve the model's accuracy.

Table 5-5. Summary of pavement features.

Number of road segments	15,603
Performance condition index (PCI) Average PCI	1-100 52
International roughness index (IRI) Average IRI	0 – 13.9 5
Rutting (m) Average rutting	0-50 4.79
Pavement coating	Asphalt, cobblestone, concrete, crushed stone
Average length (m)	212
Average surface area (m^2)	2,245.1
Category	Arterial, local
Pavement type	Rigid, flexible
Pavement condition	**N, D, R**

As shown in Table 2-4, apart from some water pipe features (i.e., depth, soil, and pressure), most of the features used by other researchers were also used in this research in addition to others not listed in the table (e.g., age at the time of break (*break_age*) and break rate). The failure data for the water pipe model was only available for 30% of the total number of pipes in the dataset. Its inclusion in the model was necessary to determine the conditions of the water pipes, although this meant reducing the dataset. The output of the data preparation and preprocessing phases on the water pipe dataset resulted in 13 features.

In terms of the sewer condition classification, several features such as the slope, pressure values, and soil type, alongside failure data, are unavailable for this research. Therefore, the sewer model uses 13 features in the classification process as shown in Table 5-1.

Unlike the pavement model, data normalization was performed on all the numeric features in the water and sewer pipe model. Other data preprocessing methods, such as discretization and the conversion of nominal to numeric data types, were applied; however, they did not improve the accuracy of the models. Also, several feature selection techniques (i.e., forward selection, backward elimination, and optimized selection) alongside dimensionality reduction processes (i.e.,

Principal component analysis) were applied at this stage of data preprocessing. However, these processes did not improve the classification accuracy of the models.

The sewer dataset was imbalanced as most pipes had the *N* condition. The SMOTE upsampling process was applied twice to the training/cross-validation dataset to rectify the imbalance of the *D* and *R* classes.

Finally, the cross-validation process was applied to ten mutually exclusive subsets of equal folds for all three models. However, stratified sampling was used for the sewer pipe model to create each fold randomly. Using stratified sampling further ensured an equal class distribution of the classes in each fold. At the same time, both the pavement and water pipe models used shuffled sampling.

Table 5-6. Summary of water pipe features.

Number of pipes	127,716
Mean age (yrs.), Std. Dev.	73.84 40.79
Major materials	Gray cast iron, ductile iron, copper, reinforced concrete, etc.
Jurisdiction	Local, metropolitan area, centre ville, etc.
Diameter range (mm)	15-3,900
Average pipe length (m)	215.4
Break rate (brk/km/yr) Average break rate	0-15 0.5
Break age	1–149
N_failures (Number of failures in the section) Average	0–15 0
R_life (age/estimated useful life) Average	0–1.68 0.55
T_length (Average total length of pipes in a section) (m)	286.3
N_p_bad (Number of pipes in a street section with a bad or very bad status) Average	0–8 0.21
N_p_segment (Number of pipes in a street section) Average	1-27 1.48
Water pipe condition	**N, D, R**

Table 5-7. Summary of sewer pipe features.

Number of pipes	119,857
Major materials	Reinforced concrete, grey font, brick, PVC, ductile iron, etc.
Pipe type	Combined, sanitary
Hierarchy	I, II, III
Installation year	1900-2015
Diameter range (mm)	75-5,325
Average length (m)	54.19
T_length (Average total length of pipes in a section) (m)	254.19
T_n_pipes (Average number of pipes in a section) (m)	5
R_life (Inspection age/estimated useful life**)** Average	0–3.48 0.45
Rem_life (Remaining life) Average	1-212 71
N_p_bad (Number of pipes in a street section with a bad or very bad status) Average	0-12 1.14
Inspection year	1993-2015
Jurisdiction	Local, arterial
Sewer pipe condition	**N, D, R**

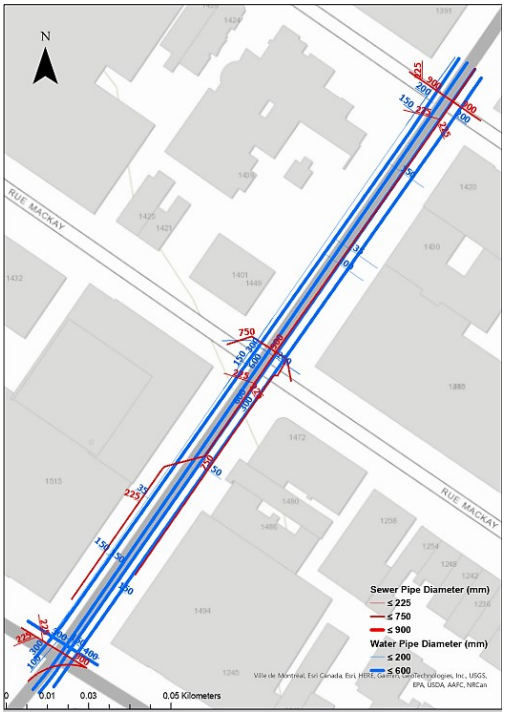

Figure 5-8. Sample street segment.

5.5.1 Data preparation and preprocessing

Data used in this research was obtained from three primary sources, including intervention and network data for all three assets and the failure data for only the water pipes. The collected datasets were combined with the intersect tool of the ArcGIS geoprocessing toolbox. The resulting Shapefiles were converted to excel files using the ArcGIS Table-to-Excel toolbox (Esri, 2016b).

5.5.2 Feature importance

The weights assigned by each classifier determine the importance or contribution of each feature in the ML classification process. In addition to the weights assigned to each feature, the DL algorithm also assigns weights to each feature value with a nominal data type. All three base learners in the ensemble assign different weights to each feature. This difference results in different classification outputs. For example, as shown in Figure 5-9(b) and Figure 5-9(c), both GBT and DL assign the highest weight to PCI, followed by IRI, whereas the RF model assigned the highest weight to pavement length as shown in Figure 5-9(a). Furthermore, Figure 5-10 shows that all three base learners assigned the number of pipes in a street section with a bad or very bad status (*n_p_bad*) feature as the most important in classifying the sewer pipes. In addition, Figure 5-11 shows that all three algorithms assigned the highest weight to different features in the water pipe model.

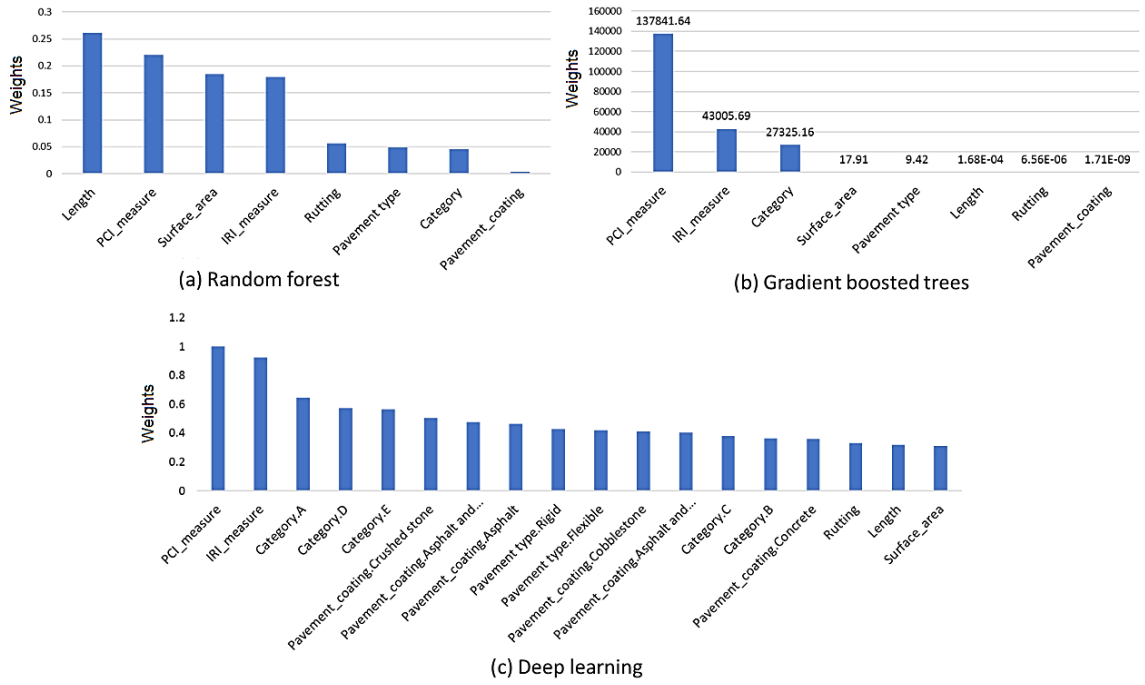

Figure 5-9. Pavement feature weights

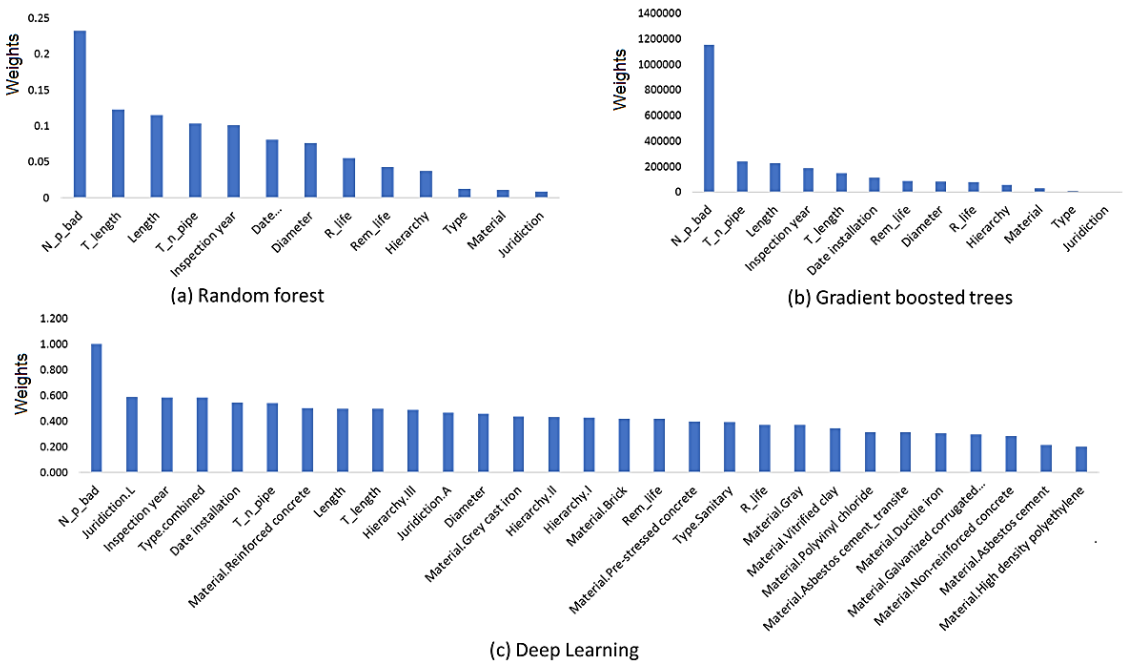

Figure 5-10. Sewer pipe feature weights.

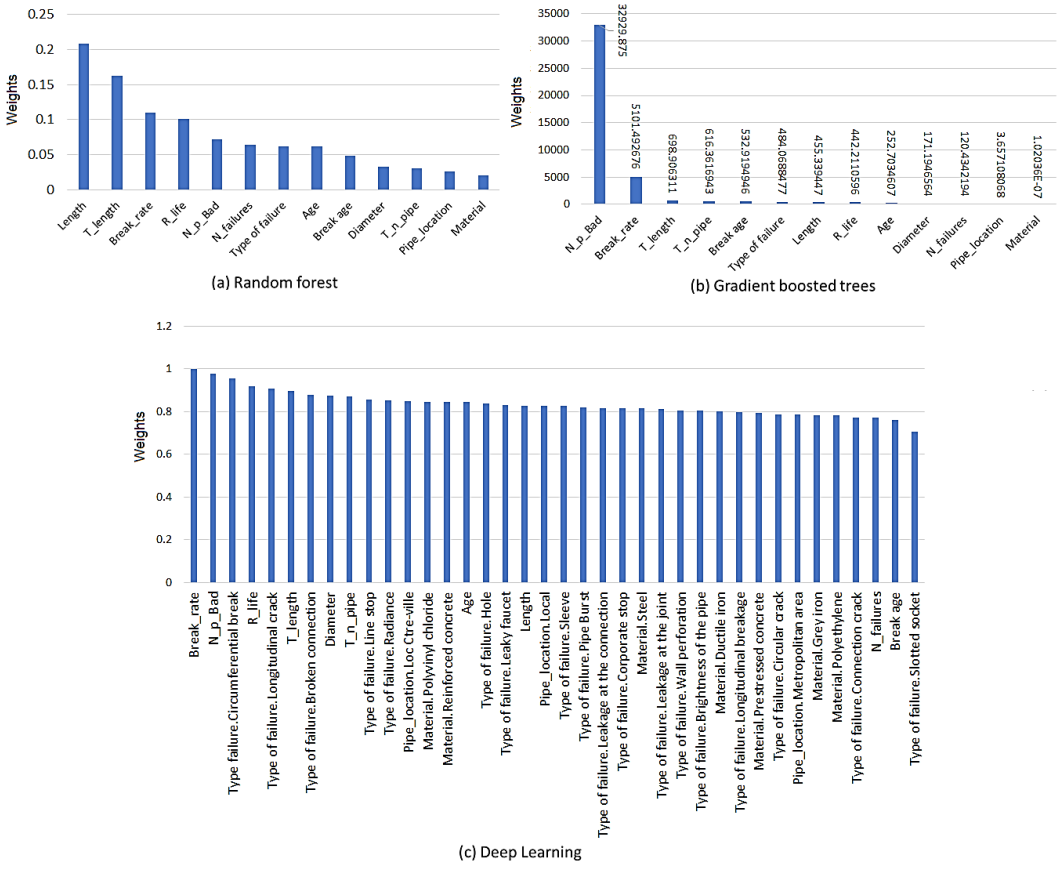

Figure 5-11. Water pipe feature weights.

5.5.3 ML modelling

5.5.3.1 Hyperparameter tuning

Hyperparameter tuning was done on the parameters of all three models using a grid search (Guo *et al.*, 2021; Pei *et al.*, 2022). Table 5-8 shows the hyperparameter values, the search range, and the selected values used to obtain the accuracies of each ML model for all three infrastructure assets. The models are trained using the combination of every single value (i.e., exhaustive search) in the search range, to find an optimal parameter set that is guided toward improving the accuracy of each model. Different parameters have different effects on the learning algorithm and the selected parameters had the highest influence on the performance of each base learner. For example, a high number of trees in the RF model may lead to a generalized model however, it may also increase the complexity of the model and slow down the training process. On the other hand, the GBT model generally requires relatively more trees as presented in Table 5-8. The maximal depth signifies the nodes of each tree in the forest. The higher the number of nodes, the more the splits and captured information. However, a relatively high maximal depth may lead to overfitting and a failure to generalize the model. Therefore, as presented in Table 5-8 each of these two base learners (i.e., RF and GBT) are trained using relatively low maximal depths. In the case of the GBT algorithm, the use of a small learning rate helps prevent overfitting by reducing the overall variance of the model. Due to the imbalanced nature of the sewer dataset, a relatively high number of epochs was used in its DL model as compared to the other DL models. This high number of epochs resulted in a significant increase in training time because the weights are recalculated for each layer during each pass of the entire training dataset. The value of k (i.e., the number of neighbors to consider) was the only parameter changed in the SMOTE upsampling process. All other parameter values for each algorithm retain their default values. The following sections elaborate on the performance of the ML models based on the outcome of the hyperparameter tuning.

Table 5-8. Searched range and hyperparameter values for the ML algorithms.

ML algorithm	Hyperparameters	Range searched	Selected values		
			Pavement	Water pipes	Sewer pipes
RF	Number of trees	{30-500}	190	41	90
	Splitting criterion	Gain ratio, Gini index, Information gain	Gini index	Gini index	Gini index
	Maximal depth	{1-40}	19	16	8
GBT	Number of trees	{10-1000}	500	200	300
	Maximal depth	{4-8}	5	5	8
	Learning rate	{0.01-1}	0.08	0.01	0.01
DL	Activation	Tanh, Rectifier	Rectifier	Rectifier	Rectifier
	Number of hidden layers {Size of hidden layers}	1-5{1-200}	3{200,100,200}	3{100,100,100}	3{150, 150,150}
	Epochs	{10-2000}	10	11	1000
SMOTE upsampling	K	{2-5}	-	-	2

5.5.3.2 Pavement classification model performance

Table 5-9 presents the comparison of the base models with the ensemble model of the pavement classification model. The results presented in the table are based on the test dataset and the hyperparameters of each base model are the same as those presented in Table 5-8. Based on the performance metrics used in the multi-class classification of the pavement conditions, the ensemble model outperformed all the individual base learners. The difference in the accuracies of the RF, GBT, and DL base models when compared with the ensemble algorithm is 0.06%, 0.23%, and 1.89%, respectively.

Table 5-9. Comparison of the base and the ensemble models on the pavement test dataset.

Algorithms	Accuracy (%)	Precision (%)	Recall (%)	Kappa
Random Forest	98.58	98.49	97.85	0.98
GBT	98.41	98.17	97.68	0.95
DL	96.75	96.72	95.67	0.95
Ensemble	98.64	98.58	97.92	0.98

Table 5-10 shows that using the ensemble algorithm on the training/cross-validation dataset generated an accuracy of 98.66% and Kappa = 0.98. Applying the model to the test dataset generated an accuracy of 98.64%, Kappa = 0.98. The breakdown of the classification of all three

classes is in the confusion matrix presented in Table 5-11. The confusion matrix shows that the model correctly classified all street pavements with N and D conditions with a precision of 100%. However, only 71 street segments with actual R conditions were misclassified as D; this brought the precision for D conditions to 95.73%.

Table 5-10. Pavement ensemble model performance.

	Accuracy (%)	Kappa
Training dataset	98.66	0.98
Test dataset	98.64	0.98

Table 5-11. Confusion matrix of the pavement ensemble model applied on the test dataset.

	True N	True D	True R	Class precision (%)
Predicted N	2498	0	0	100
Predicted D	0	1593	71	95.73
Predicted R	0	0	1066	100
Class recall (%)	100	100	93.76	

5.5.3.3 Water pipe classification model performance

The comparison between the base models and the ensemble model is presented in Table 5-12. Like the pavement comparison results, the RF model has the highest accuracy when compared to the other two base models with a slightly lower accuracy when compared to the ensemble model. Furthermore, the DL model has the lowest accuracy, which could be associated with the relatively small datasets used in the water pipe classification model.

Table 5-12. Comparison of the base and the ensemble models on the water pipe test dataset.

Algorithms	Accuracy (%)	Precision (%)	Recall (%)	Kappa
Random Forest	96.31	89.21	89.50	0.90
GBT	95.59	87.95	88.05	0.89
DL	94.85	85.92	86.19	0.87
Ensemble	96.37	89.86	89.93	0.91

Table 5-13 shows the performance of the water pipe classification model on both the training/cross-validation and testing datasets. The model's accuracy on the training and testing datasets is 97.27% and 96.37%, respectively. The test dataset's Kappa value (0.91) shows that only a small number of the expected classification is achieved by chance. Furthermore, all pipes in class *N* were correctly classified with precision and recall at 100%, as shown in Table 5-14. In addition, pipes in classes

D and *R* were also classified with a precision of 80.13% and 89.44%, respectively. However, the *D* and *R* classes have 88.97% and 80.89% recall values.

Table 5-13. Water pipe ensemble model performance.

	Accuracy (%)	Kappa
Training dataset	97.27	0.93
Test dataset	96.37	0.91

Table 5-14. Confusion matrix of the water pipe ensemble model applied on the test dataset.

	True N	True D	True R	Class precision (%)
Predicted N	946	0	0	100
Predicted D	0	121	15	80.13
Predicted R	0	30	127	89.44
Class recall (%)	100	88.97	80.89	

5.5.3.4 Sewer pipe classification model performance

Table 5-15 presents the comparison between the ensemble models and the base models for the sewer pipe condition classification. The results show the diversity in the classification results of the base models and how their combination in an ensemble improved the overall classification of the sewer pipe condition model. Unlike the water and pavement models where the DL algorithm is outperformed by the other two algorithms, the DL algorithm has the highest accuracy. This relatively higher accuracy can be attributed to the size of the dataset, as the sewer dataset is larger than both the water and pavement datasets. Also, the RF algorithm has the lowest performance and a relatively low kappa value of 0.58.

Table 5-15. Comparison of the base and the ensemble models on the sewer pipe test dataset.

Algorithms	Accuracy (%)	Precision (%)	Recall (%)	Kappa
Random Forest	74.97	66.56	71.51	0.58
GBT	78.21	67.34	70.86	0.61
DL	79.62	66.60	65.88	0.61
Ensemble	82.38	89.86	89.93	0.67

The sewer condition model results are presented in Tables 5.17 and 5.18. The model's training/cross-validation and test datasets accuracies are 86.22 and 82.38%, respectively. The corresponding Kappa values for both datasets are 0.79 and 0.67. The test dataset also shows the

imbalance of the test dataset, with condition labels N and R having relatively higher instances than the D label. In addition, the Kappa value of 0.67 for the test dataset shows a substantial strength of agreement as only 0.33 was observed by chance.

Table 5-16. Sewer pipe model performance.

	Accuracy (%)	Kappa
Training dataset	86.22	0.79
Test dataset	82.38	0.67

Table 5-17. Confusion matrix of the sewer model test.

	True N	True D	True R	Class precision (%)
Predicted N	7485	432	277	91.35
Predicted D	476	2851	420	76.09
Predicted R	285	473	710	48.37
Class recall (%)	90.77	75.91	50.46	

5.5.4 Intervention strategies

Finally, the ML model was applied to the dataset used to test segment-level interventions and street closures. The accuracies of all ML models on this dataset are presented in Table 5-18. Based on the segment-level intervention strategies, Figure 5-12 shows the actual intervention map, and Figure 5-13 is the predicted intervention map for street segments. Both maps show street segments where no intervention, unsynchronized, or synchronized interventions are needed and the nature of the street closures. Street segments with no information on the collocated assets are labeled as no data. When comparing the actual and predicted sets of segment-level interventions, there was a 79.92% similarity.

Table 5-18. Accuracy of the models on the street closure dataset.

Ville Marie subset data	Accuracy (%)
Pavement	96.79
Water pipe	94.70
Sewer pipes	70.17

5.6 Sensitivity Analyses

In this research, the sensitivity analysis is achieved by systematically ablating the most influential input features identified in Section 5.4.2 to see how they affect each asset model's performance.

Apart from the removed input feature of each model, other input features remain unchanged. Processes that include hyperparameter tunning and cross-validation are performed while retraining the ensemble models, and the results on the street closure dataset are compared using the evaluation metric used in the previous section.

Firstly, in the ensemble pavement classification model, the results of the feature importance show that both DL and GBT are influenced by the *PCI measure.* Therefore, it is ablated from the ensemble model. Secondly, in the sewer pipe model, the number of pipes in a street section with a bad or very bad status (*n_p_bad*) is removed since all base models assigned it as the most important feature in their classification processes. Lastly, the sensitivity of the water pipe classification model to *pipe length*, *n_p_bad*, and *break rate* features was conducted by removing each feature one after another, while keeping the other two features. Table 5-19 presents the results of the sensitivity analysis on all three models and the degree of influence of each ablation process.

According to the results of the sensitivity analysis on the pavement model, the removal of the *PCI_measure* from the input features reduced the model's accuracy by 12.02%. This difference in accuracy shows that the pavement condition classification is sensitive to *PCI*, which is consistent with the results of previous studies. On the sewer classification model, the removal of the *n_p_bad* feature resulted in reducing the model's accuracy by 18.84% and a relatively low Kappa value of 0.29.

Table 5-19. Sensitivity analyses on the ensemble models using the street closure dataset.

Model	Accuracy before ablation (%)	Feature removed	Accuracy after ablation (%)	Kappa after ablation
Pavement	96.79	*PCI measure*	84.77	0.76
Sewer	70.17	*n_p_bad*	51.33	0.29
Water	94.70	*Pipe length*	92.93	0.81
		n_p_bad	80.65	0.55
		break rate	88.94	0.71

Considering that all three base models assigned the highest importance to this feature, this result is expected. Based on the three ablated features, the water pipe classification model is more sensitive to the *n_p_bad* feature which, when removed from the input features, reduced the accuracy by 14.05% with a Kappa value of 0.55. The sensitivity of the model to the *pipe length* and *break rate* is significantly lower, as their ablation resulted in a drop of the accuracy of 1.77% and 5.76%, respectively.

Figure 5-12. Actual segment interventions and street closures.

***Notes**: N.I.: No intervention; S: Sewer pipe, P: Pavement; W: Water pipes; Sync: Synchronized; Unsync: Unsynchronized; RH: Rehabilitation; RC: Reconstruction, RP: Replacement; PC: Partial closure; CC: Complete closure*

Figure 5-13. Predicted segment intervention strategies and street closures.

***Notes**: N.I.: No intervention; S: Sewer pipe, P: Pavement; W: Water pipes; Sync: Synchronized; Unsync: Unsynchronized; RH: Rehabilitation; RC: Reconstruction, RP: Replacement; PC: Partial closure; CC: Complete closure; MUT: Multi-purpose utility tunnel*

5.7 Discussion

This research presents a combination of three independent ML models used to classify the conditions of pavement and underground assets to determine the needed asset-level interventions and the corresponding segment-level interventions leading to street closures. Classifying each asset using a uniform scale enabled the combination of the outcomes of the three models.

This paper uses three labels (*N, D*, and *R*) to signify the different asset condition levels. The pavement condition classification model uses eight essential features in the ML process, including two condition indicators (PCI and IRI), rutting length, pavement material, etc. After hyperparameter tuning, the ensemble ML algorithm generated a classification accuracy of 98.64% with a Kappa value of 0.98 for test data. In addition to pipe features such as break rate, number of failures, etc., the water pipe model also uses the number of bad pipes, the sum of pipes, and the total length of pipes in the street segment for the classification process. Therefore, emphasizing the relationship in the conditions of spatially collocated assets. After optimizing the parameter values of all three ML algorithms in the ensemble, the model generated an accuracy of 96.37% and a Kappa value of 0.91 for the test data.

The classification of sewer pipes uses similar features to the water pipe classification model. However, the model's accuracy (82.38%) is lower than the pavement and water pipe classification models. This relatively low performance is partly due to the imbalanced nature of the sewer pipe dataset and the limited features available. For example, the slope, groundwater level, history of failure, and depth are missing from the dataset.

When the ensemble models were tested on the reserved data meant for implementing the interventions and street closures, the model's accuracy was 96.79%, 94.70%, and 70.17% for the pavement, water, and sewer pipes, respectively, with a segment-level accuracy of 79.92%.

Although the use of an ensemble model, hyperparameter tuning, and SMOTE upsampling, improved sewer accuracy, one main source of uncertainty is the imbalanced nature of the sewer dataset. The relatively low performance of the sewer classification model as compared to both the water and pavement models reduced the overall segment-level accuracy, therefore increasing the uncertainty of the overall model.

Furthermore, each asset condition determined the asset-level intervention strategy (i.e., replacement, rehabilitation, or reconstruction (pavements only)) needed to restore its condition. Based on the intervention strategy needed at the segment level, interventions can be synchronized or not, and the nature of street closures is determined. Some asset-level interventions are changed at a segment level. For instance, pipes with a *D* condition will require rehabilitation at an asset level. However, when combined with an *R*-condition pipe requiring a replacement at an asset level, replacement is done rather than rehabilitating the *D*-condition pipe.

The results also show that some street segments undergo partial and complete street closures to accommodate the pipe rehabilitation phase and the subsequent pavement reconstruction or rehabilitation phase of the intervention. This type of closure reduces the accrued social cost on the street segment because road users can access the street during partial closures. In addition, Figure 13 reveals instances, where neighboring street segments with similar segment-level interventions can be combined into a single intervention, thus, reducing the accrued social costs. The results also reveal street segments where the implementation of the MUT could serve as an alternative to the synchronized method. Although several criteria determine the placement of MUTs on a street segment (Genger et al., 2021), this research can aid in identifying potential street segments which can be subsequently ranked using the criteria for determining the MUT placement.

Although synchronized interventions increase utility cost savings by reducing the number of repeated excavations, introducing the MUT as an alternative technique for street sections, where the combined condition of the assets is in a critical state, increases the lifespan and ease of maintenance of underground utilities. This method of utility placement increases sustainability while avoiding future excavations related to utility interventions in the implemented street segment. GIS maps were used to display the street closures where interventions and subsequent street closures are imminent. These visualizations aid in traffic management (alternative route selection based on the impact on travel time) and intervention budget estimation (direct and social costs) based on the conditions of the individual assets. By classifying the individual conditions of the pipes in a road segment, a more accurate intervention duration can be ascertained.

To our knowledge, the combination of machine learning outputs for multiple assets to aid synchronization has not been done before. Therefore, it is not possible to compare the accuracy of our results with previous research. Instead, Table 5-20 shows the comparison of the results of each model to individual classification models in the literature review. The pavement and water models

outperformed all the previous classification models, and the sewer condition model outperformed all the models except (Tavakoli *et al.*, 2020). However, with a balanced sewer dataset, there is the possibility of improving the accuracy of the sewer classification model.

Table 5-20. Model accuracy comparison.

Asset	**Reference**	**Accuracy%**	**Accuracy % (This research)**
Water	Winkler *et al.* (2018)	96	**96.37**
	Robles-Velasco *et al.* (2020)	85	
	Kumar et al. (2018)	62	
Sewer	Harvey and McBean (2014)	76	**82.38**
	Mohammadi *et al.* (2019)	81	
	Laakso *et al.* (2018)	62	
	Tavakoli *et al.* (2020)	93	
Pavement	(Piryonesi and El-Diraby, 2021a)	88	**98.64**
	Hoang and Nguyen (2018)	87.5	

5.8 Summary

This chapter presents an approach to determining street closures based on the combined conditions of spatially collocated municipal infrastructure assets at the segment level. The use of ensemble ML methods for classifying multi-asset conditions while using a uniform scale for all assets made it applicable for enhancing synchronized interventions at the segment level.

The contributions of this research are as follows:

(1) Developing an ML-based method for systematic condition classification of different spatially collocated underground municipal assets (i.e., pavements, water and sewer pipes) within a segment. Based on this contribution, the following conclusions can be stated:

- The high accuracy of each ensemble machine learning model indicates an acceptable performance in the classification of the spatially collocated municipal assets as shown in Table 5-20.
- Using a uniform classification scale for all three municipal assets enabled the determination of asset-level interventions, whose combination led to segment-level interventions and street closure decisions.

(2) Applying a heuristic approach for determining street closures based on the synchronized or unsynchronized interventions at the segment level induced by combining the interventions of individual assets within each segment. Based on this contribution, the following conclusions can be stated:

- The intervention strategies derived from the applied heuristics were used to determine the intervention unique to restoring the condition of each asset while taking a holistic approach to restoring the conditions of all spatially collocated assets within a segment.
- The predicted segment-level interventions have an accuracy of 79.92%.
- Based on the segment-level interventions, potential street segments for MUT location selections have been identified.
- The segment-level intervention strategies resulted in both synchronized and unsynchronized interventions leading to complete or partial street closures. Some street segments require partial and complete street closures to accommodate the initial pipe rehabilitation phase and the subsequent pavement reconstruction or rehabilitation phase of the intervention.

This research was implemented using a part of the City of Montreal (reserved dataset) that includes approximately 200 street segments. Moreover, this research shows the potential to be scaled up to an entire city with a similar combination of asset features, coupled with the intervention strategies unique to the infrastructure asset owners. This research can also be scaled up to include both municipal and private infrastructure assets.

CHAPTER 6. MULTI-CRITERIA DECISION-MAKING FOR MUT LOCATION SELECTION[4]

6.1 Introduction

As discussed in Section 2.3, due to the limited research in the area of MUT location selection, this chapter is focused specifically on MUT location selection from the point of view of the decision-makers and the data itself. The focus is on analyzing spatial data as input in the MCDM process of selecting the ideal candidate street segment for MUT placement. The objective is to gain insights into how spatial data can be utilized as input to a process to rank pre-selected street segments as potential MUT locations. This objective is accomplished through five specific goals (1) defining the criteria that influence the MUT location selection, (2) defining the required GIS datasets for quantifying these criteria and transforming them into scores for each candidate street segment, (3) analyzing the impacts of the dependencies between the criteria by comparing the ranking results of two MCDM methods (i.e., AHP and ANP) combined with the TOPSIS, (4) analyzing the difference between using subjective weights and objective weights obtained by applying the Entropy MCDM method, and (5) developing a prototype system to integrate the MCDM methods in a GIS platform. The ultimate aim of this chapter is to provide a comprehensive understanding of the MUT location selection process and the crucial role that spatial data can play in this decision-making process.

6.2 MCDM Module

This chapter provides a general method for MUT location selection using a combination of MCDM techniques and GIS spatial analysis, as shown in Figure 6-1. The method is broken into four phases: the criteria definition, selection and scoring of the alternatives, aggregation, and decision-making. This research focuses on the ranking of street segments for MUT placement using 12 criteria that are based on the literature review. They include annual average daily traffic, road class, the density of the utilities, population density, number of expected excavations, underground development projects, land-use, proximity to public facilities, proximity to high-rise buildings, soil type, the slope of the terrain, and proximity to the floodplain.

[4]This chapter is based on the following journal paper:

Genger, K.T., Luo, Y. and Hammad, A. (2021), "Multi-criteria spatial analysis for location selection of multi-purpose utility tunnels", Journal of Tunnelling and Underground Space Technology, Pergamon, Vol. 115, p. 104073.

Different sets of weights are estimated using both AHP and ANP. The ranking of the street segments is achieved using TOPSIS. To determine the effects of the dependencies considered in the ANP methodology, the weights and the subsequent ranking results are compared. However, both ranking results are then compared to the output obtained from using Entropy weights applied in TOPSIS to determine which method (AHP or ANP) closely relates to an objective approach for a set of alternative MUT locations.

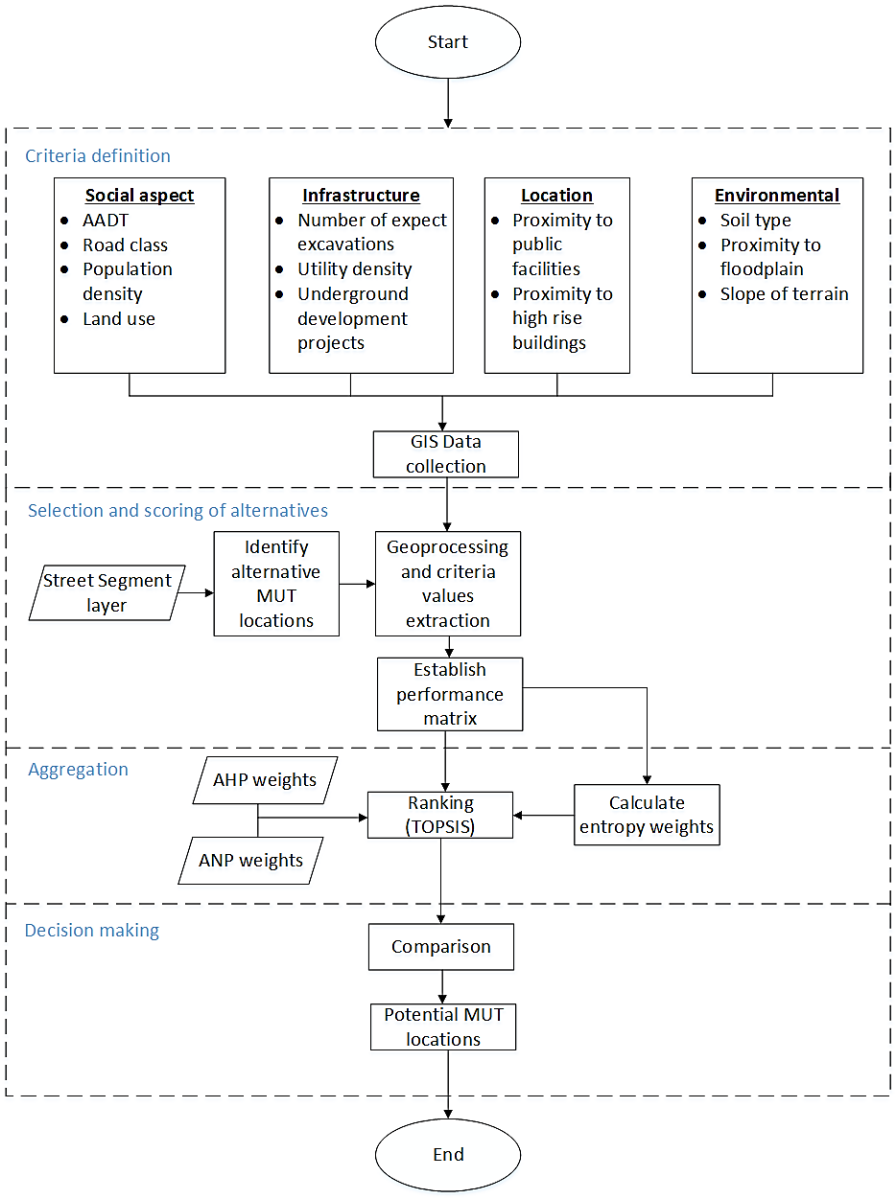

Figure 6-1. Proposed MCDM method.

6.2.1 Criteria definition

The MCDM process starts with defining the criteria and gathering the data related to each criterion in the MUT location selection process. Table 6-1 contains the 12 criteria used in the MCDM process and the possible GIS layers that could be used in generating the value of each criterion. Both the AHP and ANP models comprise four groups of criteria that further contain sub-criteria. These groups address different aspects of selecting a location for MUT placement in an urban or existing city. The social aspects and location groups address issues relating to the end-users (e.g., social cost generated from vehicular traffic and pedestrian delays, etc.) and the justification of the high construction cost with regard to the benefits of MUTs. The infrastructure cluster focuses on the benefits to the utility network infrastructure and the utility owners and the opportunities that could be constructed alongside MUTs. The environment cluster is mainly related to the method of construction and the utilities hosted in the MUT. The details of calculating or extracting each criterion are as follows.

Table 6-1. GIS data related to criteria.

#	**Criteria**	**GIS Layer**
1	AADT	Road traffic layer
2	Road class	Road class
3	Population density	Population distribution (e.g., Census data)
4	Land-use categories	Land-use layer
5	Number of expected excavations for utility intervention	Future intervention plan, history excavation data for intervention
6	Utility density	Utility networks (water, sewage, steam cool water and gas pipes, electricity and telecom cables, etc.)
7	Underground development projects	A layer of future underground projects (i.e., metro, underground roads, tunnels, etc.)
8	Public facilities	A layer of health facilities, colleges, universities, police departments, commercial centers, etc.
9	High-rise buildings	High-rise buildings layer
10	Slope	The slope of the terrain layer
11	Floodplain	Floodplain layer
12	Soil type	Soil layer

6.2.1.1 Social aspects cluster

(a) Annual average daily traffic (AADT): MUTs reduce the need for excavation for underground asset maintenance; and consequently, they reduce the impact of traffic delays resulting from intervention activities. Therefore, selecting street segments with relatively higher AADT is

paramount. The GIS layer representing the AADT at road intersections can be integrated with the road layer to obtain the AADT for each street segment.

(b) Road class: MUTs should be built under higher class roads (e.g., such as national roads, provincial roads, highways, etc.) because of the transitive relationship between road classification and AADT, and the importance of the continuity of traffic flow. Although there is a dependency between the classification of roads and AADT, road class is also influenced by additional variables such as transit routes and the needs of pedestrians and cyclists. These variables account for the road users that are not captured in the AADT. The road class is scored by assigning each classification a value between 0 and 1 based on its relevance to MUT location selection. This value is assigned using experts' opinions.

(c) Population density: MUTs should provide services to areas with high population density (number of persons per square kilometer) as a means of justifying their high initial cost of construction. Furthermore, areas of high population density tend to have a higher demand for utilities, and this translates to a high utility density. Equation 6-1 is used to calculate the average population density of street segments whose entire length is surrounded by areas with different population densities.

$$PD_{st} = \frac{\sum_{i=1}^{n} length_i \times PD_i}{\sum_{i=1}^{n} length_i} \qquad (6\text{-}1)$$

where PD_{st}=average population density of a street segment; PD_i=population density of a length *i*.

(d) Land-use: Areas with different land-use categories have different needs of MUTs, and they also reflect the number of potential users that do not show in the population density (e.g., day-time users that are reflected in the institution or educational land-use category). Each land-use category is assigned a score between 0 and 1 according to its relevance to the MUTs based on experts' judgment. Furthermore, the average score for street segments surrounded by different land-use categories is estimated using Equation 6-2.

$$LS_{st} = \frac{\sum_{i=1}^{n} length_i \times LS_i}{\sum_{i=1}^{n} length_i} \qquad (6\text{-}2)$$

where LS_{st}=land-use score of the street segment; LS_i=land-use score of a length *i*.

6.2.1.2 Infrastructure cluster

(a) Number of expected excavations for utility repair activities: MUTs would reduce the need for excavations for utility repair activities. Therefore, street segments with a relatively large number of excavations for utility interventions have a high priority for building MUTs. There is a relationship between utility density and the number of expected excavations. It can be assumed that street segments with a higher utility density will have a higher probability of utility interventions. Also, this criterion represents problematic street segments where excavations are frequent due to factors such as the age of the utility assets, material, level of deterioration, etc.

(b) Utility density: MUTs would reduce the frequency of excavation for intervention activities of underground utilities. Furthermore, there is also a higher probability of utility strikes occurring on streets with a high utility density. Therefore, building MUTs under roads with high utility density eliminates utility strikes and their associated costs, and reduces downtime as a result of the disruption of service.

Utility density takes into consideration: (1) The total number of utility pipes and cables, and (2) the sub-type of each utility: based on the diameters of water pipes, the type of electricity cables (single-phase, two-phase, etc.), the pressure of gas pipes, etc. The utility density of a street segment is calculated using Equation 6-3. The utilities buried under the street segments (e.g., electricity cables, sewage, gas, and water pipes) are considered to calculate utility density. The utility sub-type score (e.g., diameter of pipes, type of cables) of each utility type is assigned based on experts' opinions. For each street segment, the length covered by each utility sub-type is multiplied by the score attached to this sub-type. Subsequently, the summation of these values for all utilities is divided by the length of the street segment.

$$UD_{st} = \frac{\sum_{i=1}^{n}\sum_{j=1}^{m} l_{ij}s_{ij}}{l_{st}} \qquad (6\text{-}3)$$

where UD_{st}= utility density of a street segment *st*; n= number of utility types under a road segment; m = number of utility sub-types for each utility of type i; l_{ij}= length of utility type i and sub-type j; s_{ij}= utility score; l_{st} = length of the street segment.

(c) Underground development projects: MUTs can be constructed simultaneously with underground development projects as this will significantly reduce the cost of construction. Therefore, MUTs should be built under roads with new construction of underground

passageways, metro lines, malls, etc. Boolean logic is used to normalize the underground project criterion. Street segments with future underground development projects are assigned 1 and street segments without any underground developments are assigned 0.

6.2.1.3 Location cluster

(a) Proximity to public facilities: Public facilities have a relatively higher demand for utilities (e.g., hospitals, schools, factories, etc.), and the social cost accrued when there is service disruption is relatively higher than regular end-users. Therefore, public facilities would maximize the use of MUTs. The distance of the public facilities to the alternative street segments is calculated. This method was used in scoring the street segments because proximity determines the cost of lateral connections (i.e., longer lateral connections increase the cost of construction). Therefore, the shorter the distance from the MUT to the public facilities, the higher the score and vice versa.

(b) Proximity to high-rise buildings: MUTs should be built near high-rise buildings because the ratio between the number of end-users to the number of lateral connections is higher than that of low-rise buildings. Also, high-rise buildings are correlated to the high density of utility networks. The scoring process is like the criterion of proximity to public facilities.

6.2.1.4 Environmental cluster

(a) Soil type: Different soil types determine the method of construction, construction materials, etc., and consequently, it may increase the initial construction cost. The soil types are assigned a value between 0 and 1 based on their suitability for the location of MUTs. This score is also assigned using experts' opinions.

(b) Slope of terrain: This criterion affects the utility type selection to be hosted in MUTs. The hosting of gravity-based sewage pipes in the MUT may increase construction costs due to the extra excavations needed to meet the slope requirements. Therefore, the slope of the terrain is a factor for MUT location selection.

(c) Proximity to the Floodplain: MUT construction in floodplain areas may considerably increase construction costs. To avoid additional construction costs and the likelihood of future flooding of the MUT, MUTs should not be built in proximity to the floodplain. The distance between

each alternative street segment and the floodplain is calculated. Each alternative is scored based on the distance (i.e., the longer the distance the higher the score, and vice versa).

6.2.2 Selection and scoring of alternatives

The processes involved in this phase include identifying the alternative MUT locations and the use of several geoprocessing techniques in GIS in the extraction or calculation of the criteria scores for each alternative location from the data. These criteria scores are the values that make up the performance (decision) matrix.

6.2.3 Aggregation

This phase of the MCDM process identifies the most suitable alternatives from the available locations. Two sets of criteria weights are calculated using the AHP and ANP methods. These weights and the decision matrix generated in the selection and scoring phase are used in the TOPSIS process to obtain two sets of priority rankings that both represent the subjective ranking of each alternative for the MUT location selection.

The decision matrix is also used in calculating the Entropy criteria weights for the identified alternative locations. The Entropy weights and the decision matrix are subsequently used in generating a third set of priorities using TOPSIS. These priorities signify the objective ranking of the MUT alternative locations. The following sections describe the AHP and ANP models used in generating the subjective weights.

6.2.3.1 AHP model

In the AHP hierarchy, the MUT location selection is the goal and the highest node in the hierarchy. This is followed by the criteria and sub-criteria in the middle and lower levels of the hierarchy as shown in Figure 6-2. All the experts' judgments for each pairwise comparison is aggregated to a single value using the geometric mean (Saaty, 2008), which is then incorporated into the pairwise comparison matrix (PCM). The priority vector (weights) for each criterion is computed from the Eigenvector of the PCM. This represents the weights for each criterion that will be subsequently used in the ranking of the alternatives.

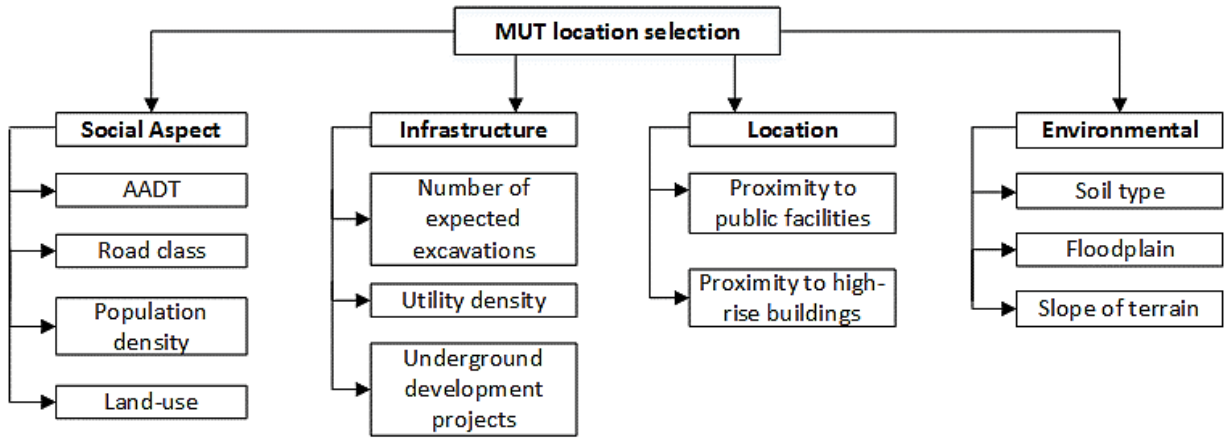

Figure 6-2. AHP model.

6.2.3.2 ANP model

Dependencies exist between some of the criteria that make up the MCDM. Figure 6-3 represents the ANP structure for the MUT location selection problem. The ANP model shows five clusters and the dependencies that exist between/within them. Four clusters group the criteria, and one cluster represents the goal of the MCDM process.

6.3 List of dependencies

Based on the criteria selected for the MCDM process, the relationships that exist are both inner dependencies within a cluster and outer dependencies that exist between clusters. The inner dependencies considered in the social aspect cluster are (1) Land-use and population density: Certain land-use categories have relatively higher population densities than others (e.g., residential land-use has a relatively higher population density than agricultural land-use). To maximize the benefits, MUTs should be built in land-use categories associated with relatively higher population densities. (2) Road class and AADT: The relationship between road classification and traffic volume is such that, higher-classed roads serve both regional and inter-regional traffic movement over long distances. While lower-order classes handle local traffic movements over shorter distances. This does not necessarily mean that higher classed roads always have higher AADT. Although, their importance in terms of traffic interruption due to utility intervention is higher than roads of lower classification where alternative routes may exist, resulting in lower social costs. (3) AADT and Population density: There is a positive correlation between AADT and population density.

The inner dependency considered in the Infrastructure Cluster is; Utility density and Number of expected excavations: Street segments with high utility density tend to have a higher number of excavations regardless of other factors such as age, level of deterioration of the utilities, etc.
The outer dependencies considered are: (1) Utility density and Population density: Ideally, there is a positive correlation between utility density and population density i.e., the demand for utility increases as the population density increases. (2) Land-use and Location Cluster: High-rise buildings or public facilities are mainly concentrated around downtown areas or areas with a diverse mix of residential or commercial land-use categories. Therefore, building MUTs near public facilities or high-rise buildings will also be of benefit to the surrounding users captured by the land-use category. (3) Population density and Location Cluster: This is similar to (2). (4) Utility density and Location Cluster: Public facilities and high-rise buildings generally require more utilities and need a certain level of service to operate efficiently. The cost-of-service disruption due to damage to utility services poses a threat to public safety and human lives in the case of health centers.
Capturing dependencies in the model ensures that the influence these criteria have with respect to MUT placement or with respect to other criteria is recognized by the decision-maker. This recognition is converted to a value via the decision-makers opinions in the pairwise comparison using the nine-point fundamental scale proposed by (Saaty, 2004).

6.3.1 Decision making

All three techniques are based on different concepts; for example, AHP and ANP are based on decomposition, comparative judgments, and priority synthesis (Saaty, 1987). While TOPSIS is based on the distance principle (Jahanshahloo *et al.*, 2006). In Step 4, the ranking results of AHP/ANP are compared to the results obtained from the ranking using Entropy weights applied to TOPSIS. These techniques are compared to determine the variance and similarities in the results obtained from each combination.

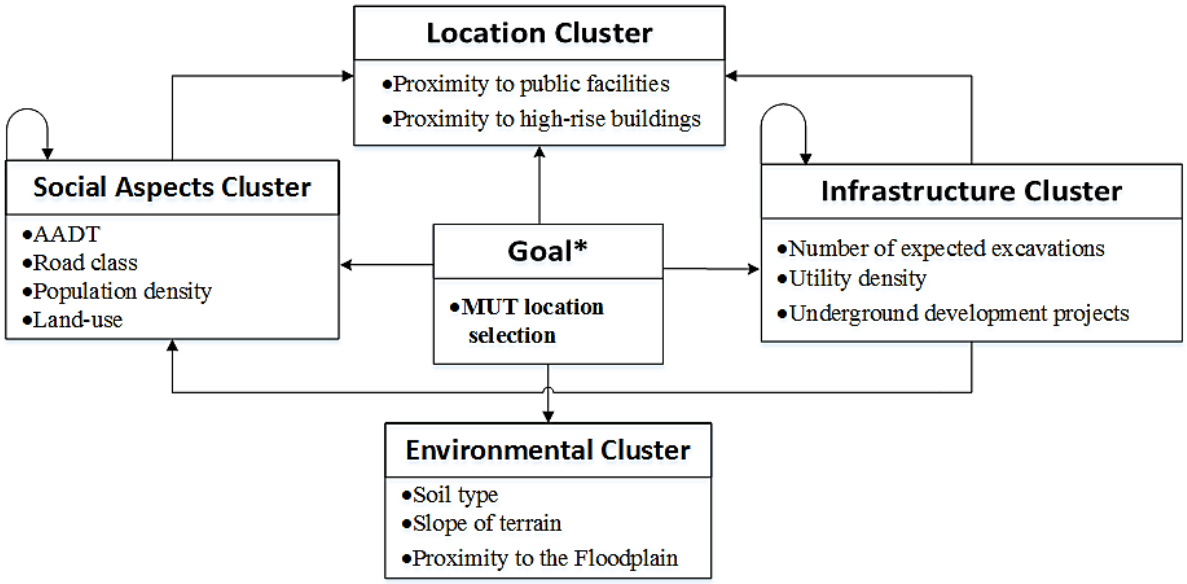

Figure 6-3. ANP model for MUT location selection.

6.4 Implementation and Case Study

6.4.1 Study area and related GIS data

The study area used in the implementation of the MCDM module is shown in Figure 4-2. Table 6-2 presents information on the GIS data used in generating the criteria values for the ten alternative MUT locations. Figure 6-4 shows the locations of the ten street segments that have been selected as the alternative MUT locations. The labels in the figures represent the unique identifiers of each street segment. To have comparable MUT projects of a similar scale, the length of each alternative street segment is about 200 m. The alternative street segments were selected based on attributes like the street's significance in terms of the activities (commercial, education, industrial, etc.) surrounding the street, data availability, and the topology of the utility networks. The maps in Figure 6-5 show the spatial maps generated for 11 criteria, excluding the soil type data which is, currently unavailable. Therefore, all alternatives will be assigned a value of one for this criterion. Figure 6-5 also contains four additional maps that show the utilities (electricity cables, water, sewer, and gas pipes) used in estimating the utility density.

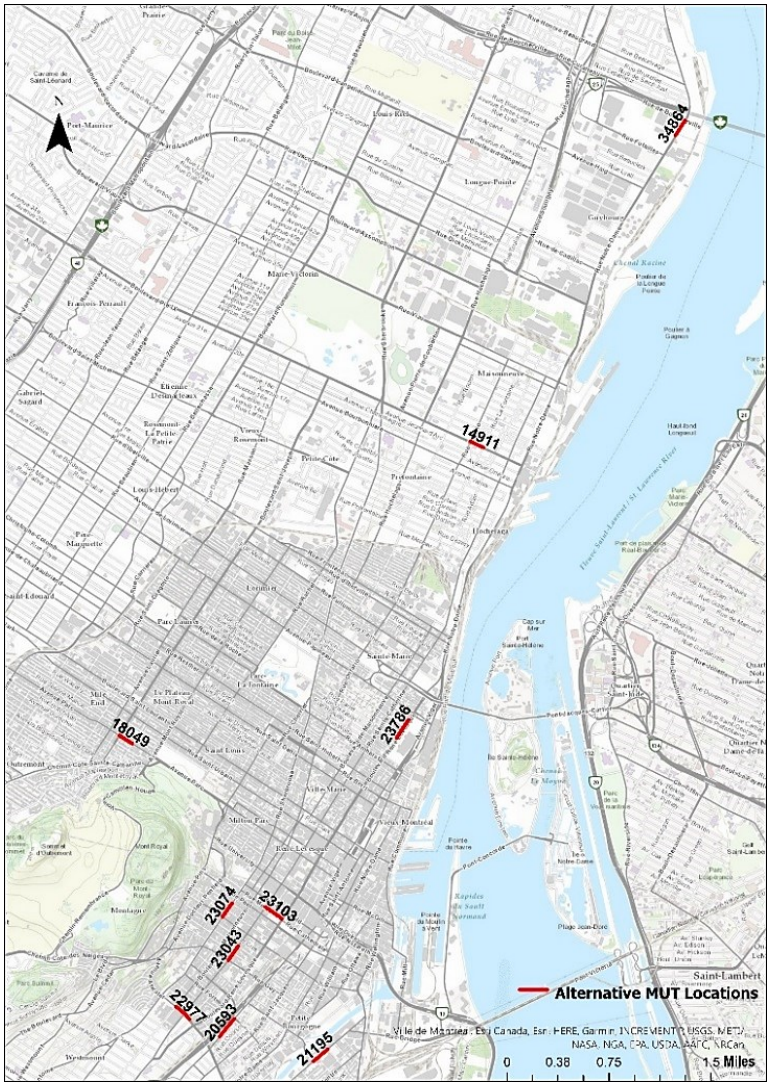

Figure 6-4. The locations and IDs of the alternative street segments.

Table 6-2. Criteria and data sources.

#	Content	Layer	Data Type	Data source	Derived map
1	AADT	Traffic	Polylines	Map of AADT at intersections*	AADT
2	Road	Roads		Map of the existing road network**	Road class
3	Population	Population density	Polygons	Map of census information***	Population density
4	Land-use	Land-use		Map of land-use**	Land-use
5	Intervention plan	Road intervention plan	Polylines	Map of the intervention plan for road, water and sewer network**	Break rate (the number of expected excavations) for the water pipes
6	Utility networks	Water pipes		Map of the water pipe network**	Utility density
		Sewages pipes		Map of the sewer pipe network**	
		Electricity cables		Map of the electricity cable network**	
		Gas pipes		Map of the Gas pipe network*	
7	Future city projects			Map of future underground projects**	Underground development projects
8	Public facilities	Health facilities	Points	Map of hospitals, colleges, universities, police departments, and commercial centers**	Public facilities
		Colleges			
		Universities			
		Police departments			
		Commercial centers			
9	High-rise buildings	High-rise buildings	Points	Lidar point cloud and building footprints**	High-rise buildings
10	Slope	Road network slope	Polylines	Lidar point cloud and road network**	Slope of road segments
11	Floodplain	Floodplain	Polygons	Map of the floodplain**	Floodplain

* Traffic Department, City of Montreal, Geomatics Department of the City of Montreal

**Montreal Open Data Portal

*** Statistics Canada

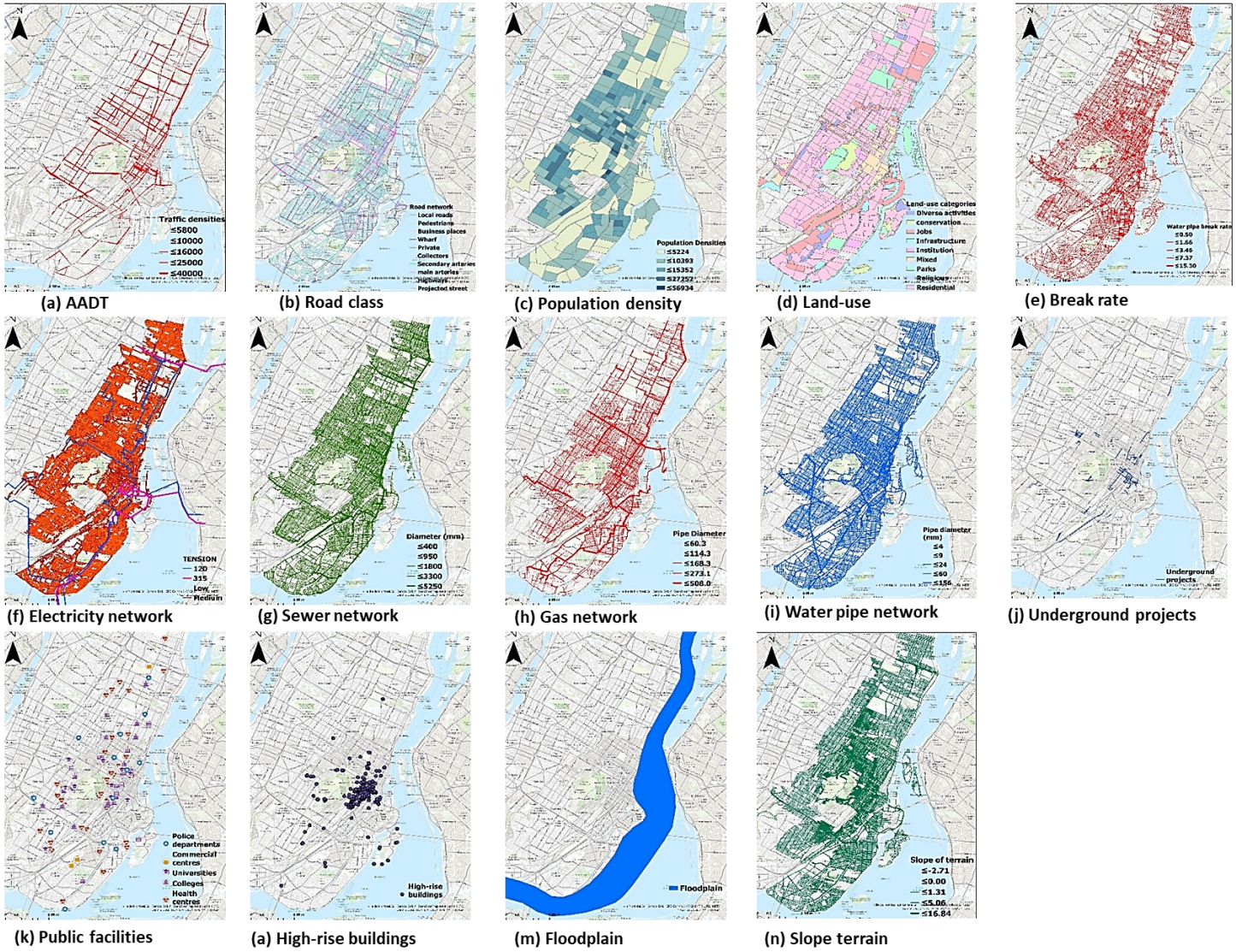

Figure 6-5. Criteria spatial maps.

6.4.2 Criteria data analysis

This section elaborates on the retrieval/estimation of each criterion value from the available datasets.

AADT: Determining the AADT for any street segment required intersecting the AADT layer with the street segments layer. Figure 6-6 shows a GIS representation of a section of the AADT dataset with the color-coding signifying the different traffic densities for several intersections in the study area.

Figure 6-6. AADT layer.

Road class: Table 6-3 contains the 10 classes that represent the road classification in the study area and the score assigned to each class using experts' opinions. This score represents the value of the road class criterion for each alternative.

Utility density: Four types of utilities (i.e., electricity cables, sewage, gas, and water pipes) are considered in calculating utility density. Figure 6-7 is the GIS representation of a typical street segment showing the utilities buried underground. The utilities and the utility sub-types under each street segment are initially extracted from their respective GIS layers and the score for each utility sub-type is assigned. Table 6-4 is an example of the scores assigned to the description of the electricity cables. The total score (utility density) for each alternative street segment is then calculated using Equation (6-1).

Number of expected excavations: This criterion was extracted from two types of GIS data: (1) Historical number of excavations and (2) Intervention plan of utilities and roads. The intervention plan layer contains an attribute about the water pipe break rate. This refers to the number of water

pipe breaks per km per year. Due to the lack of breakage data for other utilities, only the water pipe break rate was used to estimate the number of expected excavations for utility repair. The value of this criterion is extracted for all the alternative street segments. Street segments with missing values were assigned zero values.

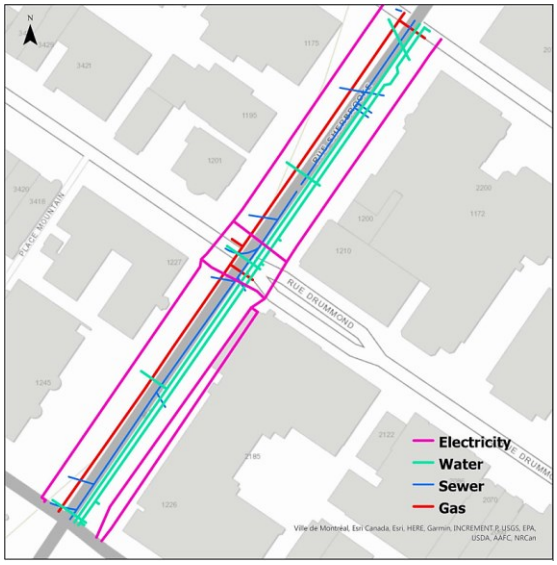

Figure 6-7. Utilities under street segment.

Table 6-3. Assigned road class scores.

Class name	Scores
Main arteries	1.0
Highways	1.0
Collectors	0.8
Secondary arteries	0.8
Business places	0.6
Local roads	0.5
Projected street	0.3
Pedestrians	0.2
Wharf	0.1
Private	0.1

Table 6-4. Sub-type scores of electricity cables.

	Level Score
Neutral	0.9
Secondary principal	0.9
Three-phase	0.7
Two-phase	0.6
Street lighting	0.5
Single-phase	0.4
Connection	0.1

Table 6-5.Assigned land-use scores.

Land-use category	Scores
Diversified activities	1.0
Employment	1.0
Institution	0.9
Mix	0.8
Infrastructure	0.7
Residential	0.6
Religious	0.2
Agricultural	0.1
Preservation	0.1
Park	0.1

Underground development projects: The map for the future city projects of the City of Montreal was intersected with the streets segments layer to identify the alternatives with future underground projects.

Population density: The street segments layer was intersected with the population density layer. Equation (6-2 was used to calculate the average population density for segments that cut across two or more population density polygons (e.g., Figure 6-8).

Land-use: Table 6-5 shows the score assigned to each land-use category. Estimating the score for the land-use criterion is similar to the population density criterion. The criterion score for street segments with more than one surrounding land-use category was calculated using Equation 6-3.

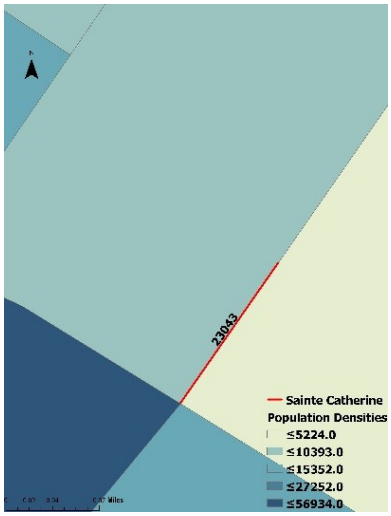

Figure 6-8. A segment surrounded by population density polygons.

Proximity to public facilities: The maps used in determining the proximity to public facilities include health facilities, colleges, universities, police departments, and commercial centers layer. Using the Near method in ArcGIS, the distance between each alternative location and the closest public facility was estimated. The value is used in calculating the score for this criterion. The shorter the distance, the higher the score, and vice versa.

Proximity to high-rise buildings: Like the proximity to public facilities criterion, the distance between the alternatives and the nearest high-rise building is calculated and the criterion value is based on the calculated distance.

The slope of the road segment: Figure 6-9 shows the GIS model for calculating the slope of a road segment**.** Ground points are filtered from the point cloud data (LAS files) and saved in an LASD dataset using the *Make LAS dataset layer* tool in ArcGIS. The subsequent layer is converted to the Digital Terrain Model (DTM) by using the *LAS dataset to raster* tool. The street intersection

layer is converted to points using the *feature vertices to point* tool. This tool iterates through all the line features of the intersection layer and converts all the vertices that make up its geometry to point features. The new feature class is combined with the DTM layer to extract the cell values of the DTM raster. These values represent the elevation of the start and endpoints of the street intersections. This criterion is calculated using the difference in elevation between the start and endpoints of the street segment divided by the length of the road.

Proximity to the floodplain: The Near method was also used in determining the proximity to the floodplain. Alternatives that are farthest away from the floodplain have higher scores. Alternatives with a score of zero are located within the floodplain.

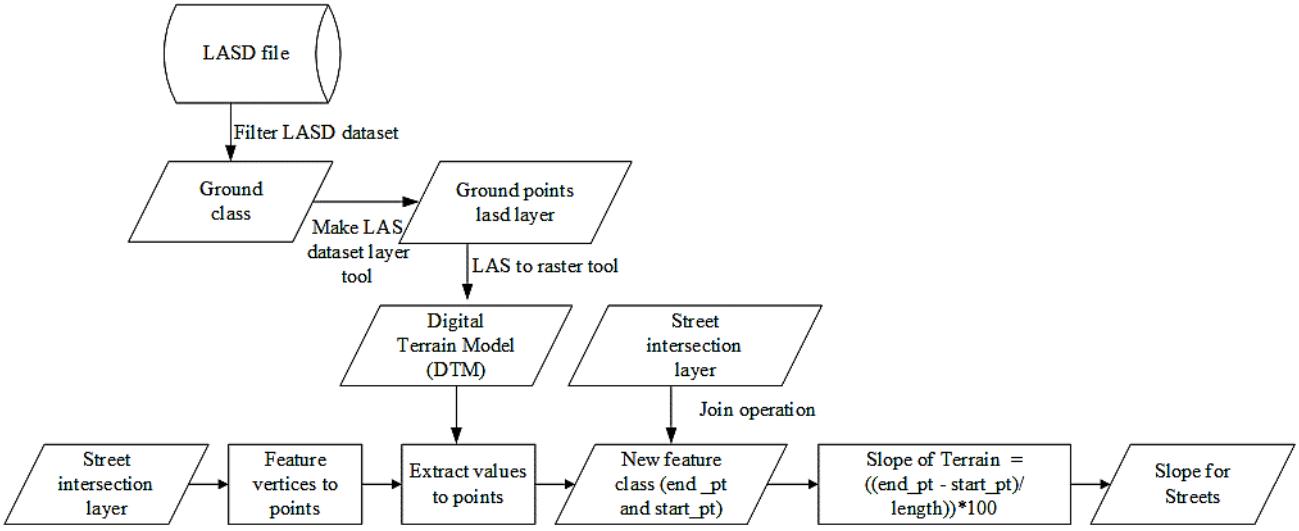

Figure 6-9. Calculating the slope of a street segment.

6.5 GIS Software Prototype Implementation

The tool, *PlaceMUT,* was designed to provide a user-friendly interface that aids decision-making by eliminating the need for calculating the weights for each criterion and the need to generate the attribute scores by using several geoprocessing techniques for each road segment. The user does not need to have prior knowledge of any geoprocessing or database manipulation techniques. The intended use of this software is the automated ranking of street segments based on 12 criteria for the location selection of the placement of MUTs. This software calculates the TOPSIS ranking based on weights obtained from AHP and ANP for the alternative road segments. It also estimates

the objective Entropy weights from the performance values of the street segments selected by the user.

6.5.1 Software architecture

PlaceMUT is implemented in Python 3.6.8 with several open-source libraries. For example, geoprocessing operations are implemented using the Arcpy library (Esri, 2020), and data visualization and numerical operations are done using Matplotlib (John, 2003) and NumPy (Numpy, 2020) respectively. Also, the GUI was designed using Tkinter libraries (Python Software Foundation, 2021), and both the input map (for selecting street segments) and output map (for visualizing the ranking scores) were implemented using C#. In addition, the *archook* module (Ramm, 2017) was used to locate ArcGIS and *arcpy,* thus making them available outside an active ArcGIS Conda environment. Finally, the SQLite3 (SQLite.org, 2014) SQL database engine was used to store the criteria scores for calculating the weights, the normalized scores, and the ranking results. The normalization, TOPSIS ranking codes, and Entropy processes were written from scratch in Python using the steps outlined in Sections 2.5.3 and 2.5.4. The sequence diagram in Figure 6-10 represents the sequence of operations needed to select a set of alternative street segments from the map and prioritize them using all three MCDM methods alongside two ranking methods (results from applying WLC were not included in this paper). Apart from the *User* object, the sequence diagram contains five objects: the *Mapviewer*, the *Main controller* (main Python file), *Geoprocessor*, the *GIS database*, and *MCDM*. The *Mapviewer* object is responsible for receiving and processing user commands, such as displaying selected street segment details and sending the unique identifier to the *Main controller*. The *Geoprocessor* uses queries generated by the *Main controller* to extract the criteria scores from the *GIS database* and subsequently returns the scores to the *Main controller*. The *Main controller* normalizes the scores and sends them to the *MCDM* object for ranking. Finally, the *MCDM* object sends the ranked street segments to the *Main controller*, which forwards the results to the *Mapviewer* object to display them to the *User*. Figure 6-11 is the main interface of the software. Figure 6-12 shows the study area loaded into the input map. Figure 6-13 shows a zoomed-in view of the study area with the labels in red showing the names of the alternative street segments.

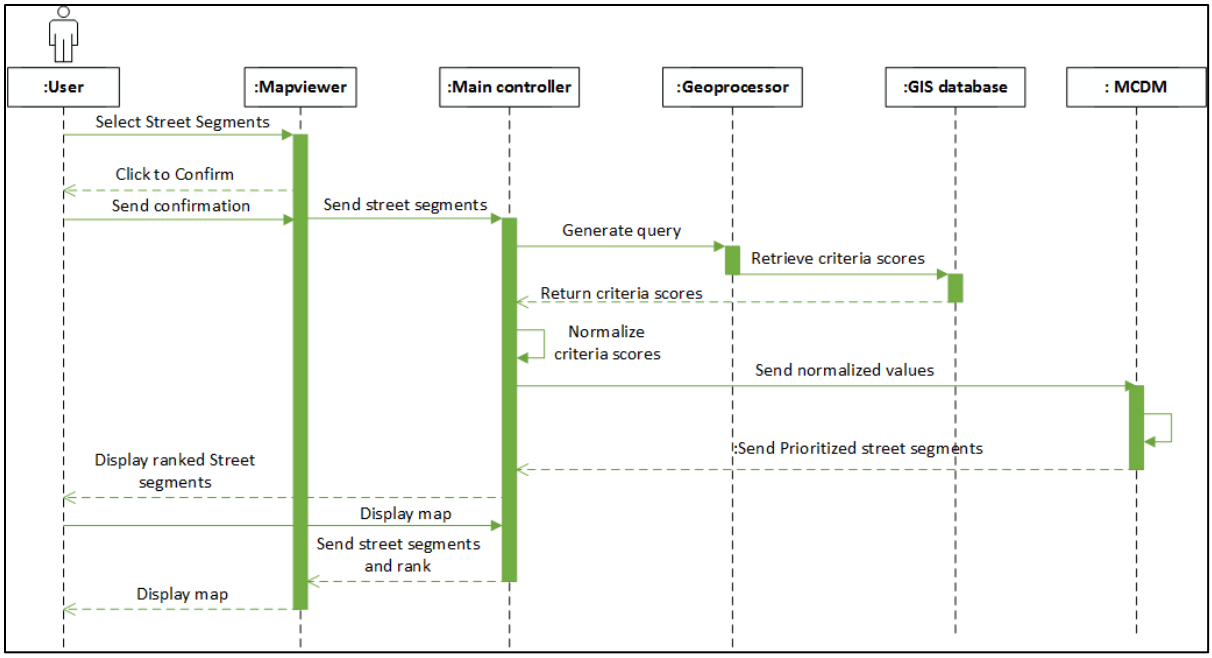

Figure 6-10. PlaceMUT sequence diagram for ranking and displaying a set of street segments.

6.6 Collecting Data for AHP and ANP Methods

The AHP and ANP questionnaires were sent to 15 experts in the fields of urban planning, utility infrastructure management (the City of Montreal, HydroQuebec), telecommunication (Bell and Videotron), engineering, and MUT researchers in the United Kingdom, and Canada to collect the relative importance (preferences) of the criteria used for both MCDM processes. Samples of both questionnaires can be found in Appendix B. By so doing, the level of inconsistency was reduced. The group of experts had a combined consistency ratio of 1.9 % and 2.2% for AHP and ANP respectively, resulting in a consistent subjective evaluation. This was achieved by giving the experts with high inconsistencies the opportunity to review their choices. The choices made by all the experts were then aggregated into a single value for each pairwise comparison using the geometric mean. This value was input as the relative importance for each pairwise comparison judgment. The Super Decisions software version 3.2.0 © (Saaty *et al.*, 2012) was used in calculating the weights derived from the AHP and ANP methods.

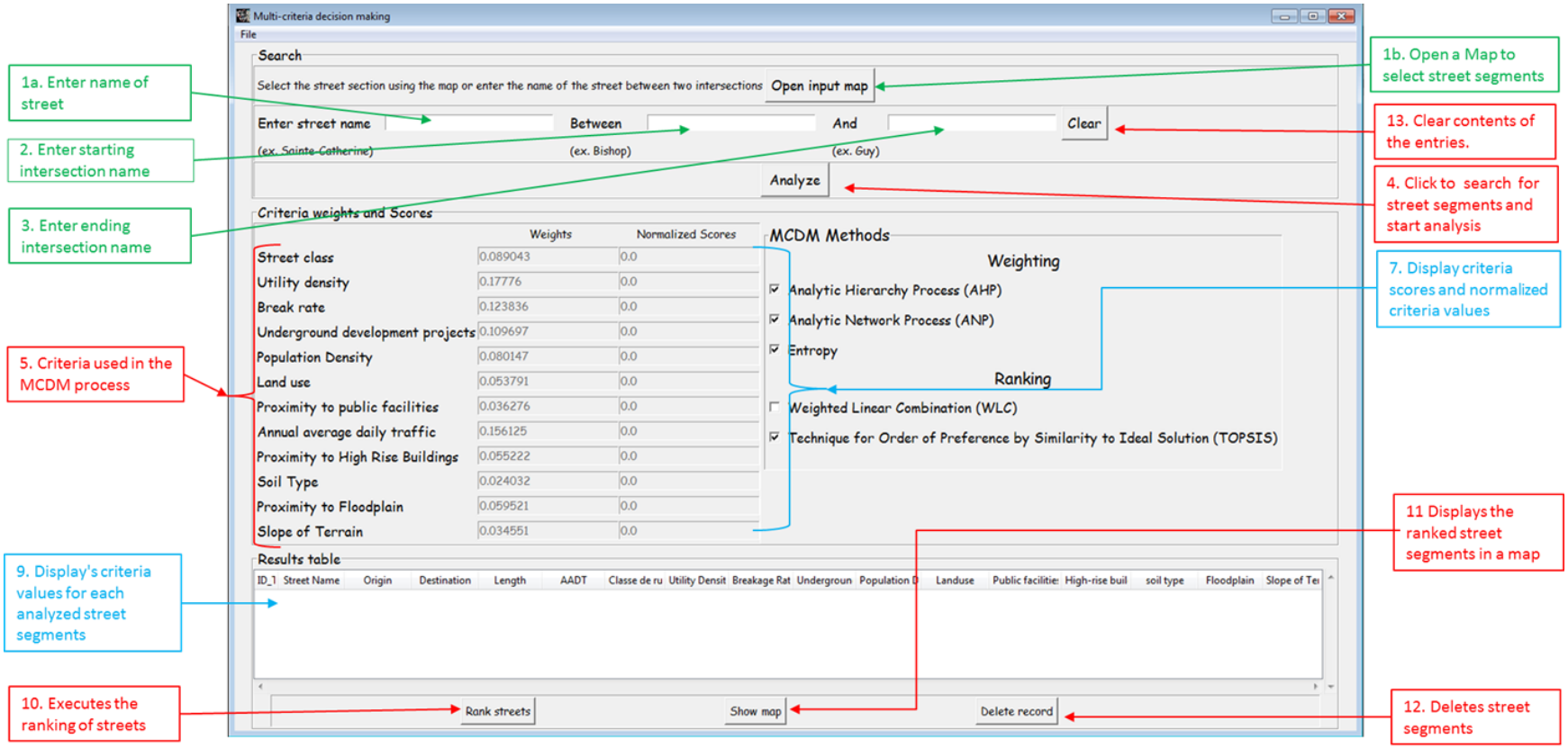

Figure 6-11. PlaceMUT main interface.

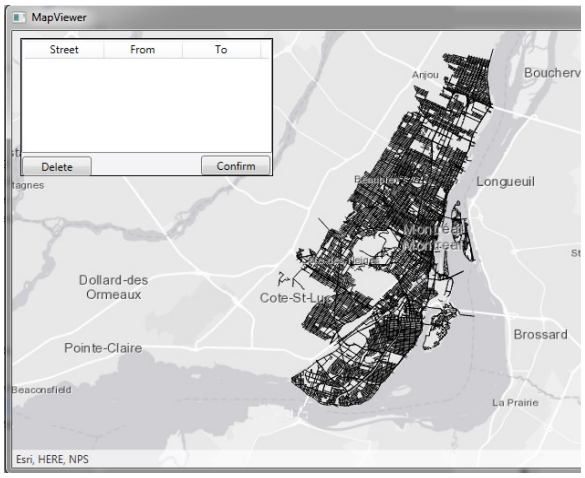

Figure 6-12. Input map.

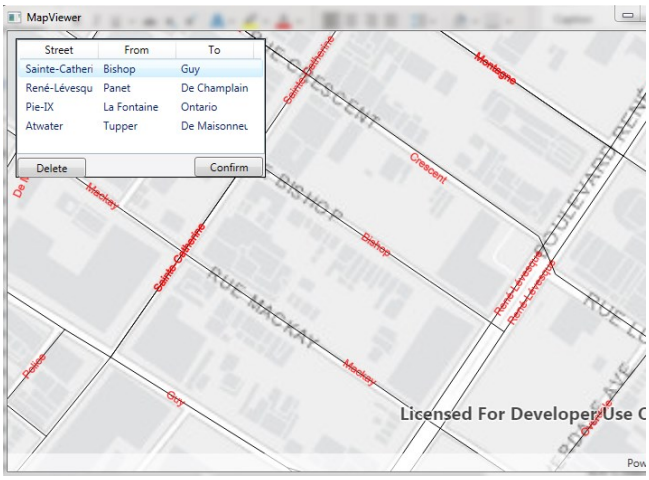

Figure 6-13. Zoomed-in map showing street segments.

6.7 Results and Discussion

This section discusses the results obtained by applying AHP, ANP, and Entropy weights. It also contains information on the ranking of the ten alternative street segments using TOPSIS. Finally, the obtained results are compared and discussed.

6.7.1 AHP weights

Table 6-6 is the aggregated decision matrix used in computing the AHP priority weights of the criteria. Based on the weights, the utility density criterion has the highest priority, followed by the AADT criterion. This shows that the experts agree that MUTs should be constructed under streets with high utility density. There are benefits to this because streets with high utility density are expected to have a relatively higher excavation rate for utility repairs than streets that have lower utility density. This could also potentially reduce the cost of construction via cost-sharing among the utility owners. There is a transitive relationship between utility density and the expected number of excavations. Prioritizing streets with a high utility density and a high expected number of excavations means reducing the excavations, which will reduce the traffic congestion caused by detours and street closures due to the excavations. This is also shown in the AHP weighting results as the experts ranked these three criteria (utility density, the expected number of excavations, and AADT) as the highest. The underground development criterion is ranked fourth. This criterion offers an opportunity to build MUTs alongside underground developments as this reduces the

initial cost of constructing the MUTs. The soil type criterion has the least priority with a weight of 2.4%. The soil type will majorly affect construction costs and its effect can be remedied.

6.7.2 ANP weights

Table 6-7 contains the ANP cluster weights and the criteria weights. Based on the criteria weights, the proximity to public facilities criterion has the highest priority weight with 20.6%. This criterion also has a high cluster weight of 55.7%, accounting for its high criterion value. It is also important to note that street segments in proximity to public facilities are usually also in proximity to high-rise buildings. The street segments that satisfy these two criteria are usually in downtown areas that have high utility density, high population density, and high traffic volume. These three criteria also have relatively high priority weights of 17.5%, 14.4%, and 6.2% respectively. This translates to the importance of building MUTs under street segments that are in proximity to both public facilities and high-rise buildings. The criteria that constitute the environmental cluster have the lowest priority weights with the soil type, distance to the floodplain, and slope of terrain having weights of 0.9%, 2.0%, and 0.9%, respectively. However, the possible impact the soil type and floodplain criteria may have on the implementation of MUTs can be remedied during the construction phase (i.e., soil and structural reinforcement of the MUT). The slope criterion affects the choice of utilities to be installed in the MUT (i.e., in the case of gravity-based pipes), which can also be remedied with the use of vacuum or pumped sewer systems (Islam, 2017).

Table 6-6. AHP aggregated decision matrix.

	AADT	Road class	Utility density	Number of expected excavations	Underground development projects	Population density	Land-use	Proximity to public facilities	Proximity to high-rise buildings	Soil type	Slope of terrain	Proximity to the Floodplain	Priority Weights (%)
AADT	1.00	2.04	0.90	1.10	1.91	1.64	3.96	3.94	2.54	4.36	6.60	2.02	15.6
Road class	0.49	1.00	0.61	0.92	0.92	1.04	1.81	2.49	1.43	4.32	2.35	1.23	8.9
Utility density	1.11	1.64	1.00	1.78	2.35	2.18	4.92	5.12	2.39	5.53	4.79	2.67	17.8
Number of expected excavations	0.91	1.08	0.56	1.00	1.64	1.84	3.73	3.20	2.02	4.32	3.09	1.63	12.4
Underground development projects	0.52	1.08	0.43	0.61	1.00	2.29	2.61	3.68	2.95	4.55	2.79	1.46	11.0
Population density	0.61	0.96	0.46	0.54	0.44	1.00	1.84	2.14	1.18	4.86	2.35	1.52	8.0
Land-use	0.25	0.55	0.20	0.27	0.38	0.54	1.00	1.50	1.35	3.44	2.35	1.22	5.4
Proximity to public facilities	0.25	0.40	0.20	0.31	0.27	0.47	0.67	1.00	1.06	1.43	0.90	0.58	3.6
Proximity to high-rise buildings	0.39	0.70	0.42	0.50	0.34	0.85	0.74	0.94	1.00	3.16	1.52	0.98	5.5
Soil type	0.23	0.23	0.18	0.23	0.22	0.21	0.29	0.70	0.32	1.00	0.68	0.54	2.4
Slope of terrain	0.15	0.43	0.21	0.32	0.36	0.43	0.43	1.11	0.66	1.48	1.00	0.74	3.5
Proximity to the Floodplain	0.49	0.81	0.37	0.61	0.68	0.66	0.82	1.72	1.02	1.84	1.35	1.00	6.0

Table 6-7. ANP cluster and criteria weights.

Cluster	Criteria	ANP cluster weights %	ANP criteria weights %
Social Aspects	AADT	22.1	6.2
	Road class	20.8	5.8
	Population density	51.6	14.4
	Land-use	5.5	1.5
Infrastructure	Number of expected excavations	22.6	7.1
	Utility density	55.7	17.5
	Underground development projects	21.7	6.8
Location	Proximity to public facilities	55.7	20.6
	Proximity to high-rise buildings	44.3	16.4
Environmental	Soil type	23.8	0.9
	Proximity to the floodplain	52.7	2.0
	Slope of terrain	23.6	0.9

6.7.3 TOPSIS ranking results based on AHP and ANP weights

Table 6-8, generated from *PlaceMUT,* presents the unnormalized scores that represent the criteria values (performance values) for the ten alternative locations. Figure 6-14 shows the TOPSIS ranking results for the alternatives using both the AHP and ANP derived weights. TOPSIS ranked the alternatives *Sainte-Catherine* and *Atwater* as the two highest priorities. The alternative *Sainte-Catherine* has the highest number of excavations for utility intervention when compared to the other alternative segments, and it is also the only location with a future underground development project. *Atwater* on the other hand has the highest population density and the second highest AADT and is located in proximity to both high-rise buildings and public facilities compared to the other alternatives. Furthermore, based on both MCDMs and TOPSIS combinations, the alternatives *Saint-Patrick and Notre-Dame* are the ninth and tenth priorities respectively. All other priority positions are slightly different when both MCDM weights are applied.

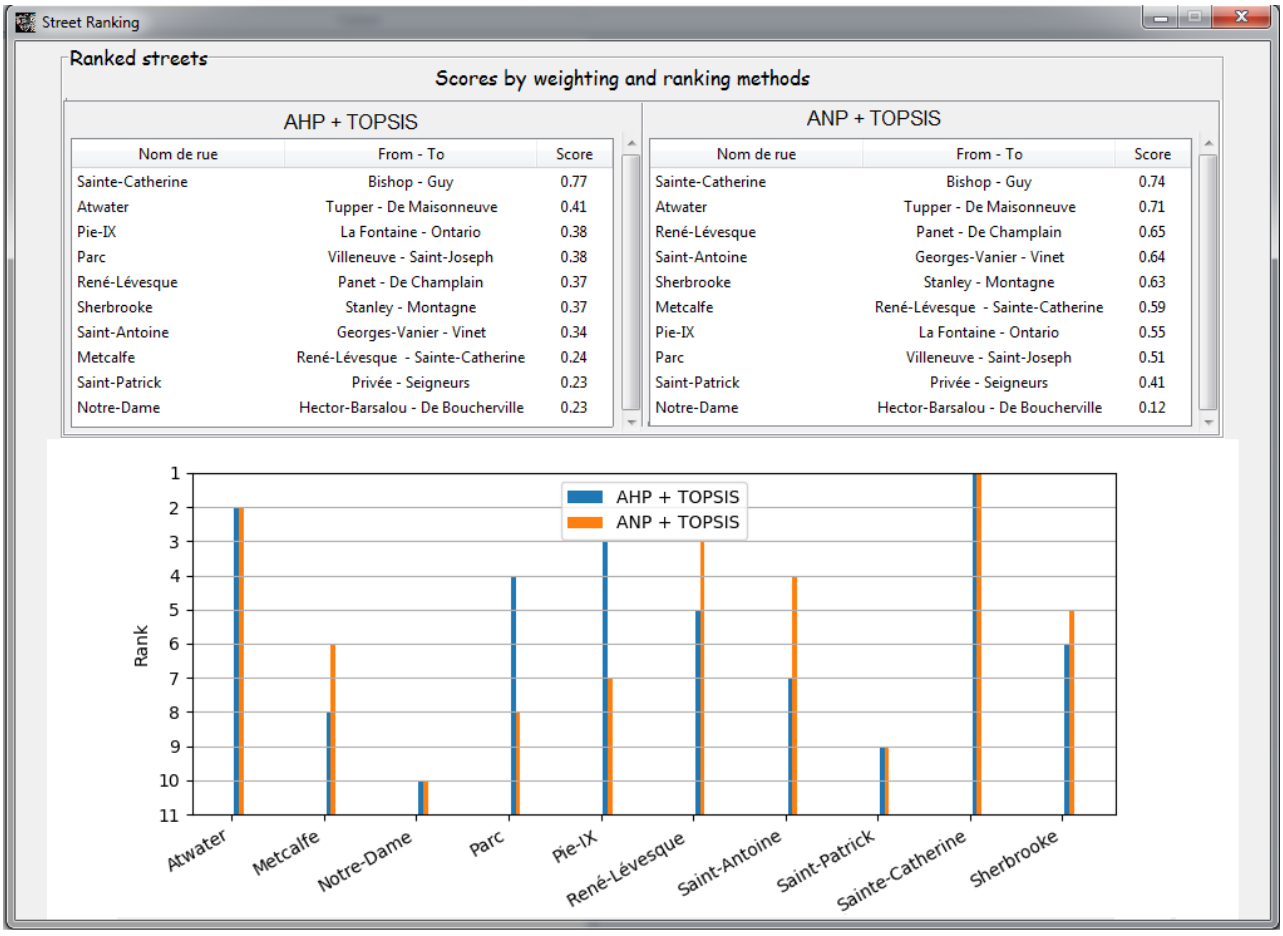

Figure 6-14. TOPSIS ranking results based on AHP and ANP weights.

Table 6-8. Performance values for ten alternative MUT locations.

Alternative / Locations	Sainte-Catherine (Bishop to Guy)	Sherbrooke (Stanley to Montagne)	René-Lévesque (Panet to De Champlain)	Atwater (Tupper to De Maisonneuve)	Metcalfe (René-Lévesque to Sainte-Catherine)	Saint-Antoine (Georges-Vanier to Vinet)	Saint-Patrick (Privée to Seigneurs)	Notre-Dame (Hector-Barsalou to De Boucherville)	Pie-IX (La Fontaine to Ontario)	Parc (Villeneuve to Saint-Joseph)
Street Segment ID	23043	23074	23786	22977	23103	20593	21195	34864	14911	18049
Length (m)	205.48	196.49	254.76	217.90	239.32	272.85	226.67	208.89	166.24	176.37
AADT	17,000	13,000	12,000	18,000	5,900	3,800	12,000	15,000	12,000	22,000
Road class	0.8	1.0	0.8	0.8	0.8	0.8	0.8	1.0	1.0	1.0
Utility density	14.60	8.17	14.35	10.08	6.66	3.76	4.72	9.60	10.05	7.70
Excavation number (brk/km/yr)	4.75	2.79	0	0	0	2.53	0	0.	3.60	0
Underground development project	1	0	0	0	0	0	0	0	0	0
Population density(per/sq.km)	5,713	9,560	10,182	27,252	3,217	13,843	7,127	848	10,122	18,038
Land-use	0.83	0.70	0.80	0.8	0.80	0.60	0.80	0.85	0.60	0.80
Proximity to public facilities (m)	18.47	115.24	329.49	96.40	133.71	294.20	998.43	1,513.83	76.45	753.80
Proximity to high-rise buildings (m)	101.06	169.28	48.58	2.22	146.10	248.83	802.42	3,131.39	2,175.32	1,033.83
Soil type	1	1	1	1	1	1	1	1	1	1
Proximity to floodplain (m)	1,581.62	0	1,567.18	2,388.27	1,047.35	1,806.42	1,169.05	0	168.41	2,967.16
Slope of terrain	1.58	0	2.40	0.86	0.83	0	0.32	0	0	0.86

6.7.4 Entropy weights and ranking

The Entropy weights are dependent on the performance values of the alternatives. Entropy weights were calculated using the values of the alternative street segments in Table 6-9. Because the soil data is unavailable, it is assumed that there is no variation in the soil type for all alternative locations. The soil type criterion was assigned a value of 1 for all alternatives. A performance value of 1 will assign an Entropy weight of 0 to the soil type criterion so as not to affect the overall ranking of the street segments. Therefore, the ranking results can be compared to the other two MCDM ranking results.

The weights in Table 6-10 show that the criterion with the highest weight is underground project development with a weight of 38.8%. Having only one alternative with a future underground project among the 10 alternatives results in a high degree of differentiation, and this accounts for the high criterion weight. Second, to this criterion is the number of expected excavations with an Entropy weight of 16%. The utility density criterion weighs 0.8%, even though this criterion is one of the main reasons for the implementation of MUTs. The slope criterion, on the other hand, has a relatively higher weight of 11.4% as opposed to AHP and ANP which gave values of 3.5% and 0.9% respectively. This is because four of the ten alternatives have zero slope values that represent flat horizontal road segments. Whereas, based on the calculation of the entropy weights, the zero values increase the level of uncertainty and therefore, increase the entropy weights.

The derived weights were applied to the TOPSIS algorithm, and the ranking results are shown in Figure 6-15. Using the Entropy weights in TOPSIS also ranked the alternative *Sainte-Catherine* as the highest priority with an evaluation score of 0.91. There is a large difference in the priority score of Sainte-Catherine and subsequent alternatives of lower priorities.

Table 6-9. Entropy weights for 10 alternatives.

Criteria	Entropy weight (%)
AADT	1.4
Road class	0.1
Population density	4.0
Land-use	0.1
Number of expected excavations	16.0
Utility density	0.8
Underground project development	38.8
Proximity to public facilities	8.9
Proximity to high rise buildings	12.2
Soil type	0.0
Proximity to the floodplain	6.2
The slope of the terrain	11.4

6.7.5 Ranking comparison of subjective and objective weights

Table 6-10 is the different criteria weights for the three MCDM techniques. The weighting methods are based on different principles. AHP assumes no relationship exists between the criteria, in contrast with ANP. Entropy weighs the criteria based on the data values themselves without considering the purpose of the data. Based on the ten alternative locations, the utility density, land-use, and road class criteria Entropy weights have relatively lower weights when compared to the weights derived from AHP and ANP. While the number of expected excavations and underground project development criteria was weighted among the top four for AHP and Entropy.

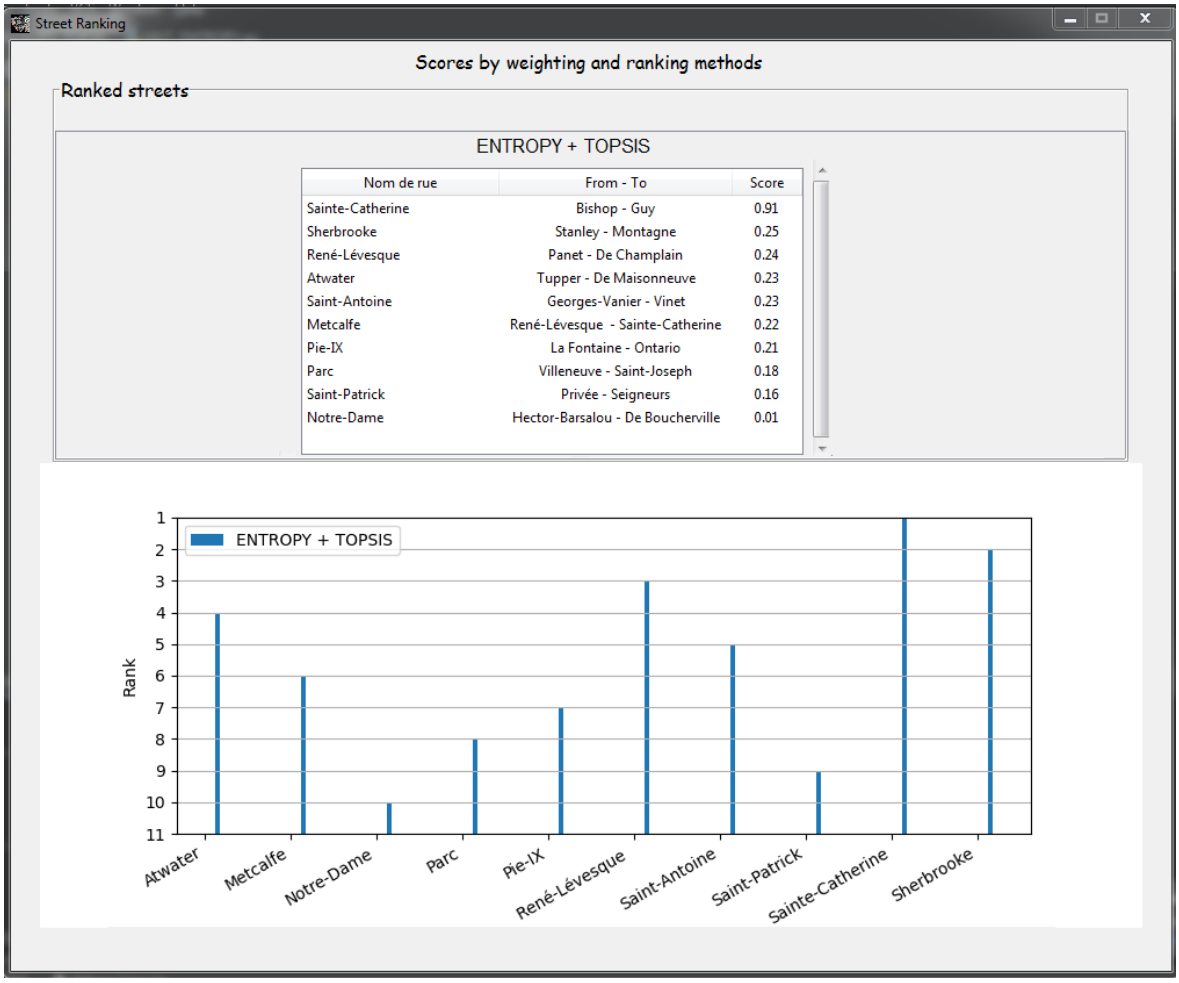

Figure 6-15. Entropy weights and TOPSIS ranking (derived using PlaceMUT).

Figure 6-16 shows the different ranking positions obtained from the combination of TOPSIS with weights derived from the AHP, ANP, and Entropy weights. Figure 6-17 is a map showing the locations of all ten alternatives and the ranking position of each combination. A comparison of the ranking results shows that the ANP method was closer in ranking priorities to the objective weights than the AHP method. All three combinations rank the alternatives *Sainte-Catherine, Saint-Patrick,* and *Notre-Dame* as the first, ninth, and tenth, respectively, amongst this set of alternatives. The ranking priorities derived from the combination of ANP+TOPSIS are equal to the combination of Entropy+TOPSIS for seven out of the ten priority positions.

Table 6-10. Criteria weights.

Criteria	Weights (%)		
	AHP	ANP	Entropy
AADT	15.6	6.2	1.4
Road class	8.9	5.8	0.1
Population density	8.0	14.4	4.0
Land-use	5.4	1.5	0.1
Number of expected excavations	12.4	7.1	16.0
Utility density	17.8	17.5	0.8
Underground Project Development	11.0	6.8	38.8
Proximity to public facilities	3.6	20.6	8.9
Proximity to high rise buildings	5.5	16.4	12.2
Soil type	2.4	0.9	0.0
Proximity to the Floodplain	3.5	2.0	6.2
The slope of the terrain	6.0	0.9	11.4

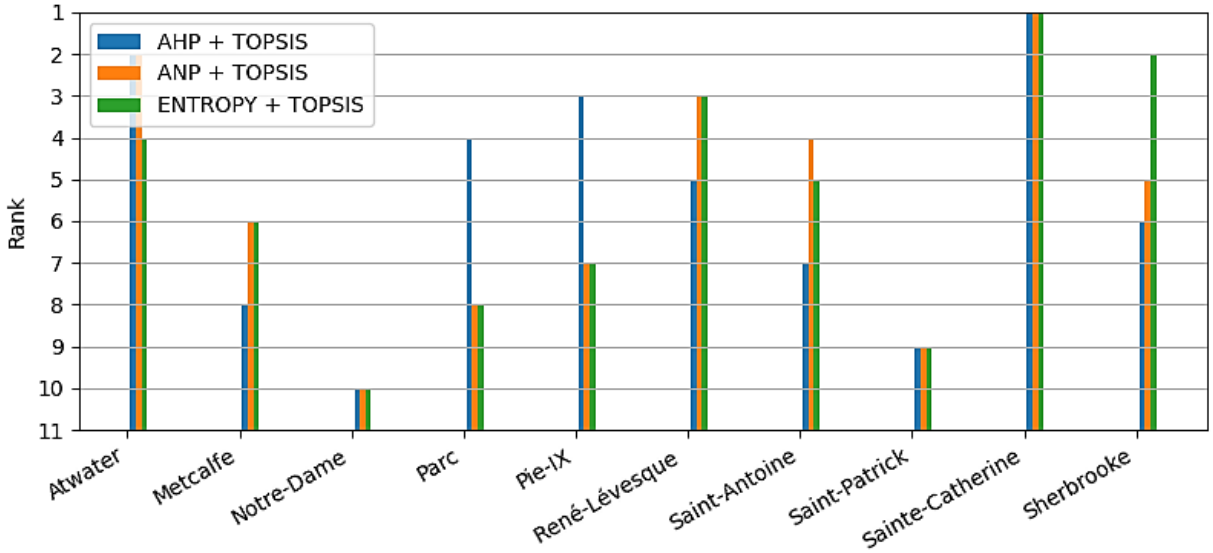

Figure 6-16. Comparing different ranking positions.

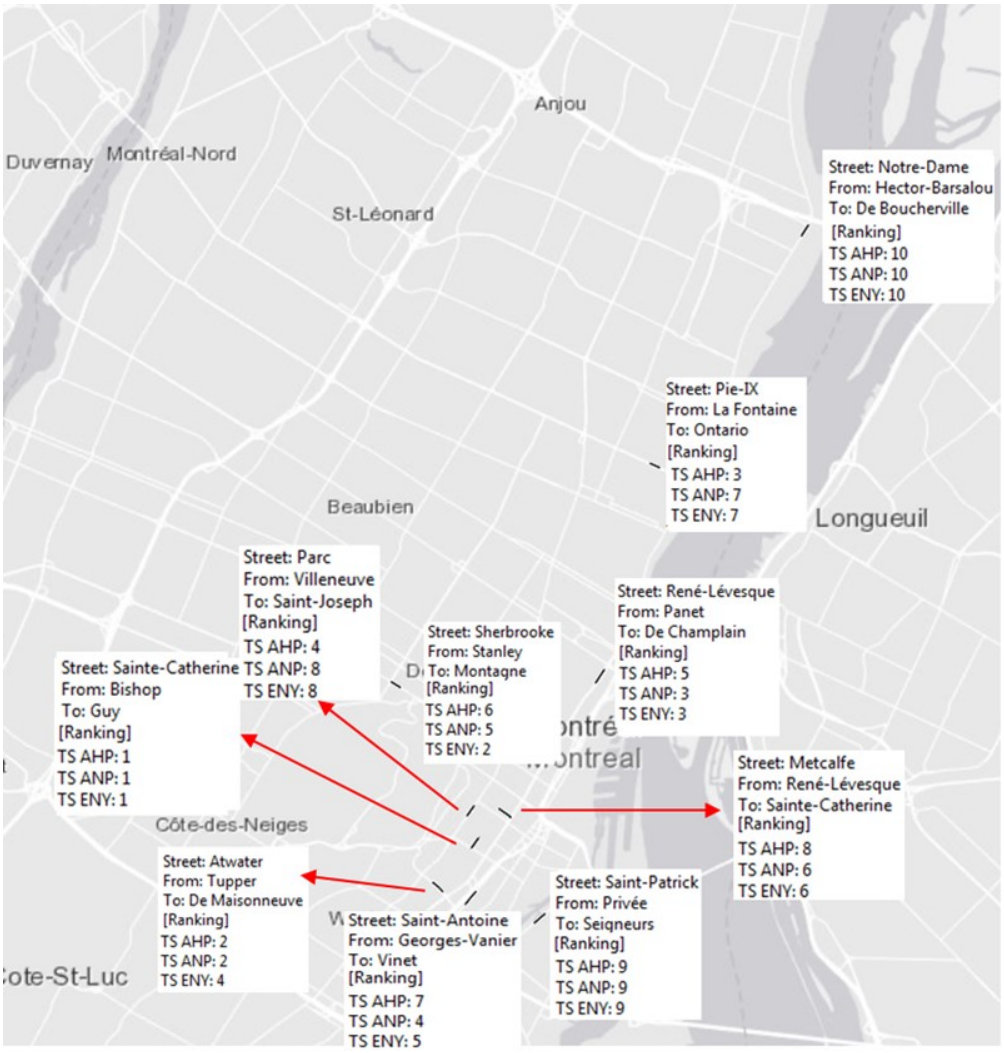

Figure 6-17. Ranked alternatives.

6.8 Summary

Considering the high initial construction cost of MUTs, this research has shown that the identification of critical street segments as candidates for MUT placement can be achieved through the application of a general method for MUT location selection based on the combination of GIS spatial analysis and MCDM. The spatial attributes of the alternative MUT locations were extracted using several geoprocessing techniques, and MCDM methods were used in weighing the criteria and subsequently ranking the potential MUT locations. The developed tool, *PlaceMUT,* automates the decision-making process of street segment selection and ranking and can be used for any city by changing the input data.

From the case study, the differences between the most critical criteria determined the ranking. The alternative *Sainte-Catherine* has an above-average utility density and the highest excavation number, and it is the only street that has a future underground development project. It is located in the downtown area of the City of Montreal. Therefore, it is selected as the most suitable location for MUT placement among the ten locations in all MCDM methods.

CHAPTER 7. MULTI-OBJECTIVE OPTIMIZATION FOR SELECTING POTENTIAL LOCATIONS OF MUT CONSIDERING SOCIAL COSTS[5]

7.1 Introduction

Chapter 6 adopted a location selection approach for MUTs based on the spatial characteristics of pre-selected locations. However, this chapter proposes a different approach to identifying the potential locations for MUTs by optimizing agency and social LCCs (life cycle costs) and network deterioration through multi-objective optimization.

This proposed approach involves estimating and comparing the savings in agency and social LCCs and network deterioration resulting from the implementation of MUTs and synchronized utility interventions at both the segment and network levels. By comparing the optimization results, the aim is to identify the street segments in the network where implementing MUTs is less expensive than the synchronized method of utility intervention while offering lifecycle savings. The end-result is a multi-year plan for MUT location selection that optimizes all three objective functions. The focus of this chapter is on using multi-objective optimization to identify the potential locations for MUTs that offer the greatest benefit in terms of LCC savings and network deterioration. The rest of this chapter includes: (1) the development of agency and social LCC models for both alternatives; (2) the use of linear deterioration models that track the yearly conditions of the spatially collocated assets; and (3) the comparison of the obtained optimization results at the network and segment levels.

7.2 Overview of the Optimization Model

Figure 7-1 represents the proposed framework at a high level of abstraction. Based on the current conditions derived from the individual datasets of each asset, asset-level interventions are determined. This research uses a condition-based method to combine the individual asset-level interventions, which enables the transition to segment-level interventions. The asset classifications alongside the asset and segment-level intervention strategies used in this module are the same used in Sections 5.2.4 and 5.2.5.

[5]This chapter is based on the following journal paper:

Genger, K.T., Hammad, A., and N. Oum (2023), "Multi-Objective Optimization for Selecting Potential Locations of Multi-Purpose Utility Tunnels Considering Agency and Social Lifecycle Costs", Journal of Tunnelling and Underground Space Technology (under review).

The assumptions (i.e., condition indicator thresholds and synchronized intervention strategies) adopted in this research are based on the practical approach used by the City of Montreal (Chacon and Normand, 2016).

The objectives of each alternative (MUT and synchronized interventions) are obtained using two independent optimization models, one for each alternative. These models will be explained in greater detail in Sections 7.5.1 and 7.5.2. The solutions contained in the Pareto fronts of the two optimization models include the LCCs and network deterioration of implementing MUTs and synchronized interventions on several street segments on a network.

The details of each optimization model will be explained in the following sections. After determining the asset conditions (Step 1) in Figure 7-1, the next step is to establish the asset-level intervention strategies unique to each asset and the segment-level intervention strategies unique to each segment (Step 2). These segment-level intervention strategies are obtained from the combination of asset-level interventions. In Step 3, the main goal is to optimize the synchronized interventions at the network level considering the agency and social LCCs and the deterioration of the assets in the network. If interventions are required, the nature of the applied intervention strategy (i.e., pipe rehabilitation or replacement, and pavement reconstruction or rehabilitation) determines the improvement in the condition of each asset. Synchronized interventions are then applied to segments where at least two assets require interventions, and their synchronization enables the transition to segment-level interventions. The agency and social costs of the intervention are calculated, and the condition of each asset is updated based on the applied intervention.

Deterioration models for each type of asset are used to determine the yearly change in asset conditions. These models keep track of the conditions of buried assets (with or without interventions). This process is repeated throughout the planning period and the LCCs are calculated at segment and network levels.

Meanwhile, MUTs are also applied to segments where the interventions require excavation (e.g., for pipe replacements), as these street segments are considered an opportunity to build MUTs (Step 4). This aggressive process means that the assets are allowed to deteriorate to the point where only interventions requiring excavations can be performed.

In Step 5, the main goal is to optimize the MUT implementation at the network level considering the agency and social LCCs and network deterioration. Similar to synchronized interventions, the

agency and social costs of implementing the MUT are calculated and the conditions of the assets (i.e., hosted in the MUT or buried) are updated. Yearly maintenance is executed on the MUT structure as well as the assets hosted in the MUT without accruing any social costs, meanwhile, the agency cost of the maintenance is calculated. Deterioration models keep track of the conditions of the assets in the MUT and these assets are replaced when their conditions get to the thresholds for intervention with no accrued social costs.

The selection of the street segments for either the implementation of the MUT or the synchronized interventions in a particular year is guided by the objectives and constraints. The multiyear location selection for the MUT and the synchronized interventions involves maximizing the network performance, which is achieved by minimizing the deterioration represented by the number of segments with *D* and *R* asset conditions at the end of the planning period. This objective function aims to minimize the network deterioration by minimizing the ratio of segments with all three assets requiring intervention versus the total number of segments in the network at the end of the planning period as will be explained in Equation *7-5*. In addition, the location selection also involves minimizing the agency and social LCCs while meeting all constraints of the system.

The second and third objective functions cover the agency and social LCCs, respectively, accrued as a result of the implementation of the MUT or synchronized interventions.

To compare both solutions at the network or segment levels, a solution that satisfies the decision maker's priority is selected from the Pareto front (Step 6). This research uses the Simple Additive Weighting (SAW) method to select a solution by assigning a score to each solution, obtained by summing the products of the normalized objective values and their weights (i.e., assigned by the decision maker). The solution with the largest score is selected from the Pareto front (Martínez-Morales *et al.*, 2010).

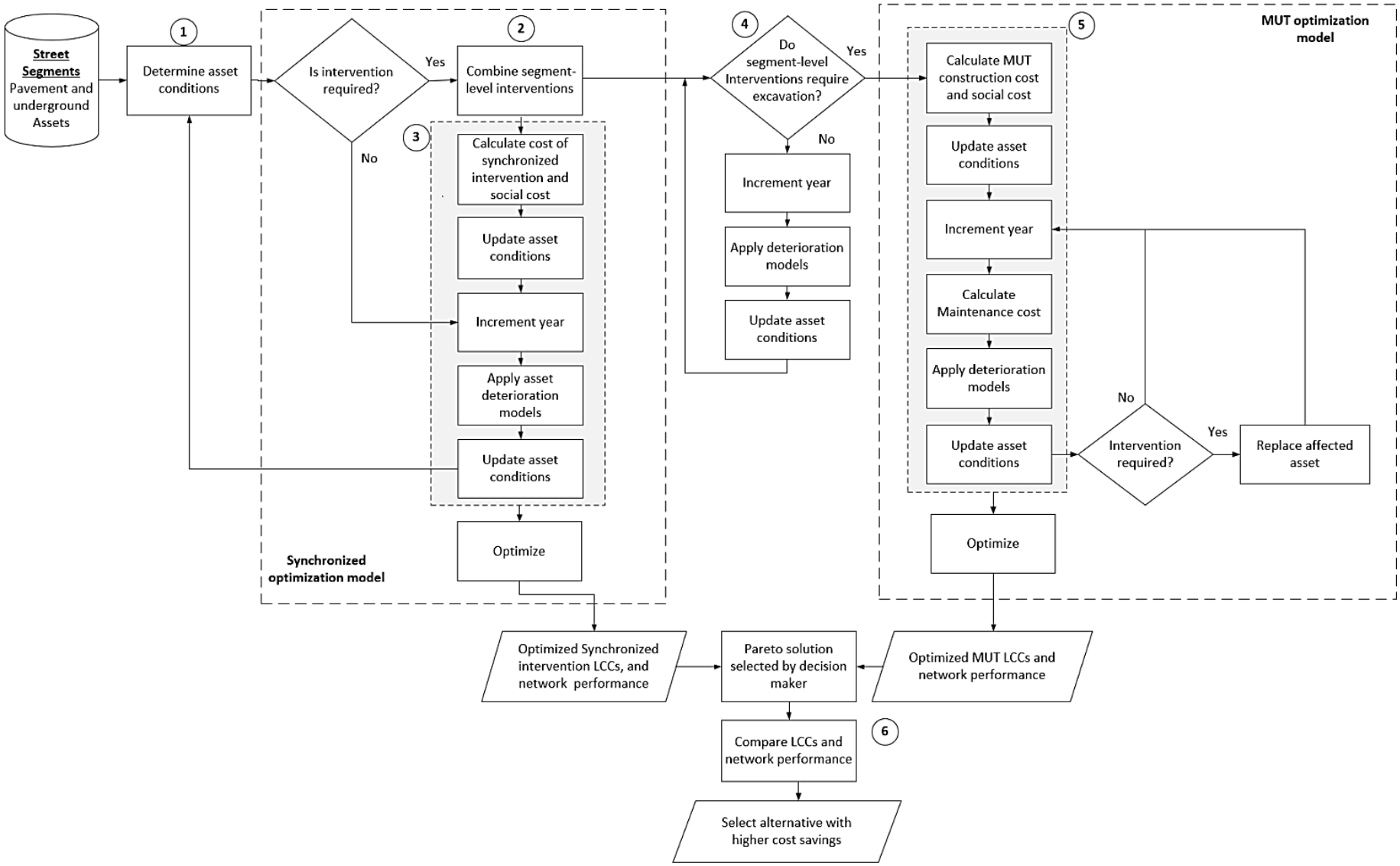

Figure 7-1. Proposed framework.

7.3 Social Cost Model

The socioeconomic impacts of both alternatives (i.e., MUTs and synchronized interventions) are estimated using three social cost indicators: vehicle maintenance and operations (VMO), vehicle delays (VED), and air pollution (AP). All three indicators are accrued during the implementation of the synchronized intervention method in the construction and maintenance phases of the lifecycle. However, they are only accrued during the construction phase of the MUT implementation. The models used for estimating each social cost indicator are presented in the sections below.

7.3.1 Social cost nonlinear regression models

The implementation of the developed models is fastidious at the macro level for the entire network. There was therefore a need to develop regression functions for the social cost indicators to ease the estimation of the social costs at the macro level. First, linear regression modeling was tested, but the results were not satisfactory, even though the R^2, measuring the proportion of variance in each social cost indicator, was acceptable. The estimated costs from linear regression often failed to match calculated social costs because some coefficients or the intercepts were negative. A negative intercept was a concern because it can lead to negative costs (Oum, 2017). Therefore, it was decided to shift to nonlinear regression modeling. For all indicators, it was observed that both the project duration (PD) and the length of the segment (L) are exponential functions, and the vehicle traffic density (VTD) is a linear function. Then, the regression functions (VED, VMO, and AP) were developed upon these observations of the three indicators.

Synchronized interventions make it necessary to guarantee worker safety and ease of movement for heavy machinery and equipment. Therefore, most interventions on the right-of-way require complete or partial closures of street segments (le Gauffre et al., 2002; Matthews et al., 2015). The regression coefficients are determined for both partial and complete street closures. The coefficients for complete street closures are used to calculate the social cost indicators for synchronized interventions, while the coefficients for partial street closures are used to calculate the social cost indicators for the MUT construction. This assumption is mainly due to the selected method of construction used in the implementation of MUT (i.e., microtunneling) which requires an input shaft and an exit shaft.

The regression functions for all three social cost indicators were built in a way to find the predicted VED, VMO, and AP costs (in $), based on VTD (in vehicles), L (in meters), and PD (in days). The regression was performed by minimizing the sum of the squares of the errors, i.e., differences between modeled and measured values. The statistical tests, F-test, and t-test were performed for complete and partial closures.

7.4 Deterioration Models

The deterioration of all three assets is determined using linear deterioration models adopted from the models used by the City of Montreal (Chacon and Normand 2016). Due to the lack of models that capture the rate of asset deterioration in MUTs, it is assumed that assets hosted in the MUT deteriorate at the same rate as those buried under the subsurface. Therefore, the condition threshold required for the implementation of the intervention strategies before building the MUT is the same. In addition, replacements and yearly maintenance are carried out on the assets hosted in the MUT.

7.4.1 Sewer and water pipe deterioration models

It is assumed that both the sewer and water pipes buried underground follow a linear deterioration model, which is expressed by the age of the pipe divided by the expected life (Equation *7-1*). Furthermore, the expected life of sewer and water pipes is based on their respective materials and diameters as will be explained in Section 7.7.

$$D_t = \frac{Age_t}{Expected\ life} \qquad (7\text{-}1)$$

where D_t is the degree of deterioration of the pipe at year t

Both intervention strategies (i.e., pipe rehabilitation and replacement) restore the deterioration degree of a pipe to 0. However, the expected life of these intervention strategies differs.

7.4.2 Pavement deterioration models

In this research, the pavement condition index (PCI) is used to determine pavement condition. At year 0 (i.e., time of intervention), PCI is 100. At the end of the elapsed life, the PCI approaches 0 (Piryonesi and El-Diraby, 2021b). Assuming a pavement deteriorates at a rate ($rate_{det}$) between 1 to 2 PCI points/year (Chacon and Normand 2016). The pavement deterioration model can be

expressed as presented in Equation *7-2*. To capture the random nature of the pavement deterioration rate, a random value between 1 and 2 is assigned yearly to each street segment.

$$PCI_t = PCI_{t-1} - rate_{det} \qquad (7\text{-}2)$$

Different intervention strategies have different impacts on pavement conditions. Although both minor and major pavement rehabilitation strategies improve the condition of the pavement, only a pavement reconstruction restores it to the original state (i.e., PCI = 100). The impact of applying both major and minor rehabilitation interventions is achieved by randomly assigning a PCI value between 100 – 70 and 70-40 for major and minor rehabilitation respectively.

7.5 Optimization Model (NSGA-II Adaptation)

The optimization problem considered in this work is a combinatorial multi-objective problem because it involves selecting a combination of street segments based on their current conditions, future conditions, and the timing and nature of the intervention, all subject to budgetary constraints. The search space for finding the optimal or near-optimal solutions is very large because several variables are considered. These variables include the street segments in the network, the collocated utility assets in a segment (i.e., water and sewer pipes, telecommunication and electricity cables, and pavement), the type of synchronized intervention strategies (e.g., pipe rehabilitation or replacement and pavement rehabilitation or reconstruction), the year of the applied intervention, and the planning period.

The optimization model is implemented using the Non-dominated Sorting Genetic Algorithm (NSGA-II) optimization algorithm (Deb *et al.*, 2002) because it is a well-established and widely used multiobjective optimization algorithm capable of solving complex combinatorial problems. The NSGA-II is implemented by randomly initializing a population according to the number of solutions (chromosomes). Figure 7-2 presents the proposed optimization model for identifying the optimal MUT locations as well as the optimal intervention plan for implementing the synchronized interventions over a planning period.

The fitness functions are evaluated using Equations 7-3 to 7-5 for the synchronized intervention model which is subject to the constraints in Equations 7-6 and 7-7. Furthermore Equations *7-6* and 7-7 ensure that the agency cost and the social costs in year *t* are within budgets limits of their

respective the present values. Details on the synchronized intervention optimization model are provided in Section 7.5.1.

The objective functions for synchronized interventions are:

$$Minimize\ AG\_SYNC\_LCC = \sum_{s=1}^{S}\sum_{t=1}^{N}\frac{AG\_SYNC\_LCC_{st}}{(1+r)^t} \quad (7\text{-}3)$$

$$Minimize\ SC\_SYNC\_LCC = \sum_{s=1}^{S}\sum_{t=1}^{N}\frac{SC\_SYNC\_LCC_{st}}{(1+r)^t} \quad (7\text{-}4)$$

$$Minimize\ Network\_deterioration\ = \sum_{s=1}^{S}\sum_{i=1}^{n}\sum_{j=1}^{m}\frac{D_{Nsij} + R_{Nsij}}{S} \quad (7\text{-}5)$$

where AG_SYNC_LCC is the agency LCC achieved by implementing the synchronized intervention; SC_SYNC_LCC is the social LCC achieved by implementing the synchronized intervention; *r* is the discount rate; *t* is the year of intervention; *N* is the length of the planning period*; S* is the number of segments in the network; D_{Nsij} and R_{Nsij} is the number of segments with D-condition assets and R-condition assets, respectively.

Subject to the following constraints:

$$\sum_{s=1}^{S} AG\_SYNC\_LCC_s \leq \frac{AG_B}{(1+r)^t} \quad (7\text{-}6)$$

$$\sum_{s=1}^{S} SC\_SYNC\_LCC_s \leq \frac{SC_B}{(1+r)^t} \quad (7\text{-}7)$$

where AG_B is the yearly agency cost budget; and SC_B is the social cost budget.

While for the MUT optimization problem, the fitness functions are evaluated using Equation 7-5 (this fitness is common to both optimization problems), and Equations 7-8 to 7-9. The MUT optimization problem is subject to the constraints in Equations 7-10 to 7-11. Equation *7-10* ensures that the combined maintenance cost of existing MUTs and cost of implementation new MUTs in year *t* does not exceed the present value of the yearly agency. On the other hand, Equation *7-11* ensures that the social cost of implementing new MUTs does not exceed the present value of the yearly social cost budget at year *t*. Details of the MUT optimization model are provided in Section 7.5.2.

The objective functions for MUT implementation are:

$$Minimize\ AG\_MUT\_LCC = \sum_{s=1}^{S}\sum_{t=1}^{N}\frac{AG\_MUT\_LCC_{st}}{(1+r)^t} \quad (7\text{-}8)$$

$$Minimize\ SC\_MUT\_LCC = \sum_{s=1}^{S}\sum_{t=1}^{N}\frac{SC\_MUT\_LCC_{st}}{(1+r)^t} \quad (7\text{-}9)$$

where AG_MUT_LCC is the agency LCC; s is the street segment; SC_MUT_LCC is the social LCC; Subject to the following constraints:

$$\sum_{s=1}^{S} AG\_MUT\_LCC_s + \sum_{s=1}^{S} OMC_s \leq \frac{AG_B}{(1+r)^t} \quad (7\text{-}10)$$

$$\sum_{s=1}^{S} SC\_MUT\_LCC_s \leq \frac{SC_B}{(1+r)^t} \quad (7\text{-}11)$$

where OMC_s is the cost of existing MUT maintenance and operation

The representation of the solution for optimizing the multi-year MUT locations is presented in Table 7-1. Each solution (i.e., chromosome) is a vector with a length equal to the multiplication of the length of the planning period and the number of street segments in the network. Table 7-2 is the solution representation for one year of a synchronized intervention. Each chromosome comprises the interventions for each utility in each segment in each year of the planning period. The length of a solution is the multiplication of the planning period, the number of segments in the network, and the intervention strategies applied based on the asset condition and the number of assets.

Table 7-1. MUT solution representation.

S_1	S_2	…	S_X	S_a	S_b	…	S_y	…	S_i	S_j	…	S_z
Year 1				Year 2				…	Year N			

Table 7-2. Solution representation for the synchronized intervention for year t.

Sewer pipe	Water pipe	Pavement	Sewer pipe	Water pipe	Pavement	...	Sewer pipe	Water pipe	Pavement
2	2	3	1	1	3		0	0	0
Segment X			Segment Y			...	Segment Z		
Year t									

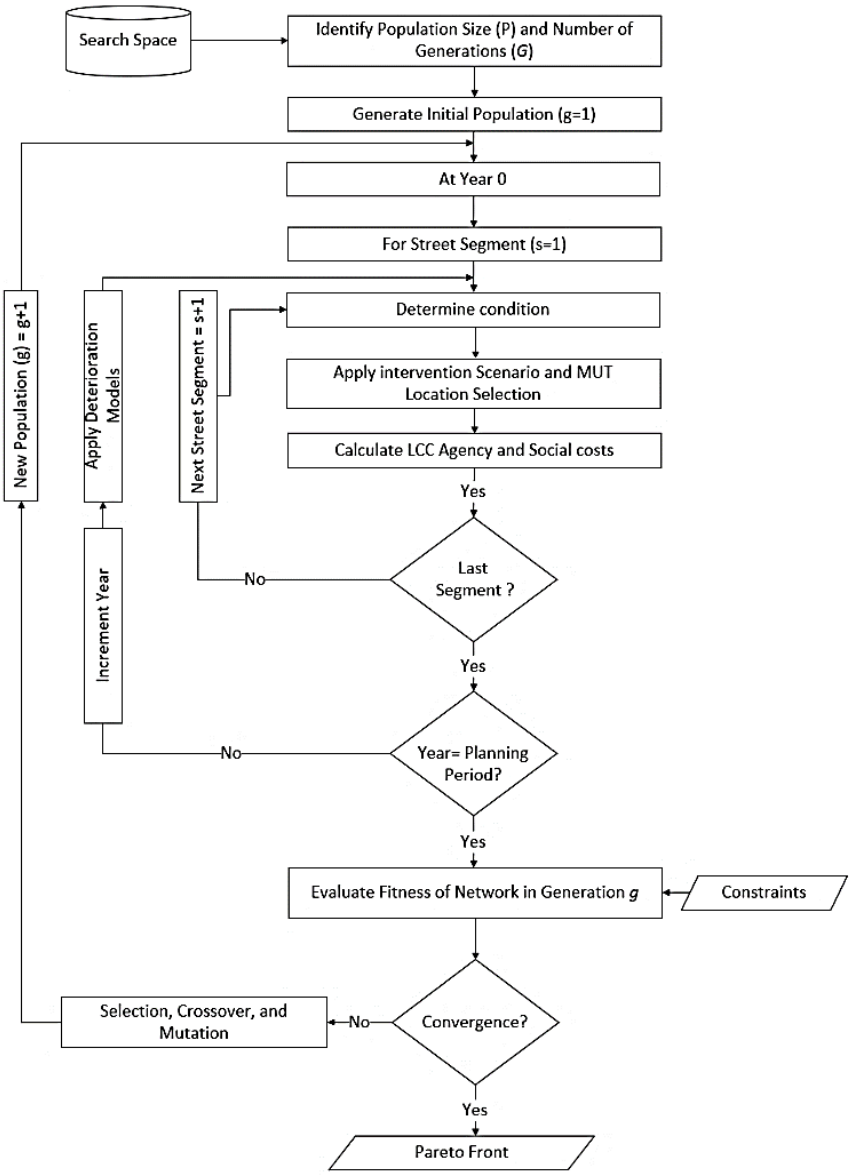

Figure 7-2. Optimization model.

An intervention strategy is assigned to each collocated asset based on its current condition. The intervention strategies for all the collocated assets are encoded using an integer representation. Each type of intervention strategy is assigned a unique integer. For example, no intervention strategy is assigned 0, the rehabilitation of sewer and water pipes is assigned 1, and the replacement is assigned 2. Segments where the initial intervention on the sewer pipe is 1 (i.e., rehabilitation), are changed to a 2 (i.e., replacement) when the intervention of the water pipe is 2 and vice versa. This decision means that both the water and sewer pipes will undergo synchronized replacement requiring excavations or they will both undergo synchronized rehabilitation using trenchless

methods such as cured-in-place pipes (CIPP) or sliplining (Najafi, 2010). Also, due to the need for excavation during the replacement of underground assets, pavement interventions are dependent on the interventions of the underground assets. This means that the underground interventions will be also synchronized with pavement interventions. Based on the current asset conditions, some segments may not require any intervention, for example, Table 7-2 includes a street segment *z* where all the underground assets and the pavement do not require intervention hence the intervention strategy is 0. All these conditions are accounted for when generating each solution in a population. The value of each objective function is calculated, and each solution is assigned a fitness value.

The selection of potential individuals to construct a new population is done by binary tournament selection, which initially sorts the population using the dominance principle and a comparison operator that calculates the crowding distance. Each individual in the new population either has a lower (i.e., better) or equal rank that is located in a lesser crowded region (i.e., new solutions have greater crowding distances than the old solutions).

Crossover is achieved by selecting a random single cut-point for two random parent solutions as shown in Figure 7-3 for the case of synchronized interventions. The crossover operator then creates two child solutions by combining the left side of the cut-point of parent 1 and the right side of the cut-point of parent two for child one, followed by a switch of selected sides for child two. After the crossover operation, both parents and children are merged, and a new Pareto front is computed for that generation.

The mutation process is carried out to ensure a good spread of solutions. Mutation is achieved by randomly changing, one or more intervention strategies on the utilities in a segment in a specific solution as shown in Figure 7-4. The crossover and mutation will also reflect the impact of the implemented interventions of the underground assets on the intervention of the pavement as shown in Figure 7-3. This entire process is carried out for all generations until convergence is obtained or the maximum number of generations is reached.

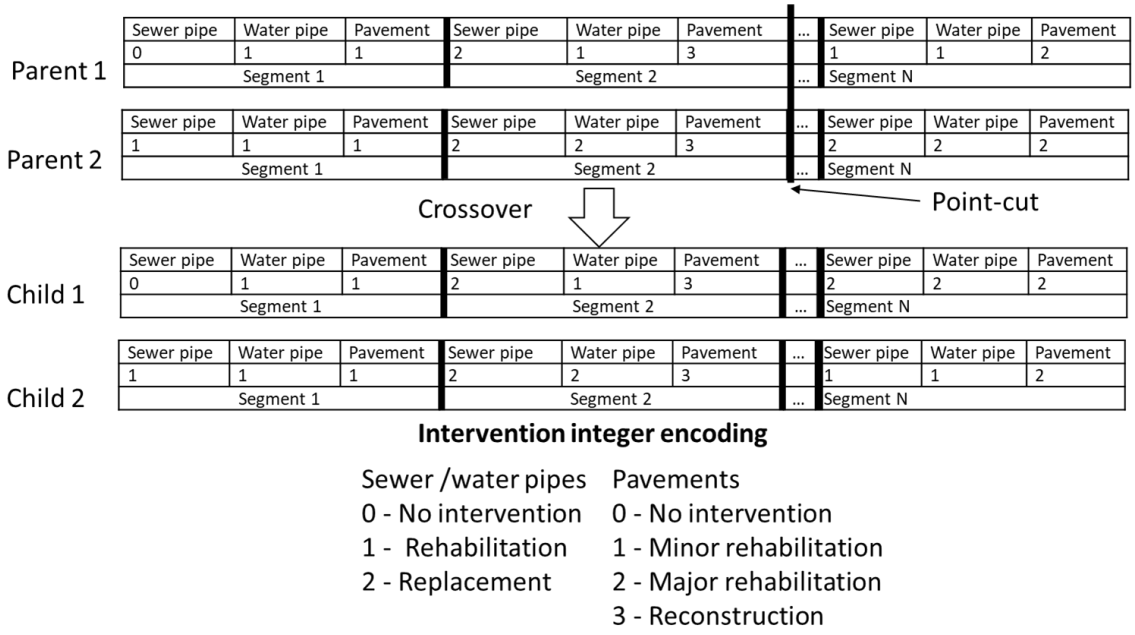

Figure 7-3. Crossover operation (case of synchronized interventions).

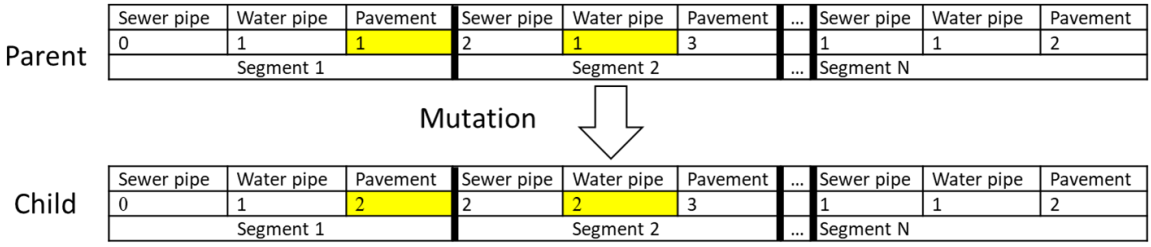

Figure 7-4. Mutation operation.

7.5.1 Synchronized utility intervention optimization model

In the case of optimizing the synchronized intervention model, at the start of the planning period, the initial conditions of all assets in the segment will determine the nature of the respective interventions. The condition for subsequent years is determined using a deterioration model for each asset. The derived conditions will further determine the nature and timing of an applied intervention strategy. Adopted from the intervention strategies used by the City of Montreal (Chacon and Normand, 2016), the intervention strategies applied to water and sewer pipes include: *No Intervention* for pipes still in a good condition, *Structural Rehabilitation* for pipes in a desirable condition (i.e., extending the service life of an existing sewer or water pipe using methods such as inserting a sheath inside the pipe), and *Replacement* for pipes in a critical condition. Similar to the intervention strategies of water and sewer pipes, pavements in a good condition (i.e., PCI $\geq$ 70)

will require *No Intervention*, *Minor Rehabilitation* (i.e., restoring the structural capacity of a pavement structure, by rout and crack sealing) is applied to pavements in a desirable condition (i.e., 70 > PCI ≥ 40), *Major Rehabilitation* (i.e., increasing the structural load carrying capacity of the pavement using structural overlays), or *Reconstruction* (i.e., the complete removal and replacement of existing pavement including granular layers) for pavement in a critical condition (i.e., PCI < 39). The timing and nature of the selected intervention will have agency costs and social costs implications, as well as implications on the level of deterioration of the asset.

Equation *7-12* represents the agency LCC for synchronizing the intervention of utilities under a street segment and the road pavement. The equation accounts for the intervention cost of the underground assets and the cost of pavement intervention.

$$AG\_SYNC\_LCC_s = \sum_{t=1}^{N}\sum_{i=1}^{n}\sum_{j=1}^{m}\frac{IC_{stij} + PIC_{st}}{(1+r)^t} \qquad (7\text{-}12)$$

where $AG\_SYNC\_LCC_s$ is the agency life-cycle cost for conducting a synchronized intervention on street segment *s*; for an underground asset of type *i* and sub-type *j*, over a planning period *N;* IC_{stij} and PIC_{st} are the intervention costs of underground assets and pavement interventions, respectively; *r* is the discount rate.

Equation *7-13* is the social LCC associated with the intervention, which is the sum of all social cost indicators discounted to the present value.

$$SC\_SYNC\_LCC_s = \sum_{t=1}^{N}\sum_{k=1}^{K}\frac{SCI_{stk}}{(1+r)^t} \qquad (7\text{-}13)$$

where $SC\_SYNC\_LCC_s$ is the social cost accrued during all interventions at segment *s*; *k* is the number of social cost indicators; SCI_{stk} is the social cost accrued during interventions on segment *s* at time *t*.

7.5.2 MUT optimization model

Based on the initial conditions of the collocated assets on each segment, several street segments are selected as the target of MUT construction and both the agency and social LCC are estimated. For subsequent years in the planning period, linear deterioration models are applied to each asset in the network and based on future conditions, more street segments are selected as the target of

MUT construction. The selection of the street segments in any particular year is constrained by a social cost budget and an agency cost budget.

The LCC components considered in this research include the tunnel construction, utility replacement and installation, tunnel system equipment, and maintenance phase of the MUT. According to Jorjam (2022), the two main methods used in MUT construction are cut and cover (C&C) and microtunneling. The tradeoff between these methods is that while the microtunneling is faster and has relatively lower socioeconomic impacts, it is more expensive than the C&C method. In addition, microtunneling is applicable in mature cities with high traffic densities, because it requires fewer street closures, and is less disruptive to traffic. The selected construction method is a major factor in estimating the initial construction cost and the duration of the construction. In this study, microtunneling is selected as the construction method of MUTs because of the above-mentioned advantages. This research assumes that all the existing utilities previously buried in the underground are replaced by new ones in the MUT.

Another factor that affects the cost of MUT implementation is the cost of utility asset replacement and installation. Equation *7-14* represents the agency LCC of implementing a MUT under a street segment. The agency LCC is the summation of the initial cost of construction, the cost of MUT system equipment (e.g., appurtenances, auxiliary systems, detection and communication systems, control systems, etc.), utility handling (i.e., replacement and installation), and utility and tunnel maintenance.

$$AG\_MUT\_LCC_s = ICC_s + MUT\_SEq_s + \sum_{i=1}^{n}\sum_{j=1}^{m}(CP_{REP} + CP_{INS})_{sij} + OMC_s \qquad (7\text{-}14)$$

where $AG\_MUT\_LCC_s$ is the agency LCC of implementing a MUT on a street segment *s*; ICC_s is the initial cost of MUT construction on segment *s*; MUT_SEq_s is the cost of MUT system equipment; CP_{REP} and CP_{INS} are the costs of replacing and installing the pipes and cables, respectively; *i* is the number of utility assets to be replaced and installed, *j* is the number of utility sub-types (e.g., pipes with different materials and diameters); and OMC_s is the utility operation and maintenance cost of the MUT after the first year of construction.

ICC_s is calculated by multiplying the unit cost of tunnel construction (C_d) by the length of the tunnel l_s as shown in Equation *7-15*.

$$ICC_s = C_d * l_s \qquad (7\text{-}15)$$

MUT_SEq_s is calculated by multiplying the unit cost per meter of MUT requirements (REQ_s) by the length of the tunnel as shown in Equation *7-16*.

$$MUT\_SEq_s = REQ_s * l_s \quad (7\text{-}16)$$

Equation *7-17* is the sum of the unit cost of yearly maintenance per meter of each asset multiplied by the length, cost of the asset repair, and the cost of tunnel maintenance. The repair of an asset hosted in the MUT is determined by the same linear deterioration models in Equation 7-1.

$$OMC_s = \sum_{t=1}^{T} \sum_{i=1}^{n} \sum_{j=1}^{m} (U_{sij}\, l_{sij} + CR_{stij} + TM_s)(1+r)^{-t} \quad (7\text{-}17)$$

where U_{sij} is the unit cost of asset maintenance; l_{sij} is the length utility asset; CR_{stij} is the cost of replacement; TM_s is the cost of tunnel maintenance; r is the discount rate; t is the intervention year; T is the maintenance period (i.e., from the year of construction till the end of the planning period).

Equation *7-18* is the social cost (i.e., the sum of all social cost indicators) accrued on a street segment only during the MUT construction phase.

$$SC\_MUT\_LCC_s = \sum_{t=1}^{N} \sum_{k=1}^{K} \frac{SCI_{sk}}{(1+r)^t} \quad (7\text{-}18)$$

where $SC\_MUT\_LCC_s$ is the social cost accrued during the construction phase; SCI_{sk} is a social cost indicator.

7.6 LCC Savings

To determine if there are LCC savings achieved via the implementation of the MUT as opposed to the synchronized intervention on a street segment, the best solutions are selected and compared from the Pareto fronts of each optimization model. This research uses Simple Additive Weighting (SAW) method to rank and select one solution from the Pareto front of each model (Martínez-Morales *et al.*, 2010). The SAW method calculates an evaluation score ES_i for each solution *i* in the Pareto front by multiplying the relative importance weights w_j of the objective functions *j* and the normalized values of each solution v_{ij} as expressed in Equation *7-19*. Equal weights are assigned to each objective function and the non-dominated solution with the highest evaluation

score is selected and the LCC savings are calculated. The normalization is achieved using Equation *7-20*.

$$ES_i = \sum_{j=1}^{M} w_j v_{ij} \qquad \text{for } i = 1,2,3,\ldots,P \qquad (7\text{-}19)$$

$$v_{ij} = \frac{min_i(x_{ij})}{x_{ij}} \qquad (7\text{-}20)$$

where *P* is the size of the Pareto front; *M* is the number of objective functions; and x_{ij} is the value of the objective functions for each solution.

LCC savings are calculated as the differences between the LCC (agency or social) of implementing the MUT and the synchronized intervention as expressed in Equations *7-21* and *7-22*, respectively.

$$AG\_LCC\_savings = AG\_SYNC\_LCC - AG\_MUT\_LCC \qquad (7\text{-}21)$$

$$SC\_LCC\_savings = SC\_SYNC\_LCC - SC\_MUT\_LCC \qquad (7\text{-}22)$$

7.7 Case Study

Due to the limited amount of data, three municipal assets (pavement, sewer, and water pipes) are used in this analysis. However, this framework can be extended to accommodate private utility networks such as gas, telecommunication cables, electricity cables, etc., if the related data is available on the cost of interventions, the deterioration patterns, and maintenance strategies. To examine the approach proposed in this research, the case study area is presented in Figure 7-5. The geographic information system (GIS) map shown in the figure contains street segments in ten boroughs spread across the City of Montreal. The boroughs include Rosemont-La Petite-Patrie, Anjou, Saint-Léonard, Mercier-Hochelaga-Maisonneuve, Le Plateau-Mont-Royal, Rivière-des-Prairies-Pointe-aux-Trembles, Ville-Marie, Villeray-Saint-Michel-Parc-Extension, Le Sud-Ouest, and Outremont. 1,151 street segments totaling 259.71 km make up this study area. It should be noted that social cost indicators related to municipal works have never been assessed in previous research at a large scale, but rather they were addressed at a project level due to the complexity of their assessment.

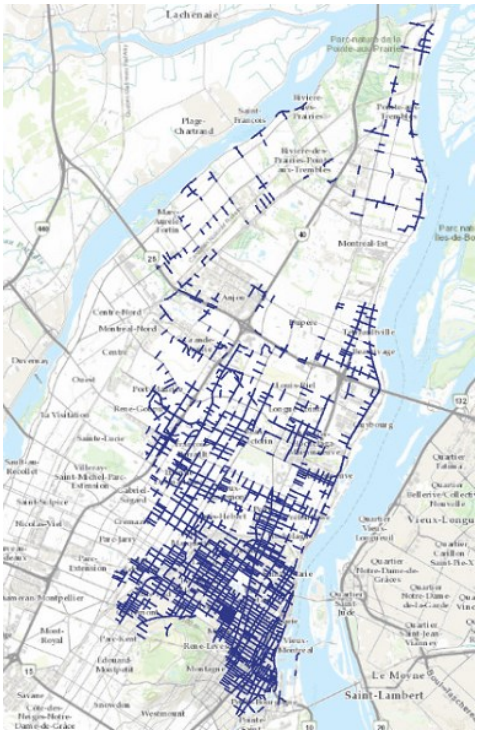

Figure 7-5. Case study area showing street segments.

Figure 5-2 shows the schematic view of a street segment (between two intersections) and the spatially collocated assets in the segment. Table 7-3 is a summary of the assets used in this analysis. The information presented in the table includes the asset age, material, expected life, condition thresholds, etc. Included in Table 7-3 are some of the major sewer pipe materials and their respective expected life. In addition, it is assumed that sewer pipes with larger diameters made from the same material have higher expected life (Chacon and Normand 2016). For example, the average expected life of a 400 mm - 600 mm prestressed concrete pipe is 115 years, whereas that of a 750 mm – 1,350 mm pipe is 165 years.

Table 7-4 outlines the cost components that make up the LCC of the MUT on a street segment. Included in the table is the range for tunnel construction cost per unit length (m), which is used to randomly assign a cost to the segments in the network following a uniform distribution function adopted from (Jorjam, 2022). Table 7-4 also presents the cost of routine tunnel structure maintenance. The costs in the references have been adjusted by considering the average yearly inflation rate of 3.03% (Bank of Canada, 2022).

Table 7-5 outlines the cost components used in estimating the LCC of synchronized interventions. The table shows the cost of the different intervention strategies for each of the assets used in this

research. Table 7-6 presents a sample of pavement and traffic attributes, for 11 street segments. Table 7-7 presents a sample of the attribute values for the sewer and water pipes located under the 11 street segments. Most asset infrastructure systems are managed on a short planning period. For example, the City of Montreal uses a six-year intervention plan. However, for this research, the planning period is taken as 100 years (i.e., the service life span of the MUT), as this enables a rational comparison between the two alternatives. The discount rate is assumed fixed at 3% and the effect of inflation on future unit costs is not considered. The yearly agency and social cost budgets for both alternatives are fixed at \$140M and \$8.5M, respectively. The value of the agency cost budget is based on the budget for the City of Montreal's intervention plan for all the municipal assets for the period 2016-2021. In addition, the value of the agency cost budget is also set to accommodate the implementation of MUTs as special projects. The social cost budget signifies the amount of delays and pollution that can be tolerated yearly, and its value is assumed to be approximately ten percent of the agency cost. According to (Rahman *et al.*, 2005) the social cost can amount to 400% of a construction project.

Table 7-3. Asset summary.

Asset	**Attribute**	**Attribute values**	
Pavements	Average age (years)	65.14	
	Average length (m)	224.05	
	Average surface area (m^2)	2,556.16	
	Pavement categories	A (numbered lane), B (artery), C (collector), D (others), and E (local road)	
	Average PCI	45	
	PCI intervention thresholds	No intervention	PCI ≥ 70
		Intervention desirable	69 ≥ PCI ≥ 40
		Intervention critical	PCI < 39
Sewer pipes	Average age (years)	81.24	
	Average length (m)	55.90	
	Diameter range (mm)	200 – 3,850	
	Major materials | average expected life (years)	Prestressed concrete (400 - 600 mm)	115
		Prestressed concrete (750 – 1,350 mm)	165
		Reinforced concrete (≤ 1970)	90
		Reinforced concrete (> 1970)	120
		brick	145
		grey cast iron	100
		Polyvinyl chloride	90

Table 7-3. Asset summary (cont'd).

Asset	Attribute	Attribute values	
Sewer pipes	Ductile iron	80	
	Deterioration level D = Age/expected life	No intervention	$D \leq 0.50$
		Desirable intervention	$0.90 \geq D > 0.50$
		Intervention critical	$D > 0.90$
	Average initial deterioration level	0.60	
Water pipes	Average age (years)	82.85	
	Average length (m)	204.9	
	Diameter range (mm)	100 – 2,100	
	Major materials | average expected life (years)	Pre-stressed concrete (<1966 or < 1987)	120
		Pre-stressed concrete (1966-1987)	35
		Ductile iron	63
		Grey cast iron (<1921)	172
		Grey cast iron (1921 - 1935)	124
		Gray cast iron (1936 - 1956)	87
		Grey cast iron (>1956)	78
		Polyvinyl chloride	100
		Reinforced concrete	90
		Steel	100
	Deterioration level D = Age/expected life	No intervention	$D \leq 0.50$
		Desirable intervention	$0.90 \geq D > 0.50$
		Intervention critical	$D > 0.90$
	Average initial deterioration level	0.66	

Table 7-4. MUT cost components.

Item	Unit ($/m)	Reference
Tunnel construction cost	117,000 - 308,000	Jorjam (2022)
Utility tunnel requirements		
Occupancy costs	130.62	Boileau (2013)
Service equipment	500	
Utility replacement and Utility installation	2,400	
Maintenance		
Water pipes	16	Boileau (2013)
Sewer pipes	26	
Tunnel structure	21.24	(Riera and Pasqual, 1992)

Table 7-5. The average cost for synchronized intervention.

Asset		**Diameter (mm)**	**Replacement cost ($/m)**	**Rehabilitation cost ($/m)**	**Reference**
Water pipes		150	1,520	1,165	Chacon (2016)
		375 - 400	2,050	1,573	
		600	2,500	2,193	
		900	3,270	3,013	
		1,200	3,550	3,823	
		3,000	8,200	8,743	
Sewer pipes		200 - 300	2,170	425 - 445	
		600	4,080	574	
		900	4,340	1,025	
		1,200	5,530	1,147	
		3000	11,500	9,530	
Pavement		**Minor rehabilitation cost ($/m^2)**	**Major rehabilitation cost ($/m^2)**	**Reconstruction cost ($/m^2)**	
Category	A - D	295	319	395	
	E	251	319	335	

Table 7-6. Sample pavement and traffic attribute values.

Segment ID					**AADT**			
ID	**Length (m)**	**Surface area (mm^2)**	**PCI**	**Pavement category**	**Bus**	**Autos**	**Heavy trucks**	**Light trucks**
17820	133.52	983.37	74	B	0	8,256	354	3,919
17822	115.96	1,261.76	29	E	0	1,098	47	521
17823	292.96	3,398.87	23	D	0	1,098	47	521
17825	228.31	2,651.99	28		12	1,953	84	927
17830	154.23	1,633.44	52		55	3,423	164	0
17831	188.26	2638.04	39	C	314	15,352	493	35
17834	215.36	2,518.34	33	E	36	6,084	0	2,888
17837	208.34	1,934.98	24		98	16,037	688	7,611
17838	388.01	3,523.25	61		98	16,037	688	7,611
17842	305.62	2,781.32	44		22	3,686	0	1,749
17844	307.42	3,349.80	33		36	6,084	0	2,888

Table 7-7. Sewer and water pipe attribute values.

Segment ID	Sewer pipes							Water pipes						
	ID	Material	Age	Diameter (mm)	Length (m)	Expected life (yrs.)	Initial condition	ID	Material	Age	Diameter (mm)	Length (m)	Expected life (yrs.)	Initial condition
17820	5297446	Reinforced concrete	63	750	25.95	165	0.38	88355	Ductile iron	8	350	81.89	63	0.13
17822	5297431		56	750	14.39	165	0.34	33732		51	200	124.88	63	0.81
17823	5293854		56	375	12.54	105	0.53	33733	Grey cast iron	113	150	315.21	172	0.66
17823	5293903	Brick	110	900	43.6	145	0.76	47530	Grey font	88	900	60.7	172	0.51
17825	5296284		110	900	70.05	145	0.76	33749		121	150	225.56	172	0.70
17830	5292687		117	900	73.22	145	0.70	87960	Reinforced concrete	58	900	154.3	58	0.87
17830	5302985		117	900	65.2	145	0.70	87961	Ductile iron	19	300	161	117	0.16
17831	5292688		130	900	53.8	145	0.9	33767	Steel	111	900	186.7	100	0.9
17831	5292813		130	900	53.8	145	0.9	33770	Ductile iron	15	300	194.6	63	0.24
17834	5292811		99	900	81.00	145	0.68	33801	Grey font	115	150	216.38	172	0.67
17837	5293864		98	900	13.67	145	0.68	33804		115	150	215.34	172	0.67
17838	5293900	Reinforced concrete	32	750	8.51	165	0.19	33805		118	100	388.47	172	0.69
17842	5302735		32	600	13.28	115	0.28	33809	Ductile iron	32	200	313.25	63	0.51
17844	5292267	Brick	99	900	41.42	145	0.68	33811	Grey font	117	150	308.24	172	0.68

7.7.1 Estimating the social cost indicators

Table 7-8 presents the social cost components. The duration of the synchronized interventions has been extracted from past projects executed on the street segments. The value of the duration for the microtunnelling is randomly assigned between 1.6 - 2.2 days/m to account for uncertainties (e.g., soil type) in the construction phase following a uniform distribution function adopted from (Jorjam, 2022). Annual average daily traffic (AADT) is broken down into four types of vehicles, namely: automobiles, light trucks, heavy trucks, and buses (Open Government Portal, 2023).

Table 7-8. Social cost components.

Component	Duration (days)	Source
Synchronized intervention (segment)	4 - 14	City of Montreal
MUT (microtunnelling) (m)	1.6 - 2.2	Jorjam (2022)
AADT		City of Montreal

7.7.1.1 Regression functions for *VED* costs

VED costs represent the costs of travel delays borne by vehicle passengers because of increased travel routes or time. Table 7-9 presents the results of the statistical tests for both partial and complete closures for the *VED*, *VMO*, and *AP* costs. In modeling the *VED* for partial closures, the F-statistic = 1.02 < $F_{0.05}$ = 1.09; therefore H_0 ($\sigma_1 = \sigma_2$) is accepted. The t-test assuming equal variances has a p-value = 0.44, so H_0 ($\mu_1 = \mu_2$) is accepted. For complete closures, the F-statistic = 1.01 < $F_{0.05}$ = 1.09; so H_0 ($\sigma_1 = \sigma_2$) is accepted. The t-test assuming equal variances has a p-value = 0.56, so H_0 ($\mu_1 = \mu_2$) is accepted. It can be concluded that the regression function for complete closure is adequate. Refer to Appendix E for the assumptions of the literature related to the interpretation of the statistical tests.

Table 7-9. Statistical tests for VED, VMO, and AP cost regression models.

	F-statistic	p-value
VED for partial closure	1.020	0.44
VED for complete closure	1.010	0.56
VMO for partial closure	1.010	0.54
VMO for complete closure	1.010	0.54
AP for partial closure	1.095	0.88
AP for complete closure	1.078	0.70

Equation *7-23* represents the regression model used in calculating the *VED* costs. The coefficients for each of the variables of the model are presented in Table 7-10. The coefficients show that *PD* has the highest statistical significance on *VED* costs irrespective of the nature of street closures, while the *VTD* of buses has the lowest.

$$VED_{costs} = \left(x_1 \times VTD_{auto} + x_2 \times VTD_{light\ truck} + x_3 \times VTD_{heavy\ truck} + x_4 \times VTD_{bus}\right) \times e^{x_5 \times L} \times PD^{x_6} \quad (7\text{-}23)$$

Table 7-10. Regression coefficients for VED costs.

Variables	**Coefficients**	**Partial closure**	**Complete closure**
VTD $_{auto}$	x_1	0.0124	0.0873
VTD $_{light\ truck}$	x_2	0.0074	0.0076
VTD $_{heavy\ truck}$	x_3	0.1122	0.6335
VTD $_{bus}$	x_4	0.0001	0.0001
L	x_5	0.0040	0.0040
PD	x_6	1.0306	1.0306

7.7.1.2 Regression function for *VMO* costs

Similar to the tests applied to the *VED* in Section7.7.1.1, the coefficients of the *VMO* costs are presented in Table 7-9. The *VMO* costs is calculated using Equation *7-24*. The coefficients for each variable are presented in Table 7-11. Similar to *VED* costs, the *PD* has the highest statistical significance on *VMO* costs while L has the lowest significance on *VMO* for both partial and complete closures.

$$VMO_{costs} = \left(x_1 \times VTD_{auto} + x_2 \times VTD_{light\ truck} + x_3 \times VTD_{heavy\ truck} + x_4 \times VTD_{bus}\right) \times e^{x_5 \times L} \times PD^{x_6} \quad (7\text{-}24)$$

Table 7-11. Regression coefficients for VMO costs.

Variables	Coefficients	Partial closure	Complete closure
VTD $_{auto}$	x_1	0.0230	0.1373
VTD $_{light\ truck}$	x_2	0.0072	0.0073
VTD $_{heavy\ truck}$	x_3	0.0440	0.3205
VTD $_{bus}$	x_4	0.3546	0.4067
L	x_5	0.0040	0.0040
PD	x_6	1.0256	1.0325

7.7.1.3 Regression functions for vehicle AP cost

The coefficients of the *AP* costs are presented in Table 7-9. AP costs is estimated using Equation *7-25* and the values of coefficients for partial and complete closures are presented in Table 7-12. Similar to *VED* and *VMO* costs, PD also has the highest significance on *AP* costs while *VTD* for autos and buses has the lowest significance during partial closures, and *VTD* for heavy trucks has no significance on AP costs during complete closures.

$$AP_{cost} = \left(x_1 \times VTD_{auto} + x_2 \times VTD_{light\ truck} + x_3 \times VTD_{heavy\ truck} + x_4 \times VTD_{bus}\right) \times e^{x_5 \times L} \times PD^{x_6} \quad (7\text{-}25)$$

Table 7-12. Regression coefficients for AP from vehicle emissions.

Variables	Coefficients	Partial closure	Complete closure
VTD $_{auto}$	x_1	0.0001	0.0107
VTD $_{light\ truck}$	x_2	0.0018	0.0071
VTD $_{heavy\ truck}$	x_3	0.0006	0.0000
VTD $_{bus}$	x_4	0.0001	0.3493
L	x_5	0.0039	0.0043
PD	x_6	1.0297	1.0151

7.7.2 Optimization results and discussion

This section presents the results of the optimization of both intervention alternatives. The calculations were carried out in the MATLAB R2020b (MathWorks, 2019) environment on a

computer with Intel(R) Core (TM) i7-3840QM CPU @ 2.80GHz and 32 GB RAM. The NSGA-II parameters adopted for the synchronized optimization problem include a population size of 250, a maximum number of generations set at 50, the probability of crossover set at 80%, and the mutation probability set at 1%. While the NSGA-II parameters for the MUT optimization problem include a population size of 300, a maximum number of generations of 50, the probability of crossover set at 70%, and the mutation probability set at 2%. These parameter values are the output of a hyperparameter tunning that produced the highest 3D hypervolume with a reference point as the largest possible value for all three objective functions (Bradstreet, 2011).

The selection of a single solution from the Pareto fronts of both optimization problems was achieved by selecting the solution in the Pareto front with the largest score calculated using the SAW method, assuming all objectives have equal weights as explained in Section 7.6. Figure 7-6 presents the scores for the synchronized optimization problem and Figure 7-7 presents the SAW scores for all the solutions in the Pareto front for the MUT optimization. The bar chart presents, the normalized social and agency LCCs, network deterioration, and the SAW score. Both graphs are ordered based on their descending SAW scores.

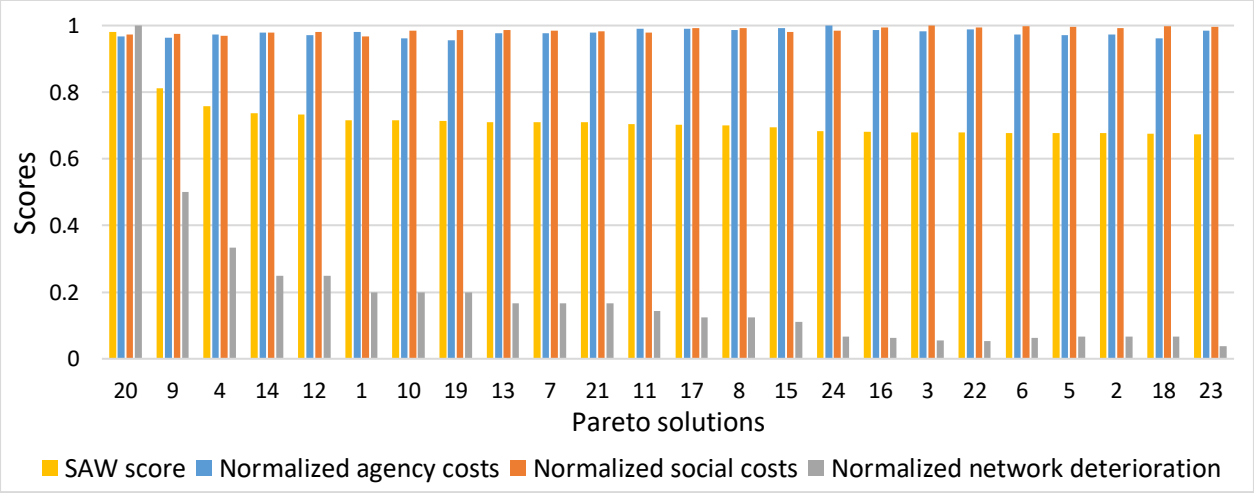

Figure 7-6. SAW weights for solutions in the Pareto front (Synchronized).

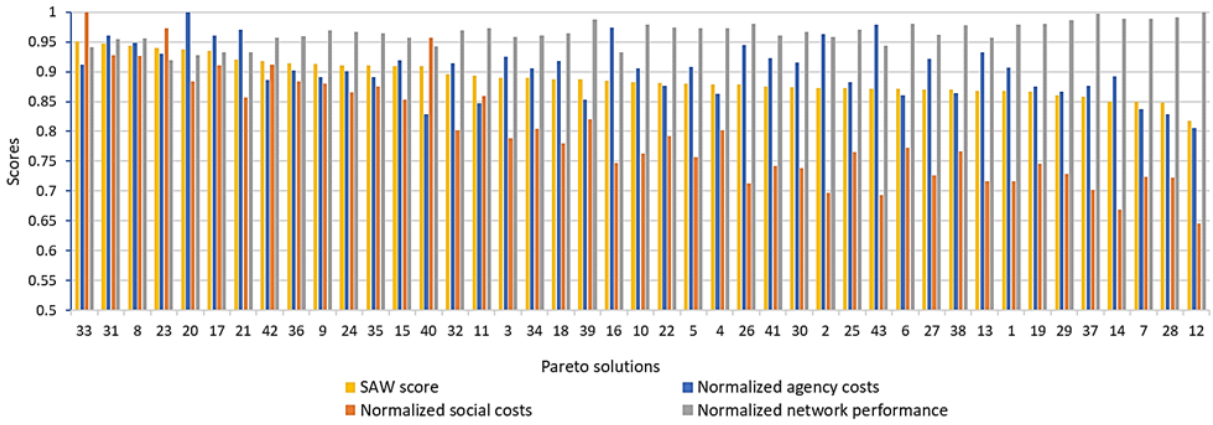

Figure 7-7. SAW weights for solutions in the Pareto front (MUT).

7.7.2.1 Synchronized intervention results

Figure 7-8 presents the generated solutions of the synchronized optimization problem. The Pareto front includes 24 solutions. Figure 7-8(a) shows the tradeoff between the synchronized agency LCC and the network deterioration. The present value for the synchronized agency LCC generated by the solutions in the Pareto front ranges from approximately CAD$2.80B to CAD$2.93B, with an average LCC of CAD$2.87B over the planning period. Figure 7-8(b) shows the tradeoff between the synchronized social LCC and the network deterioration. The synchronized social LCC across the network ranges from approximately CAD$254M to CAD$263M, with an average of CAD$258M. Meanwhile the network deterioration for all solutions in the Pareto front ranges from 0.09% to 2.26%, with an average network deterioration of 0.85%. Meaning that at the end of the planning period, only 0.09% to 2.26% of the assets in the network will require any intervention.

Figure 7-8(c) shows the tradeoff between the synchronized social LCC and synchronized agency LCC and Figure 7-8(d) presents the 3D view of all three objective functions.

The selected optimal solution for the synchronized intervention contains all the street segments, with a network agency and social LCC of CAD$2.90B and CAD$261M, respectively. The network deterioration of this solution is approximately 0.09%. The results indicate that on the segment level, the non-dominated solutions yield maximum values of CAD$7.89M and CAD$3.86M for the present values of the agency and social LCCs, respectively. In contrast, the minimum values for the agency and social LCCs are CAD$0.42M and CAD$2,267, respectively. The average values for the agency and social LCCs are CAD$2.52M and CAD$0.23M, respectively. These findings suggest that there is considerable variation in the performance of the solutions, with some

outperforming others in terms of both agency and social LCCs. The average number of segments undergoing synchronized interventions throughout the planning period is approximately 63 per year, with a maximum of 103 and a minimum of 30. In addition, the average number of interventions per segment throughout the planning period is approximately six, with a maximum of eight and a minimum of three. These values do not account for the interventions due to sudden damages that occur when assets are not regularly maintained due to the limitation in the placement of utilities under the subsurface.

7.7.2.2 MUT optimization results

Figure 7-9 shows the generated solutions of the MUT optimization problem. The Pareto front includes 43 solutions. Figure 7-9(a) presents the tradeoff between the MUT agency LCC and the network deterioration. The MUT agency LCC generated by the solutions in the Pareto front ranges from approximately CAD$3.02B to CAD$3.75B, with an average of CAD$3.35B, over the planning period, which is slightly higher than the agency LCC for the synchronized intervention. Furthermore, the maximum number of street segments selected for MUT implementation by all 43 solutions in the Pareto front are 362 and the minimum is 292 (out of 1,150 segments) with an average of 333 over the planning period. These results corroborate with the literature, as not all street segments have the potential to maximize the benefits of the MUT due to their location, street class, AADT, etc. (Genger et al., 2021). This is especially relevant when resources are limited. Meanwhile, the resulting network deterioration ranges from 68.55% to 74.63%, with an average of 71.08%. These values mean that at the end of the planning period, 68.55% to 74.63%, of the street segments will have assets requiring some form of intervention.

Figure 7-9(b) shows the tradeoff between the MUT social LCC and the network deterioration. The MUT social LCC ranges from CAD$77M to CAD$120M, with an average social LCC of CAD$98M. Figure 7-9(c) shows the tradeoff between the MUT social LCC and the agency LCC and Figure 7-9(d) shows the tradeoff between all three objective functions.

The solution in the Pareto front selected for the MUT optimization contains 312 street segments with a MUT agency LCC and social LCC of CAD$3.32B and CAD$77M, respectively, and a network deterioration of 72.89%. Furthermore, on a segment level, the maximum MUT agency and social LCC values generated are CAD$70.5M and CAD$3.92M, respectively. Meanwhile, the

minimum values are both zeros (i.e., street segments where no MUTs are implemented yet) with average values of CAD$10.62M and CAD$0.25M for the agency and social LCCs, respectively.

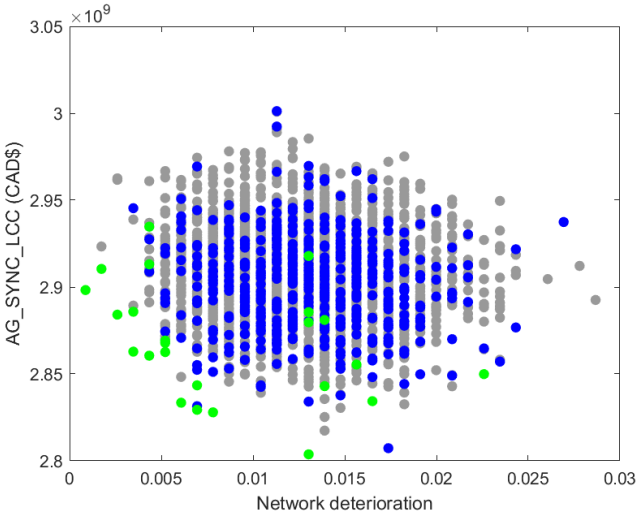

(a) Synchronized agency LCC vs Network deterioration

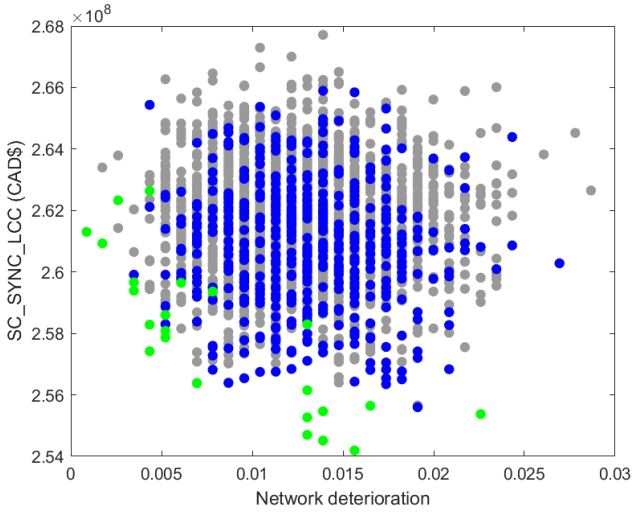

(b) Synchronized social LCC vs Network deterioration

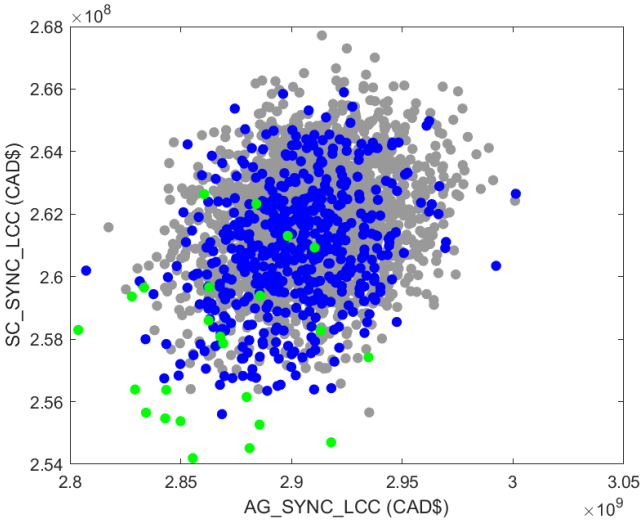

(c) Synchronized social vs Synchronized agency LCCs

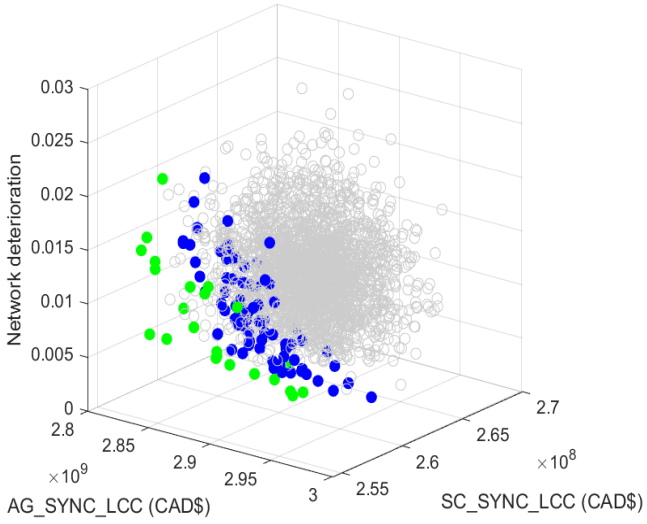

(d) Network deterioration vs Synchronized social LCC vs Synchronized agency LCC

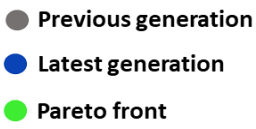

Figure 7-8. Comparison of the values of the objective functions (synchronized interventions)

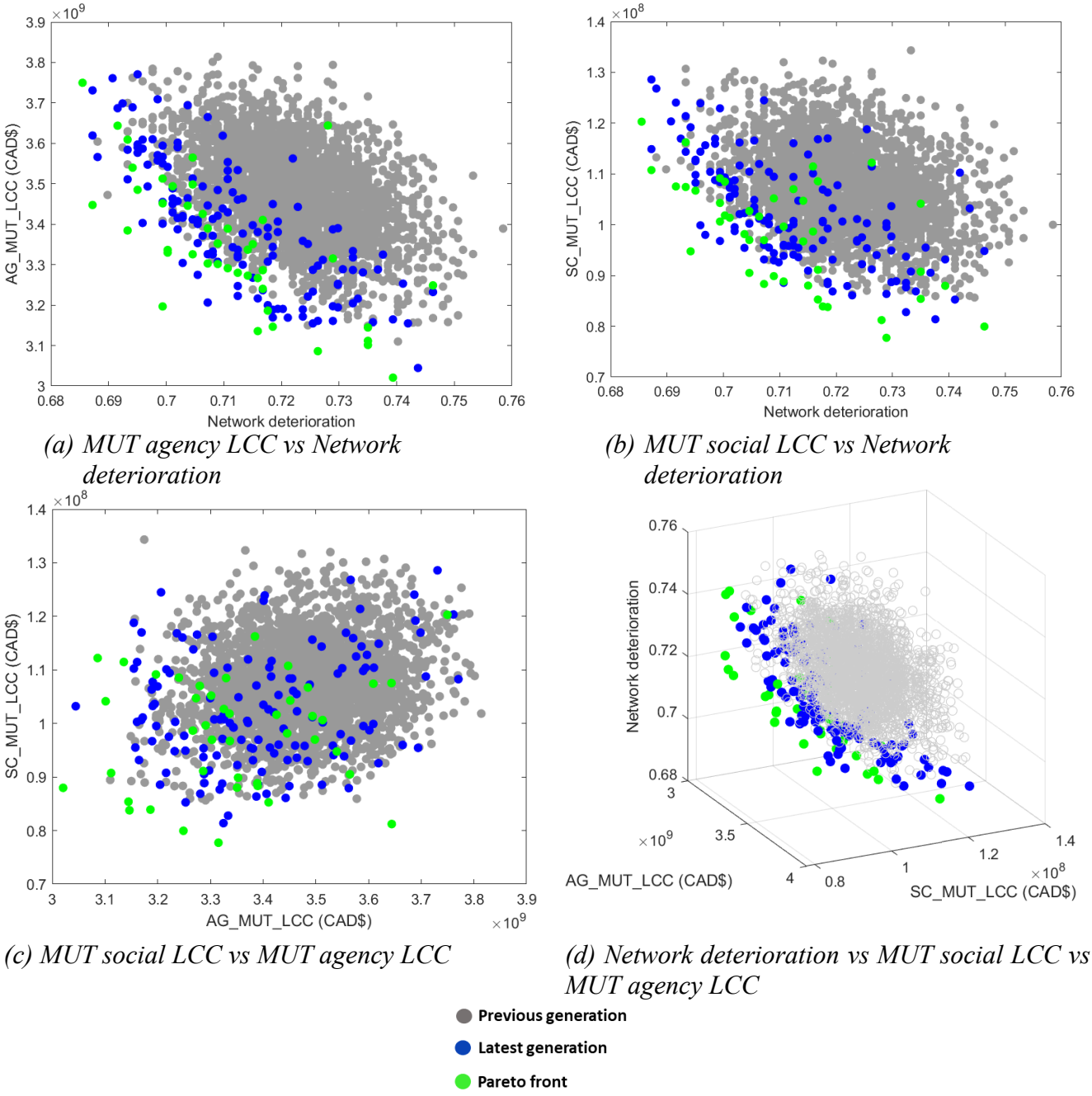

(a) MUT agency LCC vs Network deterioration

(b) MUT social LCC vs Network deterioration

(c) MUT social LCC vs MUT agency LCC

(d) Network deterioration vs MUT social LCC vs MUT agency LCC

Figure 7-9. Comparison of the values of the objective functions (MUT)

Every year (other than the initial year in the planning period), the cost of maintenance and repair of assets in existing MUTs is always considered, and therefore deducted from the present value of the yearly agency cost budget. The remainder of the budget is then used for the construction of new

MUTs. This budgetary constraint, coupled with the conditions and their respective intervention strategies that serve as an opportunity for MUT implementation in a particular year, may result in no new MUTs being built in certain years. On the other hand, some years have as many as seven segments selected for MUT implementation.

7.7.3 Location selection

Coupled with the values of the objective functions for the solutions in the Pareto front, an interventions plan showing the segments and the year in the planning period for the proposed interventions (synchronized and MUT) is also generated for each solution in the Pareto front. Based on the SAW scores, solutions 20 and 33 have the highest scores for the synchronized and MUT Pareto fronts, respectively, as shown in Figure 7-6 and Figure 7-7.

The results presented in Figure 7-10 and Figure 7-11 illustrate the distribution of the number of synchronized interventions conducted during each decade of the planning period and the present values of the agency and social LCCs, respectively. Both figures reveal that the first decade of the planning period experienced a relatively high number of street segments selected for synchronized interventions, as well as relatively high agency LCC. Subsequently, there are small variations in the number of synchronized interventions although the present values of the agency and social LCCs decrease down the planning period.

These decreases are reflecting the effect of the discount rate. Furthermore, the highest number of interventions are experienced during the fourth and seventh decades of the planning period.

Figure 7-12 and Figure 7-13 displays the distribution of the number of potential street segments selected for implementation of the MUT for each decade in the planning period and the corresponding present values of the agency and social LCCs, respectively. Similar to the distribution of synchronized interventions, both figures show a steady decrease in the present value of both LCCs with a slight variation in the number of potential street segments selected for MUT implementation across the planning period. Meanwhile, the lowest and highest number of segments are obtained in the third and eighth decades, respectively.

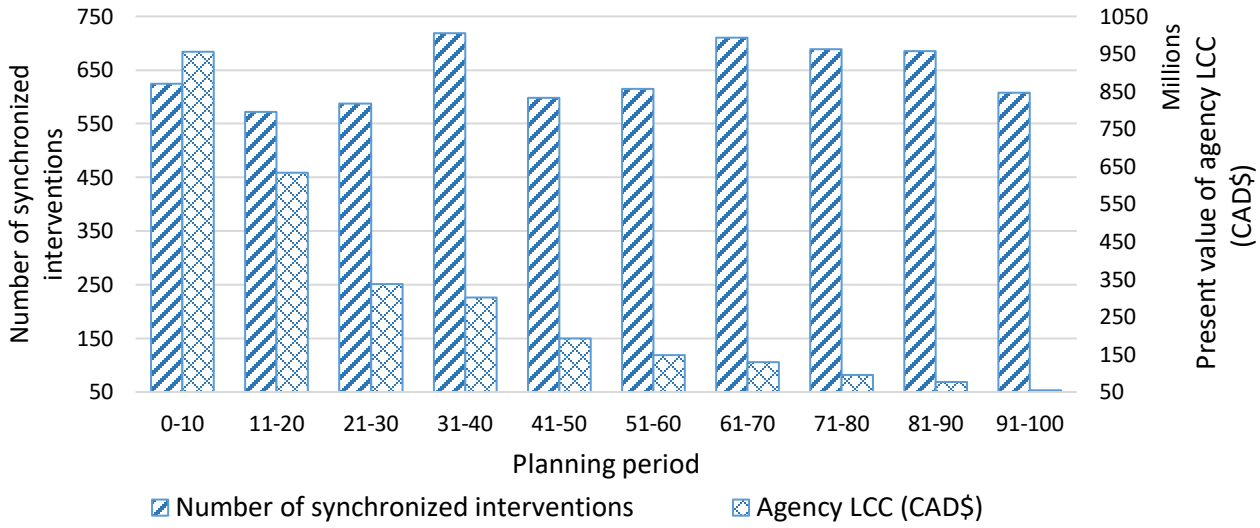

Figure 7-10. Number of synchronized interventions vs present value of agency LCC for the planning period.

These figures (Figure 7-10 to Figure 7-13) also show the difference in the number of synchronized interventions as compared to the number of potential MUTs and their corresponding LCCs. The figures clearly show that although the number of potential MUTs only make a fraction of the number street segments for synchronized intervention, the have a higher agency LCC and a lower social LCC.

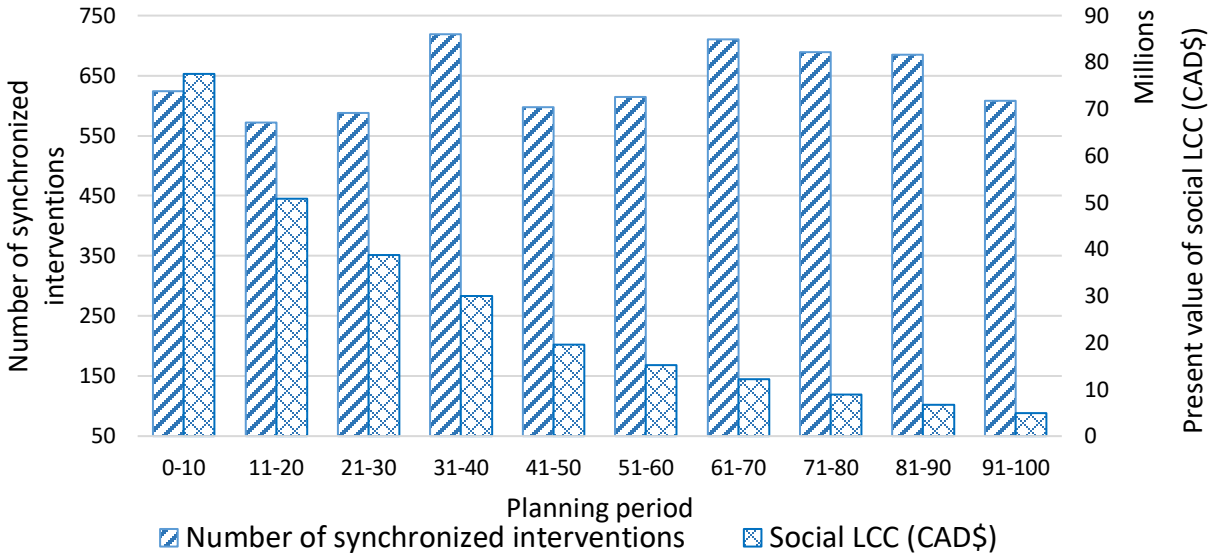

Figure 7-11. Number of synchronized interventions vs present value of social LCC for the planning period.

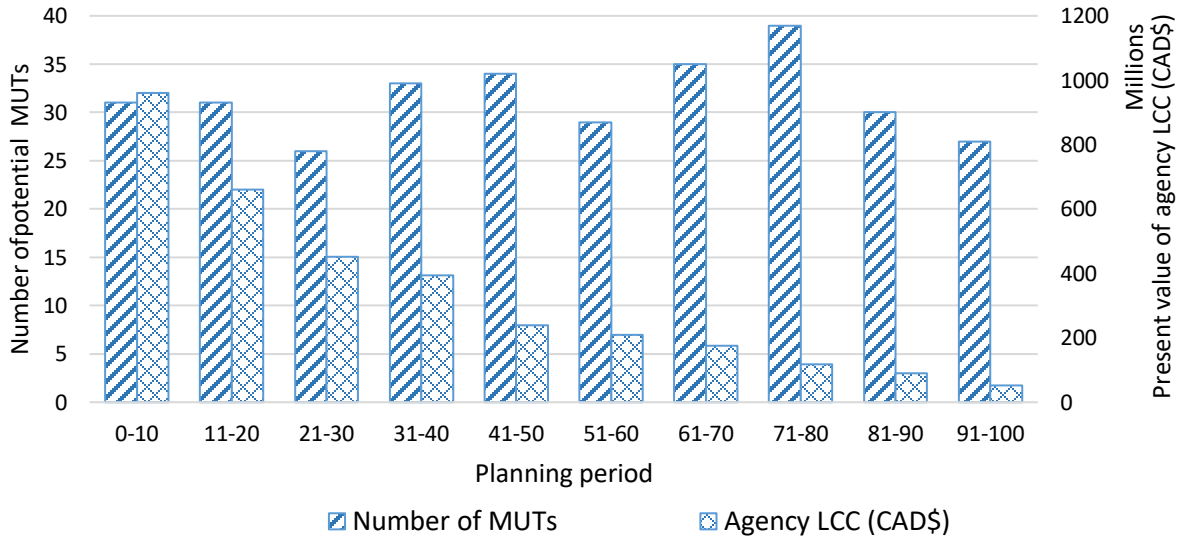

Figure 7-12. Number of MUTs vs present value of agency LCC for the planning period

Table 7-13 presents the network-level optimization results and the budgets for both alternatives. Based on the network comparison of both alternatives across the planning period, the present value of the MUT agency LCC surpasses the synchronized agency LCC with a significant difference of about CAD$417M. However, the MUT has a lower social LCC with a difference of about CAD$184M. These values agree with the literature because the implementation of MUTs is expected to offer social LCC savings although the cost of implementation is higher.

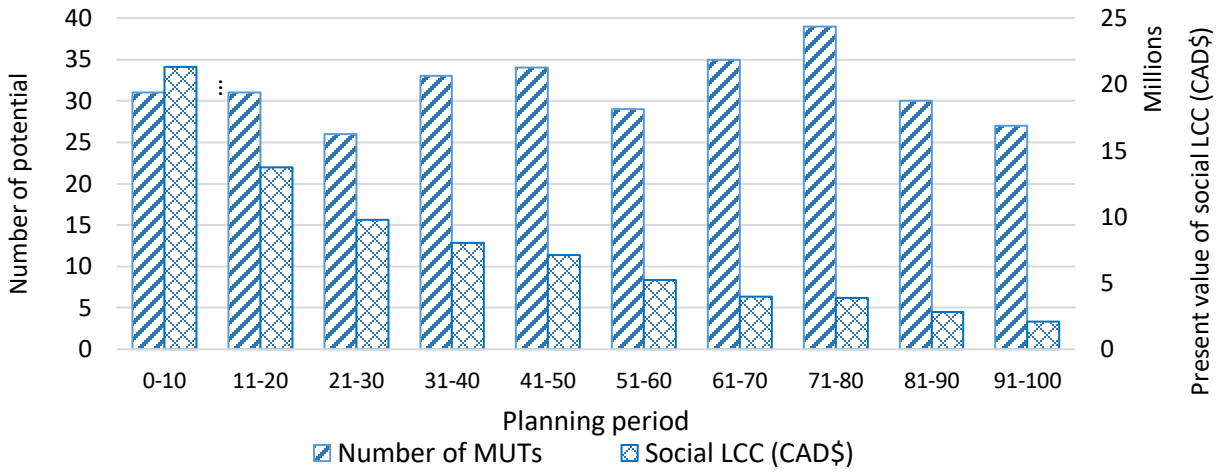

Figure 7-13. Number of MUTs vs present value of social LCC for the planning period

Based on the selected solution from the Pareto front, Figure 7-14 shows the potential street segments selected for MUT implementation and the range of years for their implementation. The GIS map shows that the majority of the selected street segments are located in the downtown area, and even though these segments will generate high social costs during MUT construction. However, they will also offer the highest level of benefits of implementing the MUT in the rest of their lifecycle.

Table 7-13. Summary of network optimization results

	Agency LCC (CAD$)	**Social LCC (CAD$)**	**Network deterioration (%)**
Synchronized intervention	2.90 B	261 M	0.09
MUT	3.32 B	77 M	72.89
Yearly budget	140 M	8.5 M	-
Total present value of the budget (100Y)	4.56 B	277 M	-

Using the synchronized interventions and MUT implementation plans, a segment-level comparison was done on the 312 segments (i.e., the potential MUT segments) that are common to both plans. The results show that 70 street segments offer agency LCC savings ranging from CAD$24,161 to CAD$5.15M with an average of CAD$1.34M and a total agency LCC savings of about CAD$93.48M. Meanwhile, 136 street segments offer social LCC savings ranging from as low as CAD$89 to a high of CAD$0.63M, with an average of approximately CAD$99,821 and a total social LCC of approximately CAD$6.99M. Furthermore, 51 street segments offer both agency and social LCC savings of about CAD$69.52M and CAD$4.5M, respectively. In addition, the results

also show that MUTs are suitable in certain locations, as only 51 out of the 312 potential segments selected for MUT implementation offer both agency and social LCC savings. Figure 7-15 and Figure 7-16 show the locations of the street segments with agency and social LCC savings, respectively, and Figure 7-17 shows the street segments with both LCC savings.

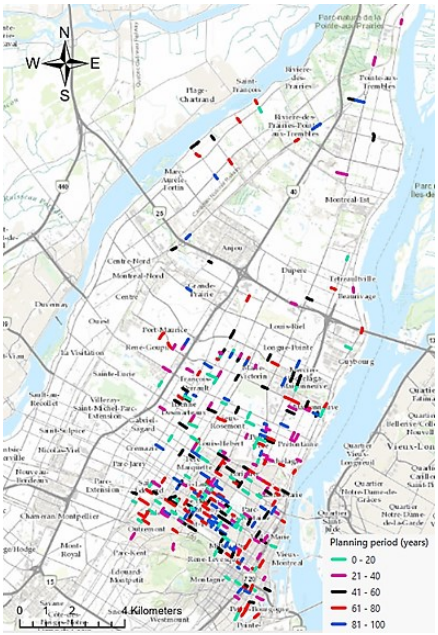

Figure 7-14. MUT selected locations in the Pareto front.

7.7.4 Discussion

The implementation of MUTs on street segments is a special intervention that should be carefully considered due to potential social costs during construction that may exceed those of regular interventions such as pipe replacements or pavement reconstructions. The inclusion of privately owned and managed assets (e.g., telecom, electricity, and gas) in synchronized interventions has the potential to increase social costs further, resulting in greater social LCC savings with MUTs. In addition to the quantifiable benefits of MUTs, such as ease of maintenance and longer pavement lifespan, there are also less quantifiable benefits that should be considered in LCC analysis. However, the current study has not factored in additional costs associated with damage to buried utilities over their lifecycle, which can result in service loss, repair costs, and reduced quality of life. It is also important to note that while social LCC savings from MUT implementation are continuous throughout the lifespan of the MUT, it is difficult to estimate these savings in the current optimization model. For example, MUTs implemented in the later part of the planning period will

continue to offer benefits and savings for the rest of their service lives, whereas synchronized interventions will continue to accrue social costs with each intervention in the planning period.

7.8 Summary

This chapter developed a framework to optimize the location selection of MUTs based on the agency and social LCCs and network deterioration using the NSGA-II algorithm. The use of two multi-objective optimization models for minimizing the agency and social LCCs, as well as the network deterioration, ensured the optimal cost and timing of implementing both the synchronized method of utility interventions and the MUT were obtained.

By quantifying the socioeconomic impacts of implementing both the MUT and the synchronized utility interventions at the network level and segment level, the costs of both intervention alternatives have been optimized and compared.

The results show that the tradeoff between the social LCC and agency LCC significantly affects the location selection. Although the literature argues that MUTs are more sustainable in general, this study shows that by estimating the social costs associated with each alternative at the network and segment levels, the tradeoff between the objectives makes MUT only suitable in certain street segments in urban locations. Meanwhile, as shown in the results, at the network and segment levels, there is a significant difference in the LCC of implementing the MUT compared to the synchronized interventions. Although at the network level, the MUT has a higher agency LCC, the social LCC of implementing synchronized interventions is higher. Furthermore, the benefits of the implementation of MUTs will continue for decades after their construction.

The contributions of this chapter are as follows:

The main objective of this research is to optimize the agency and social LCCs and network deterioration using multi-objective optimization for identifying the potential locations of MUTs. This selection involves modeling the agency and social cost savings and the network deterioration resulting from the implementation at the network and segment levels. Comparing the optimization results in identifying the street segments in a network where the LCC of implementing MUTs is less than the LCC of the synchronized utility intervention. While doing so, a multi-year plan for MUT location selection that optimizes the three objective functions and offers lifecycle savings is achieved.

(1) Defining a multi-objective optimization model that was able to identify the potential MUT locations and a multi-year plan for MUT implementation that optimizes the three objective functions and offers lifecycle savings. The candidate MUTs locations have been identified purely based on mathematical optimization without any subjective reasoning as was done in previous research (Genger *et al.*, 2021). This is a novel approach that increases the objectivity and reliability of the decision-making process.

(2) Developing a systematic method for comparing the results of the MUT optimization with those of the synchronized interventions. This comparison is based on the agency and social LCCs, and the network deterioration generated by the MUTs and synchronized method of utility interventions at the network and segment levels. Based on this comparison, it can be concluded that, when compared with the optimized results of the synchronized interventions, 51 out of 312 potential MUT locations (optimized from a network of 1,151 street segments) provided both agency and social LCC savings.

(3) Developing three regression models for capturing the social cost of both alternatives at the network and segment levels. The three social cost indicators resulting from the regression models are effective tools for capturing the benefits of MUTs in reducing the negative impacts on traffic and environment. Quantifying the social cost benefits of MUTs using these models provided valuable insights into the potential advantages of implementing MUTs.

Furthermore, the MUT optimization model does not contain intangible agency and social cost components such as the ease of maintenance, added protection of assets hosted in the MUT, etc. Methods for calculating these costs will further improve the optimization results.

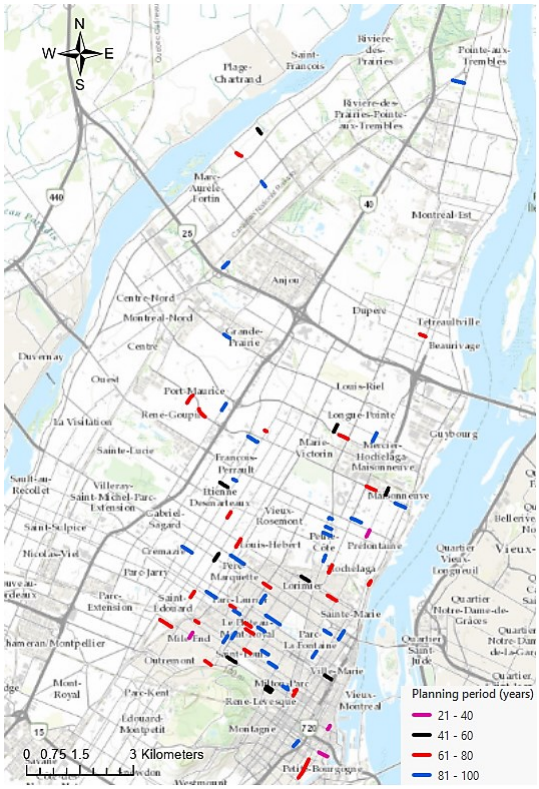

Figure 7-15. Street segments with agency LCC savings

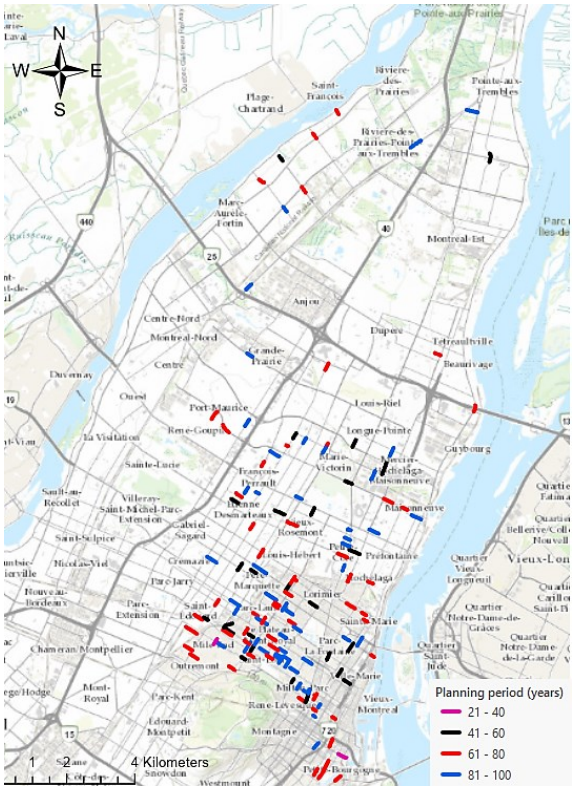

Figure 7-16. Street segments with social LCC savings

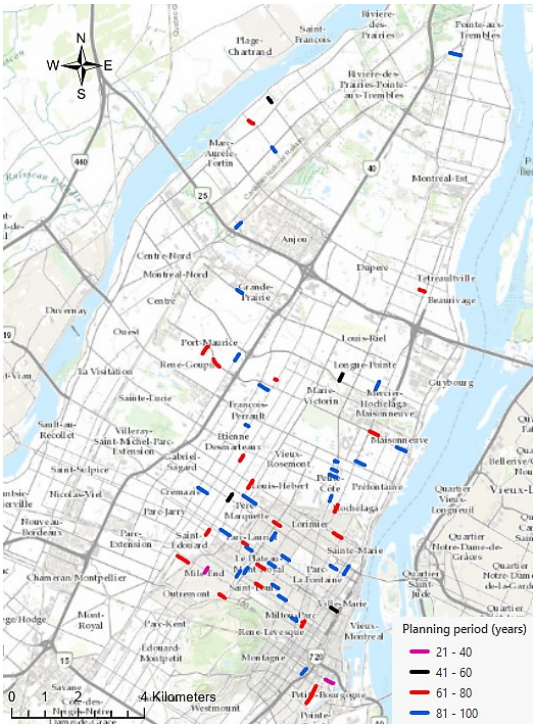

Figure 7-17. Street segments with both LCC savings

CHAPTER 8. SUMMARY, CONCLUSIONS, CONTRIBUTIONS, AND FUTURE WORK

8.1 Introduction

This chapter provides a summary of both the conceptual and practical implications of the research, highlighting its contributions to the existing body of knowledge. In addition, it presents key conclusions drawn from the findings and outlines potential avenues for future research.

8.2 Summary of the Research

The complex and multidimensional nature of the MUT location selection problem is addressed in the proposed framework, which incorporates geospatial visual analytics to aid decision-making (Chapter 4). By utilizing spatial analysis and visual and statistical methods, the framework presents the socioeconomic impact of utility interventions, enabling stakeholders to make informed decisions. This aspect of the research module facilitates the quantification of the relationship between current practices and their corresponding effects on the surrounding areas.

Chapter 5 explored the application of condition-based classification of underground utility assets, utilizing three ensemble ML algorithms. The implementation of a uniform classification scale allowed for the transition from asset-level to segment-level interventions, enabling the identification of street segments suitable for MUT implementation and the determination of the necessary segment-level interventions. In addition, this approach is applicable for enhancing synchronized interventions at the segment level, which is considered best practice and a short-term solution to utility interventions. The proposed methodology provides a useful tool for stakeholders involved in underground utility management, facilitating more effective decision-making and improving the efficiency of infrastructure maintenance and upgrade programs.

The methodology provided in Chapter 6 incorporates both subjective and objective MCDM methods to determine the location selection for MUTs by analyzing spatial data. This approach allows for the weighting of various criteria, providing a more holistic assessment of potential locations. By combining the weights and criteria scores of preselected locations, the framework generates a ranking of the most suitable locations for MUT implementation. Overall, this approach represents an effective tool for decision-makers involved in the selection of MUT locations, providing a comprehensive and data-driven approach to infrastructure planning and management.

Chapter 7 examines the use of mathematical optimization algorithms to identify street segments suitable for MUT implementation. This module involves quantifying, optimizing, and comparing agency and social LCC savings, as well as minimizing network asset deterioration. By analyzing both network and segment levels, the module determines which street segments are best suited for MUT implementation. This approach ensures that the identified MUT locations are optimal, guaranteeing long-term LCC savings.

8.3 Research Contributions and Conclusions

The contributions of this research are as follows:

(1) Developing a geospatial visual analytics model that supports the understanding of the socioeconomic impacts of unsynchronized intervention practices. Based on this contribution, the following conclusions can be stated:

- The proposed geospatial visual analytics model represents a valuable tool for identifying, visualizing, and quantifying the negative socioeconomic implications of unsynchronized utility interventions on a multi-utility network. By utilizing this model, stakeholders can more effectively assess the impact of infrastructure maintenance and upgrade programs and make informed decisions about the implementation of MUTs.

(2) Developing an ML method for systematic condition classification of different spatially collocated underground municipal assets (i.e., pavements, water and sewer pipes) within a segment. To the best of our knowledge, there is no existing research about determining street closures based on the combined conditions of spatially collocated municipal infrastructure assets at the segment level. Based on this contribution, the following conclusions can be stated:

- The high accuracy of each ensemble machine learning model indicates an acceptable performance in the classification of the spatially collocated municipal assets as shown in Table 5-20.
- Using a uniform classification scale for all three municipal assets enabled the determination of asset-level interventions, whose combination led to segment-level interventions and street closure decisions.
- The proposed solution also identifies segments where MUTs can be considered as an alternative to synchronized interventions that require excavations.

(3) Applying a heuristic approach for determining street closures based on the synchronized or unsynchronized interventions at the segment level induced by combining the interventions of individual assets within each segment. Based on this contribution, the following conclusions can be stated:

- The intervention strategies derived from the applied heuristics were used to determine the intervention unique to restoring the condition of each asset while taking a holistic approach to restoring the conditions of all spatially collocated assets within a segment.
- The predicted segment-level interventions have an accuracy of 79.92%.
- Based on the segment-level interventions, potential street segments for MUT location selections have been identified.
- The segment-level intervention strategies resulted in both synchronized and unsynchronized interventions leading to complete or partial street closures. Some street segments require partial and complete street closures to accommodate the initial pipe rehabilitation phase and the subsequent pavement reconstruction or rehabilitation phase of the intervention.

(4) Defining a comprehensive MCDM model that identifies and quantifies the criteria that influence the MUT location selection using subjective and objective methods. Based on this contribution, the following conclusions can be stated:

- The use of AHP and ANP showed considerable differences in the calculated criteria weights and subsequent ranking of the alternatives. However, factoring in the dependencies affected the criteria weights and the subsequent ranking as only 40% of the ranking positions were similar for the combination of both AHP and ANP with TOPSIS.
- Comparing the ranking results also showed that 70% of the results obtained from the combination of ANP+TOPSIS were similar to the results obtained from the Entropy+TOPSIS combination, unlike the AHP+TOPSIS combination which had a 30% similarity.
- The results show that a systematic process for MUT location selection can be achieved using spatial data.
- The developed software enables the automated ranking of street segments for the location selection of the placement of MUTs.

(5) Defining a multi-objective optimization model that was able to identify the potential MUT locations and a multi-year plan for MUT implementation that optimizes the three objective functions and offers lifecycle savings. The candidate MUTs locations have been identified purely based on mathematical optimization without any subjective reasoning as was done in previous research (Genger *et al.*, 2021). This is a novel approach that increases the objectivity and reliability of the decision-making process.

(6) Developing a systematic method for comparing the results of the MUT optimization with those of the synchronized interventions. This comparison is based on the agency and social LCCs, and the network deterioration generated by the MUTs and synchronized method of utility interventions at the network and segment levels. Based on this comparison, it can be concluded that, when compared with the optimized results of the synchronized interventions, 51 out of 312 potential MUT locations (optimized from a network of 1,151 street segments) provided both agency and social LCC savings.

(7) Applying three regression models for capturing the social cost of both alternatives at the network and segment levels. The three social cost indicators resulting from the regression models are effective tools for capturing the benefits of MUTs in reducing the negative impacts on traffic and environment. Quantifying the social cost benefits of MUTs using these models provided valuable insights into the potential advantages of implementing MUTs.

8.4 Limitations and Future Work

Despite the contributions listed above, some limitations of this research need to be addressed in the future.

(1) The methods applied in this research rely on data related to several attributes of water and sewer pipes and pavements. In some instances, where these assets are not managed together, data availability and coordination may become an issue.

(2) Only municipal assets were considered in this research. However, other buried assets such as gas pipes and electrical cables could be combined in determining street closures and MUT location selection.

(3) The relationships presented in Chapter 4 do not necessarily represent a cause and effect, due to the lack of temporal precedence and sequential data representing the cause-and-effect timelines.

(4) Issues such as the lack of motivation of the different stakeholders and data-sharing platforms can also hamper synchronized segment-level interventions. Future research should include estimating the impact of uncertainties on the use of methods that require risk assessment or the probability of failure and ML methods.

(5) In addition to a balanced sewer pipe dataset, including features like the slope, pressure, soil, etc., could improve the sewer pipe condition model.

(6) Furthermore, the pavement intervention strategy could integrate indicators such as frost susceptibility and road bearing capacity.

(7) In Chapter 5, some alternatives have missing criterion values for the number of expected excavations, which could affect the Entropy weights for the criteria, and therefore, the overall ranking of the alternatives.

(8) Furthermore, the MUT optimization model does not contain intangible agency and social cost components such as the ease of maintenance, added protection of assets hosted in the MUT, etc. Methods for calculating these costs will further improve the optimization results.

REFERENCES

Abdelaziz, N., Abd El-Hakim, R.T., El-Badawy, S.M. and Afify, H.A. (2020), "International Roughness Index prediction model for flexible pavements", *International Journal of Pavement Engineering*, Vol. 21 No. 1, pp. 88–99, doi: 10.1080/10298436.2018.1441414.

Abu-Samra, S., Ahmed, M. and Amador, L. (2020), "Asset Management Framework for Integrated Municipal Infrastructure", *Journal of Infrastructure Systems*, American Society of Civil Engineers (ASCE), Vol. 26 No. 4, p. 04020039, doi: 10.1061/(asce)is.1943-555x.0000580.

Abu-Samra, S., Ahmed, M., Hammad, A. and Zayed, T. (2018a), "Multiobjective Framework for Managing Municipal Integrated Infrastructure", *Journal of Construction Engineering and Management*, Vol. 144 No. 1, doi: 10.1061/(ASCE)CO.1943-7862.0001402.

Abu-Samra, S., Ahmed, M., Hammad, A. and Zayed, T. (2018b), "Multiobjective Framework for Managing Municipal Integrated Infrastructure", *Journal of Construction Engineering and Management*, Vol. 144 No. 1, doi: 10.1061/(ASCE)CO.1943-7862.0001402.

Alaghbandrad, A. and Hammad, A. (2018), "PPP Cost-Sharing of Multi-purpose Utility Tunnels", in Smith, I.F.C. and Domer, B. (Eds.), *Advanced Computing Strategies for Engineering*, Springer International Publishing, Cham, pp. 554–567.

Alaghbandrad, A. and Hammad, A. (2020), "Framework for multi-purpose utility tunnel lifecycle cost assessment and cost-sharing", *Tunnelling and Underground Space Technology*, Vol. 104, p. 103528, doi: 10.1016/j.tust.2020.103528.

al Amari, C., ben Hassine, S., Bruxelle, C. and Modieli, S. (2013), *Guide d'élaboration d'un Plan d'intervention Pour Le Renouvellement Des Conduites d'eau Potable, d'égouts et Des Chaussées. Guide Destiné Au Milieu Municipal Québécois.*

American Public Works Association (APWA). (1971), *Feasibility of Utility Tunnels in Urban Areas*, Chicago.

Amin, S.R. and Amador-Jiménez, L.E. (2017), "Backpropagation Neural Network to estimate pavement performance: dealing with measurement errors", *Road Materials and Pavement Design*, Taylor & Francis, Vol. 18 No. 5, pp. 1218–1238, doi: 10.1080/14680629.2016.1202129.

Andrienko, G., Andrienko, N., Fuchs, G., Rüping, S., Cordero, J.M., Scarlatti, D., Vouros, G.A., *et al.* (2020), "Visual analytics in the aviation and maritime domains", *Big Data Analytics for Time-Critical Mobility Forecasting: From Raw Data to Trajectory-Oriented Mobility*

Analytics in the Aviation and Maritime Domains, Springer International Publishing, pp. 59–84, doi: 10.1007/978-3-030-45164-6_3.

Andriy, B. (2019), *The Hundred-Page Machine Learning*, Andriy Burkov.

Arhin, S.A., Noel, E.C. and Ribbiso, A. (2015a), "Acceptable International Roughness Index Thresholds based on Present Serviceability Rating", *Journal of Civil Engineering Research*, Vol. 2015 No. 4, pp. 90–96.

Arhin, S.A., Williams, L.N., Ribbiso, A. and Anderson, M.F. (2015b), "Predicting Pavement Condition Index Using International Roughness Index in a Dense Urban Area", *Journal of Civil Engineering Research*, Vol. 10 No. 17, doi: 10.5923/j.jce.20150501.02.

Bank of Canada. (2022), "Inflation Calculator - Bank of Canada", available at: http://www.bankofcanada.ca/rates/related/inflation-calculator/ (accessed 5 December 2022).

Bashar, M.Z. and Torres-Machi, C. (2021), "Performance of Machine Learning Algorithms in Predicting the Pavement International Roughness Index", *Transportation Research Record: Journal of the Transportation Research Board*, SAGE PublicationsSage CA: Los Angeles, CA, Vol. 2675 No. 5, pp. 226–237, doi: 10.1177/0361198120986171.

Behzadian, M., Khanmohammadi Otaghsara, S., Yazdani, M. and Ignatius, J. (2012), "A state-of the-art survey of TOPSIS applications", *Expert Systems with Applications*, Elsevier Ltd, 1 December, doi: 10.1016/j.eswa.2012.05.056.

Bobylev, N. (2011), "Comparative analysis of environmental impacts of selected underground construction technologies using the analytic network process", *Automation in Construction*, Vol. 20 No. 8, pp. 1030–1040, doi: 10.1016/j.autcon.2011.04.004.

Bradstreet, L. (2011), *The Hypervolume Indicator for Multi-Objective Optimisation: Calculation and Use*, University of Western Australia Perth.

Braun, A.J. (2012), "Planning an Integrated Utility /Roadway Project Brings Asset Management to Life", *Proceedings of the Water Environment Federation*, Water Environment Federation, Vol. 2003 No. 3, pp. 216–220, doi: 10.2175/193864703784830054.

Brownlee, J. (2019), *XGBoost with Python*, *Machine Learning Mastery*.

BVH Integrated Services, P. (2018a), "Utility Tunnel, Central Connecticut State University".

BVH Integrated Services, P. (2018b), "University of Massachusetts Boston", available at: http://www.bvhis.com/university-of-massachusetts-boston.html (accessed 24 January 2019).

CAA. (2013), “Driving Costs Beyond the price tag: Understanding your vehicle’s expenses Canadian automobile association 2013 Edition”.

Caffoor, I. (2019), *Robotics and Autonomous Systems (RAS) for Buried Pipe Infrastructure and Water Operations*, *TWENTY65*.

Calvo-Peña, V., Curiel-Esparza, J. and Canto-Perello, J. (2006), “Risk assessment of urban utilidors”.

Candel, A. and Parmar, V. (2015), “Deep Learning with H2O ’ s R Package Introduction”, pp. 1–21.

Cano-Hurtado, J.J. and Canto-Perello, J. (1999), “Sustainable development of urban underground space for utilities”, *Tunnelling and Underground Space Technology*, Vol. 14 No. 3, pp. 335–340, doi: 10.1016/S0886-7798(99)00048-6.

Canto-Perello, J. and Curiel-Esparza, J. (2001), “Human factors engineering in utility tunnel design”, *Tunnelling and Underground Space Technology*, Vol. 16 No. 3, pp. 211–215, doi: 10.1016/S0886-7798(01)00041-4.

Canto-Perello, J. and Curiel-Esparza, J. (2013), “Assessing governance issues of urban utility tunnels”, *Tunnelling and Underground Space Technology*, Elsevier Ltd, Vol. 33, pp. 82–87, doi: 10.1016/j.tust.2012.08.007.

Canto-Perello, J., Curiel-Esparza, J. and Calvo, V. (2009), “Analysing utility tunnels and highway networks coordination dilemma”, *Tunnelling and Underground Space Technology*, Vol. 24 No. 2, pp. 185–189, doi: 10.1016/j.tust.2008.07.004.

Canto-Perello, J., Curiel-Esparza, J. and Calvo, V. (2013), “Criticality and threat analysis on utility tunnels for planning security policies of utilities in urban underground space”, *Expert Systems with Applications*, Elsevier Ltd, Vol. 40 No. 11, pp. 4707–4714, doi: 10.1016/j.eswa.2013.02.031.

Canto-Perello, J., Curiel-Esparza, J. and Calvo, V. (2016), “Strategic decision support system for utility tunnel’s planning applying A’WOT method”, *Tunnelling and Underground Space Technology*, Elsevier Ltd, Vol. 55, pp. 146–152, doi: 10.1016/j.tust.2015.12.009.

Caradot, N., Riechel, M., Fesneau, M., Hernandez, N., Torres, A., Sonnenberg, H., Eckert, E., *et al.* (2018), “Practical benchmarking of statistical and machine learning models for predicting the condition of sewer pipes in Berlin, Germany”, doi: 10.2166/hydro.2018.217.

Carey, B.D. and Lueke, J.S. (2013), "Optimized holistic municipal right-of-way capital improvement planning", *Canadian Journal of Civil Engineering*, NRC Research Press, Vol. 40 No. 12, pp. 1244–1251, doi: 10.1139/cjce-2012-0183.

Chacon, N. and Normand, H. (2016), *Plan D'Intervention Ville de Montreal*, Montreal.

Chatti, K. and Zaabar, I. (2012), *Estimating the Effects of Pavement Condition on Vehicle Operating Costs*, *Estimating the Effects of Pavement Condition on Vehicle Operating Costs*, doi: 10.17226/22808.

Chawla, N. v, Bowyer, K.W., Hall, L.O. and Kegelmeyer, W.P. (2002), "SMOTE: Synthetic Minority Over-sampling Technique", *Journal of Artificial Intelligence Research*, Vol. 16, pp. 321–357.

Chen, C.H. (2020), "A novel multi-criteria decision-making model for building material supplier selection based on entropy-AHP weighted TOPSIS", *Entropy*, MDPI AG, Vol. 22 No. 2, p. 259, doi: 10.3390/e22020259.

Chen, S., Lin, L. and Yuan, X. (2017), "Social Media Visual Analytics", *Computer Graphics Forum*, Blackwell Publishing Ltd, Vol. 36 No. 3, pp. 563–587, doi: 10.1111/cgf.13211.

Chris, C. (2015), *University of {Rochester}'s {Tunnel} {System} – {Rochester}, {NY}*.

City of Charleston. (2013), "Steel Plates Requirements Used in Connection with Roadway Utility Excavations", No. April.

Clarke, B.G., Magee, D., Dimitrova, V. and ... (2017), "A decision support system to proactively manage subsurface utilities", *... Symposium for Next ...*.

Curiel-Esparza, J. and Canto-Perello, J. (2013), "Selecting utilities placement techniques in urban underground engineering", *Archives of Civil and Mechanical Engineering*, Elsevier, Vol. 13 No. 2, pp. 276–285, doi: 10.1016/j.acme.2013.02.001.

Curiel-Esparza, J., Canto-Perello, J. and Calvo, M.A. (2004), "Establishing sustainable strategies in urban underground engineering", *Science and Engineering Ethics*, Vol. 10 No. 3, pp. 523–530, doi: 10.1007/s11948-004-0009-5.

Deb, K., Pratap, A., Agarwal, S. and Meyarivan, T. (2002), "A fast and elitist multiobjective genetic algorithm: NSGA-II", *IEEE Transactions on Evolutionary Computation*, Vol. 6 No. 2, pp. 182–197, doi: 10.1109/4235.996017.

Dehdasht, G., Salim Ferwati, M., Zin, R.M. and Abidin, N.Z. (2020), "A hybrid approach using entropy and TOPSIS to select key drivers for a successful and sustainable lean construction

implementation", edited by Xue, B.*PLoS ONE*, Public Library of Science, Vol. 15 No. 2, p. e0228746, doi: 10.1371/journal.pone.0228746.

DHURD.Liaoning. (2016), "Liaoning Province Urban Underground Multi-utility Tunnel Project Planning Guidelines", Department of Housing & Urban-Rural Development. Liaoning.

Dietterich, T.G. (2000), "Ensemble Methods in Machine Learning", *Lecture Notes in Computer Science (Including Subseries Lecture Notes in Artificial Intelligence and Lecture Notes in Bioinformatics)*, Springer, Berlin, Heidelberg, Vol. 1857 LNCS, pp. 1–15, doi: 10.1007/3-540-45014-9_1.

Dong, Y. and Frangopol, D.M. (2016), "Probabilistic Time-Dependent Multihazard Life-Cycle Assessment and Resilience of Bridges Considering Climate Change", *Journal of Performance of Constructed Facilities*, American Society of Civil Engineers (ASCE), Vol. 30 No. 5, p. 04016034, doi: 10.1061/(ASCE)CF.1943-5509.0000883.

Elsawah, H., Bakry, I. and Moselhi, O. (2016), "Decision Support Model for Integrated Risk Assessment and Prioritization of Intervention Plans of Municipal Infrastructure", *Journal of Pipeline Systems Engineering and Practice*, American Society of Civil Engineers (ASCE), Vol. 7 No. 4, p. 04016010, doi: 10.1061/(asce)ps.1949-1204.0000245.

Elsawah, H., Guerrero, M. and Moselhi, O. (2014), "Decision support model for integrated intervention plans of municipal infrastructure", *ICSI 2014: Creating Infrastructure for a Sustainable World - Proceedings of the 2014 International Conference on Sustainable Infrastructure*, American Society of Civil Engineers (ASCE), Reston, VA, pp. 1039–1050, doi: 10.1061/9780784478745.098.

Elshaboury, N. and Marzouk, M. (2022), "Prioritizing water distribution pipelines rehabilitation using machine learning algorithms", *Soft Computing*, Springer Science and Business Media Deutschland GmbH, Vol. 26 No. 11, pp. 5179–5193, doi: 10.1007/S00500-022-06970-8/TABLES/7.

Esri. (2016a), "How Band Collection Statistics works—ArcMap | Documentation", available at: https://desktop.arcgis.com/en/arcmap/10.3/tools/spatial-analyst-toolbox/how-band-collection-statistics-works.htm (accessed 23 January 2022).

Esri. (2016b), "Table To Excel (Conversion)—ArcGIS Pro | Documentation", available at: https://pro.arcgis.com/en/pro-app/latest/tool-reference/conversion/table-to-excel.htm (accessed 1 April 2022).

Esri. (2020), “What is ArcPy?—ArcGIS Pro | Documentation”, available at: https://pro.arcgis.com/en/pro-app/latest/arcpy/get-started/what-is-arcpy-.htm (accessed 26 February 2021).

Ester, M., Kriegel, H.P. and Xu, X. (1995), “Knowledge discovery in large spatial databases: Focusing techniques for efficient class identification”, *Lecture Notes in Computer Science (Including Subseries Lecture Notes in Artificial Intelligence and Lecture Notes in Bioinformatics)*, Vol. 951, Springer Verlag, pp. 67–82, doi: 10.1007/3-540-60159-7_5.

FCM and NRC. (2003), “Coordinating infrastructure works: a best practice by the national guide to sustainable municipal infrastructure”, *National Research Council of Canada. NRC Institute for Research in Construction*, No. 1.

Ferreira, N., Poco, J., Vo, H.T., Freire, J. and Silva, C.T. (2013), “Visual exploration of big spatio-temporal urban data: A study of New York city taxi trips”, *IEEE Transactions on Visualization and Computer Graphics*, Vol. 19 No. 12, pp. 2149–2158, doi: 10.1109/TVCG.2013.226.

Flintsch, G.W. and Chen, C. (2004), “Soft Computing Applications in Infrastructure Management”, *Journal of Infrastructure Systems*, Vol. 10 No. 4, pp. 157–166, doi: 10.1061/(asce)1076-0342(2004)10:4(157).

Frangopol, D.M. and Liu, M. (2007), “Maintenance and management of civil infrastructure based on condition, safety, optimization, and life-cycle cost”, *Structure and Infrastructure Engineering*, Vol. 3, pp. 29–41, doi: 10.1080/15732470500253164.

French, S. and Roy, B. (1997), “Multicriteria Methodology for Decision Aiding.”, *The Journal of the Operational Research Society*, Springer US, Boston, MA, Vol. 48 No. 12, p. 1257, doi: 10.2307/3010757.

Friedman, J., Hastie, T. and Tibshirani, R. (2000), “Additive logistic regression: a statistical view of boosting (With discussion and a rejoinder by the authors)”, *Https://Doi.Org/10.1214/Aos/1016218223*, Institute of Mathematical Statistics, Vol. 28 No. 2, pp. 337–407, doi: 10.1214/AOS/1016218223.

Friedman, J.H. (2001), “Greedy Function Approximation: A Gradient Boosting Machine”, *Source: The Annals of Statistics*, Vol. 29 No. 5, pp. 1189–1232.

Fu, G., Kapelan, Z., Kasprzyk, J.R. and Reed, P. (2012), “Optimal Design of Water Distribution Systems Using Many-Objective Visual Analytics”, *Journal of Water Resources Planning and*

Management, American Society of Civil Engineers, Vol. 139 No. 6, pp. 624–633, doi: 10.1061/(ASCE)WR.1943-5452.0000311.

Gao, Z. (2010), "Design of Lake Reservoir municipal multi-purpose utility tunnel in Xiamen City", *Water & Wastewater*, Vol. 36 No. 10, pp. 116–119, doi: 10.3969/j.issn.1002-8471.2010.10.033.

le Gauffre, P., Baur, R., Laffréchine, K. and Miramond, M. (2002a), "CARE-W: WP 3-Decision support for annual rehabilitation programmes. D7-Survey of multi-criteria techniques and selection of relevant procedures".

le Gauffre, P., Baur, R., Laffréchine, K. and Miramond, M. (2002b), "CARE-W: WP 3-Decision support for annual rehabilitation programmes. D7-Survey of multi-criteria techniques and selection of relevant procedures".

Genger, T.K. and Hammad, A. (2022), "Geospatial Visual Analytics for Supporting Decision Making for Underground Utility Integrated Interventions", *International Conference on Transportation and Development 2022*, American Society of Civil Engineers, Reston, VA, pp. 46–59, doi: 10.1061/9780784484364.005.

Genger, T.K., Luo, Y. and Hammad, A. (2021), "Multi-criteria spatial analysis for location selection of multi-purpose utility tunnels", *Tunnelling and Underground Space Technology*, Pergamon, Vol. 115, doi: 10.1016/j.tust.2021.104073.

Gilchrist, A. and Allouche, E.N. (2005), "Quantification of social costs associated with construction projects : state-of-the-art review", *Tunnelling and Underground Space Technology*, Pergamon, Vol. 20 No. 1, pp. 89–91, doi: 10.1016/j.tust.2004.04.003.

Grimaldi, M., Pellecchia, V. and Fasolino, I. (2017), "Urban plan and water infrastructures planning: A methodology based on spatial ANP", *Sustainability (Switzerland)*, MDPI AG, Vol. 9 No. 5, doi: 10.3390/su9050771.

Guo, R., Fu, D. and Sollazzo, G. (2021), "An ensemble learning model for asphalt pavement performance prediction based on gradient boosting decision tree", *International Journal of Pavement Engineering*, Taylor & Francis, pp. 1–14, doi: 10.1080/10298436.2021.1910825.

Guo, Z., Ward, M.O. and Rundensteiner, E.A. (2009), "Model space visualization for multivariate linear trend discovery", *VAST 09 - IEEE Symposium on Visual Analytics Science and Technology, Proceedings*, pp. 75–82, doi: 10.1109/VAST.2009.5333431.

Hafskjold, L.S. (2010), *SIP-Future Rehabilitation Strategies for Physical Infrastructure: COORDINATION OF REHABILITATION PLANNING AND MEASURES-CO-INFRASTRUCTURE INTERACTIONS Water and Environment*.

Hafskjold, L.S. and Bertelsen, D. (2008), *SIP - Future Rehabilitation Strategies for Physical Infrastructure : Studieområde Nonnegata: Hva Var Planlagt Og Hva Ble Resultatet? Er Det Noe å Lære?*, SINTEF construction research.

Hao, T., Rogers, C.D.F., Metje, N., Chapman, D.N., Muggleton, J.M., Foo, K.Y., Wang, P., *et al.* (2012), "Condition assessment of the buried utility service infrastructure", *Tunnelling and Underground Space Technology*, Vol. 28, pp. 331–344, doi: 10.1016/j.tust.2011.10.011.

Harvey, R.R. and McBean, E.A. (2014a), "Predicting the structural condition of individual sanitary sewer pipes with random forests", *Canadian Journal of Civil Engineering*, NRC Research Press, Vol. 41 No. 4, pp. 294–303, doi: 10.1139/cjce-2013-0431.

Hernández, N., Caradot, N., Sonnenberg, H., Rouault, P. and Torres, A. (2021), "Optimizing SVM models as predicting tools for sewer pipes conditions in the two main cities in Colombia for different sewer asset management purposes", *Structure and Infrastructure Engineering*, Taylor and Francis Ltd., Vol. 17 No. 2, pp. 156–169, doi: 10.1080/15732479.2020.1733029.

Heyermann, B., Li, J., Li, L., Unzaki, S., Xu, Q. and Yang, C. (2022), *Life Cycle Cost Benefit Analysis to Support the Creation of the Smart City Infrastructure Authority/New York City*, New York, NY.

Hoang, N.-D. and Nguyen, Q.-L. (2018), "A novel method for asphalt pavement crack classification based on image processing and machine learning", *Engineering with Computers 2018 35:2*, Springer, Vol. 35 No. 2, pp. 487–498, doi: 10.1007/S00366-018-0611-9.

Hojjati, A., Jefferson, I., Metje, N. and Rogers, C.D.F. (2018), "Sustainability assessment for urban underground utility infrastructure projects", *Proceedings of the Institution of Civil Engineers - Engineering Sustainability*, Vol. 171 No. 2, pp. 68–80, doi: 10.1680/jensu.16.00050.

Huck, P.J., Iyengar, M.N., Makeig, K.S. and Chipps, J. (1976), *Combined Utility/Transportation Systems-Economic , Technical and Institutional Feasibility*, Chicago.

Hunt, D.V.L., Jefferson, I., Drinkwater, N.K.K. and Rogers, C.D.F.D.F. (2012), "Sustainable Utility Placement for University Campuses", *GeoCongress 2012*, American Society of Civil Engineers, Oakland, California, United States, No. Table 1, pp. 4309–4318, doi: 10.1061/9780784412121.443.

Hunt, D.V.L., Nash, D. and Rogers, C.D.F. (2014a), "Sustainable utility placement via Multi-Utility Tunnels", *Tunnelling and Underground Space Technology*, Vol. 39 No. May, pp. 15–26, doi: 10.1016/j.tust.2012.02.001.

Hunt, D.V.L., Nash, D. and Rogers, C.D.F. (2014b), "Sustainable utility placement via Multi-Utility Tunnels", *Tunnelling and Underground Space Technology*, Vol. 39 No. May, pp. 15–26, doi: 10.1016/j.tust.2012.02.001.

Hunt, D.V.L. and Rogers, C.D.F. (2005), "Barriers to sustainable infrastructure in urban regeneration", *Engineering Sustainability*, Vol. 158 No. 2, pp. 67–81, doi: 10.1680/ensu.158.2.67.67124.

Islam, M.S. (2017), "Comparative evaluation of vacuum sewer and gravity sewer systems", *International Journal of System Assurance Engineering and Management*, Springer, Vol. 8 No. 1, pp. 37–53.

Jafar, R., Shahrour, I. and Juran, I. (2010), "Application of Artificial Neural Networks (ANN) to model the failure of urban water mains", *Mathematical and Computer Modelling*, Vol. 51 No. 9–10, pp. 1170–1180, doi: 10.1016/j.mcm.2009.12.033.

Jahanshahloo, G.R., Lotfi, F.H. and Izadikhah, M. (2006), "Extension of the TOPSIS method for decision-making problems with fuzzy data", *Applied Mathematics and Computation*, Vol. 181 No. 2, pp. 1544–1551, doi: 10.1016/j.amc.2006.02.057.

Jat, M.K., Garg, P.K. and Khare, D. (2008), "Monitoring and modelling of urban sprawl using remote sensing and GIS techniques", *International Journal of Applied Earth Observation and Geoinformation*, Vol. 10 No. 1, pp. 26–43, doi: https://doi.org/10.1016/j.jag.2007.04.002.

Jiang, Y. and Wang, H. (2016), "Study on the Multi-Utility Tunnel Layout of Yining Old City Based on ArcGIS", *Engineering Technology*, Vol. 6, pp. 278–279.

John, H.D. (2003), "Matplotlib: Python plotting", *Matplotlib*, available at: https://matplotlib.org/stable/index.html (accessed 26 February 2021).

Jorjam, S. (2022a), *Stochastic Simulation of Construction Methods of Multi-Purpose Utility Tunnels - Spectrum: Concordia University Research Repository*, Concordia University.

Jorjam, S. (2022b), *Stochastic Simulation of Construction Methods of Multi-Purpose Utility Tunnels - Spectrum: Concordia University Research Repository*, Masters, Concordia University.

Justin, B. and Ryan, B. (2012), “MYTH: The Education building used to have rooftop gardens.”, *The Gateway*, available at: https://www.ualberta.ca/newtrail/spring2012/features/campusmythsrevealed.

Kerwin, S., Garcia de Soto, B., Adey, B., Sampatakaki, K. and Heller, H. (2020), “Combining recorded failures and expert opinion in the development of ANN pipe failure prediction models”, *Sustainable and Resilient Infrastructure*, pp. 1–23, doi: 10.1080/23789689.2020.1787033.

Kirbaş, U. and Karaşahin, M. (2016), “Performance models for hot mix asphalt pavements in urban roads”, *Construction and Building Materials*, Elsevier, Vol. 116, pp. 281–288, doi: 10.1016/j.conbuildmat.2016.04.118.

Klimas, R. (2020), “Engineering & Construction Services Division Standard Specifications for Road Works Construction Specification for Steel Plates Used in Connection with Roadway Utility Excavations Construction Specification for Steel Plates Used in Connection with Roadway”.

Kolektory Praha. (2014), *PRAGUE’S COLLECTORS*.

Kuhn, B.T., Jasek, D., Brydia, R., Parham, A., Blaschke, B. and Ullman, B. (2002), “Utility corridor structures and other utility accommodation alternatives in TXDOT right of way”, *Technical Report*, Vol. 7 No. 2.

Kuhn, M. and Johnson, K. (2013), *Applied Predictive Modeling*, *Applied Predictive Modeling*, Springer New York, doi: 10.1007/978-1-4614-6849-3.

Kumar, A., Ali Asad Rizvi, S., Brooks, B., Vanderveld, A.R., Wilson, K.H., Kenny, C., Edelstein, S., *et al.* (2018), “Using Machine Learning to Assess the Risk of and Prevent Water Main Breaks”, *ACMSIGKDD*, pp. 1–9, doi: 10.1145/nnnnnnn.nnnnnnn.

Kumar, S.S., Zamenian, H., Abraham, D.M. and Iseley, D.T. (2018), “An Evaluation of the Failure Modes and Condition Assessment Technologies for Small Diameter Ductile Iron Pipes”, *Construction Research Congress 2018: Safety and Disaster Management - Selected Papers from the Construction Research Congress 2018*, American Society of Civil Engineers, Vol. 2018-April, pp. 678–687, doi: 10.1061/9780784481288.066.

Kumar, S.S., Zamenian, H., Abraham, D.M., Iseley, D.T. and Student, P.D. (2018), “An Evaluation of the Failure Modes and Condition Assessment Technologies for Small Diameter Ductile Iron Pipes”, *Construction Research Congress*, p. 10.

Kuncheva, L.I. and Rodríguez, J.J. (2012), "A weighted voting framework for classifiers ensembles", *Knowledge and Information Systems 2012 38:2*, Springer, Vol. 38 No. 2, pp. 259–275, doi: 10.1007/S10115-012-0586-6.

Laakso, T., Kokkonen, T., Mellin, I. and Vahala, R. (2018), "Sewer Condition Prediction and Analysis of Explanatory Factors", *Water 2018, Vol. 10, Page 1239*, Multidisciplinary Digital Publishing Institute, Vol. 10 No. 9, p. 1239, doi: 10.3390/W10091239.

Laistner, A. (2012), "proven sustainability", *Real Corp*, No. May.

Laistner, A. and Laistner, H. (2012), "Utility Tunnels – Proven Sustainability Above and Below Ground Axel Laistner, Hermann Laistner", *REAL CORP 2012*, Selbstverl. des Vereins CORP - Competence Center of Urban and Regional Planning, Schwechat, Vol. 0 No. May, pp. 1445–1456.

Landis, J.R. and Koch, G.G. (1977), "The Measurement of Observer Agreement for Categorical Data", *Biometrics*, JSTOR, Vol. 33 No. 1, p. 159, doi: 10.2307/2529310.

Lee, C., Kim, Y., Jin, S., Kim, D., Maciejewski, R., Ebert, D. and Ko, S. (2020), "A Visual Analytics System for Exploring, Monitoring, and Forecasting Road Traffic Congestion", *IEEE Transactions on Visualization and Computer Graphics*, IEEE Computer Society, Vol. 26 No. 11, pp. 3133–3146, doi: 10.1109/TVCG.2019.2922597.

Lee, H.-C. and Chang, C.-T. (2018), "Comparative analysis of MCDM methods for ranking renewable energy sources in Taiwan", doi: 10.1016/j.rser.2018.05.007.

Leon, F., Floria, S.A. and Badica, C. (2017), "Evaluating the effect of voting methods on ensemble-based classification", *Proceedings - 2017 IEEE International Conference on INnovations in Intelligent SysTems and Applications, INISTA 2017*, Institute of Electrical and Electronics Engineers Inc., pp. 1–6, doi: 10.1109/INISTA.2017.8001122.

Li, T., Liu, L., Li, J. and Yin, M. (2019), "Economic Analysis for Installation of Electrical Cables into Utility Tunnels in China", doi: 10.1145/3328886.3328900.

LLA. (2007), "Condition assessment program".

Lu, Y., Garcia, R., Hansen, B., Gleicher, M. and Maciejewski, R. (2017), "The State-of-the-Art in Predictive Visual Analytics", *Computer Graphics Forum*, Vol. 36 No. 3, pp. 539–562, doi: 10.1111/cgf.13210.

Luo, Alaghbandrad, A., Genger, T.K. and Amin, H. (2019), "SMART MULTI-PURPOSE UTILITY TUNNELS", in ANJALI, A. (Ed.), *Sustainable City Logistics Planning: Methods and Applications. Volume 3*, Volume 3., Nova Science Publishers, Montréal, Québec.

Luo, Y. (2019a), "Multi-Criteria Spatial Analysis of Multi-Purpose Utility Tunnels".

Luo, Y. (2019b), *Multi-Criteria Spatial Analysis of Multi-Purpose Utility Tunnels*, Concordia University.

Luo, Y., Alaghbandrad, A., Genger, T.K. and Hammad, A. (2020), "History and recent development of multi-purpose utility tunnels", *Tunnelling and Underground Space Technology*, Pergamon, 1 September, doi: 10.1016/j.tust.2020.103511.

Luo, Y., Genger, T.K. and Hammad, A. (2020), "Multi-criteria decision making for multi-purpose utility tunnel location selection", *Pipelines 2020: Planning and Design - Proceedings of Sessions of the Pipelines 2020 Conference*, pp. 339–349, doi: 10.1061/9780784483190.038.

de Magalhães, R.F., Danilevicz, Â. de M.F. and Palazzo, J. (2019), "Managing trade-offs in complex scenarios: A decision-making tool for sustainability projects", *Journal of Cleaner Production*, doi: 10.1016/j.jclepro.2018.12.023.

Makana, L., Metje, N., Jefferson, I., Sackey, M. and Rogers, C. (2018), "Cost Estimation of Utility Strikes: Towards Proactive Management of Street Works", *Infrastructure Asset Management*, Vol. 7, pp. 1–34, doi: 10.1680/jinam.17.00033.

Makana, L.O., Jefferson, I., Hunt, D.V.L. and Rogers, C.D.F. (2016), "Assessment of the future resilience of sustainable urban sub-surface environments", *Tunnelling and Underground Space Technology*, Vol. 55, pp. 21–31, doi: 10.1016/j.tust.2015.11.016.

Malczewski, J. (2007), "International Journal of Geographical Information Science GIS-based multicriteria decision analysis: a survey of the literature GIS-based multicriteria decision analysis: a survey of the literature", doi: 10.1080/13658810600661508.

Maleti, M., Maleti, D., Dahlgaard, J.J., Mi Dahlgaard-Park, S. and stjan Gomi cek, B. (2014), "Sustainability exploration and sustainability exploitation: from a literature review towards a conceptual framework", doi: 10.1016/j.jclepro.2014.05.045.

Manuilova, A., Dormuth, D.W. and Vanier, D.J. (2009), "A Case Study of User and External Components of Social Costs that are related to Municipal Infrastructure Rehabilitation", *Municipal Infrastructure Investment Planning (MIIP) Report*, Vol. B-5123.15, doi: Resolve DOI: https://doi.org/10.4224/20374147.

Marcelino, P., de Lurdes Antunes, M., Fortunato, E. and Gomes, M.C. (2020), "Transfer learning for pavement performance prediction", *International Journal of Pavement Research and Technology*, Springer, Vol. 13 No. 2, pp. 154–167, doi: 10.1007/s42947-019-0096-z.

Marcelino, P., de Lurdes Antunes, M., Fortunato, E. and Gomes, M.C. (2021), "Machine learning approach for pavement performance prediction", *International Journal of Pavement Engineering*, Taylor and Francis Ltd., Vol. 22 No. 3, pp. 341–354, doi: 10.1080/10298436.2019.1609673.

de Marcellis-Warin, N., Peignier, I., Mouchikhine, V. and Mahfouf, M. (2013), *Évaluation Des Coûts Socio-Économiques Reliés Aux Bris Des Infrastructures Souterraines Au Québec*, *Rapport de Recherche Préparé Pour l'APISQ-Rapport de Recherche CIRANO 2013RP-22*, Montreal.

Martínez-Morales, J.D., Pineda-Rico, U. and Stevens-Navarro, E. (2010), "Performance comparison between MADM algorithms for vertical handoff in 4G networks", *Program and Abstract Book - 2010 7th International Conference on Electrical Engineering, Computing Science and Automatic Control, CCE 2010*, pp. 309–314, doi: 10.1109/ICEEE.2010.5608646.

Marzouk, M. and Osama, A. (2017), "Fuzzy-based methodology for integrated infrastructure asset management", *International Journal of Computational Intelligence Systems*, Taylor and Francis Ltd., Vol. 10 No. 1, pp. 745–759, doi: 10.2991/ijcis.2017.10.1.50.

MathWorks. (2019), "R2019a - Updates to the MATLAB and Simulink product families - MATLAB & Simulink", *The MathWorks, Inc.*

Matthews, J.C. and Allouche, E.N. (2010), "A social cost calculator for utility construction projects", *North American Society for Trenchless Technology No-Dig Show 2010*, Vol. Chicago, I No. September, p. F-403-1.

Matthews, J.C., Allouche, E.N. and Sterling, R.L. (2015), "Social cost impact assessment of pipeline infrastructure projects", *Environmental Impact Assessment Review*, Elsevier, Vol. 50, pp. 196–202, doi: 10.1016/j.eiar.2014.10.001.

Max, A. (2022), "How to Bring the Utilities in Below Ground - This Old House", available at: https://www.thisoldhouse.com/concord-cottage/21015418/how-to-bring-the-utilities-in-below-ground (accessed 18 April 2022).

McKim, R.A. (1997), "Bidding strategies for conventional and trenchless technologies considering social costs", *Canadian Journal of Civil Engineering*, Vol. 24 No. 5, pp. 819–827, doi: 10.1139/l97-036.

MHURD. (2015a), "Interpretation of experts for 'Guiding Opinions on Promoting the Construction of Urban Underground Multi-utility tunnels'", *Ministry of Housing and Urban-Rural Development of the People's Republic of China*.

MHURD. (2015b), *Notice of Organizing to Declare the Underground Multi-Utility Tunnel Pilot City*.

MHURD. (2015c), "Index of investment estimation of urban utility tunnel projects (for trial implementation)", June.

MHURD. (2015d), "Notice of Ministry of Housing and Urban-Rural Development on the issuance of 'Urban Underground Multi-Utility Tunnel Project Planning Guidelines'", *MHURD*.

Mohammadi, M.M., Najafi, M., Tabesh, A., Riley, J. and Gruber, J. (2019), "Condition prediction of sanitary sewer pipes", *Pipelines 2019: Condition Assessment, Construction, and Rehabilitation - Proceedings of Sessions of the Pipelines 2019 Conference*, American Society of Civil Engineers, pp. 117–126, doi: 10.1061/9780784482490.013.

Montreal City. (2018), "Results of the intervention plan for the assets of the drinking water, sewer and road networks of the City of Montreal - Datasets - Open data portal", available at: http://donnees.ville.montreal.qc.ca/dataset/resultats-plan-intervention-actifs-eau-voirie (accessed 31 May 2020).

Montreal City. (2021), "Bienvenue - Welcome", available at: https://donnees.montreal.ca/ (accessed 25 February 2021).

Morioka, S.N. and Monteiro De Carvalho, M. (2016), "A systematic literature review towards a conceptual framework for integrating sustainability performance into business", doi: 10.1016/j.jclepro.2016.01.104.

Motamedi, A., Hammad, A. and Asen, Y. (2014), "Knowledge-assisted BIM-based visual analytics for failure root cause detection in facilities management", *Automation in Construction*, Elsevier, Vol. 43, pp. 73–83, doi: 10.1016/j.autcon.2014.03.012.

Nabipour, N., Karballaeezadeh, N., Dineva, A., Mosavi, A., Mohammadzadeh S., D. and Shamshirband, S. (2019), "Comparative analysis of machine learning models for prediction

of remaining service life of flexible pavement", *Mathematics*, Multidisciplinary Digital Publishing Institute, Vol. 7 No. 12, p. 1198, doi: 10.3390/MATH7121198.

Najafi, Dr.M., Gokhale, Dr.S., Calderón, D.R. and Ma, Dr.B. (2021), *Social Costs of Utility Construction: A Life Cycle Cost Approach*, *Trenchless Technology: Pipeline and Utility Design, Construction, and Renewal*, McGraw-Hill Education.

Najafi, Mohammad. (2010), *Trenchless Technology Piping: Installation and Inspection*, McGraw-Hill Professional.

National Research Council. (2013), *Underground Engineering for Sustainable Urban Development*, *Underground Engineering for Sustainable Urban Development*, The National Academy Press, Washington, DC, doi: 10.17226/14670.

Numpy. (2020), "NumPy", available at: https://numpy.org/ (accessed 26 February 2021).

Open Government Portal. (2023), "Counts of vehicles, cyclists and pedestrians at intersections with traffic lights - Open Government Portal", available at: https://open.canada.ca/data/en/dataset/584de76b-13b9-47ea-af12-0c37b8eb5de5 (accessed 24 January 2023).

Ormsby, C. (2009), *A Framework for Estimating the Total Cost of Buried Municipal Infrastructure Renewal Projects: A Case Study in Montreal*, *[Master's Thesis]*, McGill University, Montreal.

Osman, H. (2016), "Coordination of urban infrastructure reconstruction projects", *Structure and Infrastructure Engineering*, Taylor & Francis, Vol. 12 No. 1, pp. 108–121, doi: 10.1080/15732479.2014.995677.

Oum, N. (2017), *Modeling Socio-Economic Impacts of Municipal Infrastructure Works*, PhD. Thesis, Concordia University.

Packer, E., Bak, P., Nikkila, M., Polishchuk, V. and Ship, H.J. (2013), "Visual analytics for spatial clustering: Using a heuristic approach for guided exploration", *IEEE Transactions on Visualization and Computer Graphics*, Vol. 19 No. 12, pp. 2179–2188, doi: 10.1109/TVCG.2013.224.

Paige, D.C. (2021), "Can You Run Electrics And Plumbing In The Same Trench? - Cohesive Homes", available at: https://www.cohesivehomes.com/electrics-plumbing-same-trench (accessed 18 April 2022).

Palsat, B., Eng, P., Liu, Q., Luo, C., Jago, B. and Duriez, C. (2020), "Characteristics of Utility Cuts and Their Impacts on Pavement Serviceability in the City of Saskatoon", *Transportation Association of Canada 2020 Conference and Exhibition - The Journey to Safer Roads*.

Papathanasiou, J. and Ploskas, N. (2018), *Multiple Criteria Decision Aid*, Vol. 136, Springer International Publishing, Cham, doi: 10.1007/978-3-319-91648-4.

Parker, J. (2008), "Briefing: The real cost of street works", *Proceedings of the Institution of Civil Engineers - Transport*, Vol. 161 No. 4, pp. 175–176, doi: 10.1680/tran.2008.161.4.175.

Pavlov, Y.L. (2019), *Random Forests*, *Random Forests*, Vol. 45, Routledge, London, doi: 10.4324/9781003109396-5.

Pei, L., Yu, T., Xu, L., Li, W. and Han, Y. (2022), "Prediction of Decay of Pavement Quality or Performance Index Based on Light Gradient Boost Machine", *Lecture Notes on Data Engineering and Communications Technologies*, Vol. 80, Springer, Cham, pp. 1173–1179, doi: 10.1007/978-3-030-81007-8_135.

Peng, F., Yang, C. and Ma, C. (2018), *Introduction to Planning and Construction for Utility Tunnels*, Tongji University Press.

Peng, J. and Peng, F.-L. (2018), "A GIS-based evaluation method of underground space resources for urban spatial planning: Part 1 methodology", *Tunnelling and Underground Space Technology*, Vol. 74, pp. 82–95, doi: 10.1016/j.tust.2018.01.002.

Piryonesi, S.M. and El-Diraby, T.E. (2021a), "Using Machine Learning to Examine Impact of Type of Performance Indicator on Flexible Pavement Deterioration Modeling", *Journal of Infrastructure Systems*, American Society of Civil Engineers, Vol. 27 No. 2, p. 04021005, doi: 10.1061/(ASCE)IS.1943-555X.0000602.

Piryonesi, S.M. and El-Diraby, T.E. (2021b), "Examining the relationship between two road performance indicators: Pavement condition index and international roughness index", *Transportation Geotechnics*, Elsevier, Vol. 26, p. 100441, doi: 10.1016/j.trgeo.2020.100441.

Poldrack, R.A. (2018), *Statistical Thinking for the 21st Century*, Russell Poldrack.

Praha Kolektory. (2018), *TECHNICKÉ STANDARDY*.

Python Software Foundation. (2021), "tkinter — Python interface to Tcl/Tk", *Python*, available at: https://docs.python.org/3/library/tkinter.html (accessed 26 February 2021).

Rahbaralam, M., Modesto, D., Cardús, J., Abdollahi, A. and Cucchietti, F.M. (2020), "Predictive Analytics for Water Asset Management: Machine Learning and Survival Analysis".

Rahman, S., Vanier, D.J. and Newton, L.A. (2005), "MIIP Report: Social Cost Considerations for Municipal Infrastructure Management.", *NRC Publications Archive*, doi: 10.4224/20377011.

Ramanujan, D., Bernstein, W.Z., Chandrasegaran, S.K. and Feddersen, D.W. (2017), "Karthik Ramani Visual Analytics Tools for Sustainable Lifecycle Design: Current Status, Challenges, and Future Opportunities", doi: 10.1115/1.4037479.

Ramm, J. (2017), "archook · PyPI", available at: https://pypi.org/project/archook/ (accessed 7 June 2021).

RapidMiner. (2020a), "Deep Learning - RapidMiner Documentation", available at: https://docs.rapidminer.com/latest/studio/operators/modeling/predictive/neural_nets/deep_learning.html (accessed 15 February 2022).

RapidMiner. (2020b), "Deep Learning - RapidMiner Documentation".

RapidMiner. (2021), "Gradient Boosted Trees", *RapidMiner*, available at: https://docs.rapidminer.com/latest/studio/operators/modeling/predictive/trees/gradient_boosted_trees.html (accessed 16 February 2022).

Rashedi, R. and Hegazy, T. (2016), "Holistic Analysis of Infrastructure Deterioration and Rehabilitation Using System Dynamics", *Journal of Infrastructure Systems*, American Society of Civil Engineers (ASCE), Vol. 22 No. 1, p. 04015016, doi: 10.1061/(asce)is.1943-555x.0000273.

RCCAO. (2020), *The Need to Protect Ontario's Infrastructure Investments Averting a Crisis: NOVEMBER 2020 A Report by Prism Economics and Analysis for the Residential and Civil Construction Alliance of Ontario*, Ontario.

Reinert, A., Snyder, L.S., Zhao, J., Fox, A.S., Hougen, D.F., Nicholson, C. and Ebert, D.S. (2020), "Visual Analytics for Decision-Making during Pandemics", *Computing in Science and Engineering*, Vol. 22 No. 6, pp. 48–59, doi: 10.1109/MCSE.2020.3023288.

Rey, S., Anselin, L., Li, X., Pahle, R., Laura, J., Li, W. and Koschinsky, J. (2015), "Open Geospatial Analytics with PySAL", *ISPRS International Journal of Geo-Information*, MDPI AG, Vol. 4 No. 2, pp. 815–836, doi: 10.3390/ijgi4020815.

Riera, P. and Pasqual, J. (1992), "The importance of urban underground land value in project evaluation: a case study of Barcelona's utility tunnel", *Tunnelling and Underground Space Technology*, Pergamon, Vol. 7 No. 3, pp. 243–250, doi: 10.1016/0886-7798(92)90005-3.

Roberts, G., Meng, X., Taha, A. and Montillet, J.-P. (2006), *TS 38-Engineering Surveys for Construction Works I The Location and Positioning of Buried Pipes and Cables in Built Up Areas*.

Robles-Velasco, A., Cortés, P., Muñuzuri, J. and Onieva, L. (2020), "Prediction of pipe failures in water supply networks using logistic regression and support vector classification", *Reliability Engineering and System Safety*, Elsevier Ltd, Vol. 196, p. 106754, doi: 10.1016/j.ress.2019.106754.

Rogers, C. and Hunt, D. (2006), "Sustainable utility infrastructure via multi-utility tunnels", *1st International Constrution Specialty Conference May 23-26*, No. May, pp. 1–10.

Saad, D.A., Mansour, H. and Osman, H. (2018), "Concurrent bilevel multi-objective optimisation of renewal funding decisions for large-scale infrastructure networks", *Structure and Infrastructure Engineering*, Taylor & Francis, Vol. 14 No. 5, pp. 594–603, doi: 10.1080/15732479.2017.1378238.

Saaty, R.W. (1987), "The analytic hierarchy process-what it is and how it is used", *Mathematical Modelling*, Pergamon, Vol. 9 No. 3–5, pp. 161–176, doi: 10.1016/0270-0255(87)90473-8.

Saaty, T.L. (1982), "The analytic hierarchy process: A new approach to deal with fuzziness in architecture", *Architectural Science Review*, Vol. 25 No. 3, pp. 64–69, doi: 10.1080/00038628.1982.9696499.

Saaty, T.L. (2002), "Decision making with the Analytic Hierarchy Process", *Scientia Iranica*, Vol. 9 No. 3, pp. 215–229, doi: 10.1504/ijssci.2008.017590.

Saaty, T.L. (2004), "Fundamentals of the analytic network process — Dependence and feedback in decision-making with a single network", *Journal of Systems Science and Systems Engineering*, Vol. 13 No. 2, pp. 129–157, doi: 10.1007/s11518-006-0158-y.

Saaty, T.L. (2008), "Decision making with the analytic hierarchy process", *IJSSCI*, Vol. 1 No. 1, p. 83, doi: 10.1504/IJSSCI.2008.017590.

Saaty, T.L., Adams, W.J. and Rokou, E. (2012), "Super Decisions Software Guide Version 3.0.0".

Sambe, A.M. and Dogoua, F. (2016), *Guide de l'analyse Avantages-coûts Des Projets Publics En Transport Routier*, doi: https://doi.org/10.4224/20377011.

Savikhin, A., Maciejewski, R. and Ebert, D.S. (2008), "Applied visual analytics for economic decision-making", *VAST'08 - IEEE Symposium on Visual Analytics Science and Technology, Proceedings*, pp. 107–114, doi: 10.1109/VAST.2008.4677363.

Shad, R., Khorrami, M. and Ghaemi, M. (2017), "Developing an Iranian green building assessment tool using decision making methods and geographical information system: Case study in Mashhad city", *Renewable and Sustainable Energy Reviews*, Elsevier Ltd, 1 January, doi: 10.1016/j.rser.2016.09.004.

Shah, Y.U., Jain, S.S., Tiwari, D. and Jain, M.K. (2013), "Development of Overall Pavement Condition Index for Urban Road Network", *Procedia - Social and Behavioral Sciences*, Elsevier, Vol. 104, pp. 332–341, doi: 10.1016/j.sbspro.2013.11.126.

Shahata, K.F. (2013), *Decision-Support Framework for Integrated Asset Management of Major Municipal Infrastructure*, Thesis, Concordia University.

Shannon, C.E. (1948), "A mathematical theory of communication", *The Bell System Technical Journal*, Vol. 27 No. 3, pp. 379–423, doi: 10.1002/j.1538-7305.1948.tb01338.x.

Soliman, A. (2018), *Coordination and Multi-Objective Optimization Framework for Managing Municipal Infrastructure Under Performance-Based Contracts*, Thesis, Concordia University.

SQLite.org. (2014), "SQLite Home Page".

Statistics Canada. (2020), "Canada's national statistical agency - Statistics Canada", available at: https://www.statcan.gc.ca/eng/start (accessed 25 February 2021).

Tallón-Ballesteros, A.J. and Riquelme, J. (2014), "Data Mining Methods Applied to a Digital Forensics Task for Supervised Machine Learning", *Studies in Computational Intelligence*, Vol. 555, pp. 413–428, doi: 10.1007/978-3-319-05885-6-17.

Tavakoli, R., Sharifara, A. and Najafi, M. (2020), "Prediction of Pipe Failures in Wastewater Networks Using Random Forest Classification", *Pipelines 2020: Condition Assessment, Construction, Rehabilitation, and Trenchless Technologies - Proceedings of Sessions of the Pipelines 2020 Conference*, American Society of Civil Engineers (ASCE), pp. 90–102, doi: 10.1061/9780784483206.011.

The Canadian Press. (2022), "Montreal's downtown has the second highest growth rate in the country | Montreal Gazette", *Montreal Gazette*, available at: https://montrealgazette.com/pmn/news-pmn/canada-news-pmn/census-2021-a-snapshot-of-quebecs-population-and-dwelling-data/wcm/984d791e-227c-4657-be6b-16aa40a92a87 (accessed 10 March 2022).

Tighe, S., Lee, T., McKim, R. and Haas, R. (1999), "Traffic Delay Cost Savings Associated with Trenchless Technology", *Journal of Infrastructure Systems*, American Society of Civil Engineers (ASCE), Vol. 5 No. 2, pp. 45–51, doi: 10.1061/(ASCE)1076-0342(1999)5:2(45).

Ting, C.Y., Ho, C.C., Yee, H.J. and Matsah, W.R. (2018), "Geospatial Analytics in Retail Site Selection and Sales Prediction", *Big Data*, Mary Ann Liebert Inc., Vol. 6 No. 1, pp. 42–52, doi: 10.1089/big.2017.0085.

Uddin, W., Hudson, W.R. and Haas, R. (2013), *Public Infrastructure Asset Management, Second Edition*, 2nd ed., McGraw-Hill Education, New York.

Valdenebro, J.V. and Gimena, F.N. (2018), "Urban utility tunnels as a long-term solution for the sustainable revitalization of historic centres: The case study of Pamplona-Spain", *Tunnelling and Underground Space Technology*, Elsevier, Vol. 81 No. July, pp. 228–236, doi: 10.1016/j.tust.2018.07.024.

Valdenebro, J.-V., Gimena, F.N. and López, J.J. (2019), "Construction process for the implementation of urban utility tunnels in historic centres", *Tunnelling and Underground Space Technology*, Elsevier Ltd, Vol. 89, pp. 38–49, doi: 10.1016/j.tust.2019.03.026.

Vehlow, C., Kao, D.P., Bristow, M.R., Hunter, L.E., Weiskopf, D. and Görg, C. (2015), "Visual analysis of biological data-knowledge networks", *BMC Bioinformatics*, BioMed Central Ltd., Vol. 16 No. 1, p. 135, doi: 10.1186/s12859-015-0550-z.

Visalakshi, S. and Radha, V. (2014), "A literature review of feature selection techniques and applications: Review of feature selection in data mining", doi: 10.1109/ICCIC.2014.7238499.

Wang, E., Alp, N., Shi, J., Wang, C., Zhang, X. and Chen, H. (2017), "Multi-criteria building energy performance benchmarking through variable clustering based compromise TOPSIS with objective entropy weighting", *Energy*, Elsevier Ltd, Vol. 125, pp. 197–210, doi: 10.1016/j.energy.2017.02.131.

Wang, J. (2018), "Construction and development of urban multi-purpose utility tunnel projects", Macau, China.

Wang, T., Tan, L., Xie, S. and Ma, B. (2018), "Development and applications of common utility tunnels in China", *Tunnelling and Underground Space Technology*, Elsevier, Vol. 76 No. March, pp. 92–106, doi: 10.1016/j.tust.2018.03.006.

Wang, T.C. and Lee, H. da. (2009), "Developing a fuzzy TOPSIS approach based on subjective weights and objective weights", *Expert Systems with Applications*, Elsevier Ltd, Vol. 36 No. 5, pp. 8980–8985, doi: 10.1016/j.eswa.2008.11.035.

Weeraddana, D., Liang, B., Li, Z., Wang, Y., Chen, F., Bonazzi, L., Phillips, D., *et al.* (2019), "Machine learning for water mains maintenance", *Water E-Journal*, Vol. 4 No. 3, pp. 1–13, doi: 10.21139/wej.2019.017.

Wilde, W.J., Grant, C.A. and Nelson, P.K. (2002), "*manual for controlling and reducing the frequency of pavement utility cuts final report*".

Winkler, D., Haltmeier, M., Kleidorfer, M., Rauch, W. and Tscheikner-Gratl, F. (2018), "Pipe failure modelling for water distribution networks using boosted decision trees", *Structure and Infrastructure Engineering*, Vol. 14 No. 10, pp. 1402–1411, doi: 10.1080/15732479.2018.1443145.

Wu, C., Wu, P., Jiang, R., Wang, J., Wang, X. and Wan, M. (2020), "Evaluating the economic and social benefits of multiutility tunnels with an agent-based simulation approach", *Engineering, Construction and Architectural Management*, Emerald Group Holdings Ltd., doi: 10.1108/ECAM-07-2019-0399.

Yang, C. and Peng, F. Le. (2016), "Discussion on the Development of Underground Utility Tunnels in China", *Procedia Engineering*, Elsevier B.V., Vol. 165, pp. 540–548, doi: 10.1016/j.proeng.2016.11.698.

Yildirim, V., Yomralioglu, T., Nisanci, R., Çolak, H.E., Bediroğlu, Ş. and Saralioglu, E. (2017), "A spatial multicriteria decision-making method for natural gas transmission pipeline routing", *Structure and Infrastructure Engineering*, Taylor and Francis Ltd., Vol. 13 No. 5, pp. 567–580, doi: 10.1080/15732479.2016.1173071.

Yoon, K. and Hwang, C.-L. (1981), *Multiple Attribute Decision Making Methods and Applications A State-of-the-Art Survey*, *Lecture Notes In Economics and Mathematical Systems*, Vol. 186, Springer Berlin Heidelberg, Berlin, Heidelberg, doi: 10.1007/978-3-642-48318-9.

Zamojska, A. and Próchniak, J. (2017), "Measuring the Social Impact of Infrastructure Projects: The Case of Gdańsk International Fair Co.", *Journal of Entrepreneurship, Management and Innovation*, Fundacja Upowszechniajaca Wiedze i Nauke Cognitione, Vol. 13 No. 2017, pp. 25–42, doi: 10.7341/20171342.

Zangenehmadar, Z., Moselhi, O. and Golnaraghi, S. (2020), "Optimized planning of repair works for pipelines in water distribution networks using genetic algorithm", *Engineering Reports*, Wiley, Vol. 2 No. 6, doi: 10.1002/eng2.12179.

Zhang, G. (2016a), "Design and construction of Jimei Road multi-purpose utility tunnel in Xiamen City", *Fujian Building Materials*, No. 7, pp. 66–67.

Zhang, J. (2016b), "Urban underground space development and construction management standards-introduction to multi-utility tunnel in Guangzhou Higher Education Mega Center", *Civil Engineering & Architecture*, No. 2, pp. 72–86.

Zhou, J., Li, Z., Zhang, Z., Liang, B. and Chen, F. (2016), "Visual Analytics of Relations of Multi-Attributes in Big Infrastructure Data", *2016 Big Data Visual Analytics, BDVA 2016*, Institute of Electrical and Electronics Engineers Inc., doi: 10.1109/BDVA.2016.7787052.

Zhou, Q., Okte, E. and Al-Qadi, I.L. (2021), "Predicting Pavement Roughness Using Deep Learning Algorithms", *Transportation Research Record: Journal of the Transportation Research Board*, SAGE Publications, p. 036119812110237, doi: 10.1177/03611981211023765.

Ziari, H., Sobhani, J., Ayoubinejad, J. and Hartmann, T. (2015), "Prediction of IRI in short and long terms for flexible pavements: ANN and GMDH methods", *International Journal of Pavement Engineering*, Taylor & Francis, Vol. 17 No. 9, pp. 776–788, doi: 10.1080/10298436.2015.1019498.

APPENDICES

Appendix A. Ph.D. Related Publications and Awards

Awards and achievements:

(1) CERIU Prix Relève

(2) Concordia International Tuition Award of Excellence

Journal papers:

(1) **Genger, K.T**., Hammad, A., and N. Oum (2023), "*Multi-Objective Optimization for Selecting Potential Locations of Multi-Purpose Utility Tunnels Considering Agency and Social Lifecycle Costs*", Journal of Tunnelling and Underground Space Technology. Under review.

(2) **Genger, K.T.** and Hammad, A. (2023), "*Street closure prediction based on the combined conditions of spatially collocated municipal infrastructure assets at the segment level*", Expert Systems with Applications, Vol. 219, doi: 10.1016/J.ESWA.2023.119671.

(3) **Genger, K.T.,** Luo, Y. and Hammad, A. (2021), "*Multi-criteria spatial analysis for location selection of multi-purpose utility tunnels*", Journal of Tunnelling and Underground Space Technology, Pergamon, Vol. 115, doi: 10.1016/j.tust.2021.104073

(4) Luo, Y., Alaghbandrad, A., **Genger, T.K.** and Hammad, A. (2020), "*History and recent development of multi-purpose utility tunnels*", Tunnelling and Underground Space Technology, Pergamon, 1 September, doi: 10.1016/j.tust.2020.103511.

Conference papers:

(1) **Genger, T.K.** and Hammad, A. (2023) "*Combining predictions of municipal asset conditions at the segment level to determine street closures"* 30th EG-ICE: International Conference on Intelligent Computing in Engineering. To appear.

(2) **Genger, T.K.** and Hammad, A. (2022), "*Geospatial Visual Analytics for Supporting Decision Making for Underground Utility Integrated Interventions*", International Conference on Transportation and Development 2022, American Society of Civil Engineers, Reston, VA, pp. 46–59, doi: 10.1061/9780784484364.005.

(3) Luo, Y., **Genger, T. K.**, Hammad, A. (2020). "*Multi-Criteria Decision Making for Multi-purpose Utility Tunnel Location Selection*". Utility Engineering & Surveying Institute of ASCE Pipelines 2020 Conference, doi: 10.1061/9780784483190.038.

Invited talk:
Genger, T. K., Hammad, A. (2020). Enhancing Asset Management Support Through Visual Analytics. The INFRA 2020 Conference

Book chapters:

(1) Luo, Y., Alaghbandrad, A., **Genger, T.K.** and Hammad, A. (2019). "Sustainable City Logistics Planning: Methods and Applications. Volume 3. Chapter 3: *Smart Multi-Purpose Utility Tunnels*". Nova Science Publishers, Montreal, Canada, ISBN: 978-1-53616-609-5.

(2) **Genger, T. K.**, Luo, Y., Alaghbandrad, A., Hammad, A. *"Smart Multi-Purpose Utility Tunnels*". Next-Generation Cities Institute Encyclopedia. Under review

Appendix B. ANP and AHP Questionnaires

Table B-1 ANP questionnaire

#	Questions	Extremely important	Extremely to very strongly important	Very strongly important	Very strongly to moderately important	moderately important	moderately to slightly important	Slightly important	Slightly to equally more important	Equal	Slightly to equally more important	Slightly important	Moderately to slightly important	Moderately important	Very strongly to moderately important preferred	Very strongly preferred	Extremely to very strongly important	Extremely important
		9	8	7	6	5	4	3	2	1	2	3	4	5	6	7	8	9
1	**Cluster comparisons with respect to the overall MUT placement**																	
1a	How important is **Location cluster** when it is compared to **Infrastructure cluster** when selecting the road segments for building MUTs																	
1b	How important is **Location cluster** when it is compared to **Environment cluster** when selecting the road segments for building MUTs																	
1c	How important is **Location cluster** when it is compared to **Social Aspects cluster** when selecting the road segments for building MUTs																	
1d	How important is **Infrastructure cluster** when it is compared to **Environment cluster** when selecting the road segments for building MUTs																	
1e	How important is **Infrastructure cluster** when it is compared to **Social Aspects cluster** when selecting the road segments for building MUTs																	
1f	How important is **Environmental cluster** when it is compared to **Social Aspects cluster** when selecting the road segments for building MUTs																	
2	**Cluster comparisons with respect to Infrastructure cluster (which cluster is more important when constructing MUTS)**																	
2a	How important is **Location cluster** when it is compared to **Infrastructure cluster**																	
2b	How important is **Location cluster** when it is compared to **Social Aspects cluster**																	
2c	How important is **Infrastructure cluster** when it is compared to **Social Aspects cluster**																	
3	**Cluster comparisons with respect to Social cluster**																	
3a	How important is **Location cluster** when it is compared to **Social Aspects cluster**																	
4	**Comparison with respect to AADT node in Social Aspects cluster**																	
4a	How important is **Road class when** it is compared to **Population density** (how does road class affect AADT compared to how population density affects AADT)																	
5	**Comparisons with respect to Land use node in Location cluster**																	

Table B-1 ANP Questionnaire (cont.)

		Extremely important	Extremely to very strongly important	Very strongly important	Very strongly to moderately important	moderately important	moderately to slightly important	Slightly important	Slightly to equally more important	Equal	Slightly to equally more important	Slightly important	Moderately to slightly important	Moderately important	Very strongly to moderately important preferred	Very strongly preferred	Extremely to very strongly important	Extremely important
		9	8	7	6	5	4	3	2	1	2	3	4	5	6	7	8	9
5a	How important is **Proximity to public facilities** when it is compared to **Proximity to high-rise buildings** (how does Proximity to public facilities affect Land use compared to how Proximity to high-rise buildings affects Land use)																	
6	**Comparisons with respect to Population density node in Location cluster**																	
6a	How important is **Proximity to public facilities** when it is compared to **Proximity to high-rise buildings** (compare the change in population density as the distance to public facilities/high-rise building changes)																	
7	**Comparisons with respect to Utility density node in Location cluster**																	
7	**Comparisons with respect to Utility density node in Location cluster**																	
7a	How important is **Proximity to public facilities** when it is compared to **Proximity to high-rise buildings** (compare the change in utility density as the distance to public facilities/high-rise building changes)																	
8	**Comparisons with respect to Overall Goal node in Location Cluster**																	
8a	How important is **Proximity to public facilities** when it is compared to **Proximity to high-rise buildings** (is better to place MUT close to public facilities or close to high-rise buildings)																	
9	**Comparisons with respect to Overall Goal node in Social Aspects Cluster**																	
9a	How important is **AADT** when it is compared to **Road class**																	
9b	How important is **AADT** when it is compared to **Population density**																	
9c	How important is **AADT** when it is compared to **Land use**																	
9d	How important is **Road class** when it is compared to **Population density**																	
9e	How important is **Road class** when it is compared to **Land use**																	
9f	How important is **Population density** when it is compared to **Land use**																	
10	**Comparisons with respect to Overall Goal node in Infrastructure Cluster**																	
10a	How important is **Number of expected excavations** when it is compared to **Utility density**																	
10b	How important is **Number of expected excavations** when it is compared to **Underground development projects**																	
10c	How important is **Utility density when** it is compared to **Underground development projects**																	
11	**Comparisons with respect to Overall Goal node in Environmental Cluster**																	
11a	How important is **Soil type** when it is compared to **Floodplain**																	
11b	How important is **Soil type** when it is compared to **Slope of utilities**																	
11c	How important is **Floodplain** when it is compared to **Slope of utilities**																	

Table B-2 AHP Questionnaire

#	Questions	Extremely more important	Very strongly more important	Moderately more important	Slightly more important	Equal	slightly less important	Moderately less important	Very strongly less important	Extremely less important
		9	7	5	3	1	1/3	1/5	1/7	1/9
1	How important is Annual average daily traffic (AADT) when it is compared to Road class									
2	How important is Annual average daily traffic (AADT) when it is compared to Utility density									
3	How important is Annual average daily traffic (AADT) when it is compared to Number of expected excavations for utility repair activities									
4	How important is Annual average daily traffic (AADT) when it is compared to Underground development projects									
5	How important is Annual average daily traffic (AADT) when it is compared to Population density									
6	How important is Annual average daily traffic (AADT) when it is compared to Land use									
7	How important is Annual average daily traffic (AADT) when it is compared to Near to public facilities									
8	How important is Annual average daily traffic (AADT) when it is compared to Near to high-rise buildings									
9	How important is Annual average daily traffic (AADT) when it is compared to Soil type									
10	How important is Annual average daily traffic (AADT) when it is compared to Slope of utilities									
11	How important is Road class when it is compared to Utility density									
12	How important is Road class when it is compared to Number of expected excavations for utility repair activities									
13	How important is Road class when it is compared to Underground development projects									
14	How important is Road class when it is compared to Population density									
15	How important is Road class when it is compared to Land use									
16	How important is Road class when it is compared to Near to public facilities									
17	How important is Road class when it is compared to Near to high-rise buildings									
18	How important is Road class when it is compared to Soil type									
19	How important is Road class when it is compared to Slope of utilities									
20	How important is Utility density when it is compared to Number of expected excavations for utility repair activities									
21	How important is Utility density when it is compared to Underground development projects									
22	How important is Utility density when it is compared to Population density									
23	How important is Utility density when it is compared to Land use									
24	How important is Utility density when it is compared to Near to public facilities									
25	How important is Utility density when it is compared to Near to high-rise buildings									
26	How important is Utility density when it is compared to Soil type									
27	How important is Utility density when it is compared to Slope of utilities									

Table B-2 AHP Questionnaire (Cont.)

	Questions	Extremely more important	Very strongly more important	Moderately more important	Slightly more important	Equal	slightly less important	Moderately less important	Very strongly less important	Extremely less important
28	How important is Number of expected excavations for utility repair activities when it is compared to Underground development projects									
29	How important is Number of expected excavations for utility repair activities when it is compared to Population density									
30	How important is Number of expected excavations for utility repair activities when it is compared to Land use									
31	How important is Number of expected excavations for utility repair activities when it is compared to Near to public facilities									
32	How important is Number of expected excavations for utility repair activities when it is compared to Near to high-rise buildings									
33	How important is Number of expected excavations for utility repair activities when it is compared to Soil type									
34	How important is Number of expected excavations for utility repair activities when it is compared to Slope of utilities									
35	How important is Underground development projects when it is compared to Population density									
36	How important is Underground development projects when it is compared to Land use									
37	How important is Underground development projects when it is compared to Near to public facilities									
38	How important is Underground development projects when it is compared to Near to high-rise buildings									
39	How important is Underground development projects when it is compared to Soil type									
40	How important is Underground development projects when it is compared to Slope of utilities									
41	How important is Population density when it is compared to Land use									
42	How important is Population density when it is compared to Near to public facilities									
43	How important is Population density when it is compared to Near to high-rise buildings									
44	How important is Population density when it is compared to Soil type									
45	How important is Population density when it is compared to Slope of utilities									
46	How important is Land use when it is compared to Near to public facilities									
47	How important is Land use when it is compared to Near to high-rise buildings									
48	How important is Land use when it is compared to Soil type									
49	How important is Land use when it is compared to Slope of utilities									
50	How important is Near to public facilities when it is compared to Near to high-rise buildings									
51	How important is Near to public facilities when it is compared to Soil type									
52	How important is Near to public facilities when it is compared to Slope of utilities									
53	How important is Near to high-rise buildings when it is compared to Soil type									
54	How important is Near to high-rise buildings when it is compared to Slope of utilities									
55	How important is Soil type when it is compared to Slope of utilities									

Appendix C. *PlaceMUT* Software User Guide

LOCATION SELECTION OF THE PLACEMENT OF MULTI-PURPOSE UTILITY TUNNELS - SOFTWARE USER GUIDE

SUPERVISOR: DR. AMIN HAMMAD

RESEARCH ASSISTANT: KELECHUKWU T. GENGER (Ph.D. CANDIDATE)

Concordia Institute for Information and Systems Engineering
Sir George William Campus
1455 De Maisonneuve Blvd. W.
Montreal, Quebec, Canada. H3G 1M8

Dr. Amin Hammad - Phone: 514-261-5640 • Email: amin.hammad@concordia.ca
Kelechukwu T. Genger – Phone: 438-884-9448 • Email: lktersoo@gmail.com

Table of Contents

Table of Figures

Introduction

This chapter gives a general overview of the developed software and its working principles. The software implementation is based on the results of the multi-criteria decision-making (MCDM) model, which aims to identify the street segments with the highest potential for establishing a MUT. The MCDM model, shown in Figure C-1, is based on eight criteria: (Average Annual Daily Traffic (AADT), road class, utility density, number of expected excavations for utility repair activities, underground development projects, population density, land use, and near to public facilities/high-rise buildings). These criteria form the backbone of the decision-making process. The criteria values for each street segment represent the criteria scores for that street segment. The summation of the multiplication of each criterion score and its corresponding weight, derived from the Analytic Hierarchy Process (AHP) results, is the evaluation score for that street segment. This process is subsequently repeated for all the streets in the group of streets within the analysis. Street segments are ranked based on their total evaluation scores. The segment with the highest score is ranked highest and vice versa (Caffoor, 2019).

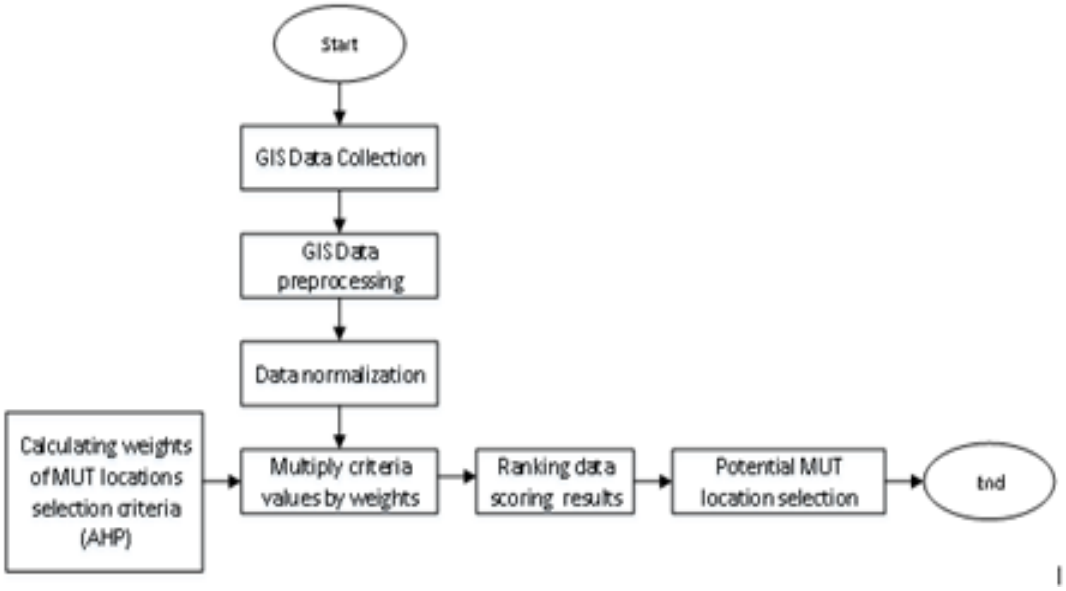

Figure C-1. MCDM model

Languages and software components

The languages and software components used in the development are as follows:

-Python (Programming language)

-ArcGIS (Arcpy libraries) (Geoprocessing)

-SQLite (Database)

-C# (Visualization)

Intended Use

The intended use of this software is the automated ranking of street segments based on eight criteria for the location selection of the placement of MUTs. This software aids decision-making by eliminating the need for calculating the priority weights for each criterion and the need to generate the attribute scores by using several geoprocessing techniques for each street segment. The user does not need to have prior knowledge of any programming, geoprocessing, and database manipulation techniques.

Installation

To run the software, a licensed copy of ArcGIS Pro (version 2.6.3 or above) or ArcGIS Desktop (version 10.7.1 or above) is needed. The following is the sequence of steps necessary to execute the program:

Copy and unzip the MUT_EXE file into any location. After unzipping the MUT_EXE folder, click the MUT-AHP.exe executable file.

The software is not installed in a way that requires uninstalling. It's enough to delete the folder that is generated after unzipping the provided software file. However, keeping this folder is not going to affect any other functionality of your computer.

Database

This application uses an SQLite database. The database schema is called *MUTDB* and it contains three tables, namely:

Road_details: This table contains approximately 18,000 street segment records. The columns of the table are the data source for the autocomplete feature (i.e., the user can type the first few letters of the street name and the names will be completed automatically) of the three street input entries in the GUI. The values were extracted from the PIM_TRONCON_UNIFIE (road intervention plan) layer.

Results_table: This table stores the criteria values extracted after the geoprocessing stage.

Rank_db: This table stores the normalized values.

Functionalities

Figure C-2 shows the main window that is displayed when the program is executed. The message box presents an option for the user to either use their custom files or use preprocessed files. If the user decides to use custom files, a warning is generated as shown in Figure C-3. The interface in Figure C-4 is displayed when the user decides to use custom files. Using the custom file interface is explained in Section 6. The following sequence of activities is executed when using preprocessed files.

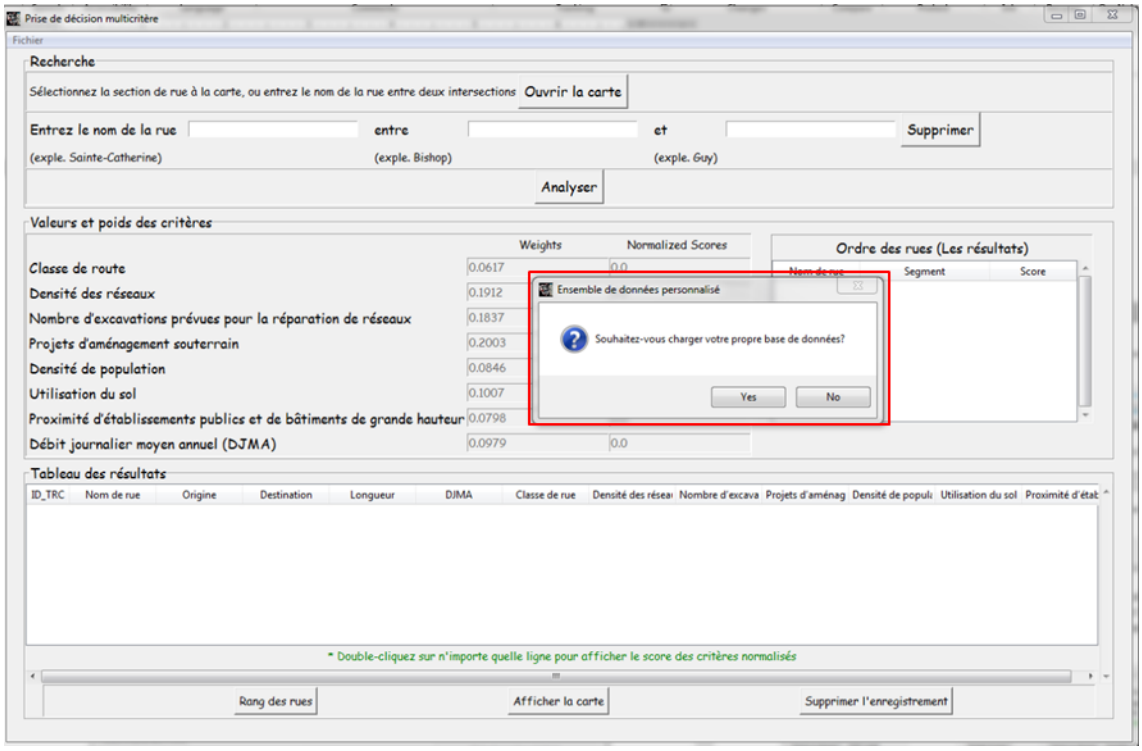

Figure C-2. The select custom file message box.

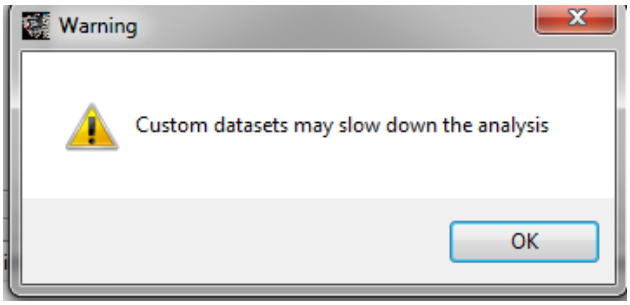

Figure C-3. Warning for using custom datasets.

Figure C-5 shows a description of the features of the main window of the application. The numbers in each text box represent the sequence of operations of actions that must be executed for a successful ranking of street segments. The green boxes represent inputs, the blue text boxes represent outputs, and the red text boxes represent processes.

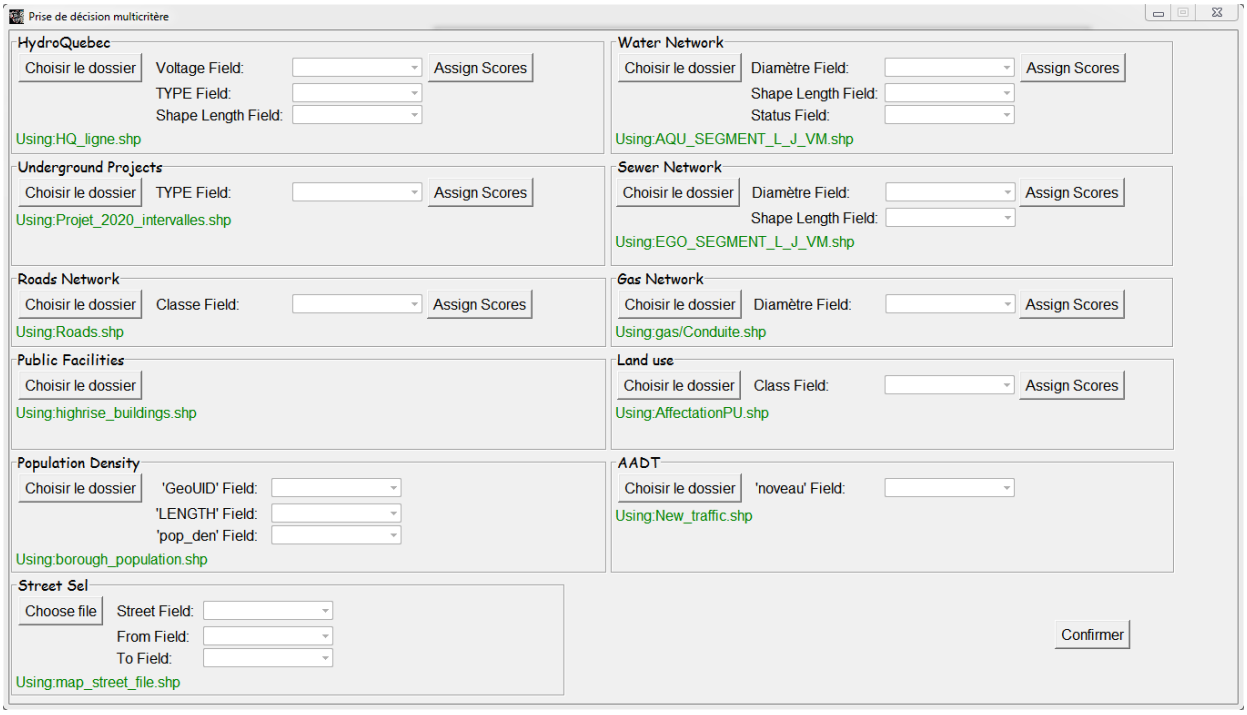

Figure C-4 Custom files

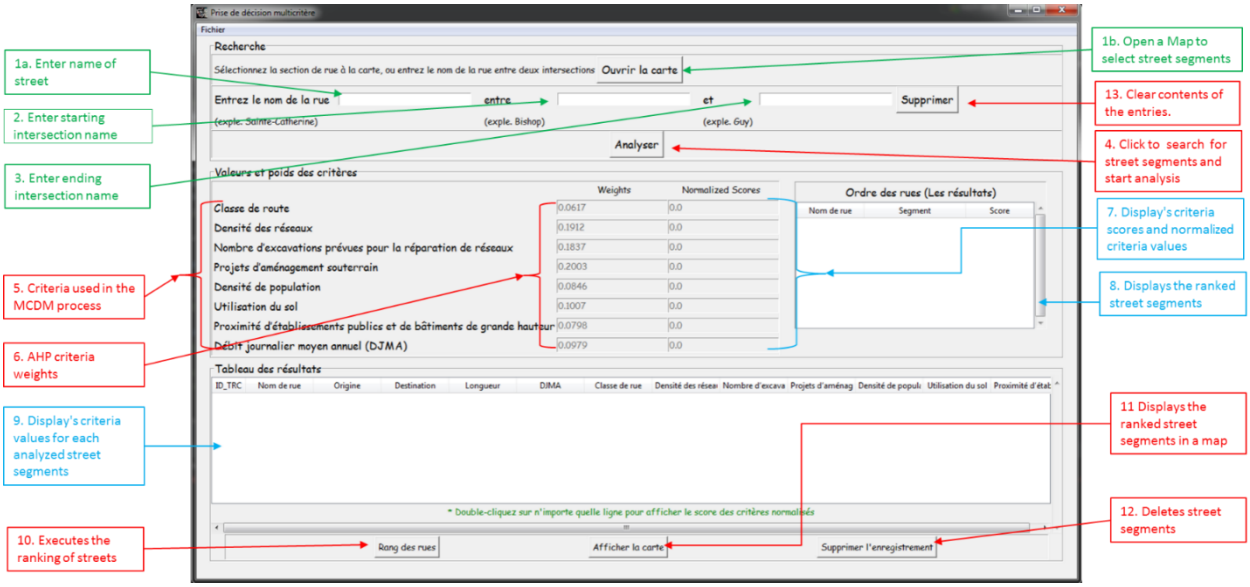

Figure C-5 Main interface window

Selecting street segments: This step selects the street segments and extracts all the criteria values that are available. The source of the street segment data is the road intervention plan. This limits the search for street segments to records that exist in the road intervention plan. Intersections that exist in the intervention plan, may or may not be exactly as desired (e.g., "Sainte-Catherine between Guy

and Bishop" vs. "Sainte-Catherine between Guy and Mackay" or "Sainte-Catherine between Mackay and Bishop").

Searching for a street segment is done in two ways.

- Visually locating the street segment using the map.
- Typing the details of the street segment (i.e., the name, starting intersection, and end intersection) into the entries in the user interface.

Using the map. To visually select street segments, the user clicks the button shown in Figure C-6. This opens an interface displaying the available street segments as shown in Figure C-7.

Figure C-6. Open Map button

Figure C-7. Map input

To zoom in and zoom out, use the mouse wheel to scroll up and down respectively. Furthermore, to identify the desired street, the user should hover the mouse around the area and zoom in as shown in Figure C-8. As the user zooms further down, labels appear to guide the user in identifying the desired street segment. Figure C-9 shows the streets segments labels.

Figure C-8. Zooming into the map

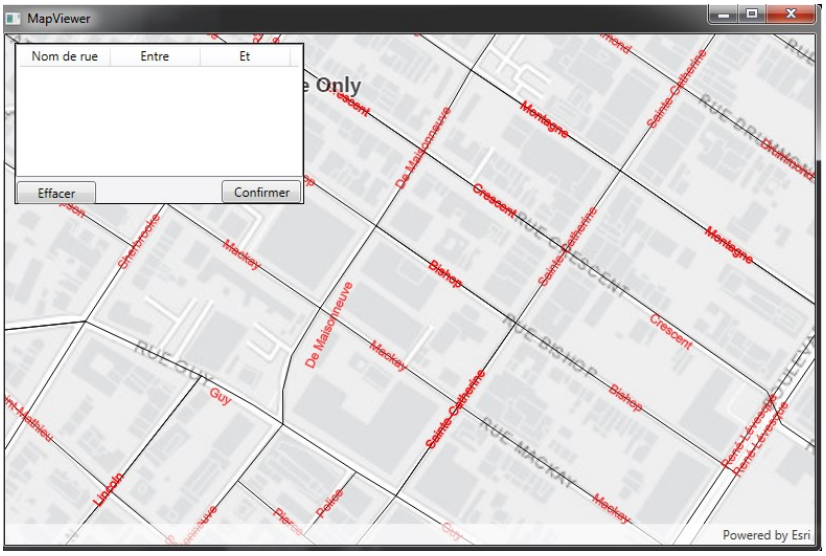

Figure C-9. Street segments showing labels

After identifying the desired street segment, the user right-clicks the mouse, and the details of the street segment pop as shown in Figure C-10. The user can either confirm the selection by clicking OK or cancel the selection by clicking CANCEL. Clicking OK sends the selected segment to the list in the table as shown in Figure C-11. Multiple segments can be selected and added to the table as shown in Figure C-12. After selecting all the desired segments, the user clicks on the CONFIRM button and all the segments are processed in a First-in First-Out (FIFO) order. Clicking the CONFIRM button generates a popup (Figure C-13) showing the progress of the processing of each street in the street segments table. When the process is complete (Figure C-14), the user should click on the PROCEED button.

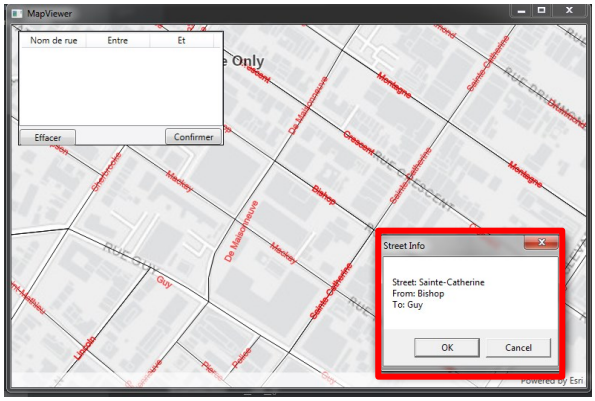

Figure C-10. Map showing selected segment details

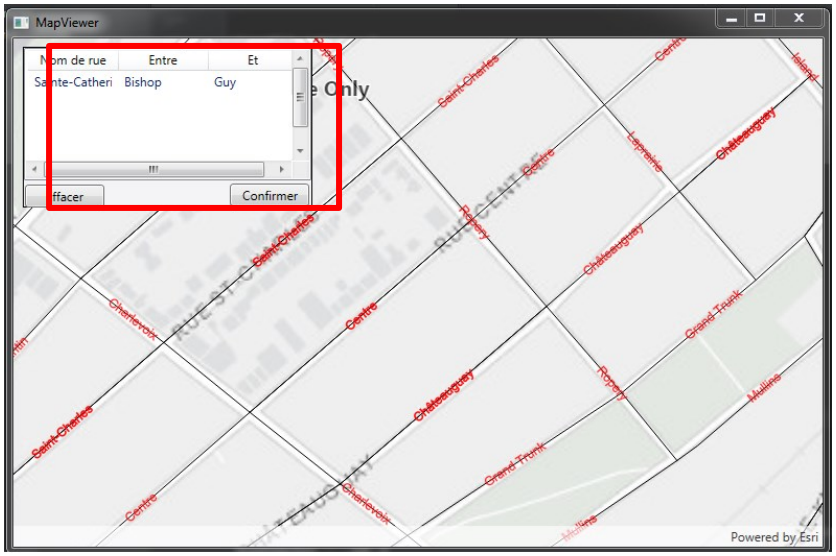

Figure C-11. Text area showing one street segment

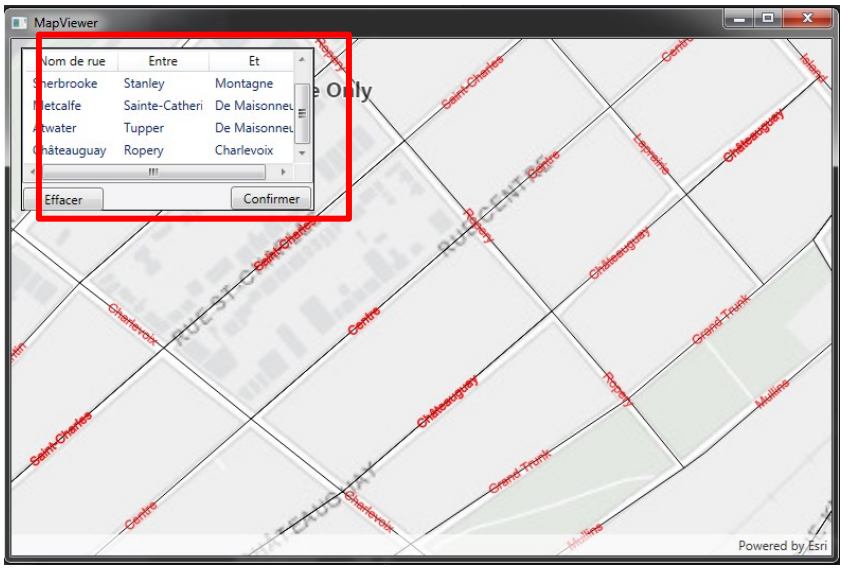

Figure C-12. Text area showing multiple street segments

After clicking the PROCEED button, the interface in Figure C-15 is displayed showing extracted criteria values for all the selected street segments.

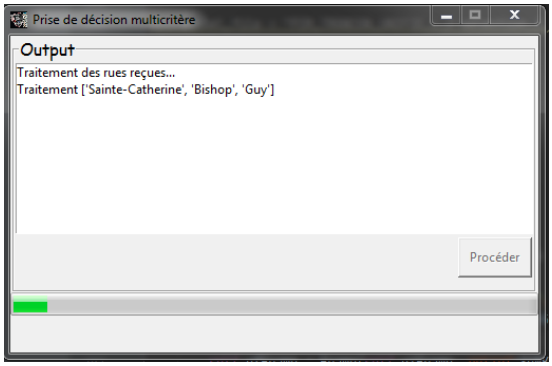

Figure C-13. Process initiated

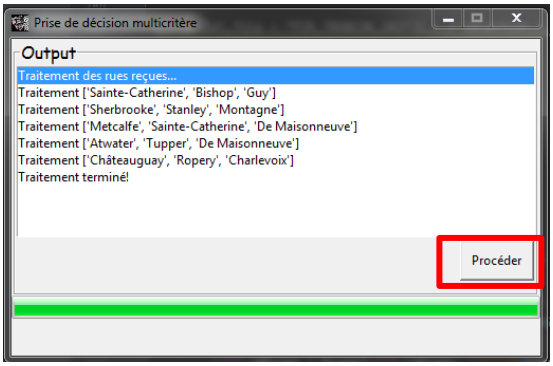

Figure C-14. Process completed

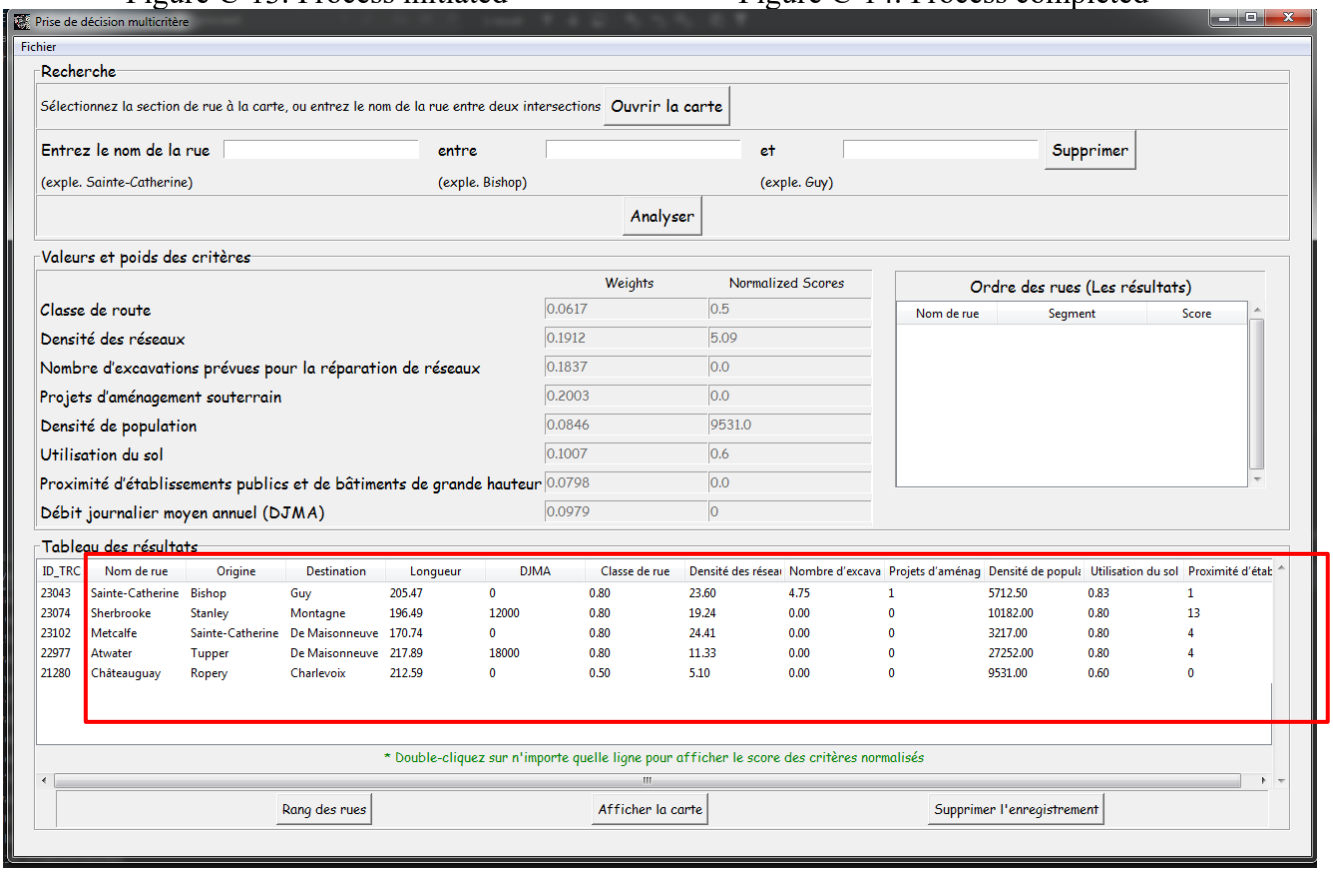

Figure C-15. Results table showing extracted criteria values.

Alternatively, searching can be done by first entering a valid street name along with the names of a start and a stop intersection. Entries 1, 2, and 3 represent the street name, start intersection and stop intersection, respectively. All three entries have auto-complete features embedded in them as shown in Figure C-16. This feature suggests street names as the user types. To select the intended street, use the UP or DOWN keys to navigate to the name and use the RIGHT KEY to select.

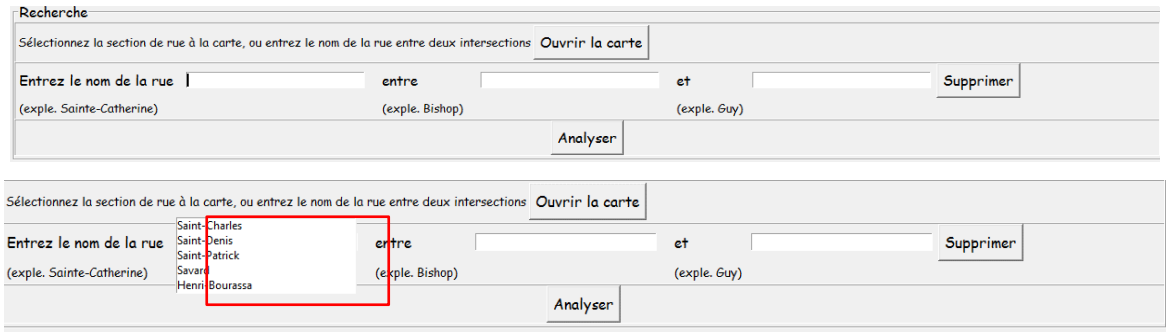

Figure C-16. Autocomplete feature.

French characters do not appear correctly in the autocomplete entries (e.g. René-Lévesque is displayed as "Ren?-L?vesque"). The error message in Figure C-17 pops up when searching for street names with French characters. To avoid this error, the names should be entered manually.

If the street segment is found in the database, its attribute values are generated and displayed in the *Criteria Scores* section (Figure C-18) across each corresponding criterion. The same values are displayed in the *Result Table* in Figure C-18. Furthermore, Figure C-18 also shows the analysis conducted on a road segment on Sainte-Catherine Street between Bishop and Guy.

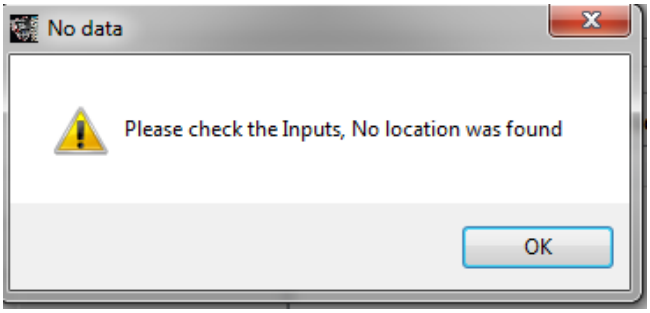

Figure C-17. Check input warning!

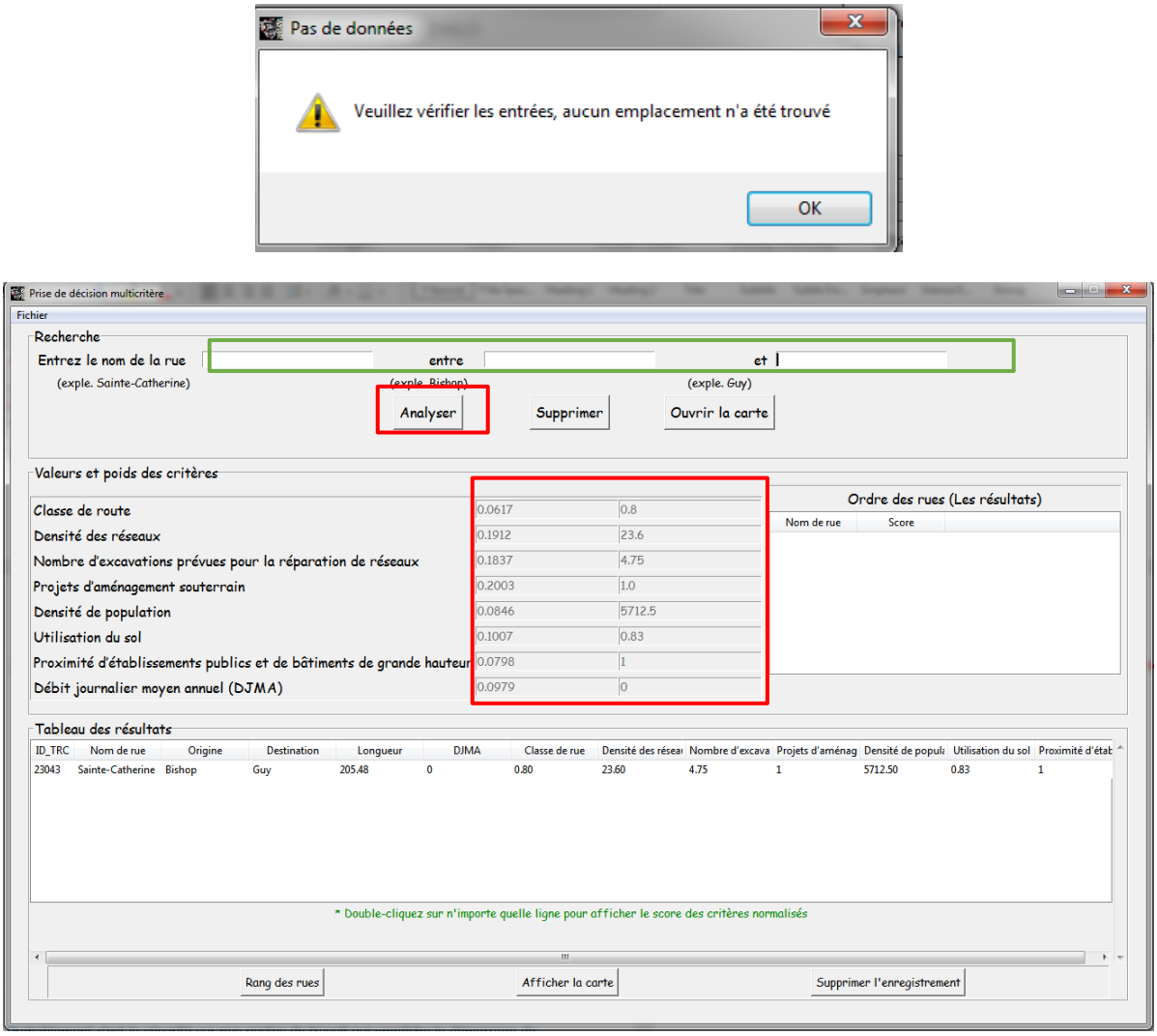

Figure C-18. Example of a search and analyze function

Ranking: Ranking can only be performed on two or more street segments. The steps involved are:

First, enter the details of at least two or more valid street segments.

Normalization (please refer to Equation 12 of the phase 2 report) is performed and the results of each normalized road segment can be seen by double-clicking the row corresponding to that road segment on the *Result Table*. Figure C-19 shows the normalized values for the highlighted row in the Criteria Scores section of the GUI.

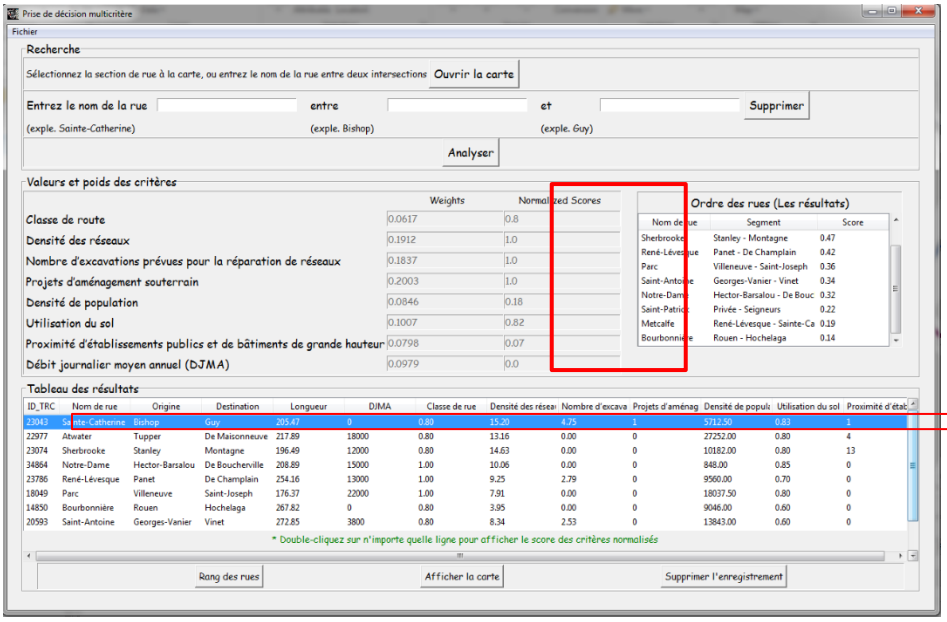

Figure C-19. Displaying normalized results

Finally, by clicking the *Rank Streets* button, the street segments are ranked, and the ranking is displayed in descending order in the *Ranked Streets* table as shown in Figure C-20. The street segment with the highest value is considered the most suitable for MUT placement based on the criteria values.

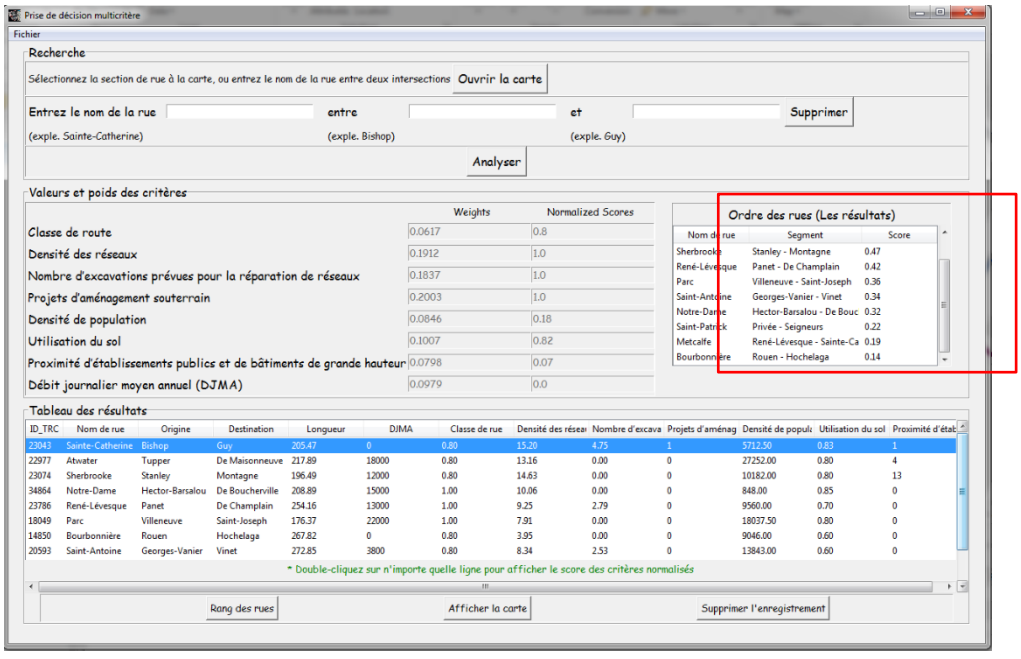

Figure C-20. Ranking results

Map Display: This feature displays the ranked segments on a map. Displaying a map is done by first clicking the *Display Map* button shown in Figure C-21. The generated map is shown in Figure C-22. The width of the street segments signifies their ranks (i.e., the thicker the width, the higher the rank of the street). Clicking on a street segment generates a pop-up that displays the street name and the score as shown in Figure C-23. Maps are generated for a minimum of 2 segments and a maximum of 10 street segments. The error message in Figure C-24 is generated if the user attempts to generate a map outside this range.

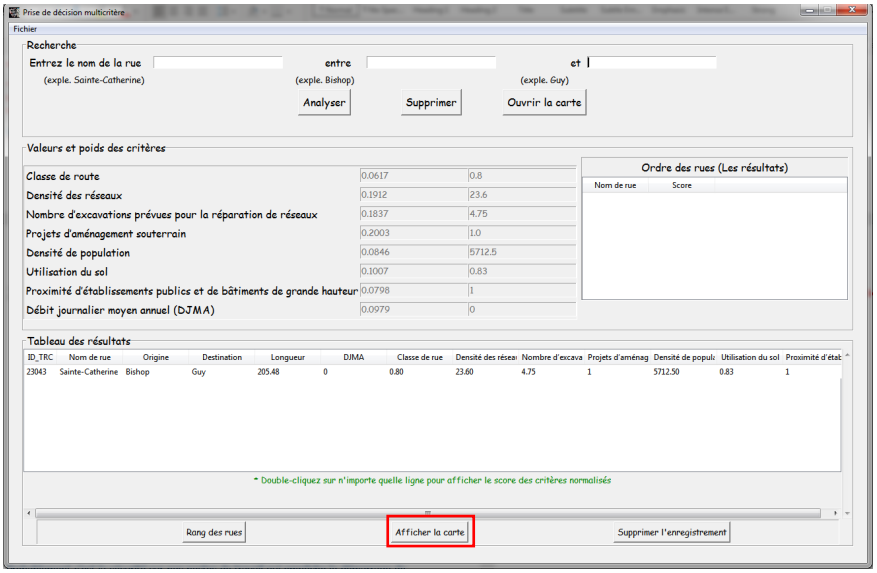

Figure C-21. Open map button

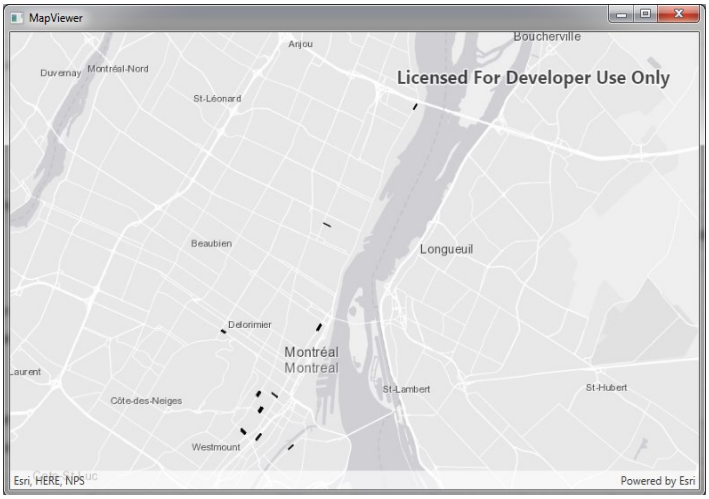

Figure C-22. Map showing ranked street segments

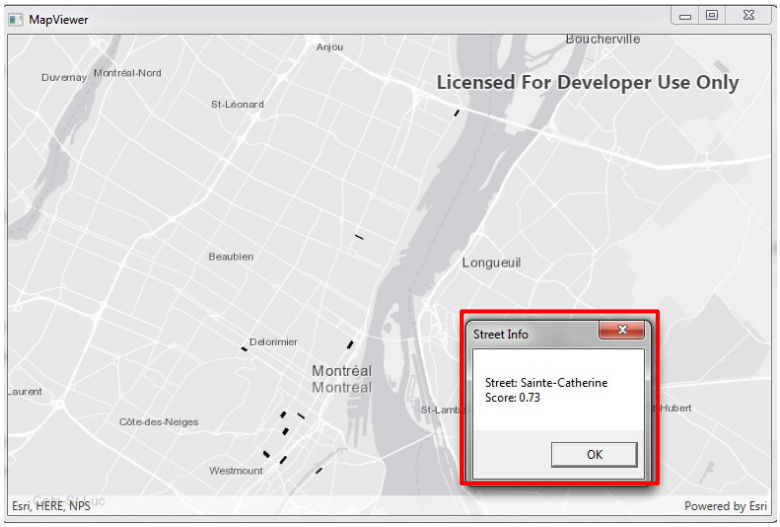

Figure C-23. Pop-up showing street name and rank score

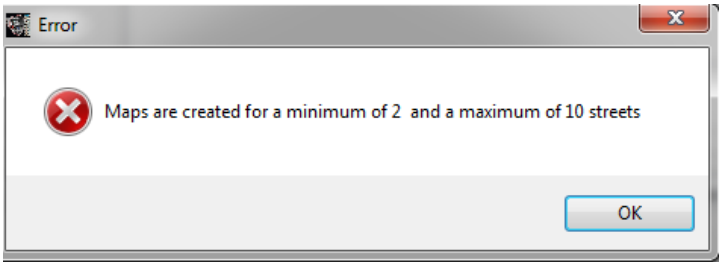

Figure C-24. Map error message

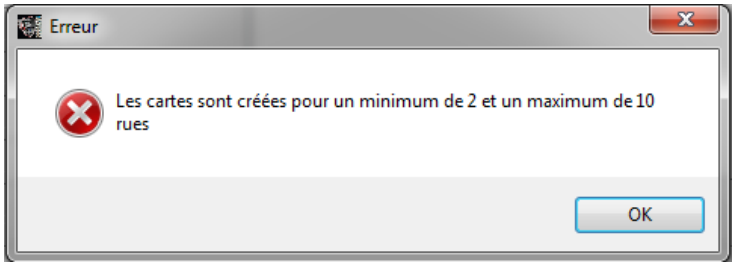

Delete: This feature allows the user to delete a street segment from the analysis. Records of street segments can be deleted from the analysis by selecting the row in the *Result Table* and then clicking the *Delete Record* button. When the deletion is confirmed (Figure 25), the ranking is recomputed, and the new scores are updated as shown in Figure 26.

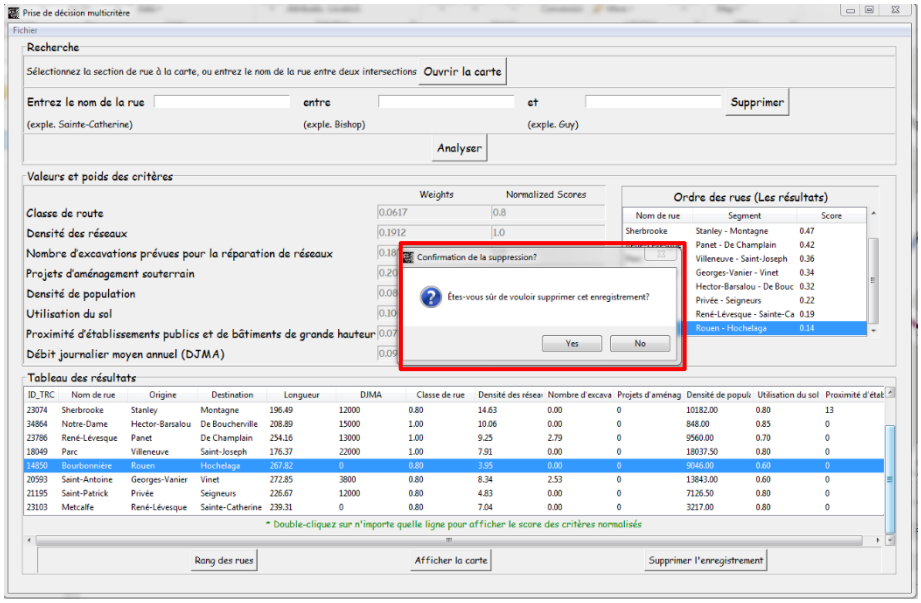

Figure C-25. Delete confirmation

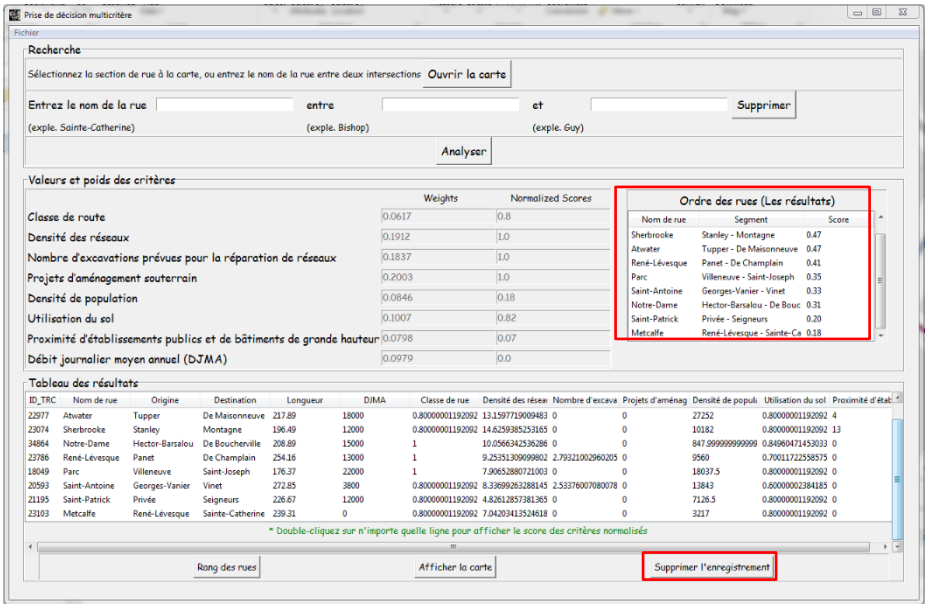

Figure C-26. Deleting a record

Saving: This feature allows the user the option of saving an analysis. The output file contains information on the extracted criteria values (unnormalized values), the normalized criteria scores, and the ranking result of the street segments that have been analyzed. An analysis is saved by clicking the *Save* option in the *Menu* toolbar as shown in Figure C-27. The user selects a location (Figure C-28) and the file is named by the user with a . TXT extension. Figure C-29 is a sample of a saved analysis.

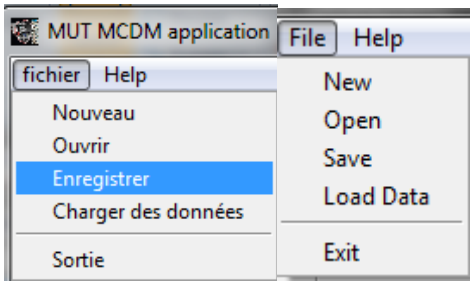

Figure C-27. Menu Toolbar

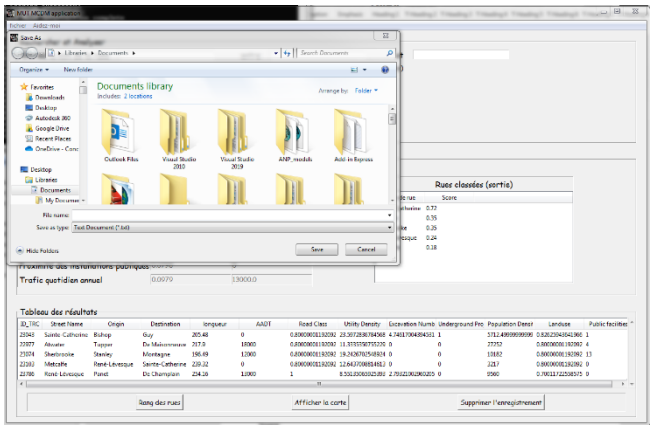

Figure C-28. Saving interface

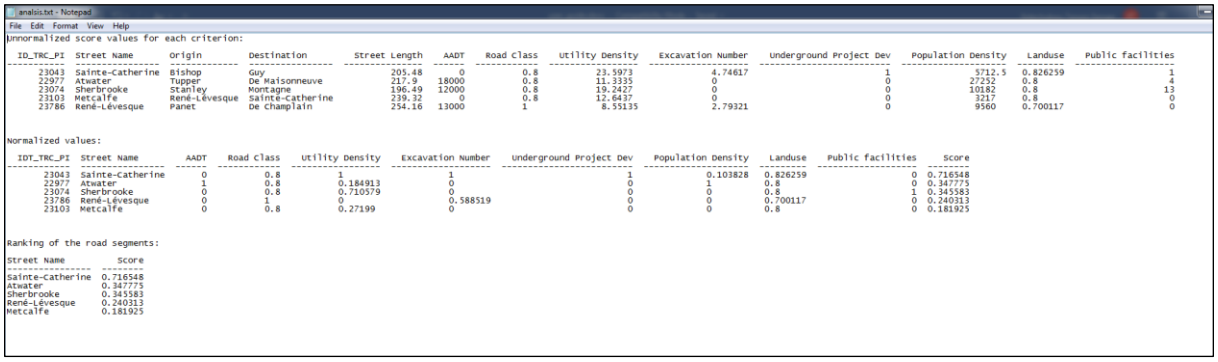

Figure C-29. Sample of output

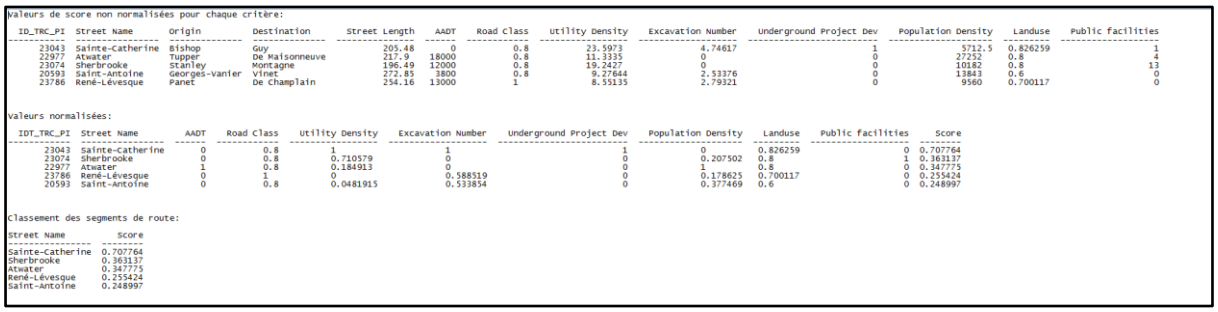

Criteria Attributes and Geoprocessing

This section gives a brief insight into the layers used for the analysis and the attributes of each layer used.

(1) Road Search

Layer used: PIM_TRONCON_UNIFIE_L_J.shp

Necessary attributes: ID_TRC_PI, RUE, DE, A, LONGUEUR

Outputs: RUE, DE, A

The beginning of analysis starts with a search for road segments. The road intervention plan layer (PIM_TRONCON_UNIFIE) was used instead of the road layer because the records capture the streets as segments in between intersections. This layer will be combined with the needed information from all other layers to get the criteria values for each street segment.

(2) Road Class

Layers used: ROAD.shp, PIM_TRONCON_UNIFIE_L_J.shp

Necessary attributes: CLASSE, LENGTH

This layer was combined with the PIM_TRONCON_UNIFIE layer to determine the class of the street segments. Please refer to Section 4.3.4 of the Phase II report for details on how the class values are assigned to road segments. The values in Table C-8 in the Phase two report are the default values that have been hard-coded into the program. To use another dataset for the road class, a column (attribute) that represents the road class must exist.

(3) AADT

Layers used: SECTION_TRAFIC.shp, PIM_TRONCON_UNIFIE_L_J.shp

Necessary attribute: nouveau__1

This layer contains section traffic for several major intersections. To derive the AADT for a street segment, this layer is combined with the road intervention plan layer (PIM_TRONCON_UNIFIE). Road segments with AADT values of 0 imply that the AADT for that segment is a missing value. Using another dataset for the AADT should contain the AADT column.

(4) Utility Density

Layers used: AGU_SEGMENT_L_J_VM, CONDUITE, EGO_SEGMENT_L_J_VM, HQ_LIGNE, PIM_TRONCON_UNIFIE_L_J

Necessary attributes:

Water: DIAMETREM_, SHAPE_Leng

Gas: diameter, SHAPE_Leng

Sewer: DIAMETRE_1, SHAPE_Leng

Hydro-Quebec: DESCRIPTION (voltage), TYPE (underground/above ground), SHAPE_Leng

Four utilities (water, gas, sewer, and Hydro-Quebec) are used in calculating the utility density for a street segment. The score for each utility type is calculated separately. For more details on the calculation of the utility density, please refer to Section 4.3.4 of the Phase II report.

(5) Number of Expected Excavations

Layer used: PIM_TRONCON_UNIFIE_L_J

Necessary attribute: Taux de bris max

The water pipe breakage rate is indicated in the "Taux de bris max (Nb/km/an)" column. This refers to the number of water breakage per km per year. Because of the lack of breakage rate data for other utilities, only the water pipe breakage rate is used to predict the number of expected excavations for utility repair.

(6) Underground Project Development

Layers used: PROJET_2020_INTERVALLES.shp, PIM_TRONCON_UNIFIE_L_J.shp

Necessary attribute: TYPE

This layer was intersected with the road intervention plan layer to determine if a street segment has an underground development project. The type of project considered in this analysis is the "*Grand Projet*".

(7) Population Density

Layers used: MONTREAL TRACTS, PIM_TRONCON_UNIFIE_L_J.shp

Source:
https://services.arcgis.com/Ywxx29kRZEPq7K5N/arcgis/rest/services/montreal_tracts10023/FeatureServer

Necessary attributes: Population density (derived), Shape_Area, GeoUID

The population layer is intersected with the road intervention plan to derive the population density of the area surrounding the road segment.

(8) Land use

Layers used: AFFECTATIONPU.shp, PIM_TRONCON_UNIFIE_L_J.shp

Necessary attributes: ID_TRC, length, categorie

This layer is intersected with the road intervention plan to determine the land use surrounding each road segment. Each category of land use is assigned a score based on its relevance to MUT placement selection (please refer to Table C-10 of the Phase II report). Several geoprocessing techniques are then applied to determine land use based on the length of the road, the category surrounding the length, and the score attached to each category of land use.

(9) Proximity to Public Facilities/High-Rise Buildings

Layers used: EQUNIVERSITAIRE, EQCOLLEGIAL, EQSANTE, HIGHRISE_BUILDING, PIM_TRONCON_UNIFIE_L_J.shp

Necessary attribute: count (derived)

The first four input layers were combined into a single feature class. This feature class was intersected with a 128 m buffer (average distance between two parallel streets) created around the road intervention plan (PIM_TRONCON_UNIFIE_L_J.shp) layer. The output was the number of high-rise /public buildings around the street segment. This number is then further normalized using Equation 12 of the Phase II report to obtain the criterion score for the road segment.

Using Custom files

A user has the option of using custom datasets. This means replacing one or all the default datasets that have already been preprocessed in the software. This interface can be executed when the program is initially run. Alternatively, the user can select the *Load data* option in the *File menu* as shown in Figure C-30. The use of custom files is executed using the interface in Figure C-31.

Replacing a criterion's preprocessed file with a custom file will require the user to select some attributes. The required attributes depend on the criteria file being replaced. Table C-1 shows the criteria, the required attributes, and the attribute description. Scoring (assigning a level of importance relative to other attributes) is required for some of the fields. This is done by assigning values between 0-1 to the unique attribute values. By default, all unique attribute values are assigned a value of 1 (i.e., equal importance). Figure C-32 is an example of scoring the Hydro Quebec voltage field.

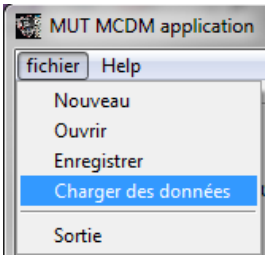

Figure C-30. Load custom files.

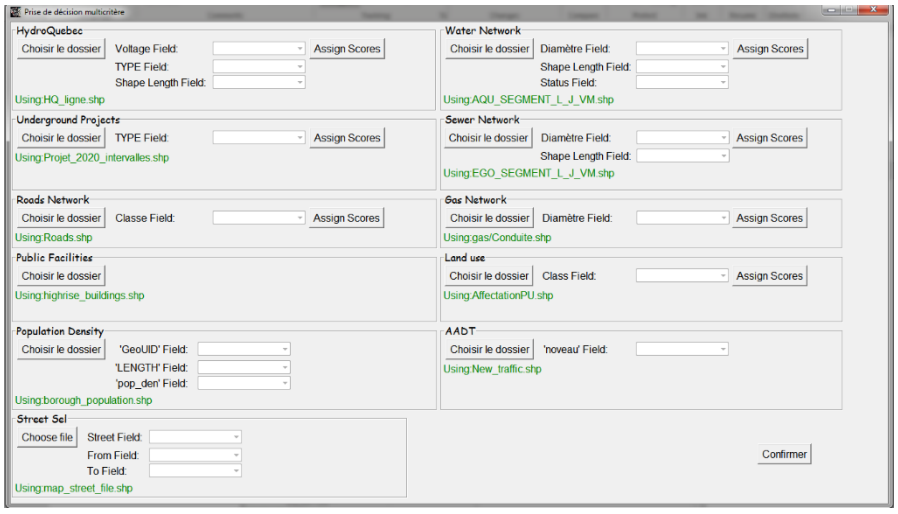

Figure C-31. Using the custom files interface

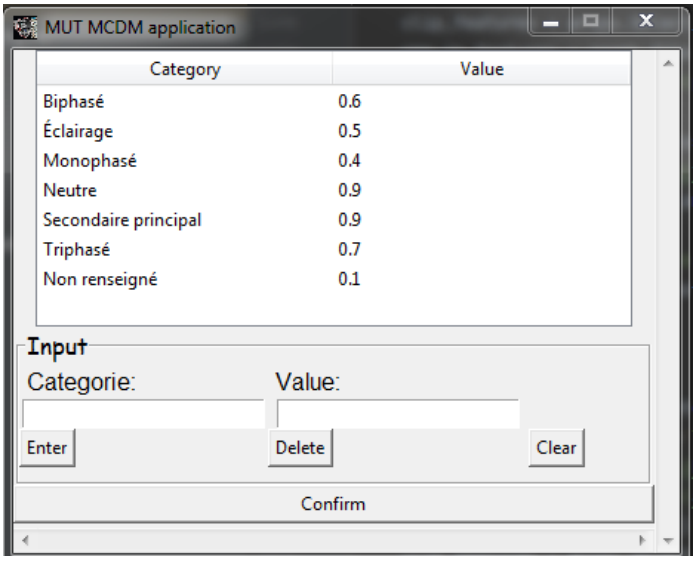

Figure C-32. Scoring attribute values

Table C-1. Criteria input description

Criteria/Layer	Required Attribute(s)/Field(s)	Description
HydroQuebec Network	Voltage	The voltage of the cables
	Type	Underground/aboveground
	Shape length	Length of the cable in that road segment
Water Network	Diameter	Water pipe diameter
	Shape length	Length of the pipe in that road segment
	Status	Pipe status e.g. abandoned pipes
Underground development projects	Type	Type/description of the project e.g. Grand projects
Sewer Network	Diameter	Water pipe diameter
	Shape length	Length of the pipe in that road segment
Road Network	Classe	Road class
Public facilities		
Land use	Category	Land use category, e.g institution, commercial.
Population Density	GeoUID	Unique ID for population densities
	Length field	Length covered by the population density
	Population density	Values representing the population densities

Limitations

This application takes in only shapefiles with the *.shp* extension. To use Feature class files from a geodatabase, the user must convert feature class files to shapefiles.

Using custom files increases the time for an analysis to complete.

French characters do not appear correctly in the autocomplete entries for example René-Lévesque is displayed as "Ren?-L?vesque". When searching for street names with French characters, the names should be entered manually. Alternatively, use the map to select the street segments.

Some road segments have missing data, this accounts for criteria values with zero scores. For example, the traffic dataset (AADT) used in this application has records for only the main segments. Using a relatively complete dataset for the criteria will improve the decision-making results.

The criteria weights are based on the AHP results in Phase II of this research. These values can be modified. However, the user must ensure that the sum of the criteria weights is equal to one.

Caffoor, I. (2019). *Robotics and Autonomous Systems (RAS) for buried pipe infrastructure and water operations*. *TWENTY65*. Retrieved from http://pipebots.ac.uk/wp-content/uploads/2019/03/robotics-report-web-4.pdf

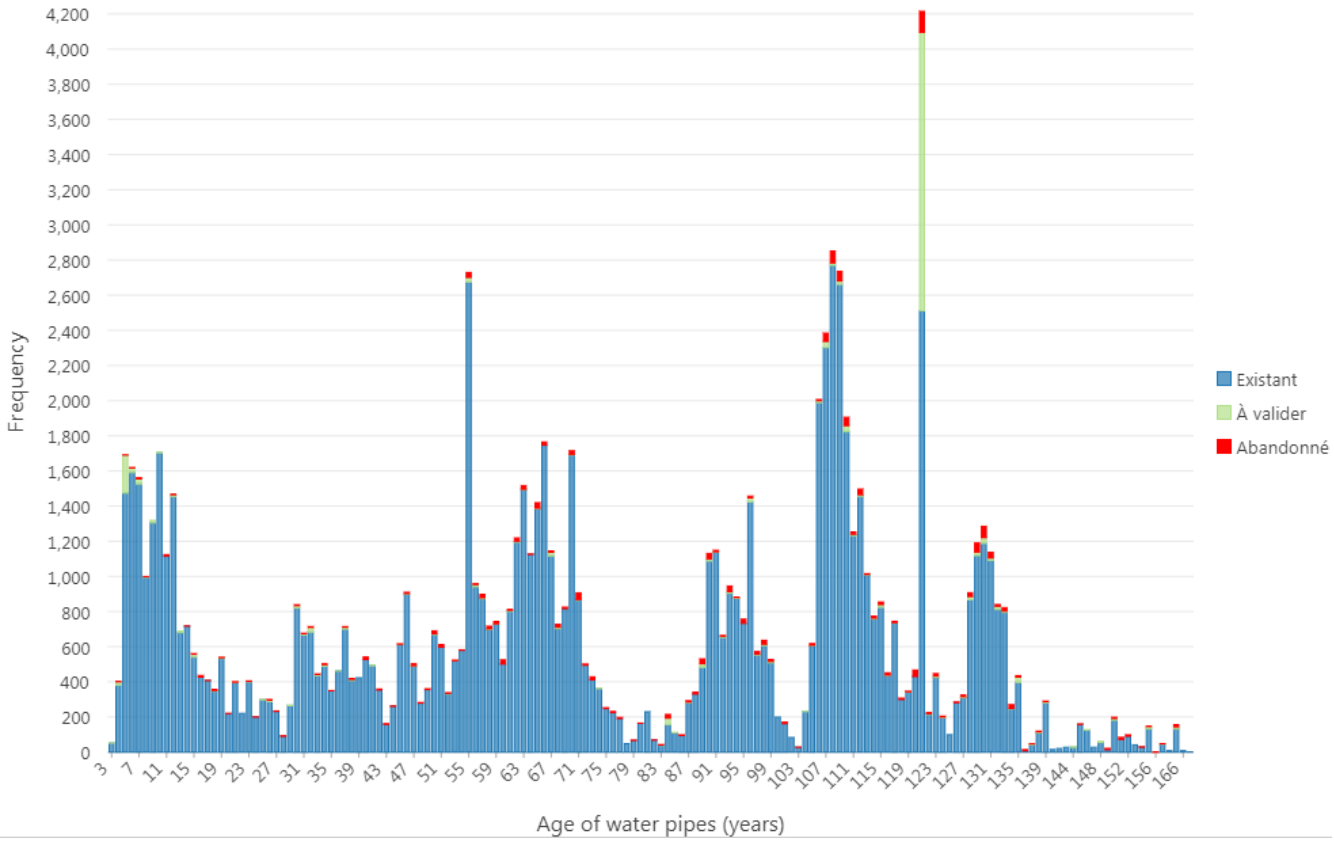

Figure C-33 Frequency and Ages of water pipes

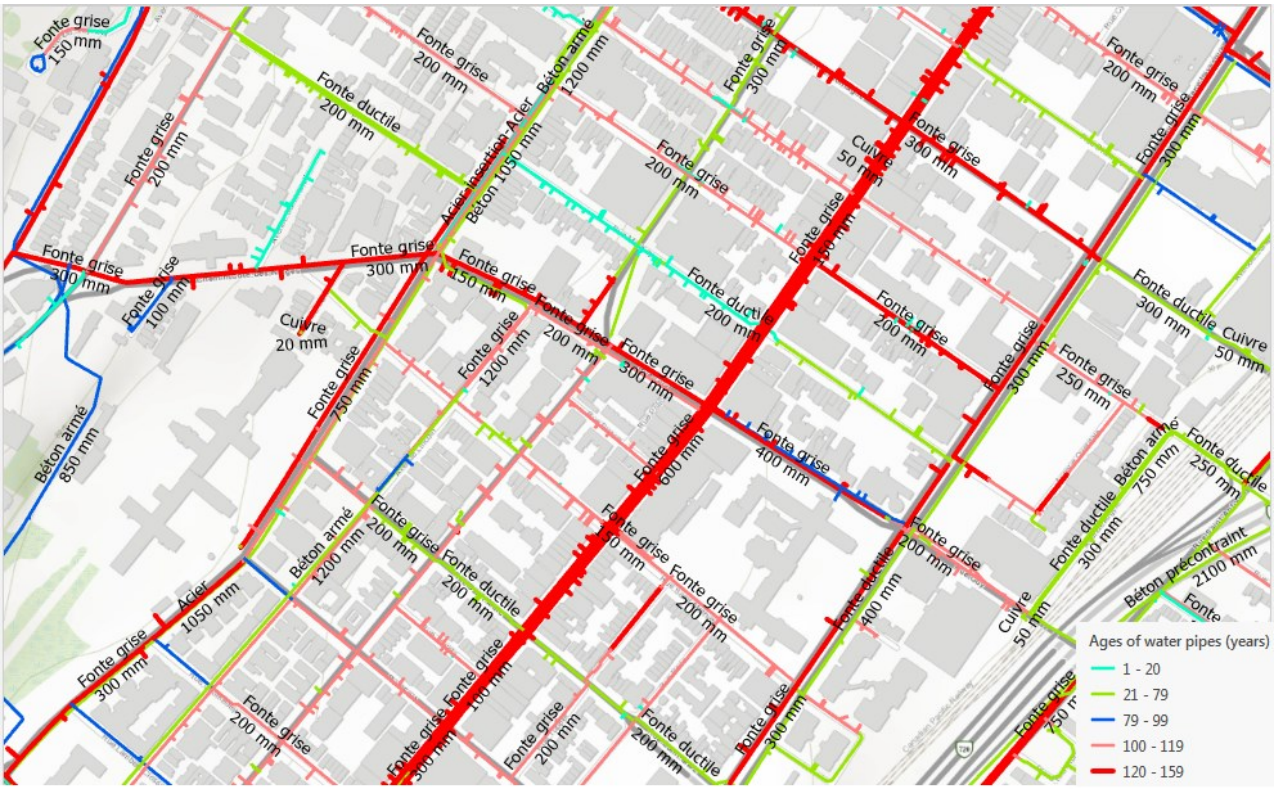

Figure C-34 GIS representation of the ages of water pipes

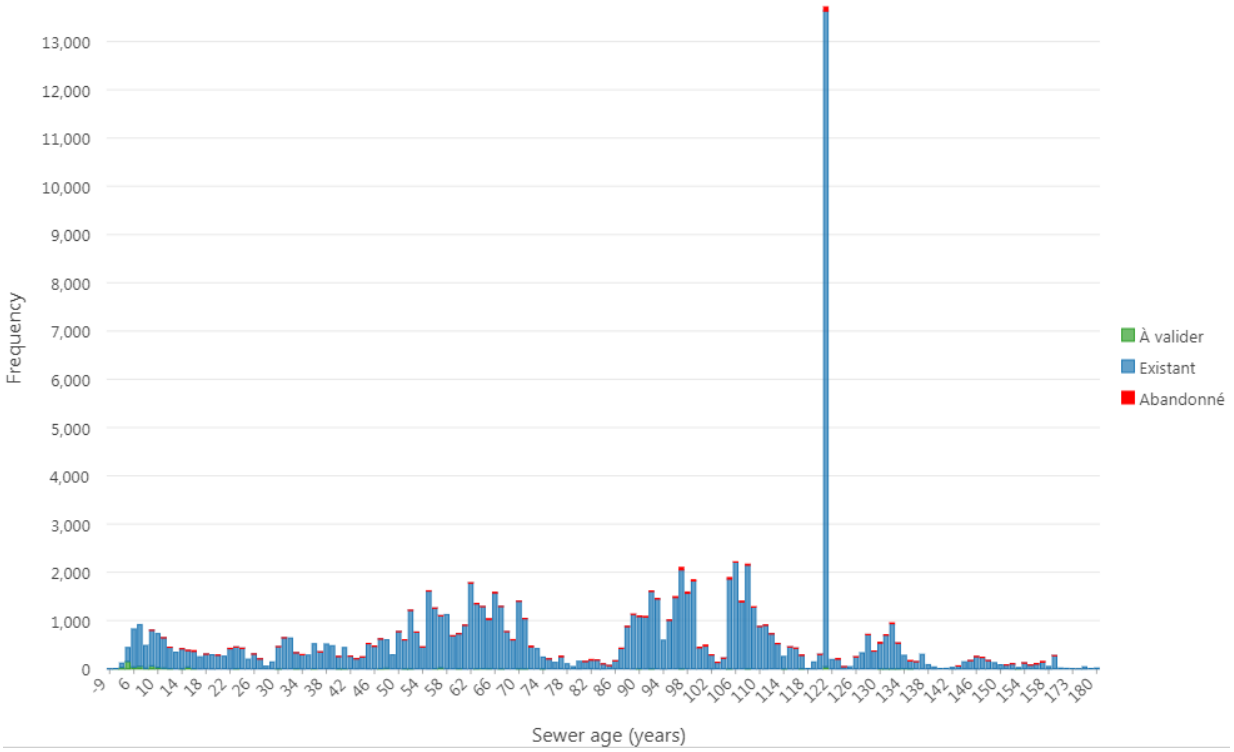

Figure C-35 Frequency and Ages of Sewer pipes

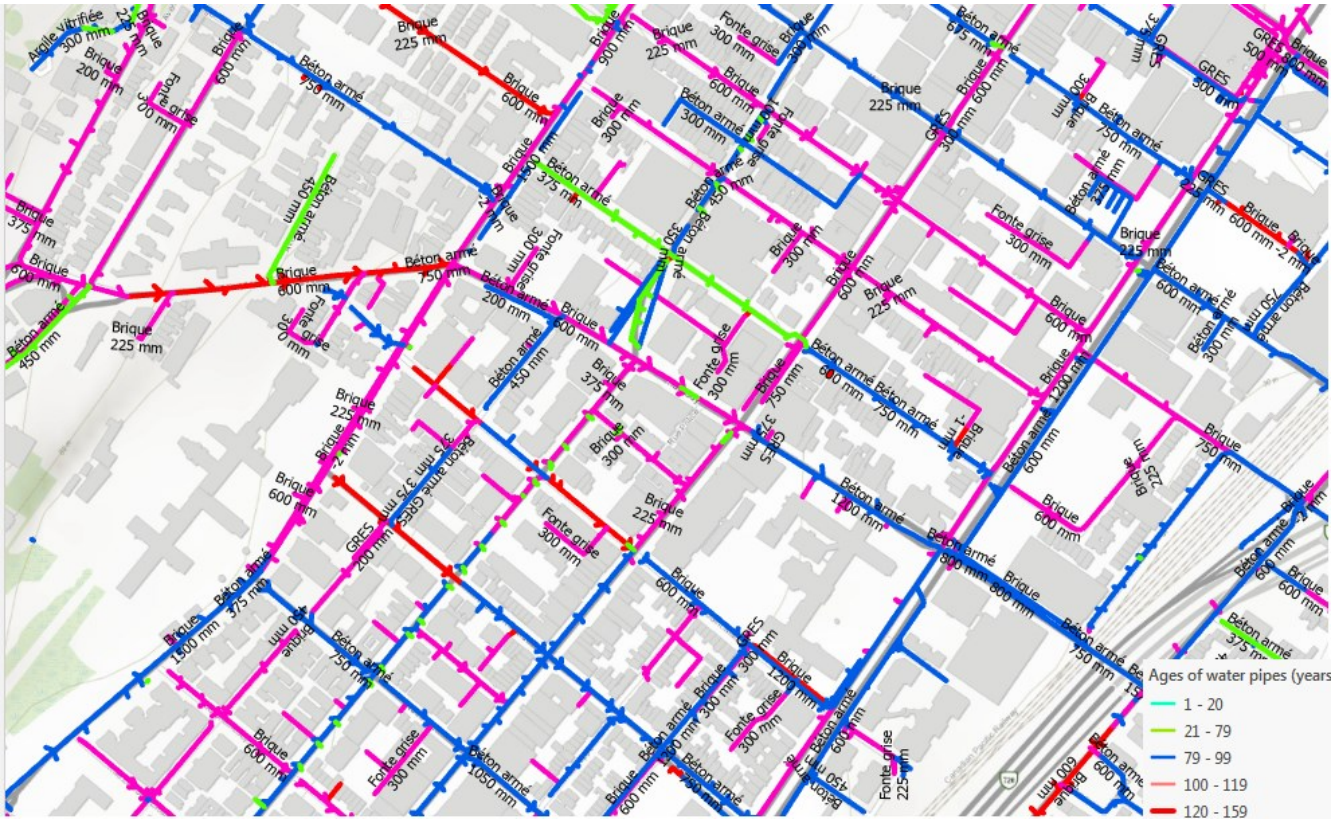

Figure C-36 GIS representation of the ages and materials of sewer pipe

	Attribute	Type	Range
Water pipe network	Pipe material	Nominal	Reinforced concrete, Steel Grey font, Ductile iron, Gray iron or ductile iron, Prestressed concrete, Polyvinyl chloride, Polyethylene, Unreinforced concrete, Asbestos cement Galvanized iron, Copper
	Diameter (mm)	Numeric	2100, 1500, 1200, 1050, 900, 850, 750, 600, 500, 450, 400, 350, 300, 250, 200, 150, 100, 75, 50
	Status	Ordinal	Existing, Abandoned, to validate offers, out of order
	Type of Pipe	Nominal	
Water pipe breaks	Date of break	Date	1900-2020
	Installation date	Date	1862- 2013
	Type of breaks	Nominal	Hole, Leak at the seal, Sparkle, Perforation in the wall, Longitudinal crack

			Circular crack Leak at the fitting Corporate shutdown (main pipe), Chipping of the pipe / Perforation in the wall, Circumferential breakage, Muff, Broken connection Leaking faucet, driving sparkle, Leak at the water connection, Longitudinal breakage, Line (or distribution) stop, Pipe chip / Longitudinal breakage, Split interlocking, Circumferential breakage / Chipping of the pipe, Perforation in the wall, Perforation, downward circumferential, shard, ramback, corrosion valve, Rift Longitudinal breakage + Perforation in the wall, Vertical, circumferential, wear pipe, Circumferential, Circular - breeze in 2 Join at the tap, Circumferential, Wear pipe, corrosion, Shine, third party damage, Breaking, Longitudinal breakage / Chipping of the pipe
	Type of repair	Nominal	Disconnection of an unused water service, Seal repair Seal repair, Replacing a pipe segment, Installation of a sleeve, Pipe replacement Repair at the connection, Valve replacement, Replacement of the pipe / Installation of a sleeve, Replacement of the water connection, Replacement of the pipe / Installation of a sleeve / Repair at the fitting

			Caliper repair, Installation of an anode, Sleeve installation Repair at the joint / Installation of a sleeve, Replacement of a segment of the pipe + Installation of a sleeve, Replacement of a pipe segment, street asphalt asphalt and earthworks - sidewalk. change the water and sewer from the BS to the main street
Intervention plan	Number of bad &very bad pipes	Numeric	0 - 8
	Age/useful life	Numeric	0 - 1.68
	Integrated class	Ordinal	A - D
	Number of historical breaks	Numeric	0 - 9
	Break rate	Numeric	0 - 9.76
	Cost ($)	Numeric	433 - 6,889,046
Public work and Info-excavation	Type of work	Nominal	
	Excavation type	Nominal	
	Duration of work	Numeric	
	AADT	Numeric	

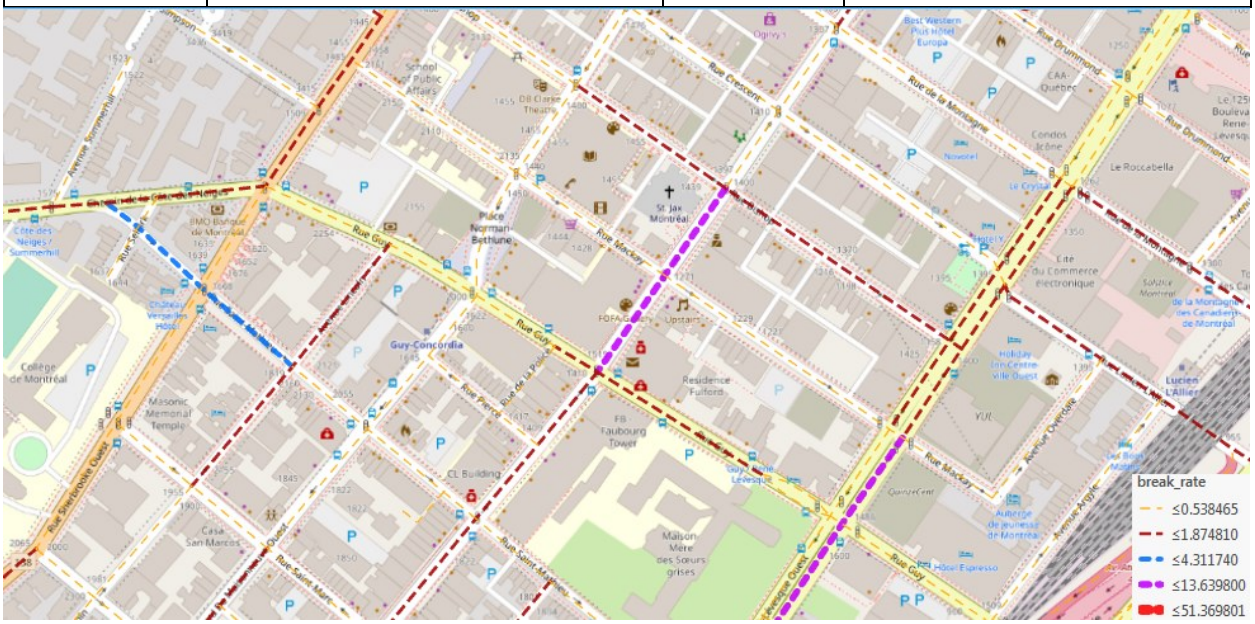

Figure C-37 Street segments showing break-rate

Appendix D. MATLAB Codes

D.1 Codes for synchronized intervention

```
% ------------------------------------------------------------------------ %
% Function NSGAII performs a Non Sorting Genetic Algorithm-II              %
%                                                                          %
%                                                                          %
%   Input parameters:                                                      %
%       - params:   Struct that contains the customized parameters.        %
%         * params.Np:           Number of chromosomes in the population. %
%         * params.maxgen:       Maximum number of generations.           %
%         * params.pc:           Probability of crossover.                %
%         * params.pm:           Probability of mutation.                 %
%         * params.NumSegments   Number of segments.                       %
%         * params.r             Discount rate.                           %
%         * params.YearlyBudget  Agency cost budget                        %
%         * params.SocialCostYearlyBudget Social cost budget               %
%         * params.years         Planning period                           %
%         * params.sewer_costs   Sewer pipe intervention cost              %
%         * params.water_costs   Water pipe intervention cost              %
%         * params.Pavement_intervention_impact pavement                   %
%
% ------------------------------------------------------------------------ %
%   Author:  Kelechukwu Tersoo Genger                                      %
%   Date:    09/03/2023                                                    %
%   E-mail:  tkgenger@gmail.com                                            %
%                                                                          %
%   Log:                                                                   %
%              1.1:  Fast Non Sorting Algorithm is now vectorized for im-  %
%                    proving the performance (much less computation time)  %
%                    (22/12/2017).                                         %
%            - 1.2:  The old mutation operator is substituted by the adding%
%                    of a , as suggested by                                %
%                    Alexander Hagg, which brings a better convergence     %
%                    (25/11/2019).                                         %
% ------------------------------------------------------------------------ %
%   References:                                                            %
%    [1] Deb, K., Pratap, A., Agarwal, S., & Meyarivan, T. A. M. T. (2002)%
%        A fast and elitist multiobjective genetic algorithm: NSGA-II.     %
%        IEEE transactions on evolutionary computation, 6(2), 182-197.     %
% ------------------------------------------------------------------------ %
```

```
function
[Plans,SocialCost,InterventionCost,Performance,years_interventioncost,years_socialcost,gen_rank_s
olutions] = SYNC_NSGAII(params)
```

```
global Water_pipe_expected_life Sewer_pipe_expected_life WaterPipeCondition Water_pipe_age
Sewer_pipe_age PavementCondition SewerCondition
    % Parameters
    Np      = params.Np;        % Number of chromosomes in the population
    maxgen  = params.maxgen;    % Maximum number of generations
    pc      = params.pc;        % Probability of crossover
    pm      = params.pm;        % Probability of mutation
    NumSegments = params.NumSegments;
    r = params.r;
    YearlyBudget = params.YearlyBudget;
    SocialCostYearlyBudget = params.SocialCostYearlyBudget;
    years = params.years;
    assets = params.assets;
    sewer_costs = params.sewer_costs;
    water_costs = params.water_costs;
    Pavement_intervention_impact = params.Pavement_intervention_impact;

   % Data
    uniqueID =  assets.ID_TRC_PI;                                   %ID of segment
    SegmentID = uniqueID(1:NumSegments)';
```

```
    function ResizeData(Nrows)
        Water_pipe_age = repmat(assets.waterPipe_age(1:NumSegments)',Nrows,1);
        Sewer_pipe_age = repmat(assets.SewerAge(1:NumSegments)',Nrows,1);
        PavementCondition = repmat(assets.PCI(1:NumSegments)',Nrows,1);
        SewerCondition = repmat(assets.sewer_initial_condition(1:NumSegments)',Nrows,1);
        WaterPipeCondition = repmat(assets.water_initial_condition(1:NumSegments)',Nrows,1);
        Sewer_pipe_expected_life =
repmat(assets.Sewer_pipe_expected_life(1:NumSegments)',Nrows,1);
        Water_pipe_expected_life =
repmat(assets.Water_pipe_expected_life(1:NumSegments)',Nrows,1);
    end
```

```
    ResizeData(Np)

    % Initialization
    UseInit = false;
    PavementInterventionInit = nan;
    SewerInterventionInit = nan;
    WaterInterventionInit = nan;
```

initial Population P

```
    [InterventionCost,
SocialCost,Performance,years_interventioncost,years_socialcost,Plans,InterventionBudgetUtilizatio
n,SocialBudgetUtilization,...
    PavementInterventionInit, SewerInterventionInit,WaterInterventionInit] =
InterventionAndSocialCost(PavementCondition,SewerCondition,WaterPipeCondition,...
```

```
    Water_pipe_age,Sewer_pipe_age,Sewer_pipe_expected_life,Water_pipe_expected_life,
assets,sewer_costs,water_costs,...
    r,Pavement_intervention_impact,YearlyBudget,years,SegmentID, SocialCostYearlyBudget,...
    PavementInterventionInit, SewerInterventionInit,WaterInterventionInit,UseInit);
```

```
    UseInit = true;
    gen   = 1;
    genPFPlans = {};
    genPFintervention_cost = [];
    genPFSocial_cost = [];
    genPFPerformance = [];
    Pfit = [sum(InterventionCost,2),sum(SocialCost,2),Performance];
    Prank = FastNonDominatedSorting_Vectorized(Pfit);
    [PavementInterventionInit, SewerInterventionInit,WaterInterventionInit,~] =
selectParentByRank(PavementInterventionInit, SewerInterventionInit,WaterInterventionInit,Prank);

    [PavementInterventionInitQ, SewerInterventionInitQ,WaterInterventionInitQ,InterventionCostQ,
SocialCostQ] = applyCrossoverAndMutation(PavementInterventionInit,...
        SewerInterventionInit,WaterInterventionInit,InterventionCost, SocialCost,pc,pm);
```

Plotting and verbose

```
    if(size(Pfit,2) == 2)
        h_fig = figure(1);
        h_par=scatter(Pfit(:,1),Pfit(:,2),20,'filled',
'markerFaceAlpha',0.3,'MarkerFaceColor',[128 193 219]./255); hold on;
        h_rep = plot(Pfit(:,1),Pfit(:,2),'ok'); hold on;
        grid on; xlabel('Intervention Cost'); ylabel('Social Cost');
        drawnow;
        axis square;
    end
    if(size(Pfit,2) == 3)
        h_fig = figure(1);
        h_rep = plot3(Pfit(:,1),Pfit(:,2),Pfit(:,3),'ok'); hold on;
        grid on; xlabel('Intervention Cost'); ylabel('Social Cost'); zlabel('Performance');
        drawnow;
        axis square;
    end
    display(['Generation #' num2str(gen) ' - First front size: ' num2str(sum(Prank==1))]);
```

Main NSGA-II loop

```
    stopCondition = false;
    gen_rank_solutions = nan;
```

```
    function update_gen_pareto_front(gen,Prank,Pfit)
        gen_rank_solution = [repmat(gen,size(Pfit,1),1),Prank,Pfit];
        if isnan(gen_rank_solutions)
            gen_rank_solutions = gen_rank_solution;
        else
            gen_rank_solutions = [gen_rank_solutions;gen_rank_solution];
```

```
        end
    end
```

% Plotting and verbose

```
 function plot_data(Rfit,Rrank)
       if(size(Rfit,2) == 2)
            figure(h_fig); delete(h_rep);
            h_par=scatter(Rfit(1:Np,1),Rfit(1:Np,2),20,'filled',
'markerFaceAlpha',0.3,'MarkerFaceColor',[128 193 219]./255); hold on;
            h_rep = plot(Rfit(1:Np,1),Rfit(1:Np,2),'ok'); hold on;
            grid on; xlabel('Intervention Cost'); ylabel('Social Cost');
            drawnow;
            axis square;
       end
        current_pf = Rrank == 1;
        RfitPF = Rfit(current_pf,:);
        NumPF = size(RfitPF,1);
        if(size(Rfit,2) == 3)
            figure(h_fig); delete(h_rep);
            h_rep = plot3(Rfit(1:Np,1),Rfit(1:Np,2),Rfit(1:Np,3),'ok'); hold on;
                try delete(h_pf); end
                h_pf =
plot3(RfitPF(1:NumPF,1),RfitPF(1:NumPF,2),RfitPF(1:NumPF,3),'s','color','green','MarkerFaceColor'
,'g'); hold on;
%             end
            grid on; xlabel('Intervention Cost'); ylabel('Social Cost');zlabel('Performance');
            drawnow;
            axis square;
        end
    end
    while ~stopCondition
```

```
        % Merge the parent P and the children Q
%         R = [P; Q];
        PavementInterventionInitR = [PavementInterventionInit;PavementInterventionInitQ];
        SewerInterventionInitR = [SewerInterventionInit;SewerInterventionInitQ];
        WaterInterventionInitR = [WaterInterventionInit;WaterInterventionInitQ];
        Nrows = size(WaterInterventionInitR,1);
        ResizeData(Nrows)
```

Compute the new Pareto Fronts

```
        [InterventionCost,
SocialCost,Performance,years_interventioncost,years_socialcost,Plans,InterventionBudgetUtilizatio
n,SocialBudgetUtilization,...
            ~] =
InterventionAndSocialCost(PavementCondition,SewerCondition,WaterPipeCondition,...
            Water_pipe_age,Sewer_pipe_age,Sewer_pipe_expected_life,Water_pipe_expected_life,
assets,sewer_costs,water_costs,...
            r,Pavement_intervention_impact,YearlyBudget,years,SegmentID,
```

```
SocialCostYearlyBudget,...
            PavementInterventionInitR, SewerInterventionInitR,WaterInterventionInitR,UseInit);

        Rfit = [sum(InterventionCost,2),sum(SocialCost,2),Performance];
        Rrank = FastNonDominatedSorting_Vectorized(Rfit);

        plot_data(Rfit,Rrank)
```

Sort by rank

```
        [Rrank,idx] = sort(Rrank,'ascend');
        Rfit = Rfit(idx,:);
        PavementInterventionInitR = PavementInterventionInitR(idx,:);
        SewerInterventionInitR = SewerInterventionInitR(idx,:);
        WaterInterventionInitR = WaterInterventionInitR(idx,:);
        Plans = Plans(idx,:);
        InterventionCost = InterventionCost(idx,:);
        SocialCost= SocialCost(idx,:);
        Performance = Performance(idx,:);

        genPFps = Plans(Rrank==1,:);
        PFintervention_cost = InterventionCost(Rrank==1,:);
        PFSocial_cost = SocialCost(Rrank==1,:);
        PFPerformance = Performance(Rrank == 1, :);

        genPFPlans = [genPFPlans;genPFps];
        genPFintervention_cost =[genPFintervention_cost;PFintervention_cost];
        genPFSocial_cost = [genPFSocial_cost;PFSocial_cost];
        genPFPerformance = [genPFPerformance; PFPerformance];

        update_gen_pareto_front(gen,Rrank,Rfit)
        if stopCondition, break; end

       display(['Generation #' num2str(gen) ' - First front size: ' num2str(sum(Rrank==1))]);
```

Compute the crowding distance index

```
        [Rcrowd,Rrank,~,PavementInterventionInitR, SewerInterventionInitR,WaterInterventionInitR]
...
            = crowdingDistances(Rrank,Rfit,PavementInterventionInitR,
SewerInterventionInitR,WaterInterventionInitR);
```

Select Parent

```
        [PavementInterventionInit, SewerInterventionInit,WaterInterventionInit] = ...
            selectParentByRankAndDistance(Rcrowd,Rrank,PavementInterventionInitR,
SewerInterventionInitR,WaterInterventionInitR);
```

Compute child

```
        [PavementInterventionInitQ, SewerInterventionInitQ,WaterInterventionInitQ,
InterventionCostQ, SocialCostQ] =...
            applyCrossoverAndMutation(PavementInterventionInit,
SewerInterventionInit,WaterInterventionInit,InterventionCost, SocialCost,pc,pm);
```

Increment generation

```
        gen = gen + 1;
        if(gen>maxgen), stopCondition = true; end
    end
    AllPF = gen_rank_solutions(gen_rank_solutions(:,2)==1,3:end);
    AllPFrank = FastNonDominatedSorting_Vectorized(AllPF);
    [AllPFrank,idx] = sort(AllPFrank,'ascend');
    genPFPlans = genPFPlans(idx,:);
    genPFintervention_cost = genPFintervention_cost(idx,:);
    genPFSocial_cost = genPFSocial_cost(idx,:);
    genPFPerformance = genPFPerformance(idx,:);
    AllPF = AllPF(idx,:);

    update_gen_pareto_front(gen,AllPFrank,AllPF);

    Plans = genPFPlans(AllPFrank == 1,:);
    InterventionCost = genPFintervention_cost(AllPFrank == 1,:);
    SocialCost = genPFSocial_cost(AllPFrank == 1,:);
    Performance = genPFPerformance(AllPFrank == 1,:);
end
```

Function that selects a new parent based on the crowding distance operator

```
function [newPavementInterventionInit, newSewerInterventionInit,newWaterInterventionInit] =...
    selectParentByRankAndDistance(Rcrowd,Rrank,PavementInterventionInitR,
SewerInterventionInitR,WaterInterventionInitR)

    % Initialization
    N = length(Rcrowd)/2;
    Npf = length(unique(Rrank));
    newPavementInterventionInit = zeros(N,size(PavementInterventionInitR,2));
    newSewerInterventionInit = zeros(N,size(PavementInterventionInitR,2));
    newWaterInterventionInit = zeros(N,size(PavementInterventionInitR,2));


    % Selecting the chromosomes
    pf = 1;
    numberOfSolutions = 0;
    while pf <= Npf
        % If there is enough space, select solutions based on rank
        if numberOfSolutions + sum(Rrank == pf) <= N
```

```
            newPavementInterventionInit(numberOfSolutions+1:numberOfSolutions+sum(Rrank == pf),:)
= PavementInterventionInitR(Rrank == pf,:);
            newSewerInterventionInit(numberOfSolutions+1:numberOfSolutions+sum(Rrank == pf),:) =
SewerInterventionInitR(Rrank == pf,:);
            newWaterInterventionInit(numberOfSolutions+1:numberOfSolutions+sum(Rrank == pf),:) =
WaterInterventionInitR(Rrank == pf,:);

            numberOfSolutions = numberOfSolutions + sum(Rrank == pf);
        % If there isn't enugh space, sort by crowding distances
        else
            rest = N - numberOfSolutions;
            lastPFPavement = PavementInterventionInitR(Rrank == pf,:);
            lastPFSewer = SewerInterventionInitR(Rrank == pf,:);
            lastPFWater = WaterInterventionInitR(Rrank == pf,:);
            lastPFdist = Rcrowd(Rrank == pf);

            [~,idx] = sort(lastPFdist,'descend');

            lastPFPavement = lastPFPavement(idx,:);
            lastPFSewer = lastPFSewer(idx,:);
            lastPFWater = lastPFWater(idx,:);

%             newParent(numberOfSolutions+1:numberOfSolutions+rest,:) = lastPF(1:rest,:);
            newPavementInterventionInit(numberOfSolutions+1:numberOfSolutions+rest,:) =
lastPFPavement(1:rest,:);
            newSewerInterventionInit(numberOfSolutions+1:numberOfSolutions+rest,:) =
lastPFSewer(1:rest,:);
            newWaterInterventionInit(numberOfSolutions+1:numberOfSolutions+rest,:) =
lastPFWater(1:rest,:);
            %newPlans(numberOfSolutions+1:numberOfSolutions+rest,:) = lastPFPlans(1:rest,:);
            numberOfSolutions = numberOfSolutions + rest;
        end
        pf = pf + 1;
    end
end
```

Function that computes the crowding distances of every single Pareto Front

```
function
[sortCrowd,sortRank,sortFit,sortPavementInterventionInitR,sortSewerInterventionInitR,sortWaterInt
erventionInitR] = ...
    crowdingDistances(rank,fitness,PavementInterventionInitR,
SewerInterventionInitR,WaterInterventionInitR)

    % Initialize
%     sortPop = [];
    sortPavementInterventionInitR = [];
    sortSewerInterventionInitR = [];
    sortWaterInterventionInitR = [];

    sortFit = [];
    sortRank = [];
```

```
    sortCrowd = [];

    Npf = length(unique(rank));
    for pf = 1:1:Npf
        index = find(rank==pf);
        temp_fit = fitness(index,:);
        temp_rank = rank(index,:);
        temp_pavementpop= PavementInterventionInitR(index,:);
        temp_sewerpop= SewerInterventionInitR(index,:);
        temp_waterpop= WaterInterventionInitR(index,:);
        %temp_planspop = PlansR(index,:);

        % Sort by first dimension
        [temp_fit,sort_idx] = sortrows(temp_fit,1);
        temp_rank = temp_rank(sort_idx);
        sortFit = [sortFit; temp_fit];
        sortRank = [sortRank; temp_rank];

%         sortPop = [sortPop; temp_pop(sort_idx,:)];
        sortPavementInterventionInitR = [sortPavementInterventionInitR;
temp_pavementpop(sort_idx,:)];
        sortSewerInterventionInitR = [sortSewerInterventionInitR; temp_sewerpop(sort_idx,:)];
        sortWaterInterventionInitR = [sortWaterInterventionInitR; temp_waterpop(sort_idx,:)];
        %sortPlansR = [sortPlansR; temp_planspop];

        % Crowded distances
        temp_crowd = zeros(size(temp_rank));
        for m = 1:1:size(fitness,2)
            temp_max = max(temp_fit(:,m));
            temp_min = min(temp_fit(:,m));
            for l = 2:1:length(temp_crowd)-1
                temp_crowd(l) = temp_crowd(l) + (abs(temp_fit(l-1,m)-
temp_fit(l+1,m)))./(temp_max-temp_min);
            end
        end
        temp_crowd(1) = Inf;
        temp_crowd(length(temp_crowd)) = Inf;
        sortCrowd = [sortCrowd; temp_crowd];
    end
end
```

Function that calculates a child population by applying crossover and mutation

```
function children = performCrossover(parent1,parent2,cut)
    temp = parent1(cut+1:end);
    child1 = [parent1(1:cut), parent2(cut+1:end)];
    child2 = [parent2(1:cut), temp];
    children = [child1;child2];
end
```

```
function [PavementInterventionInitQ, SewerInterventionInitQ,WaterInterventionInitQ,
InterventionCostQ, SocialCostQ] = applyCrossoverAndMutation(PavementInterventionInit, ...
```

```
    SewerInterventionInit,WaterInterventionInit,InterventionCost,
SocialCost,pc,pm)%,pm,ms,var_max,var_min)
    % Params
    N = size(PavementInterventionInit,1);
    nVar = size(PavementInterventionInit,2);

    % Child initialization
%     Q = parent;
    PavementInterventionInitQ = PavementInterventionInit;
    SewerInterventionInitQ =  SewerInterventionInit;
    WaterInterventionInitQ = WaterInterventionInit;
    InterventionCostQ = InterventionCost;
    SocialCostQ = SocialCost;

    % Crossover
    cross_idx = rand(N,1) < pc;
    cross_idx = find(cross_idx);
    crossed = zeros(N,1);
    next_id = 1;
    for c = 1:1:length(cross_idx)
        if any(crossed(:) == c)
            continue;
        else
            crossed(next_id) = c;
            next_id = next_id + 1;
        end
        selected = randi(N,1,1);
        while selected == c || any(crossed(:) ==selected)
            selected = randi(N,1,1);
        end
        crossed(next_id) = selected;
        next_id = next_id + 1;
        cut = randi(nVar,1,1);
%         Q(c,:) = [parent(c,1:cut), parent(selected,cut+1:nVar)];
        PavementInterventionInitQ([c,selected],:) =
performCrossover(PavementInterventionInit(c,:), PavementInterventionInit(selected,:),cut);
        SewerInterventionInitQ([c,selected],:) = performCrossover(SewerInterventionInit(c,:),
SewerInterventionInit(selected,:),cut);
        WaterInterventionInitQ([c,selected],:) = performCrossover(WaterInterventionInit(c,:),
WaterInterventionInit(selected,:),cut);
        InterventionCostQ([c,selected],:) = performCrossover(InterventionCost(c,:),
InterventionCost(selected,:),cut);
        SocialCostQ([c,selected],:) = performCrossover(SocialCost(c,:),
SocialCost(selected,:),cut);
    end

    % Mutation population with Gaussian distribution
    population_shape = size(PavementInterventionInitQ);
    total_elements = population_shape(1) * population_shape(2);
    mutatedPavementPop = reshape(randsample(0:3,total_elements,true),population_shape);
    mutatedSewerPop = reshape(randsample(0:2,total_elements,true),population_shape);
    mutatedWaterPop = reshape(randsample(0:2,total_elements,true),population_shape);
    mutatedPavementPop((mutatedSewerPop == 2) | (mutatedWaterPop == 2)) = 3;
```

```
    mut_idx = rand(N,nVar) < pm;
    PavementInterventionInitQ(mut_idx & PavementInterventionInitQ > 0) =
mutatedPavementPop(mut_idx & PavementInterventionInitQ > 0);
    SewerInterventionInitQ(mut_idx & SewerInterventionInitQ > 0) = mutatedSewerPop(mut_idx &
SewerInterventionInitQ > 0);
    WaterInterventionInitQ(mut_idx & WaterInterventionInitQ > 0) = mutatedWaterPop(mut_idx &
WaterInterventionInitQ > 0);


    PavementInterventionInitQ((SewerInterventionInitQ == 2) | (WaterInterventionInitQ == 2)) = 3;

end
```

Function that performs a binary tournament selection and extracts one parent from the initial population based on their ranks.

```
function [PavementInterventionInit1, SewerInterventionInit1,WaterInterventionInit1,P1rank]   =
selectParentByRank(PavementInterventionInit, SewerInterventionInit,WaterInterventionInit, Prank)
    % Take the couples
    N = length(Prank);
    left_idx  = randi(N,N,1);
    right_idx = randi(N,N,1);
    while sum(left_idx==right_idx)>0
        right_idx(left_idx==right_idx) = randi(N,sum(left_idx==right_idx),1);
    end

    % Make the tournament
    winners = zeros(N,1);
    winners(Prank(left_idx)<=Prank(right_idx)) = left_idx(Prank(left_idx)<=Prank(right_idx));
    winners(Prank(right_idx)<Prank(left_idx)) = right_idx(Prank(right_idx)<Prank(left_idx));

    % Select both populations
%     P1 = P(winners,:);
    PavementInterventionInit1 = PavementInterventionInit(winners,:);
    SewerInterventionInit1 = SewerInterventionInit(winners,:);
    WaterInterventionInit1 = WaterInterventionInit(winners,:);
    P1rank = Prank(winners,:);
end
```

Function that performs a vectorized version of the Fast Non Dominated Sorting algorithm which speeds up the computation time

```
function [RANK] = FastNonDominatedSorting_Vectorized(fitness)
    % Initialization
    Np = size(fitness,1);
    RANK = zeros(Np,1);
    current_vector = [1:1:Np]';
    current_pf = 1;
    all_perm = [repmat([1:1:Np]',Np',1), reshape(repmat([1:1:Np],Np,1),Np^2,1)];
    all_perm(all_perm(:,1)==all_perm(:,2),:) = [];
```

```
    % Computing each Pareto Front
    while ~isempty(current_vector)

        % Check if there is only a single particle
        if length(current_vector) == 1
            RANK(current_vector) = current_pf;
            break;
        end

        % Non-dominated particles
            % Note: nchoosek has an exponential grow in computation time, so
            % it's better to take all the combinations including repetitions using a
            % loops (quasi-linear grow) or repmats (linear grow)

        d = dominates(fitness(all_perm(:,1),:),fitness(all_perm(:,2),:));
        dominated_particles = unique(all_perm(d==1,2));

        % Check if there is no room for more Pareto Fronts
        if sum(~ismember(current_vector,dominated_particles)) == 0
            break;
        end

        % Update ranks and current_vector
        non_dom_idx = ~ismember(current_vector,dominated_particles);
        RANK(current_vector(non_dom_idx)) = current_pf;
        all_perm(ismember(all_perm(:,1),current_vector(non_dom_idx)),:) = [];
        all_perm(ismember(all_perm(:,2),current_vector(non_dom_idx)),:) = [];
        current_vector(non_dom_idx) = [];
        current_pf = current_pf + 1;
    end
end
```

Function that returns true if x dominates y and false otherwise

```
function d = dominates(x,y)
    d = (all(x<=y,2) & any(x<y,2));
end
```

This is the main function that calls the NSGAII algorithm

```
%function Optimization_09_30
```

```
%%This is the main function that calls the NSGAII algorithm
    clear; close all;
assets = readtable('Case_study_10_24Copy2.xlsx');
NanData = ~(isnan(assets.ID_TRC_PI) | isnan(assets.waterPipe_age)| isnan(assets.Autos)|
isnan(assets.Heavy_Trucks)...
    | isnan(assets.Light_Trucks)| isnan(assets.Bus)| isnan(assets.PD_arrondi)|
isnan(assets.Segment_Length)| isnan(assets.Pavement_Surface_area)...
    | isnan(assets.Sewer_length)| isnan(assets.Sewer_diameterV)| isnan(assets.water_P_length) |
```

```
isnan(assets.water_diameter));
    assets = assets(NanData,:);
    sewer_costs = readtable('Cost_replace_rehab_sewer_pipes.xlsx');
    water_costs = readtable('Cost_replace_rehab_water_pipes.xlsx');
    Pavement_intervention_impact =readtable('Pavement_Intervention_year_impact.xlsx');
    Np = 250;
    NumSegments = 1151;
    r=0.03;
    % segments in each column and row for each solution
    YearlyBudget =140000000;
    SocialCostYearlyBudget = 8500000;
    years = 100; % Planning period

    UseInit = false;

    params.Np = Np;
    params.maxgen =5;
    params.pc = 0.8;
    params.pm = 0.01;
    params.ms = 0;
    params.NumSegments = NumSegments;
    params.r = r;
    params.YearlyBudget = YearlyBudget;
    params.SocialCostYearlyBudget = SocialCostYearlyBudget;
    params.years = years;
    params.assets = assets;

    params.sewer_costs = sewer_costs;
    params.water_costs = water_costs;
    params.Pavement_intervention_impact = Pavement_intervention_impact;

    [Plans,SocialCost,InterventionCost,Performance,years_interventioncost,years_socialcost,
gen_rank_solutions] = SYNC_NSGAII(params);
    csvwrite('sync_gen_pareto_front.csv',gen_rank_solutions)
    plot_gen_SYNC_pareto_front3(gen_rank_solutions,3,'AG\_SYNC\_LCC (CAD$)',5,'Network
deterioration',2)

    plot_gen_SYNC_pareto_front3(gen_rank_solutions,5,'Network deterioration',3,'AG\_SYNC\_LCC
(CAD$)',2)
    plot_gen_SYNC_pareto_front3(gen_rank_solutions,3,'AG\_SYNC\_LCC (CAD$)',4,'SC\_SYNC\_LCC
(CAD$)',3)
    plot_gen_SYNC_pareto_front3(gen_rank_solutions,5,'Network deterioration',4,'SC\_SYNC\_LCC
(CAD$)',4)
%     loop NGSA
```

D. 2 Codes for MUT optimization

```
% ------------------------------------------------------------------------------%
% Function NSGAII performs a Non Sorting Genetic Algorithm-II                   %
%                                                                               %
%                                                                               %
%   Input parameters:                                                           %
%       - params:   Struct that contains the customized parameters.             %
%         * params.Np:                    Number of chromosomes in the population. %
%         * params.maxgen:                Maximum number of generations.        %
%         * params.pc:                    Probability of crossover.             %
%         * params.pm:                    Probability of mutation.              %
%         * params.NumSegments            Number of segments.                    %
%         * params.r                      Discount rate.                        %
%         * params.YearlyBudget           Agency cost budget                     %
%         * params.SocialCostYearlyBudget Social cost budget                    %
%         * params.years                  Planning period                       %
%         * params.req                    Cost of MUT requirement/length        %
%         * params.occupancy_costs        Occupancy costs                       %
%         * params. Service_equip         Cost of replacement                   %
%
%
% ------------------------------------------------------------------------------%
%   Author:  Kelechukwu Tersoo Genger                                           %
%   Date:    09/03/2023                                                         %
%   E-mail:  tkgenger@gmail.com                                                 %
%                                                                               %
%   Log:                                                                        %
%            1.1:  Fast Non Sorting Algorithm is now vectorized for im-         %
%                  proving the performance (much less computation time)         %
%                  (22/12/2017).                                                %
%          - 1.2:  The old mutation operator is substituted by the adding       %
%                  of a , as suggested by                                       %
%                  Alexander Hagg, which brings a better convergence            %
%                  (25/11/2019).                                                %
% ------------------------------------------------------------------------------%
%   References:                                                                 %
%    [1] Deb, K., Pratap, A., Agarwal, S., & Meyarivan, T. A. M. T. (2002)      %
%        A fast and elitist multiobjective genetic algorithm: NSGA-II.          %
%        IEEE transactions on evolutionary computation, 6(2), 182-197.          %
% ------------------------------------------------------------------------------ %
```

```
function
[construction_year,MUT_Plans,Total_MUT_SocialCost,Total_MUT_Agency_Cost,MUT_Performance,gen_rank_
solutions] = MUT_NSGAII(params)
```

```
global Water_pipe_expected_life Sewer_pipe_expected_life WaterPipeCondition Water_pipe_age
Sewer_pipe_age SewerCondition
global tunnel_length sewer_length water_length construction_year Maint_Cost
TunnelconstructionCost
    Np      = params.Np;        % Number of chromosomes in the population
    maxgen  = params.maxgen;    % Maximum number of generations
    pc      = params.pc;        % Probability of crossover
    pm      = params.pm;        % Probability of mutation
    ms      = params.ms;        % Mutation strength
    NumSegments = params.NumSegments;
    r = params.r;
    YearlyBudget = params.YearlyBudget;
    SocialCostYearlyBudget = params.SocialCostYearlyBudget;
    years = params.years;
    assets = params.assets;
    %CD = params.CD;
    req = params.req;
    Occupancy_costs = params.Occupancy_costs;
    Service_equip = params.Service_equip;
    uniqueID =  assets.ID_TRC_PI;
    SegmentID = uniqueID(1:NumSegments)';                   %ID of segment
```

```
        function ResizeData(Nrows)
        Water_pipe_age = repmat(assets.waterPipe_age(1:NumSegments)',Nrows,1);
        Sewer_pipe_age = repmat(assets.SewerAge(1:NumSegments)',Nrows,1);
        SewerCondition = repmat(assets.sewer_initial_condition(1:NumSegments)',Nrows,1);
        WaterPipeCondition = repmat(assets.water_initial_condition(1:NumSegments)',Nrows,1);
        Sewer_pipe_expected_life =
repmat(assets.Sewer_pipe_expected_life(1:NumSegments)',Nrows,1);
        Water_pipe_expected_life =
repmat(assets.Water_pipe_expected_life(1:NumSegments)',Nrows,1);
        tunnel_length = repmat(assets.Segment_Length(1:NumSegments)',Nrows,1);
        sewer_length = repmat(assets.Sewer_length(1:NumSegments)',Nrows,1);
        water_length = repmat(assets.water_P_length(1:NumSegments)',Nrows,1);
        construction_year = repmat(zeros(size(1:NumSegments)),Nrows,1);
        Maint_Cost = repmat(zeros(size(1:NumSegments)),Nrows,1);
        TunnelconstructionCost = repmat(zeros(size(1:NumSegments)),Nrows,1);

        end
```

```
    ResizeData(Np)

    %Initialization
    UseInit = false;
    SewerInterventionInit = nan;
    WaterInterventionInit = nan;
```

initial Population P

```
    [Total_MUT_Agency_Cost,
Total_MUT_SocialCost,MUT_Performance,MUT_Plans,MUT_Agency_BudgetUtilization,MUT_SocialBudgetUtili
zation,...
    construction_year,SewerInterventionInit,WaterInterventionInit] =
MUTAgency_And_SocialCost(SewerCondition,WaterPipeCondition,...
    Water_pipe_age,Sewer_pipe_age,Sewer_pipe_expected_life,Water_pipe_expected_life,assets,...
    r,YearlyBudget,years,SegmentID, SocialCostYearlyBudget,...
    construction_year,SewerInterventionInit,WaterInterventionInit,UseInit,
req,Occupancy_costs,Service_equip, tunnel_length, sewer_length,water_length);
```

```
  UseInit = true;
    gen   = 1;
    genPFPlans = {};
    genPF_MUT_Agency_cost = [];
    genPF_MUT_Social_cost = [];
    genPF_MUT_Performance = [];
    Pfit = [sum(Total_MUT_Agency_Cost,2),sum(Total_MUT_SocialCost,2),MUT_Performance];
    Prank = FastNonDominatedSorting_Vectorized(Pfit);

    [ SewerInterventionInit,WaterInterventionInit,~] =
selectParentByRank(SewerInterventionInit,WaterInterventionInit,Prank);

    [ SewerInterventionInitQ,WaterInterventionInitQ,Total_MUT_Agency_CostQ,
Total_MUT_SocialCostQ] = applyCrossoverAndMutation(
SewerInterventionInit,WaterInterventionInit,Total_MUT_Agency_Cost, Total_MUT_SocialCost,pc,pm);
```

Plotting and verbose

```
    if(size(Pfit,2) == 2)
        h_fig = figure(1);
        h_par=scatter(Pfit(:,1),Pfit(:,2),20,'filled',
'markerFaceAlpha',0.3,'MarkerFaceColor',[128 193 219]./255); hold on;
        h_rep = plot(Pfit(:,1),Pfit(:,2),'ok'); hold on;
        grid on; xlabel('Total MUT Agency Cost'); ylabel('Total MUT SocialCost');
        drawnow;
        axis square;
    end
    if(size(Pfit,2) == 3)
        h_fig = figure(1);
        h_rep = plot3(Pfit(:,1),Pfit(:,2),Pfit(:,3),'ok'); hold on;
        grid on; xlabel('Total MUT Agency Cost'); ylabel('Total MUT SocialCost');
zlabel('Performance');
        drawnow;
        axis square;
    end
    display(['Generation #' num2str(gen) ' - First front size: ' num2str(sum(Prank==1))]);
```

Main NSGA-II loop

```
    stopCondition = false;
    gen_rank_solutions = nan;
```

```
    function update_gen_pareto_front(gen,Prank,Pfit)
        gen_rank_solution = [repmat(gen,size(Pfit,1),1),Prank,Pfit];
        if isnan(gen_rank_solutions)
            gen_rank_solutions = gen_rank_solution;
        else
            gen_rank_solutions = [gen_rank_solutions;gen_rank_solution];
        end
    end
```

```
    function plot_data(Rfit,Rrank)
          % Plotting and verbose
       if(size(Rfit,2) == 2)
            figure(h_fig); delete(h_rep);
            h_par=scatter(Rfit(1:Np,1),Rfit(1:Np,2),20,'filled',
'markerFaceAlpha',0.3,'MarkerFaceColor',[128 193 219]./255); hold on;
            h_rep = plot(Rfit(1:Np,1),Rfit(1:Np,2),'ok'); hold on;
            grid on; xlabel('Total MUT Agency Cost'); ylabel('Total MUT SocialCost');
            drawnow;
            axis square;
       end
        current_pf = Rrank == 1;
        RfitPF = Rfit(current_pf,:);
        NumPF = size(RfitPF,1);
        if(size(Rfit,2) == 3)
            figure(h_fig); delete(h_rep);
            h_rep = plot3(Rfit(1:Np,1),Rfit(1:Np,2),Rfit(1:Np,3),'ok'); hold on;
                 try delete(h_pf); end
                 h_pf =
plot3(RfitPF(1:NumPF,1),RfitPF(1:NumPF,2),RfitPF(1:NumPF,3),'s','color','green','MarkerFaceColor'
,'g'); hold on;
            grid on; xlabel('Total MUT Agency Cost'); ylabel('Total MUT
SocialCost');zlabel('Performance');
            drawnow;
            axis square;
        end
    end
    while ~stopCondition
```

Merge the parent and the children R = [P; Q];

```
        SewerInterventionInitR = [SewerInterventionInit;SewerInterventionInitQ];
        WaterInterventionInitR = [WaterInterventionInit;WaterInterventionInitQ];
        Nrows = size(WaterInterventionInitR,1);
        ResizeData(Nrows)
```

```
        % Compute the new Pareto Fronts
        [Total_MUT_Agency_Cost,
Total_MUT_SocialCost,MUT_Performance,MUT_Plans,InterventionBudgetUtilization,SocialBudgetUtilizat
ion,...
```

```
            ~] = MUTAgency_And_SocialCost(SewerCondition,WaterPipeCondition,...

Water_pipe_age,Sewer_pipe_age,Sewer_pipe_expected_life,Water_pipe_expected_life,assets,...
            r,YearlyBudget,years,SegmentID, SocialCostYearlyBudget,...
            construction_year,SewerInterventionInitR,WaterInterventionInitR,UseInit,...
            req,Occupancy_costs,Service_equip, tunnel_length, sewer_length,water_length);

        Rfit = [sum(Total_MUT_Agency_Cost,2),sum(Total_MUT_SocialCost,2),MUT_Performance];
        Rrank = FastNonDominatedSorting_Vectorized(Rfit);

        plot_data(Rfit,Rrank)

        %sort by rank
        [Rrank,idx] = sort(Rrank,'ascend');
        Rfit = Rfit(idx,:);
%         R = R(idx,:);
        SewerInterventionInitR = SewerInterventionInitR(idx,:);
        WaterInterventionInitR = WaterInterventionInitR(idx,:);
        MUT_Plans = MUT_Plans(idx,:);
        Total_MUT_SocialCost = Total_MUT_SocialCost(idx,:);
        Total_MUT_Agency_Cost = Total_MUT_Agency_Cost(idx,:);
        MUT_Performance = MUT_Performance(idx,:);

        genPFps = MUT_Plans(Rrank==1,:);
        PFMUT_agency_cost = Total_MUT_Agency_Cost(Rrank==1,:);
        PFMUT_social_cost = Total_MUT_SocialCost(Rrank==1,:);
        PFMUT_performance = MUT_Performance(Rrank==1,:);

        genPFPlans = [genPFPlans;genPFps];
        genPF_MUT_Agency_cost = [genPF_MUT_Agency_cost;PFMUT_agency_cost];
        genPF_MUT_Social_cost = [genPF_MUT_Social_cost;PFMUT_social_cost];
        genPF_MUT_Performance = [genPF_MUT_Performance;PFMUT_performance];

        update_gen_pareto_front(gen,Rrank,Rfit)
        if stopCondition, break; end

        display(['Generation #' num2str(gen) ' - First front size: ' num2str(sum(Rrank==1))]);

         %compute the crowding disance index
        [Rcrowd,Rrank,~, SewerInterventionInitR,WaterInterventionInitR] ...
            = crowdingDistances(Rrank,Rfit, SewerInterventionInitR,WaterInterventionInitR);
```

Select Parent P = selectParentByRankAndDistance(Rcrowd,Rrank,R);

```
        [SewerInterventionInit,WaterInterventionInit] = ...
            selectParentByRankAndDistance(Rcrowd,Rrank,
SewerInterventionInitR,WaterInterventionInitR);
```

Compute child Q = applyCrossoverAndMutation(P,pc,pm,ms,var_max,var_min);

```
        [SewerInterventionInitQ,WaterInterventionInitQ,Total_MUT_Agency_CostQ,
Total_MUT_SocialCostQ] =...
```

```
applyCrossoverAndMutation(SewerInterventionInit,WaterInterventionInit,Total_MUT_Agency_Cost,
Total_MUT_SocialCost,pc,pm);%,pm,ms,var_max,var_min);
%
```

Increment generation

```
        gen = gen + 1;
        if(gen>maxgen), stopCondition = true; end
    end

    AllPF = gen_rank_solutions(gen_rank_solutions(:,2)==1,3:end);
    AllPFrank = FastNonDominatedSorting_Vectorized(AllPF);
    [AllPFrank,idx] = sort(AllPFrank,'ascend');
    genPFPlans = genPFPlans(idx,:);
    genPF_MUT_Agency_cost = genPF_MUT_Agency_cost(idx,:);
    genPF_MUT_Social_cost = genPF_MUT_Social_cost(idx,:);
    genPF_MUT_Performance = genPF_MUT_Performance(idx,:);
    AllPF = AllPF(idx,:);

    update_gen_pareto_front(gen,AllPFrank,AllPF);

    MUT_Plans = genPFPlans(AllPFrank == 1,:);
    Total_MUT_Agency_Cost = genPF_MUT_Agency_cost(AllPFrank == 1,:);
    Total_MUT_SocialCost = genPF_MUT_Social_cost(AllPFrank == 1,:);
    MUT_Performance = genPF_MUT_Performance(AllPFrank == 1,:);

    display(['Generation #' num2str(gen) ' - First front size: ' num2str(sum(AllPFrank==1))]);
end

function [newSewerInterventionInit,newWaterInterventionInit] =...
    selectParentByRankAndDistance(Rcrowd,Rrank, SewerInterventionInitR,WaterInterventionInitR)

    % Initialization
    N = length(Rcrowd)/2;
    Npf = length(unique(Rrank));

    newSewerInterventionInit = zeros(N,size(SewerInterventionInitR,2));
    newWaterInterventionInit = zeros(N,size(WaterInterventionInitR,2));

    % Selecting the chromosomes
    pf = 1;
    numberOfSolutions = 0;
    while pf <= Npf
        % If there is enough space, select solutions based on rank
        if numberOfSolutions + sum(Rrank == pf) <= N
            newSewerInterventionInit(numberOfSolutions+1:numberOfSolutions+sum(Rrank == pf),:) =
SewerInterventionInitR(Rrank == pf,:);
            newWaterInterventionInit(numberOfSolutions+1:numberOfSolutions+sum(Rrank == pf),:) =
WaterInterventionInitR(Rrank == pf,:);
            numberOfSolutions = numberOfSolutions + sum(Rrank == pf);
        % If there isn't enugh space, sort by crowding distances
```

```
        else
            rest = N - numberOfSolutions;
            lastPFSewer = SewerInterventionInitR(Rrank == pf,:);
            lastPFWater = WaterInterventionInitR(Rrank == pf,:);

            lastPFdist = Rcrowd(Rrank == pf);
            [~,idx] = sort(lastPFdist,'descend');
            lastPFSewer = lastPFSewer(idx,:);
            lastPFWater = lastPFWater(idx,:);


%           newParent(numberOfSolutions+1:numberOfSolutions+rest,:) = lastPF(1:rest,:);
            newSewerInterventionInit(numberOfSolutions+1:numberOfSolutions+rest,:) =
lastPFSewer(1:rest,:);
            newWaterInterventionInit(numberOfSolutions+1:numberOfSolutions+rest,:) =
lastPFWater(1:rest,:);

            numberOfSolutions = numberOfSolutions + rest;
        end
        pf = pf + 1;
    end
end
```

```
function [sortCrowd,sortRank,sortFit,sortSewerInterventionInitR,sortWaterInterventionInitR] = ...
    crowdingDistances(rank,fitness,SewerInterventionInitR,WaterInterventionInitR)

    % Initialize

    sortSewerInterventionInitR = [];
    sortWaterInterventionInitR = [];

%     sortPop = [];
    sortFit = [];
    sortRank = [];
    sortCrowd = [];

    Npf = length(unique(rank));
    for pf = 1:1:Npf
        index = find(rank==pf);
        temp_fit = fitness(index,:);
        temp_rank = rank(index,:);

%         temp_pop = pop(index,:);

        temp_sewerpop= SewerInterventionInitR(index,:);
        temp_waterpop= WaterInterventionInitR(index,:);

        % Sort by first dimension

        [temp_fit,sort_idx] = sortrows(temp_fit,1);
        temp_rank = temp_rank(sort_idx);
        sortFit = [sortFit; temp_fit];
        sortRank = [sortRank; temp_rank];
```

```
%         sortPop = [sortPop; temp_pop(sort_idx,:)];
        sortSewerInterventionInitR = [sortSewerInterventionInitR; temp_sewerpop(sort_idx,:)];
        sortWaterInterventionInitR = [sortWaterInterventionInitR; temp_waterpop(sort_idx,:)];

        % Crowded distances
        temp_crowd = zeros(size(temp_rank));
        for m = 1:1:size(fitness,2)
            temp_max = max(temp_fit(:,m));
            temp_min = min(temp_fit(:,m));
            for l = 2:1:length(temp_crowd)-1
                temp_crowd(l) = temp_crowd(l) + (abs(temp_fit(l-1,m)-
temp_fit(l+1,m)))./(temp_max-temp_min);
            end
        end
        temp_crowd(1) = Inf;
        temp_crowd(length(temp_crowd)) = Inf;
        sortCrowd = [sortCrowd; temp_crowd];
    end
end
```

Function that calculates a child population by applying crossover and mutation

```
function children = performCrossover(parent1,parent2,cut)
    temp = parent1(cut+1:end);
    child1 = [parent1(1:cut), parent2(cut+1:end)];
    child2 = [parent2(1:cut), temp];
    children = [child1;child2];
end
```

```
function [SewerInterventionInitQ,WaterInterventionInitQ,Total_MUT_Agency_CostQ,
Total_MUT_SocialCostQ] =
applyCrossoverAndMutation(SewerInterventionInit,WaterInterventionInit,...
    Total_MUT_Agency_Cost, Total_MUT_SocialCost,pc,pm)
    % Params
    N = size(SewerInterventionInit,1);
    nVar = size(SewerInterventionInit,2);

    % Child initialization
%     Q = parent;
    SewerInterventionInitQ =  SewerInterventionInit;
    WaterInterventionInitQ = WaterInterventionInit;
    Total_MUT_Agency_CostQ = Total_MUT_Agency_Cost;
    Total_MUT_SocialCostQ = Total_MUT_SocialCost;
    cross_idx = rand(N,1) < pc;
    cross_idx = find(cross_idx);
    crossed = zeros(N,1);
    next_id = 1;
    for c = 1:1:length(cross_idx)
        if any(crossed(:) == c)
            continue;
        else
```

```
            crossed(next_id) = c;
            next_id = next_id + 1;
        end
        selected = randi(N,1,1);
        while selected == c || any(crossed(:) == selected)
            selected = randi(N,1,1);
            %display(selected)
        end
        crossed(next_id) = selected;
        next_id = next_id + 1;

        cut = randi(nVar,1,1);
%         Q(c,:) = [parent(c,1:cut), parent(selected,cut+1:nVar)];
        SewerInterventionInitQ([c,selected],:) = performCrossover(SewerInterventionInit(c,:),
SewerInterventionInit(selected,:),cut);
        WaterInterventionInitQ([c,selected],:) = performCrossover(WaterInterventionInit(c,:),
WaterInterventionInit(selected,:),cut);
        Total_MUT_Agency_CostQ([c,selected],:) = performCrossover(Total_MUT_Agency_Cost(c,:),
Total_MUT_Agency_Cost(selected,:),cut);
        Total_MUT_SocialCostQ([c,selected],:) = performCrossover(Total_MUT_SocialCost(c,:),
Total_MUT_SocialCost(selected,:),cut);
    end
     population_shape = size(SewerInterventionInitQ);
    total_elements = population_shape(1) * population_shape(2);

    mutatedSewerPop = reshape(randsample(0:2,total_elements,true),population_shape);
    mutatedWaterPop = reshape(randsample(0:2,total_elements,true),population_shape);
    mutatedWaterPop ((mutatedSewerPop==2) & (mutatedWaterPop ==1))=2;  %added this
    mutatedSewerPop ((mutatedWaterPop==2) & (mutatedSewerPop ==1))=2;
      % Mutation population with Gaussian distribution
%     % Mutate the children with probability pm
    mut_idx = rand(N,nVar) < pm;
    SewerInterventionInitQ(mut_idx & SewerInterventionInitQ > 0) = mutatedSewerPop(mut_idx &
SewerInterventionInitQ > 0);
    WaterInterventionInitQ(mut_idx & WaterInterventionInitQ > 0) = mutatedWaterPop(mut_idx &
WaterInterventionInitQ > 0);

end
```

Function that performs a binary tournament selection and extracts one parent from the initial population based on their ranks.

```
function [SewerInterventionInit1,WaterInterventionInit1,P1rank]   =
selectParentByRank(SewerInterventionInit,WaterInterventionInit, Prank)
    % Take the couples
    N = length(Prank);
    left_idx  = randi(N,N,1);
    right_idx = randi(N,N,1);
    while sum(left_idx==right_idx)>0
        right_idx(left_idx==right_idx) = randi(N,sum(left_idx==right_idx),1);
    end
```

```
    % Make the tournament
    winners = zeros(N,1);
    winners(Prank(left_idx)<=Prank(right_idx)) = left_idx(Prank(left_idx)<=Prank(right_idx));
    winners(Prank(right_idx)<Prank(left_idx)) = right_idx(Prank(right_idx)<Prank(left_idx));

    % Select both populations
%     P1 = P(winners,:);

    SewerInterventionInit1 = SewerInterventionInit(winners,:);
    WaterInterventionInit1 = WaterInterventionInit(winners,:);
    P1rank = Prank(winners,:);
end
```

```
function [RANK] = FastNonDominatedSorting_Vectorized(fitness)
    % Initialization
    Np = size(fitness,1);
    RANK = zeros(Np,1);
    current_vector = [1:1:Np]';
    current_pf = 1;
    all_perm = [repmat([1:1:Np]',Np',1), reshape(repmat([1:1:Np],Np,1),Np^2,1)];
    all_perm(all_perm(:,1)==all_perm(:,2),:) = [];

    % Computing each Pareto Front
    while ~isempty(current_vector)

        % Check if there is only a single particle
        if length(current_vector) == 1
            RANK(current_vector) = current_pf;
            break;
        end

        % Non-dominated particles
            % Note: nchoosek has an exponential grow in computation time, so
            % it's better to take all the combinations including repetitions using a
            % loops (quasi-linear grow) or repmats (linear grow)
            %all_perm = nchoosek(current_vector,2);
            %all_perm = [all_perm; [all_perm(:,2) all_perm(:,1)]];
        d = dominates(fitness(all_perm(:,1),:),fitness(all_perm(:,2),:));
        dominated_particles = unique(all_perm(d==1,2));

        % Check if there is no room for more Pareto Fronts
        if sum(~ismember(current_vector,dominated_particles)) == 0
            break;
        end

        % Update ranks and current_vector
        non_dom_idx = ~ismember(current_vector,dominated_particles);
        RANK(current_vector(non_dom_idx)) = current_pf;
        all_perm(ismember(all_perm(:,1),current_vector(non_dom_idx)),:) = [];
        all_perm(ismember(all_perm(:,2),current_vector(non_dom_idx)),:) = [];
        current_vector(non_dom_idx) = [];
        current_pf = current_pf + 1;
```

```
    end
end
```

Function that returns true if x dominates y and false otherwise

```
function d = dominates(x,y)
    d = (all(x<=y,2) & any(x<y,2));
end
```

This is the main function that calls the NSGAII algorithm

```
%function MUT_optimization
    clear; close all;
    assets = readtable('Case_study_10_24Copy2.xlsx');
   NanData = ~(isnan(assets.ID_TRC_PI) | isnan(assets.waterPipe_age)| isnan(assets.Autos)|
isnan(assets.Heavy_Trucks)...
    | isnan(assets.Light_Trucks)| isnan(assets.Sewer_ID) | isnan(assets.Bus)|
isnan(assets.PD_arrondi)| isnan(assets.Segment_Length)| isnan(assets.Pavement_Surface_area)...
    | isnan(assets.Sewer_length)| isnan(assets.Sewer_diameterV)| isnan(assets.water_P_length) |
isnan(assets.water_diameter));

    assets = assets(NanData,:);%read assets data from excel sheet
    sewer_costs = readtable('Cost_replace_rehab_sewer_pipes.xlsx');                          %read
sewer_costs data from excel sheet
    water_costs = readtable('Cost_replace_rehab_water_pipes.xlsx');                          %read
water_costs data from excel sheet
    uniqueID =  assets.ID_TRC_PI;
%%read ID of segment from excel sheet

    Np = 300;
    NumSegments = 1151;
    SegmentID = uniqueID(1:NumSegments)';
    r =0.03;
    req = 2400;                                                          %Cost of MUT
    Occupancy_costs = 130;
    Service_equip = 500;
    YearlyBudget =      140000000;           %budget
    SocialCostYearlyBudget =8500000;
    years = 100;
    age_increment = 0;
    UseInit = false;
    params.Np = Np;
    params.maxgen =10;
    params.pc = 0.8;
    params.pm = 0.03;
    params.NumSegments = NumSegments;
    params.r = r;
    params.YearlyBudget = YearlyBudget;
    params.SocialCostYearlyBudget = SocialCostYearlyBudget;
    params.years = years;
    params.assets = assets;
```

```
    %params.CD = CD;
    params.req = req;
    params.Occupancy_costs = Occupancy_costs;
    params.Service_equip = Service_equip;

[construction_year,MUT_Plans,Total_MUT_SocialCost,Total_MUT_Agency_Cost,Performance,gen_rank_solu
tions] = MUT_NSGAII(params);
    csvwrite('mut_gen_pareto_front.csv',gen_rank_solutions)
plot_gen_pareto_front3(gen_rank_solutions,5,'Network deterioration',3,'AG\_MUT\_LCC (CAD$)',2)
plot_gen_pareto_front3(gen_rank_solutions,3,'AG\_MUT\_LCC (CAD$)',4,'SC\_MUT\_LCC (CAD$)',3)
plot_gen_pareto_front3(gen_rank_solutions,5,'Network deterioration',4,'SC\_MUT\_LCC (CAD$)',4)
```

This function generates the graphs

```
function plot_gen_pareto_front3(gen_rank_solutions,XCol,Xlabel,YCol,Ylabel,Fig)
    figure(Fig)

    X = gen_rank_solutions(:,XCol);
    Y = gen_rank_solutions(:,YCol);
    gen = gen_rank_solutions(:,1);
    Rank = gen_rank_solutions(:,2);
    maxgen = max(gen);
    Xold = X(gen < maxgen);
    Yold = Y(gen < maxgen);
    plot(Xold,Yold,'LineStyle', 'none', 'Marker', 'o',
'MarkerFaceColor',[0.6,0.6,0.6],'MarkerEdgeColor','none')
    hold on
    Xfinal = X(gen == maxgen);
    Yfinal = Y(gen == maxgen);
    plot(Xfinal,Yfinal,'LineStyle', 'none', 'Marker', 'o',
'MarkerFaceColor',[0,0,1],'MarkerEdgeColor','none')

    PF = (gen == maxgen) & (Rank == 1);

    plot(X(PF), Y(PF),'LineStyle', 'none', 'Marker', 'o',
'MarkerFaceColor',[0,1,0],'MarkerEdgeColor','none')

    xlabel(Xlabel)
    ylabel(Ylabel)

    hold off

    figure(Fig+1);

plot3(gen_rank_solutions(:,3),gen_rank_solutions(:,4),gen_rank_solutions(:,5),'LineStyle','none',
'Marker','o','MarkerEdgeColor',[0.8,0.8,0.8]);hold on
    plot3(gen_rank_solutions(gen == maxgen,3),gen_rank_solutions(gen ==
maxgen,4),gen_rank_solutions(gen ==
maxgen,5),'LineStyle','none','Marker','o','MarkerEdgeColor',[0,0,1],'MarkerFaceColor',[0,0,1]);

plot3(gen_rank_solutions(PF,3),gen_rank_solutions(PF,4),gen_rank_solutions(PF,5),'LineStyle','non
e','Marker','o','MarkerEdgeColor',[0,1,0],'MarkerFaceColor',[0,1,0]);
```

```
    grid on; xlabel('AG\_MUT\_LCC (CAD$)'); ylabel('SC\_MUT\_LCC (CAD$)'); zlabel('Network
deterioration');
    drawnow;
    axis square;
    hold off
end
```

Appendix E. Statistical Test Interpretation

The F-Test Two-sample for variances is used for the two populations Y_i and $\widehat{Y_i}$(estimated). It is assumed that the costs are normally distributed data. The hypotheses are:

- H_0: $\sigma_1 = \sigma_2$, variances are likely equal
- H_1: $\sigma_1 \neq \sigma_2$, variances are likely different

If $F \geq F_{0.05}$ (which is the critical value of F for the 0.05 significance level) H_0 is rejected and if $F < F_{0.05}$, H_0 is accepted. When H_0 is accepted, it means that on average the costs are spread out equally from their respective means. Now, to compare the two means (μ_1, μ_2) when the variances are known to be likely either equal or different, the Two sample T-test is used, assuming either equal ($\sigma_1 = \sigma_2$) or unequal variance ($\sigma_1 \neq \sigma_2$). The hypotheses are:

- H_0: $\mu_1 = \mu_2$, means are likely equal
- H_1: $\mu_1 \neq \mu_2$, means are likely different

If the p-value ≥ 0.05 (i.e. 5% chance there is no real difference between the two populations), H_0 is accepted, and if the p-value < 0.05 H_0 is rejected. When H_0 is accepted, it means that on average, the two means are reliably the same. Therefore, we conclude that the regression function is validated. The following section presents the results of the regression models for the three social cost indicators.